AEDC-TDR-62-51

NOX

ANALYTICAL AND EXPERIMENTAL STUDY OF ADAPTING BEARINGS FOR USE IN AN ULTRA-HIGH VACUUM ENVIRONMENT

Phase I, II, and III

By

P. H. Bowen
Materials Laboratories
Westinghouse Electric Corporation

TECHNICAL DOCUMENTARY REPORT NO. AEDC-TDR-62-51

February 1962

AFSC Program Area 850E, Project 7778, Task 777801

(Prepared under Contract No. AF 40(600)-915 by Westinghouse Electric Corporation, East Pittsburgh, Pennsylvania.)

ARNOLD ENGINEERING DEVELOPMENT CENTER

AIR FORCE SYSTEMS COMMAND

UNITED STATES AIR FORCE

NOTICES

ANALYTICAL AND EXPERIMENTAL STUDY OF ADAPTING BEARINGS FOR USE IN AN ULTRA-HIGH VACUUM ENVIRONMENT

Phase I

Screening of Wear and Friction Characteristics of Plastics, Dry Powders, Composites, and Alloys

By

P. H. Bowen

Materials Laboratories

Westinghouse Electric Corporation

East Pittsburgh, Pennsylvania

(The reproducible copy supplied by the author was used in the production of this report.)

February 1962

Contract AF 40(600)-915

ABSTRACT

This report contains the results of an investigation into the lubrication of gears and bearings for use in a vacuum environment by using dry powders as a lubricant, and dry self-lubricating materials in the bearing retainer.

The report is divided as follows:

PHASE I: The wear and friction characteristics of various dry powders and dry self-lubricating materials for use in ball bearings were evaluated and screened in a dry inert atmosphere in laboratory test apparatus under rotating speeds and loads similar to that found in 2 to 7 h.p. electric motors. The materials evaluated included reinforced thermosetting plastics, dry lubricant filled and unfilled thermoplastics and dry lubricant filled sintered alloys.

PHASE II: Dry powder and self-lubricating materials were subjected to the vacuum conditions in the range of 1×10^{-6} to 1×10^{-9} mm Hg, and at temperatures in the range of $-60^{\circ}F$ to $1000^{\circ}F$ to determine the rate of the outgassing and/or decomposition of each material.

PHASE III: Dry ball bearing (204 size, 22 mm bore) soaking and operating tests were conducted using retainers fabricated from the most promising materials determined in Phase II. The bearings were operated at a speed of 1800 rpm, radial load of 75 lbs., axial load of 5 lbs., and tested under the vacuum and temperature conditions described in Phase II. Special bearings and retainer materials were used for exploratory tests up to $1500^{\circ}F$.

TABLE OF CONTENTS

PHASE I

PHASE II

PHASE III

I. INTRODUCTION

Handling facilities are required in the positioning and testing of space vehicles and other equipment in the large ground vacuum chambers contemplated for the Arnold Air Force Station, Tennessee. This program concerns the study of bearings and lubricant systems for use in electric hoist motors operating in these ground vacuum chambers under vacuum conditions similar to those of space operation.

The initial program was divided into three phases. In Phase I the wear and friction characteristics of various dry powders and dry self-lubricating materials suitable for use in ball bearing components were evaluated in a dry inert atmosphere. In Phase II the selected materials from Phase I will be subjected to a vacuum environment to determine the rate of outgassing of each material. In Phase III the most promising self-lubricating materials of Phase II will be fabricated into retainers and evaluated along with dry powders in 20 mm ball bearings operating in a vacuum chamber at pressures in the range of 1×10^{-6} to 1×10^{-9} mm of Hg. Starts will be made at -60°F with actual bearing operation at temperatures ranging from ambient to 1000°F. All tests will be made with a radial bearing load of 75 lbs. and an axial bearing load of 5 lbs.

At the extremely low pressure levels encountered in space and also contemplated for simulation in a ground test facility, conventional bearing lubricants evaporate or sublimate causing lubricating films to disappear with a resultant tremendous increase in surface friction and wear of the ball bearings. Under such conditions clean surfaces, when rubbing on one another in laboratory tests with apparently the last monomolecular film layer removed, have been known to cold weld. In addition, in an ultra-high vacuum environment, the only natural mechanisms of heat dissipation from a bearing are by radiation or conduction to contacting surfaces. This heat reservoir effect compounds the problem, as lubricant evaporation is accelerated at higher bulk temperatures. Some bearing materials have poor heat transfer characteristics and will not dissipate the thermal energy over the entire bearing surface but retain it at the localized areas where the asperities of each material make contact.

In ball bearings, rubbing occurs between the ball surface and ball pockets of the retainer and between the retainer surface and the corresponding guide lands of the inner or outer race. In the evaluation of lubricants of Phase I, the object was to obtain or develop solids, powders or self-lubricating structural materials that would provide low friction and minimum wear when rubbing against bearing steels or when used to lubricate bearing steels rubbing against each other. The rubbing velocities selected were similar to that of the retainer rubbing the bearing race and the balls when rubbing the retainer pocket.

II. WEAR AND FRICTION STUDIES ON PLASTIC MATERIALS

A. Screening Tests

Prior work by various investigators indicated that plastic materials are the best of the many solid materials now used or considered for use as bearing components for dry lubricating applications. As a result, the wear and friction characteristics of selected plastic materials were evaluated to determine if any would be satisfactory for use as bearing components operating dry in a space environment.

Initial evaluation of the plastic materials was performed using a modified Hohman Model A4 wear and friction tester. Figure 1 is a photograph of the test apparatus used. The tester embodies the same principles used in the MacMillan and Falex testers. A test disk or plug is attached to the end of a horizontal shaft which is rotated at a selected constant speed. The shaft assembly which incorporates a torque bearing arm is supported in the pedestal by a front and rear bearing. The test specimens in the form of 1/2" x 3/4" x 0.25" test blocks are held in shoes and mounted on the torque bearing arm and can pivot in a concentric arc about the shaft. The load is applied to the blocks through a parallelogram arrangement of levers by means of an air cylinder. The cylinder located above the rotating disk, is attached to the upper end of two vertical levers that hold the shoes. An oven surrounds the test blocks to permit conducting evaluations at elevated temperatures. A bell jar was used to cover the entire assembly for conducting the test in a nitrogen atmosphere. During operation of the unit, the friction torque of the disk rotating against the test blocks was indicated by the use of a strain gage and associated equipment connected to the torque bearing arm. During the elevated temperature tests, two water jackets shielded the forward pedestal bearing, load dynamometer ring and loading cylinder against the radiated heat from the test oven. In order to obtain an inert atmosphere environment of nitrogen, the test chamber was evacuated to 1 mm of Hg, and then returned to ambient pressure by admitting dry nitrogen. This process was repeated several times prior to each test run. During the test, the chamber was held at a pressure slightly above the ambient pressure to insure no leakage of oxygen into the test area.

The tests were run using rubbing velocities of 460 ft./min. (1280 rpm) and 230 ft./min. (640 rpm) and temperatures of 86°F and 160°F. The load on the test blocks was three pounds (equivalent to a pressure of 100-300 psi between the block and disk). M-10 tool steel was used as the rotating disk material for all screening tests of all the plastic materials.

B. Selection of Materials

Plastic materials that were known to exhibit good wear and friction characteristics necessary for unlubricated bearing components were selected for screening. Since polytetrafluoroethylene (Teflon) and nylon have many of the desirable properties for unlubricated bearings, they were among the first to be considered for the severe application of operating dry in a vacuum environment. In order to obtain optimum wear and friction values when rubbing against a metal surface, various powder lubricant and fillers were incorporated in these thermoplastic materials.

Other plastics were also evaluated and were compared to polytetrafluoroethylene and nylon. These plastics were unfilled polypropylene, a chlorinated polyether and carbon-graphite solid impregnated with polytetrafluoroethylene. The fillers contained in the various plastic materials included graphite, molybdenum disulfide, glass cloth, random glass fiber, and powdered ceramic. Table I lists all of the plastic and carbon materials evaluated.

C. Test Results

The average wear and friction values for the plastic materials evaluated are shown in Table II. The variations in friction during the test runs are shown by the curves in Figures 2 to 13. Figure 14 shows a comparison of the average coefficient of friction and wear for the twelve plastic materials. The two polytetrafluoroethylene impregnated carbon materials exhibited the lowest friction and best wear characteristics. Of the remaining plastic materials, polytetrafluoroethylene filled with glass fibers and molybdenum disulfide powder exhibited the lowest coefficient of friction values and lower than average wear. Low friction values are extremely desirable because of the poor thermal conductivity of the plastic or carbon material in the bearing during operation under load in the space environment. The unfilled plastic materials were unsatisfactory as bearing components under the specific conditions of load, speed and environment for the application stated in this program. Little difference was noted between the friction values or wear rates determined in the two test conditions of temperatures or speeds.

1. Nylon

Wear of the nylon materials containing various fillers was low and was due most likely to the high hardness of the nylon. Nylon which did not contain a lubricant filler was unsatisfactory. The nylon material with 40% molybdenum disulfide filler is preferred over nylon with 20% carbon-graphite (even though the friction is higher) because of the expected poor lubricating qualities of graphite in a space environment.

2. Polytetrafluoroethylene

Duroid 5813, polytetrafluoroethylene containing glass fiber reinforcement and molybdenum disulfide powder filler, exhibited low friction values and average wear. The polytetrafluoroethylene containing mica or glass cloth filler had significantly higher wear. Polytetrafluoroethylene can withstand higher temperatures than the other thermoplastic materials, and by use of optimum fillers may be useful in bearings at elevated temperatures.

3. Carbon-Graphite

The carbon-graphite blended materials impregnated with polytetrafluoroethylene exhibited the lowest friction and wear values. Unfortunately, additional tests indicated that the carbon-graphite materials do not have the necessary mechanical strength for ball bearing retainers. These materials will continue to be evaluated for lubrication in bearings but not as a structural member such as a ball bearing retainer.

4. Other Thermoplastic Materials

Polychlorotrifluoroethylene, polypropylene and chlorinated polyether exhibited excessive friction values because of the lack of a lubricant filler.

III. FRICTION AND WEAR STUDIES ON DRY POWDERS

A. Test Procedure For Dry Powders

The wear and friction characteristics of dry powders were evaluated by using them as lubricants between two rubbing specimens made of bearing steels. Prior work had shown that graphite and molybdenum disulfide powders provided effective lubrication between metal surfaces under certain dry conditions. If these presently used dry powders or new improved powders could lubricate effectively at high temperatures in an inert atmosphere, they could be used directly as lubricating powders or be incorporated in sintered or powdered metals to provide self-lubricating bearing components. These components would have the necessary mechanical strength as well as being thermally stable.

For the dry powders to provide lubrication of metal surfaces, the particles must adhere tenaciously to the metal surfaces and the particles must also slide or shear easily in the direction of motion. To evaluate the ability of the powders to lubricate, screening tests were conducted in the Hohman tester using the test procedure similar to that for the evaluation of the plastic materials. All powders were tested in a nitrogen atmosphere as lubricants between an M-10 tool steel rotating disk and an M-10 tool steel or BG 42 stainless steel test block at a sliding velocity of 230 ft./min. (640 rpm) and a load of three pounds (approximately 150 psi for a scar width of two mm). Tests were conducted at 1000°F and/or 160°F and were of 10 minutes duration under stabilized conditions.

The test powder was contained in a reservoir and was fed by gravity flow through a 1/8" O.D. tube to the area of contact of the disk and block. Continuous flow of the powder was obtained by using a solenoid operated agitator in the powder reservoir. The flow rate of powder was approximately .005 cc/minute. The test was of sufficient duration to determine the friction and lubricating characteristics of each material. In some cases, two minutes were required before the test readings became stable. Higher flow rates of powder provided an excess that would pack in the wedge formed by the disk and block and tend to produce erratic friction values.

B. Selection of Materials

The properties of approximately 200 compounds described in the literature or studied by previous investigators were reviewed and 35 of the most promising dry powders on the basis of melting point temperature, hardness and crystalline structure were selected for further study. Prior to test, calculations were made to find the amount of energy released in the hypothetical reactions of these 35 promising dry powders with iron, nickel and cobalt to determine the probability of forming a desirable reaction product on the metal surface. Of these promising materials, a group of 27 was selected for testing. These 27 materials are listed in Table III.

C. Test Results

Significant differences existed in the ability of the various powders to provide low friction and prevent high wear of the metal surfaces. The average wear and friction values for the powders evaluated are shown in Table III. The variations in friction during the test runs are shown by the curves in Figures 15 to 34. A comparison of the data is presented in the summary chart on Figure 35. Molybdenum disulfide, graphite, antimony trisulfide, tungsten diselenide, and molybdenum diselenide powders were found to be the best lubricants. All the five powders exhibited low wear except graphite at 1000°F and all exhibited low friction except graphite at 1000°F and antimony trisulfide at both temperatures. Each of these lubricants except graphite provided the same respective degree of lubrication for either combination of M-10 tool steel or BG 42 stainless steel rubbing against the M-10 disk under each test condition.

1. Molybdenum Disulfide

Molybdenum disulfide exhibited a range of friction values when used as a lubricant between the two rubbing metal surfaces at 160°F. It was noted that even without a continuous film between the metal surfaces, the coefficient of friction ranged between .03 and .09. Wear on the metal surface of the test block was in the form of a polished area rather than a scar area. Little difference was noted in performance of the powder at 1000°F or 160°F. Several tests were made in air at 1000°F and 160°F. At 1000°F, the coefficient of friction was .50 with a corresponding wear value of 1.0 mm. During these tests the delivery tube was not cooled and most of the MoS_2 had been converted to MoO_2. Tests at 160°F in air gave equivalent values to those tested in the nitrogen atmosphere at the same temperature. During all of the tests, the molybdenum disulfide powder had a greater tendency to pack in the reservoir and delivery tube than any of the other powders.

2. Carbon

The carbon was in the form of graphite powder and had similar friction and wear values when compared to MoS_2 at 160°F; but both higher friction and wear values when compared to MoS_2 at 1000°F. Even though graphite is known to cause higher values of friction and wear of rubbing metal surfaces in a dry environment, it was included in these tests as a comparison with the other powders. Graphite later was used as a lubricant in the sintered composites.

3. Antimony Trisulfide

Antimony trisulfide exhibited higher friction values with wear rates almost equivalent to MoS_2 under similar test conditions. The powder melted at 1000°F and formed an adherent silver colored film on the metal surfaces. It was found that an extremely small amount of powder, less than any of the other powders tested, provided adequate lubrication. Additional tests showed no difference in friction or wear values at 160°F whether the antimony trisulfide was used as a powder or as a coating on the test block. The antimony trisulfide later was used to impregnate porous cobalt alloy test blocks.

4. Tungsten Diselenide and Molybdenum Diselenide

These powders exhibited extremely low friction and wear values in the sliding tests in both the 160°F and 1000°F test runs. A thin tenacious film was formed on each of the rubbing surfaces which provided excellent lubrication under all conditions of test. The annealed WSe_2 powder exhibited slightly different friction values than the unannealed powder. The unannealed WSe_2 powder (Figure 30) was heated in an oven in an inert atmosphere to make the annealed WSe_2 powder by changing the structure from turbostratic to crystalline. The oxidation stability and melting point of WSe_2 are not clearly defined, but they appear to have better properties than those of MoS_2.

5. Silver Iodide

Silver iodide exhibited low wear but rather high friction values in the 1000°F and 160°F test runs. At 1000°F, the silver iodide melted and etched the tool steel but not the stainless steel test block.

were tested in a nitrogen atmosphere as lubricants between an M-10 tool steel rotating disk and an M-10 tool steel or BG 42 stainless steel test block at a sliding velocity of 230 ft./min. (640 rpm) and a load of three pounds (approximately 150 psi for a scar width of two mm). Tests were conducted at 1000°F and/or 160°F and were of 10 minutes duration under stabilized conditions.

The test powder was contained in a reservoir and was fed by gravity flow through a 1/8" O.D. tube to the area of contact of the disk and block. Continuous flow of the powder was obtained by using a solenoid operated agitator in the powder reservoir. The flow rate of powder was approximately .005 cc/minute. The test was of sufficient duration to determine the friction and lubricating characteristics of each material. In some cases, two minutes were required before the test readings became stable. Higher flow rates of powder provided an excess that would pack in the wedge formed by the disk and block and tend to produce erratic friction values.

B. Selection of Materials

The properties of approximately 200 compounds described in the literature or studied by previous investigators were reviewed and 35 of the most promising dry powders on the basis of melting point temperature, hardness and crystalline structure were selected for further study. Prior to test, calculations were made to find the amount of energy released in the hypothetical reactions of these 35 promising dry powders with iron, nickel and cobalt to determine the probability of forming a desirable reaction product on the metal surface. Of these promising materials, a group of 27 was selected for testing. These 27 materials are listed in Table III.

C. Test Results

Significant differences existed in the ability of the various powders to provide low friction and prevent high wear of the metal surfaces. The average wear and friction values for the powders evaluated are shown in Table III. The variations in friction during the test runs are shown by the curves in Figures 15 to 34. A comparison of the data is presented in the summary chart on Figure 35. Molybdenum disulfide, graphite, antimony trisulfide, tungsten diselenide, and molybdenum diselenide powders were found to be the best lubricants. All the five powders exhibited low wear except graphite at 1000°F and all exhibited low friction except graphite at 1000°F and antimony trisulfide at both temperatures. Each of these lubricants except graphite provided the same respective degree of lubrication for either combination of M-10 tool steel or BG 42 stainless steel rubbing against the M-10 disk under each test condition.

6. Miscellaneous Powders

Many of the other compounds exhibited fair wear characteristics but excessively high friction characteristics when used to lubricate the rubbing metal surfaces. Materials such as boron nitride, potassium titanate, and rubidium diantimonide exhibited both poor wear and friction characteristics at the 1000°F test runs.

D. Crystal Structures

The symbols and nomenclature of the dry powder crystal structures used in this discussion and Table III are described in W. B. Pearson's book, "A Handbook of Lattice Spacings and Structures of Metals and Alloys".

Graphite is composed of parallel sheets of closely grouped carbon atoms. The distance between the sheets is rather large as a result of weak bonding forces. One theory of graphite lubrication based on experiments dealing with intercalation compounds and the effect of vapors on lubricating properties, suggest that π electrons that are not used in the valence bonds between a carbon atom and its three close neighbors may also be involved in interplanar bonding. Such electrons can react with materials to form graphite intercalation compounds with grossly extended interplanar distances. Water vapor or certain other gaseous materials are required for graphite to be a lubricant. These materials react with graphite with a resultant lessening of interplanar bonding and lower shear resistance or abrasiveness of the graphite. Molybdenum disulfide does not suffer this disadvantage and will lubricate in a dry atmosphere. Molybdenum disulfide has a planar structure but all the electrons are accounted for in bonding. The structure perpendicular to the planes of sulfur atoms and parallel to the hexagonal c axis may be represented as shown in Figure 36.

Around each Mo atom is a trigonal prism of sulfur atoms resulting from the d^4sp hydridization completely filling the Mo d shell. The Mo atoms are stacked in the sequence AB AB or the hexagonal sequence. Each sulfur plane is in closest packing (i.e., each sulfur is surrounded by six sulfur neighbors in the plane; only two sulfur neighbors are shown on the figure).

A few other materials have the MoS_2 C7 structure - $MoSe_2$, $MoTe_2$, WS_2, WSe_2 and all should have good lubricating properties. Several of these materials made by the Chemical Department of the Westinghouse Research Laboratories as part of another development program were tested in Phase I. $MoSe_2$ and WSe_2 were shown to have superior lubricating properties to MoS_2, heretofore the best performing solid lubricant. Since the lubrication results are, in fact, identical for $MoSe_2$ and WSe_2 it appears that the improvement comes about as a result of the substitution of Se for S rather than as a result of the tungsten substitution.

When WSe_2 and $MoSe_2$ are formed at low temperatures (700°C) an irregular structure results. The x-ray patterns of these materials show sharp hk0 and 001 lines, but extremely diffuse hkl reflections. This indicates well ordered planes stacked in a parallel manner above one another, but in which there was otherwise little order between one plane and the next. The effect is that of a spilled deck of cards. The extreme case of this type of disorder is the turbostratic structure, typical of low temperature carbons where hkl lines are completely absent. A less extreme situation would be a large concentration of stacking faults where both hexagonal AB AB and rhombohedral ABC ABC stacking co-exist. More refined measurements would be needed to completely clarify the state of disorder. When tungsten diselenide is annealed at 1200°C ordering of the crystal lattice of the normal C7 structure results as indicated by sharp x-ray lines. The ordered material viewed under the microscope could be seen to be made of typical plate-like hexagons while the disordered material is amorphous to columnar.

These materials have comparable stability limits to MoS_2 which melts at 1185°C. WS_2 is reported to decompose at 1250°C and WSe_2 was found to be stable to at least 1200°C. WSe_2 is reasonably stable in vacuum as evidenced by the lack of a mirror deposit from a sample heated at 520°C for 5 minutes in a vacuum of 1×10^{-6} mm Hg. Platinium and nickel telluride, $PtTe_2$ and $NiTe_2$, (CdI_2 structure) were tested and found to be poor lubricants. This is in spite of the fact that a double Van der Waal's layer is present in these crystal structures. The stacking arrangement is shown in Figure 36. The non-metal double layers across which Van der Waal's forces, which are operative, are identical to the MoS_2 case. There are, however, two differences between the CdI_2, C6 structure and the MoS_2, C7 structure. The metal is octahedral coordinated in the C6 case and surrounded by a trigonal prism in the C7 case. The stacking sequence of metals is A-A-A in the C6 case and A-B-A in the C7 case.

The $NbSe_2$ structure was originally expected to be of the C19 type in analogy to NbS_2. Instead it was found to be of the C27 type analogous to TaS_2 B structure. The parameters for the hexagonal cell were found to be a = 3.443 A° and c = 12.54 A°. Here the stacking of the metals are AB AB like MoS_2, but the coordination of the metal is octahedral like CdI_2. Since the material was found to be a good lubricant, the conclusion is that coordination of the metal is unimportant but that the A-A-A chain-like stacking of metals is unfavorable to lubrication.

A new class of lubricants of the type GaTe have been found. Their properties are explainable in the same terms. Included in this class are GaSe, GaS, InSe, and InS. In GaTe the net +2 charge per Ga comes through a $(Ga - Ga)^{+4}$ single bond. The structure is believed to be related to the MoS_2 type with each Mo being replaced by a Ga - Ga pair directed along the c axis.

IV. FRICTION AND WEAR STUDIES ON COMPOSITES AND ALLOYS

A. Test Procedure

Self-lubricating materials other than plastics must be considered for ball bearing retainers when the operating temperatures in the space environment exceed 500 F. As part of Phase I therefore, screening tests were made on various material composites and selected alloys to determine their wear and friction characteristics when sliding on bearing steels. The tests were conducted in a Hohman tester using the same test procedure as that for the evaluation of the plastic materials, except for the test temperature. Most of the tests were made at a sliding velocity of 230 ft./min. (640 rpm) with approximately 70% of the tests being repeated at a sliding velocity of 460 ft./min (1280 rpm). A temperature of 1000 F was selected for all runs for two reasons: (1) the materials should be capable of operating, if only for short periods of time, at this elevated temperature, (2) the amount of moisture or water vapor be a minimum on or in the vicinity of the block surfaces. The dry nitrogen reduced formation of oxides and thus the wear debris formed during the test would be somewhat similar to that occurring in bearings at elevated temperatures in a space environment. It may be possible that a nitride was formed, minor difference in work hardness of the debris occurred, or a small amount of oxide was formed due to oxygen traces in the commercially obtained liquid nitrogen used to provide N_2 gas. The flow rate of nitrogen through the Hohman tester was two liters per minute. The amount of oxygen contained in 120 liters of nitrogen during the one hour test run was approximately 0.001 liter. Since these were screening tests, only the bulk effect of friction and wear properties was being determined for selection of materials to be evaluated in ball bearings in the space chamber.

B. Selection of Materials

Many composites were made using various powdered lubricants and powdered metals. The lubricants used were carbon-graphite, antimony trisulfide, iron sulfide, zirconium chloride and zinc sulfide. The powdered metals used were iron, nickel, stainless steel, and cobalt alloys. A ceramic material, zirconium boride, was also included in this test series.

Some of the composites were impossible to make and others were made with extreme difficulty. Composites made by various organizations, and shown in the following list, were not successful because of cracking or formation of gas in the specimens. The specimens were pressed green at various pressures and then partially sintered at different temperatures for various periods of time. Some were coined, others were not.

Lubricant	(% By Vol.)	Metal	(% By Vol.)
Sb_2S_3	20	Fe	80
Sb_2S_3	10	Fe	90
FeS	20	Ni	80
SrCl	10	Fe	90
ZnS	20	Ni	80
C	40	Fe-Cr Alloy (Type 304)	60
C	20	Fe-Cr Alloy (Type 304)	80
C	10	Co Alloy (Stellite 31)	90
C	15	Co Alloy (Stellite 31)	85
C	30	Co Alloy (Stellite 31)	70
None		CrCo Alloy (Rexalloy 33)	100
C	35	CrCo Alloy (Rexalloy 33)	65
CdS	16	FeCr Alloy (Type 316)	84
CdFl	16	FeCr Alloy (Type 316)	84

The composites which were successfully made by various organizations for test are listed in Table IV. The list also includes the sintered, wrought and cast alloys which were evaluated and compared to the composite materials. Both 3/8" diameter x 1" long and 2" diameter by 2" long cylinders were made. The Ford materials contained a small percent of calcium-silicide additions to decrease the surface tension of the liquid metal and improve the wetting of graphite.

Cylinders of varying porosities (54% to 87% of theoretical density) were made using Stellite alloy No. 1 powder. These materials were pressed at various pressures into green specimens and sintered successfully using large size particles and a modified processing technique.

C. Test Results

The wear and friction characteristics determined for the various composite and alloy materials rubbing against M-10 tool steel or Lesco BG42 stainless steel are listed in Table V. The variations in the friction values during the test runs are shown on Figures 37 to 60. A comparison of the wear and friction characteristics of the composites and alloys are shown in the summary chart, Figure 61.

1. Iron Composites

The iron-graphite composites exhibited a range of coefficients of friction that varied with the iron and carbon content and speed. At a sliding velocity of 460 ft./min. the friction value was lower than that at 230 ft./min. No apparent explanation is available because only the iron-graphite composites and Fe-Mo-Co (Clevite 300HT) exhibited a significant difference in friction when evaluated at two different sliding velocities. In general, the friction force was lowest when the iron-graphite composite contained 40 to 60% graphite by volume. The iron composite materials did not exhibit constant friction values during the 60 minute tests. No conclusive correlation could be made between the variation of friction and of wear. Clevite 300HT, primarily intended for use in an oxygen atmosphere, exhibited friction values at 460 ft./min. and wear values at both 460 ft./min. and 230 ft./min., in the same range as those of the iron-graphite composites.

2. Nickel Materials

The friction values of nickel-graphite composites varied more with a change in graphite content than did the iron-graphite materials. Both the plain and coined 30% nickel - 70% graphite composites along with the coined 20% nickel - 80% graphite composite exhibited friction values consistently below .08. After a few minutes run in, friction was steady indicating continuous lubrication for the remainder of the test. This includes tests which were conducted at a temperature of 160°F. Wear for the three best nickel-graphite composites was rather high but comparable to some of the iron-graphite composites. As the nickel content increased, a corresponding increase was noted in the rubbing friction value.

The addition of other materials such as zirconium chloride or zinc sulfide to the nickel powders was attempted even though these materials were unstable or reactive with the nickel at the high coining temperature. ZrCl was chosen because it had been used as a powder lubricant at temperatures below 300°C. ZnS was selected because of the low hardness of the Zn and the possible lubricating film obtained from the sulfide, similar to the film formed in extreme pressure fluid lubrication.

Friction tests showed that the composites made with ZnS or ZrCl adversely affected the coefficient of friction and also produced high wear. Analysis of the test specimens using x-ray diffraction revealed that the Ni-ZrCl composite contained 5 to 10% ZrO_2. The Ni-ZnS_2 composite contained 5 to 10% ZnS_2. Trace amounts of unknown compounds were also found which must have resulted from a reaction of the composite and the container used in melting the sample in the furnace.

Pure nickel and two nickel alloys, Inconel X (Ni-Cr alloy with aluminum and titanium used for precipitation hardening) and Nicrotung, were evaluated for frictional and wear characteristics and compared to the nickel composites. A coefficient of friction of .70 was obtained when the Inconel X block was tested rubbing against the M-10 disk. The friction value of Nicrotung was .32 and was similar to that of pure nickel. Wear of the nickel and the nickel alloys was comparable to wear of the best composites of nickel-graphite.

Several of the nickel-graphite composites were tested at 160°F for a comparison with results at 1000°F. Friction was observed to be similar at a sliding velocity of 230 ft./min. for composites shown in Figures 44a, 45a and b and 46a and b. However, wear was significantly reduced to general values between 4.0 and 5.5 mm, a significant reduction when compared to the same materials tested at 1000°F.

3. Cobalt Materials

Although cobalt composites containing graphite were difficult to produce, separate test specimens of 30%, 49% and 50% graphite were made along with other specimens containing 85 or 93% of zirconium boride. Cobalt sintered alloys with different porosities were made. Two of the sintered porous cobalt alloys after grinding to size were impregnated with antimony trisulfide. The results of all the cobalt block tests showed that the Co-alloy (317) impregnated with antimony trisulfide exhibited the lowest friction values and an equivalent wear value when compared to the other cobalt materials. The coefficient of friction of the Co-alloy 317 "as sintered" was twice that of the impregnated 317 material. Porosity of the "as sintered" materials had little effect on friction or wear. The 50% Co-50% Carbon composite, Figure 54, had the lowest friction and was equivalent in wear rate to the other cobalt composites. A similar composite 51% Co alloy 49% Carbon, Figure 54, made by a different technique had a high coefficient of friction but a similar wear rate. Wear of all the cobalt materials was similar and was lower than any of the other materials tested except the stainless alloys. The best cobalt-graphite composites had higher friction values than the best of the Ni-graphite composites (30% Ni - 70% C and 20% Ni - 80% C) and the Fe - C composites (tested at 230 ft./min.). The cobalt composites containing 80% or 90% of zirconium boride had a high coefficient of friction but low wear. The cobalt alloy, Stellite 31, Figure 56b had a higher friction value than any of the sintered alloys or sintered composites materials excepting sintered alloy 150-1 and the cobalt-zirconium boride composites.

4. Stainless Steels

A group of 84% Fe-Cr alloy 16% graphite Figure 57a, 58% Fe-Cr alloy - 42% potassium titanate composites, were made and compared to four Fe-Cr alloys, Lesco BG42, Lesco BF16, Lesco BG11, and type 304 stainless. The friction values for the steel-graphite composites were similar to that of the best stainless steel wrought alloy, BG42. The friction of the stainless steel-potassium titanate was extremely high. During storage after test, a whitish-yellow dust continued to exude from the test specimen. An analysis of the powder using x-ray diffraction techniques revealed the material to be elemental potassium. The friction and wear of BG42 in an Argon atmosphere was similar to the values obtained in a nitrogen atmosphere.

V. CONCLUSIONS

1. Solid dry materials were successfully evaluated for wear and friction characteristics in a dry nitrogen atmosphere under loads and sliding velocities simulating the conditions of retainer components or dry powder lubricants used in ball bearings for 2 to 7 HP electric hoist motors.

2. Of the thermoplastic and carbon materials evaluated, the polytetrafluoroethylene impregnated carbon-graphite and the polytetrafluoroethylene reinforced with glass fiber and filled with molybdenum disulfide powder exhibited the most satisfactory friction and wear characteristics. However, the impregnated carbon-graphite materials must be excluded from consideration as bearing retainer components in this program because of insufficient impact strength.

3. Molybdenum disulfide, molybdenum diselenide and tungsten diselenide powders exhibited satisfactory friction and wear characteristics when used to lubricate bearing steels sliding on each other. Graphite was also a satisfactory lubricant but exhibited higher wear than the three aforementioned powders at 1000°F. Metal surfaces lubricated with an antimony trisulfide exhibited low wear and friction characteristics when either the dry powder or the powder in the molten state or solidified state was used.

4. Many composites were found to have either desirable wear or friction characteristics but no one composite exhibited both low wear and low friction values. Of the iron, nickel cobalt or iron-chrome metal based composites a 40% iron - 60% carbon (carburized), a 20% nickel - 80% carbon (coined) and porous cobalt base alloy impregnated with antimony trisulfide show sufficient promise for further evaluation in Phase III bearing tests. A modified stainless steel alloy Lesco BG 42 shows sufficient merit to also be included in the bearing evaluation.

Prepared By P.H. Bowen

P.H. Bowen
Project Engineer

Supervised By E.S. Bober

E. S. Bober
Supervisory Engineer

Approved By Harry R. Sheppard

H. R. Sheppard, Mgr.
Chemical Appl. Sec.

TABLE I

DESCRIPTION OF PLASTICS

Curve Reference (Fig. No.)	Material	Trade Name	Supplier
2	Nylon - 40% MoS_2 filler	Nylasint M4	Polymer Corp. of Pennsylvania
3	Nylon - 20% C filler	Nylasint 2G	Polymer Corp. of Pennsylvania
4	Nylon	Nylatron GS	Polymer Corp. of Pennsylvania
5	Polytetrafluoroethylene with mica filler	Fluorosint	Polymer Corp. of Pennsylvania
6	Polytetrafluoroethylene with ceramic filler	Duroid 5613	Rogers Corporation
7	Polytetrafluoroethylene with glass fiber and MoS_2 filler	Duroid 5813	Rogers Corporation
8	Polytetrafluoroethylene with glass cloth filler	Armalon	E. I. DuPont de Nemours & Co. Fabrics & Finishes Department
9	Polychlorotrifluoroethylene	Halon TVS	Allied Chemical Corporation Plastics Coal & Chemicals Dept.
10	Carbon graphite (hard) with polytetrafluoroethylene impregnate	P5W (hard)	Purecarbon Company
11	Carbon graphite (med. soft) with polytetrafluoroethylene	P2W (med. soft)	Purecarbon Company
12	Polypropylene	Profax Type 6512	Hercules Powder Company Cellulose Products Department.
13	Chlorinated polyether	Penton Type 9215	Hercules Powder Company Cellulose Products Department

TABLE II

WEAR AND FRICTION CHARACTERISTICS OF PLASTICS IN A NITROGEN ATMOSPHERE

Plastics evaluated as test blocks rubbing against a rotating M-10 Tool Steel Disk

Curve Reference (Fig. No.)	Test Material	Hardness Shore D	Tests at 86°F Slide Vel. ft./min.	Tests at 86°F Avg. Coef. of Friction	Tests at 86°F Wear After 1 Hr. (mm)	Tests at 160°F Slide Vel. ft./min.	Tests at 160°F Avg. Coef. of Friction	Tests at 160°F Wear After 1 Hr. (mm)
2a	Nylon - 40% MoS_2 filler	79	460	.17	0.7	460	.17	0.7
2b	Nylon - 40% MoS_2 filler	79	230	.20	0.7	230	.20	0.7
3a	Nylon - 20% C filler	78	460	.08	0.7	460	.09	0.7
3b	Nylon - 20% C filler	78	230	.08	0.7	230	.08	0.7
4a	Nylon	83	460	>.60	Failed	460	>.60	Failed
4b	Nylon	83	230	>.60	Failed	230	>.60	Failed
5a	PTFE* - mica filler	75	460	.14	3.2	460	.17	4.6
5b	PTFE - mica filler	75	230	.11	3.0	230	.17	3.6
6a	PTFE - ceramic filler	74	460	.20	1.7	460	.14	1.8
6b	PTFE - ceramic filler	74	230	.19	1.3	230	.21	2.0
7a	PTFE - glass fiber and MoS_2 filler	74	460	.02	1.6	460	.03	1.5
7b	PTFE - glass fiber and MoS_2 filler	74	230	.03	1.5	230	.03	1.6
8a	PTFE - glass cloth filler	75	460	.39	2.9	460	.40	3.4
8b	PTFE - glass cloth filler	75	230	.50	3.0	230	.45	3.5
9a	PTFCE**	76	460	-	-	460	.60	8.0
9b	PTFCE	76	230	.56	7.3	230	-	-
10a	Carbon (hard) - PTFE impregnate	92	460	.03	1.0	460	.02	0.5
10b	Carbon (hard) - PTFE impregnate	92	230	.02	0.7	230	.02	0.9
11a	Carbon (med. soft) - PTFE impregnate	79	460	.03	1.3	460	.02	0.7
11b	Carbon (med. soft) - PTFE impregnate	79	230	.02	1.0	230	.02	0.9
12a	Polypropylene	80	460	>.60	Failed	460	>.60	Failed
12b	Polypropylene	80	230	>.60	Failed	230	>.60	Failed
13a	Chlorinated polyether	75	460	>.60	Failed	460	>.60	Failed
13b	Chlorinated polyether	75	230	>.60	Failed	230	>.60	Failed

*Polytetrafluoroethylene
**Polychlorotrifluoroethylene

TABLE III

WEAR AND FRICTION CHARACTERISTICS OF POWDERS IN A NITROGEN ATMOSPHERE

Powders used as lubricant between BG 42 or M-10 block rubbing on M-10 disk at sliding velocity of 230 feet per minute

Curve Reference (Fig. No.)	Test Powder	Powder Melting* Point (°C)	Crystal Structure	Test Temp. (°C)	Ave. Coef. of Friction	Ave. Wear** (mm)	Block Material
15a	MoS_2	1185	Hex. D_{6h}^4	1000	.05	P	M-10
15a	MoS_2	1185	Hex. D_{6h}^4	1000	.04	P	BG 42
15b	MoS_2	1185	Hex. D_{6h}^4	160	.03	P	M-10
15b	MoS_2	1185	Hex. D_{6h}^4	160	.03	P	BG 42
16a	Graphite	3652S	Hex. D_{6h}^4	1000	.10	0.5	BG 42
16b	Graphite	3652S	Hex. D_{6h}^4	160	.04	0.2	BG 42
17a	$CaSO_4$	685	Rhombic V_h^{17}	1000	.54	0.2P	M-10
17a	$CaSO_4$	685	Rhombic V_h^{17}	1000	.52	0.2P	BG 42
17b	$CaSO_4$	685	Rhombic V_h^{17}	160	.47	0.2P	BG 42
17b	$CaSO_4$	685	Rhombic V_h^{17}	160	.35	0.2P	M-10
18a	$RhSb_2$	-	Ortho D_{2h}^{16}	1000	.42	1.2	BG 42
18b	BN	3000S	Hex. D_{6h}^4	1000	.67	2.0	BG 42
19a	$PbCrO_4$	844	Monocl. D_{2h}^5	1000	.25	0.5	M-10
19a	$PbCrO_4$	844	Monocl. D_{2h}^5	1000	.31	0.6	BG 42
19b	$PbCrO_4$	844	Monocl. D_{2h}^5	160	.21	0.2P	M-10
19b	$PbCrO_4$	844	Monocl. D_{2h}^5	160	.21	0.2P	BG 42
20a	PbS	1120	Cubic D_h^5	1000	.28	0.2P	M-10
20a	PbS	1120	Cubic D_h^5	1000	.28	1.3+	BG 42
20b	PbS	1120	Cubic D_h^5	160	.37	0.2P	M-10
20b	PbS	1120	Cubic D_h^5	160	.42	0.5	BG 42
21a	Sb_2S_3	550	Rhombic D_{2h}^{16}	1000	.12	0.2P	M-10
21a	Sb_2S_3	550	Rhombic D_{2h}^{16}	1000	.10	0.2P	BG 42
21b	Sb_2S_3	550	Rhombic D_{2h}^{16}	160	.14	0.2P	M-10
21b	Sb_2S_3	550	Rhombic D_{2h}^{16}	160	.17	0.2P	BG 42

TABLE III (Continued)

Curve Reference (Fig. No.)	Test Powder	Powder Melting* Point (°C)	Crystal Structure	Test Temp. (°F)	Ave. Coef. of Friction	Ave. Wear** (mm)	Block Material
22a	$MgSO_4$	1124	Rhombic	1000	.5	0.2	M-10
22a	$MgSO_4$	1124	Rhombic	1000	.45	0.6	BG 42
22b	$MgSO_4$	1124	Rhombic	160	.31	0.2P	M-10
22b	$MgSO_4$	1124	Rhombic	160	.5	0.3	BG 42
23a	BaF_2	1280	Cubic O_h^5	1000	.53	1.1	M-10
23a	BaF_2	1280	Cubic O_h^5	1000	.50	0.9	BG 42
23b	BaF_2	1280	Cubic O_h^5	160	.25	0.6	M-10
23b	BaF_2	1280	Cubic O_h^5	160	.21	0.6	BG 42
24a	AgI	552d	Hex. C_{6V}^4	1000	.22	0.2P++	M-10
24a	AgI	552d	Hex. C_{6V}^4	1000	.19	0.2P++	BG 42
24b	AgI	552d	Hex. C_{6V}^4	160	.17	0.2P	M-10
24b	AgI	552d	Hex. C_{6V}^4	160	.42	0.2P+	BG 42
25a	AgBr	434	Cubic O_h^5	1000	.31	0.2P	BG 42
25b	$KTiO_3$	-		1000	.84	2.4	BG 42
26a	MnTe	500	Hex. D_{6h}^4	1000	.28	1.2	BG 42
26b	MnSe	700	Cubic O_h^5	1000	.31	1.7	BG 42
27a	$NiTe_2$	700	Hex. D_{3d}^3	1000	.20	1.4	BG 42
27b	$PtTe_2$	700	Hex. D_{3d}^3	1000	.47	0.7+++	BG 42
28a	$FeTe_2$	700	Ortho D_{2h}^{12}	1000	.31	1.3	BG 42
28b	GaTe	824	Hex.	1000	.21	0.2	BG 42
29a	$OsTe_2$	600	Cubic T_h^6	1000	.33	2.1	BG 42
29b	$CdCl_2$		Cubic	1000	.17	0.6+	BG 42
30a	WSe_2(519P)	1200	Hex. D_{6h}^4	1000	.03	P	M-10
30a	WSe_2(519P)	1200	Hex. D_{6h}^4	1000	.02	P	BG 42
30b	WSe_2(519P)	1200	Hex. D_{6h}^4	160	.02	P	M-10
30b	WSe_2(519P)	1200	Hex. D_{6h}^4	160	.03	P+	BG 42

TABLE III (Continued)

Curve Reference (Fig. No.)	Test Powder	Powder Melting Point (°C)	Crystal Structure	Test Temp.(°F)	Ave. Coef. of Friction	Ave. Wear** (mm)	Block Material
31a	GaTe(619P)	824	Hex.	1000	.13	P	M-10
31a	GaTe(619P)	824	Hex.	1000	.14	P	BG 42
31b	GaTe(619P)	824	Hex.	160	.35	P	M-10
31b	GaTe(619P)	824	Hex.	160	.13	P	BG 42
32a	$MoSe_2$(551Y)	1200	Hex. D^4_{6h}	1000	.03	P	M-10
32b	$MoSe_2$(551Y)	1200	Hex. D^4_{6h}	160	.02	P	M-10
33a	$NbSe_2$(547M) annealed	800	Hex.	1000	.07	0.2P	M-10
33b	$NbSe_2$(547M) annealed	800	Hex.	160	.06	P	M-10
34a	WSe_2(544J) annealed	1200	Hex. D^4_{6h}	1000	.04	P	M-10
34b	WSe_2(544J) annealed	1200	Hex. D^4_{6h}	160	.06	P	M-10

+Powder ceased to flow during test run
++Powder melted
+++Test ended after five minutes

*Letter "S" indicates material sublimes rather than melts
**Letter "P" indicates surface was polished rather than scarred

TABLE IV

DESCRIPTION OF COMPOSITES AND ALLOYS

Curve Reference (Fig. No.)	Material Compositions (% by Vol.)	Remarks	Supplier
37a	84 Fe - 16 C	Hot coined.	SKC Research Associates, Deva Metal Division
37b	70 Fe - 30 C	Hot coined	Westinghouse Elect. Corp. Materials Laboratories
38a	70 Fe - 30 C	Hot coined.	SKC Research Associates, Deva Metal Division
38b	65 Fe - 35 C	Contained $CaSi_2$, liquid phase sintered (LPS).	Ford Motor Company, Scientific Laboratory
39a	50 Fe - 50 C HT	Contained $CaSi_2$, LPS, heat treated.	Ford Motor Company, Scientific Laboratory
39b	50 Fe - 50 C	Contained $CaSi_2$, LPS.	Ford Motor Company, Scientific Laboratory
40a	40 Fe - 60 C HT	Contained $CaSi_2$, LPS, heat treated.	Ford Motor Company, Scientific Laboratory
40b	40 Fe - 60 C	Contained $CaSi_2$, LPS.	Ford Motor Company, Scientific Laboratory
41a	30 Fe - 70 C HT	Contained $CaSi_2$, LPS, heat treated.	Ford Motor Company, Scientific Laboratory
41b	30 Fe - 70 C	Contained $CaSi_2$, LPS.	Ford Motor Company, Scientific Laboratory
42a	68 Fe - 18 Mo - 18 Co HT	Sintered, density 7.9 to 8.1 g/cc.	Clevite Corporation, Cleveland Graphite Bronze
43a	65 Ni - 35 C	Hot coined.	Westinghouse Elect. Corp., Materials Laboratories
43b	60 Ni - 40 C	Contained $CaSi_2$, LPS.	Ford Motor Company, Scientific Laboratory
44a	50 Ni - 50 C C	Contained $CaSi_2$, LPS, hot coined.	Ford Motor Company, Scientific Laboratory
44b	50 Ni - 50 C	Contained $CaSi_2$, LPS.	Ford Motor Company, Scientific Laboratory
45a	40 Ni - 60 C C	Contained $CaSi_2$, LPS, hot coined.	Ford Motor Company, Scientific Laboratory
45b	40 Ni - 60 C	Contained $CaSi_2$, LPS.	Ford Motor Company, Scientific Laboratory
46a	30 Ni - 70 C C	Contained $CaSi_2$, LPS, hot coined.	Ford Motor Company, Scientific Laboratory
46b	30 Ni - 70 C	Contained $CaSi_2$, LPS.	Ford Motor Company, Scientific Laboratory

TABLE IV (Continued)

Curve Reference (Fig. No.)	Material Compositions (% by Vol.)	Remarks	Supplier
47a	20 Ni - 80 C C	Contained $CaSi_2$, LPS, hot coined.	Ford Motor Company, Scientific Laboratory
47b	20 Ni - 80 C	Contained $CaSi_2$, LPS.	Ford Motor Company, Scientific Laboratory
48a	81 Ni - 19 ZnS	Hot coined.	Westinghouse Elect. Corp., Materials Laboratories
48b	65 Ni - 35 ZnS	Hot coined.	Westinghouse Elect. Corp., Materials Laboratories
49a	74 Ni - 26 ZrCl	Hot coined.	Westinghouse Elect. Corp., Materials Laboratories
49b	Ni	Made by thermal decomposition of nickel carbonyl.	Budd Company
50a	71 Ni - 29 Cr Alloy	Inconel X, wrought, precipitation hardened.	Westinghouse Elect. Corp., Blairsville Plant
50b	61 Ni - 12 Cr Alloy	Nicrotung, wrought.	Westinghouse Elect. Corp., Blairsville Plant
51a	Co Alloy 313 Porous	Stellite sintered alloy No. 1. Porous-bulk density of 66.0% of theoretical.	Haynes Stellite, New Products Department
51b	Co Alloy 313 Porous Sb_2S_3	Test material 313 impregnated with Sb_2S_3	Haynes Stellite, New Products Department
52a	Co Alloy 150-1	Stellite powder alloy No. 1 cold pressed and sintered.	Haynes Stellite, New Products Department
52b	Co Alloy 317 Porous	Stellite sintered alloy No. 1. Porous-bulk density of 67.0% of theoretical.	Haynes Stellite, New Products Department
53a	Co Alloy 317 Porous + Sb_2S_3	Test material 317 impregnated with Sb_2S_3	Haynes Stellite, New Products Department
53b	70 Co Alloy - 30 C	Stellite alloy 31, hot coined.	Westinghouse Elect. Corp., Materials Laboratories
54a	51 Co Alloy - 49 C	Stellite alloy 31, hot coined.	Westinghouse Elect. Corp., Materials Laboratories
54b	50 Co Alloy - 50 C	Contained $CaSi_2$, LPS.	Ford Motor Company, Scientific Laboratory
55a	15 Co - 85 ZrBr	A ceramic material, using cobalt as the binder.	Westinghouse Elect. Corp., Materials Laboratories
55b	7 Co - 93 ZrBr	A ceramic material, using cobalt as the binder.	Westinghouse Elect. Corp., Materials Laboratories
56a	Co Alloy	Stellite alloy No. 31.	Haynes Stellite, New Products Department
56b	Co Alloy X	Experimental alloy containing Co - Cr - W.	Westinghouse Elect. Corp., Materials Laboratories

TABLE IV (Continued)

Curve Reference (Fig. No.)	Material Compositions (% by Vol.)	Remarks	Supplier
57a	60 Fe-Cr Alloy - 40 C	Stainless steel type 316, hot coined.	SKC Research Associates, Deva Metal Division
57b	58 Fe-Cr Alloy - 42 $KTiO_3$	Stainless steel type 316, hot coined.	SKC Research Associates, Deva Metal Division
58a	Fe-Cr Alloy BG16	Lesco BG16, modified SS type 44C - ref. WADC 65 material.	Latrobe Steel Company, Engineering Department
58b	Fe-Cr Alloy BG11	Lesco BG11, modified SAE D-2 steel.	Latrobe Steel Company, Engineering Department
59a	Fe-Cr Alloy BG42	Lesco BG42, modified 440 stainless steel.	Latrobe Steel Company, Engineering Department
60	Fe-Cr Alloy	Stainless steel type 3[illegible].	

TABLE V

WEAR AND FRICTION CHARACTERISTICS OF COMPOSITES AND ALLOYS IN A NITROGEN ATMOSPHERE

Materials evaluated as test blocks rubbing against a rotating M-10 tool steel disk for a one hour test period

Curve Reference (Fig. No.)	Material Compositions (% by Vol.)	Sliding Velocity (ft/min)	Ave. Coef. of Friction	Total Wear (mm)
37a	84 Fe - 16 C	460	.28	7.2
37a	84 Fe - 16 C	230	.32	7.4
37b	70 Fe - 30 C	460	.19	7.0
37b	70 Fe - 30 C	230	.23	6.6
38a	70 Fe - 30 C	460	.22	5.9
38a	70 Fe - 30 C	230	.24	6.0
38b	65 Fe - 35 C	460	.18	3.0
38b	65 Fe - 35 C	230	.21	2.8
39a	50 Fe - 50 C HT	460	.14	4.0
39a	50 Fe - 50 C HT	230	.20	3.6
39b	50 Fe - 50 C	460	.14	4.0
39b	50 Fe - 50 C	230	.17	3.6
40a	40 Fe - 60 C HT	460	.09	3.4
40a	40 Fe - 60 C HT	230	.18	3.7
40b	40 Fe - 60 C	460	.12	4.0
40b	40 Fe - 60 C	230	.20	3.7
41a	30 Fe - 70 C HT	460	.13	4.2
41a	30 Fe - 70 C HT	230	.28	4.0
41b	30 Fe - 70 C	460	.21	4.2
41b	30 Fe - 70 C	230	.25	3.9
42a	68 Fe - 18 Mo - 18 Co - HT*	460	.24	3.4
42a	68 Fe - 18 Mo - 18 Co - HT*	230	.44	2.9
42b	68 Fe - 18 Mo - 18 Co (in Argon)*	460	.20	2.8
42b	68 Fe - 18 Mo - 18 Co (in Argon)*	230	-	-
43a	65 Ni - 35 C	460	-	-
43a	65 Ni - 35 C	230	.33	10.2
43b	60 Ni - 40 C	460	.28	14.3
43b	60 Ni - 40 C	230	.30	15.8
44a	50 Ni - 50 C (C)	460	.25	10.0
44a	50 Ni - 50 C (C)	230	.25	11.0
44b	50 Ni - 50 C	460	.30	17.1
44b	50 Ni - 50 C	230	.28	15.2

TABLE V (Continued)

Curve Reference (Fig. No.)	Material Compositions (% by Vol.)	Sliding Velocity (ft/min)	Ave. Coef. of Friction	Total Wear (mm)
45a	40 Ni - 60 C (C)	460	.20	11.0
45a	40 Ni - 60 C (C)	230	.18	9.4
45b	40 Ni - 60 C	460	.23	14.1
45b	40 Ni - 60 C	230	.22	12.0
46a	30 Ni - 70 C (C)	460	.10	11.0
46a	30 Ni - 70 C (C)	230	.07	6.5
46b	30 Ni - 70 C	460	.12	9.0
46b	30 Ni - 70 C	230	.07	6.9
47a	20 Ni - 80 C C	460	.06	5.3
47a	20 Ni - 80 C C	230	.05	6.0
47b	20 Ni - 80 C	460	.07	6.1
47b	20 Ni - 80 C	230	.09	6.6
48a	81 Ni - 19 Zn S	460	.45	10.7
48a	81 Ni - 19 Zn S	230	-	-
48b	65 Ni - 35 Zn S	460	.42	9.6
48b	65 Ni - 35 Zn S	230	-	-
49a	74 Ni - 26 Zr Cl	460	.42	10.2
49a	74 Ni - 26 Zr Cl	230	-	-
49b	Ni**	460	.31	2.6
49b	Ni**	230	-	-
50a	76 Ni - 15 Cr Alloy*	460	.70	5.1
50a	76 Ni - 15 Cr Alloy*	230	-	-
50b	61 Ni - 12 Cr Alloy*	460	.27	4.0
50b	61 Ni - 12 Cr Alloy*	230	.31	3.4
51a	Co Alloy 313 - Porous	460	-	-
51a	Co Alloy 313 - Porous	230	.34	2.9
51b	Co Alloy 313 - Porous Sb_2S_3 Coating	460	-	-
51b	Co Alloy 313 - Porous Sb_2S_3 Coating	230	.28	3.0
52a	Co Alloy 150 C - Porous	460	-	-
52a	Co Alloy 150 C - Porous	230	.46	2.4
52b	Co Alloy 317 - Porous	460	-	-
52b	Co Alloy 317 - Porous	230	.38	2.1
53a	Co Alloy 317 - Porous Sb_2S_3 Coating	460	-	-
53a	Co Alloy 317 - Porous Sb_2S_3 Coating	230	.15	2.1
53b	70 Co Alloy - 30 C	460	.28	2.5
53b	70 Co Alloy - 30 C	230	.28	3.3

TABLE V (Continued)

Curve Reference (Fig. No.)	Material Compositions (% by Vol.)	Sliding Velocity (ft/min)	Ave. Coef. of Friction	Total Wear (mm)
54a	51 Co Alloy - 49 C	460	.30	2.8
54a	51 Co Alloy - 49 C	230	-	-
54b	50 Co Alloy - 50 C	460	.22	2.2
54b	50 Co Alloy - 50 C	230	.22	2.5
55a	15 Co - 85 ZrBr	460	-	-
55a	15 Co - 85 ZrBr	230	.48	1.2
55b	7 Co - 93 ZrBr	460	-	-
55b	7 Co - 93 ZrBr	230	.49	1.6
56a	Co Alloy**	460	.37	2.9
56a	Co Alloy**	230	.38	2.7
56b	Co Alloy*	460	.38	1.9
56b	Co Alloy*	230	.39	1.9
57a	60 Fe-Cr Alloy - 40 C	460	.21	5.1
57a	60 Fe-Cr Alloy - 40 C	230	.23	4.6
57b	58 Fe-Cr Alloy - 42 $KTiO_3$	460	-	-
57b	58 Fe-Cr Alloy - 42 $KTiO_3$	230	.31	2.7
58a	Fe-Cr Alloy BG16**	460	.39	1.7
58a	Fe-Cr Alloy BG16**	230	.44	1.7
58b	Fe-Cr Alloy BG11**	460	.31	5.1
58b	Fe-Cr Alloy BG11**	230	.27	4.2
59a	Fe-Cr Alloy BG42**	460	.23	1.5
59a	Fe-Cr Alloy BG42**	230	.28	1.2
59b	Fe-Cr Alloy BG42** (Argon)	460	.24	2.3
59b	Fe-Cr Alloy BG42** (Argon)	230	.21	1.5
60a	Fe-Cr Alloy (Type 304)**	460	.7 - 1.0	7.7

*Composition on a % by wt. basis
**Deposited, cast or wrought alloy

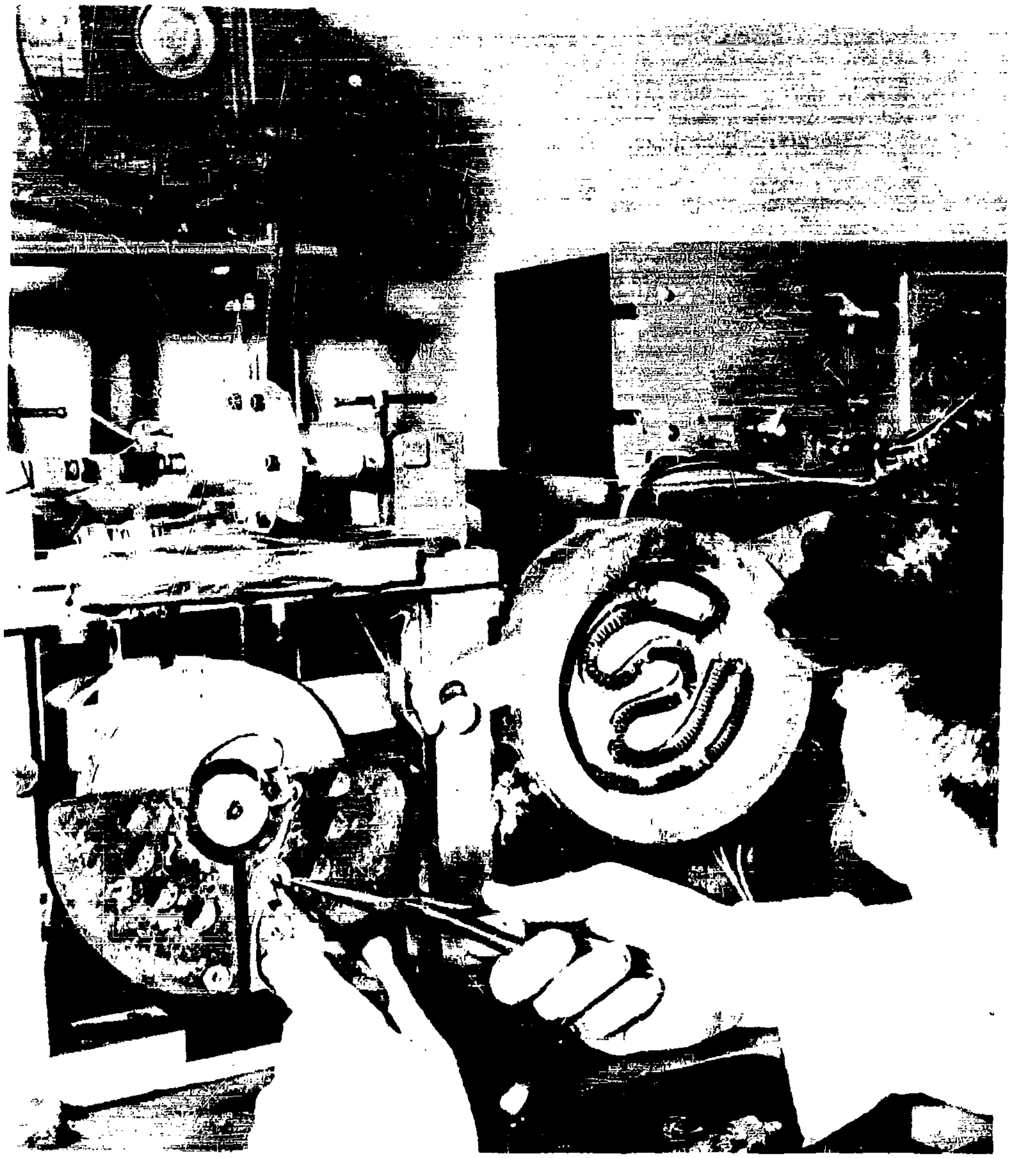

FIGURE 1

CLOSE UP OF WEAR AND FRICTION TESTER USED
TO EVALUATE DRY MATERIALS

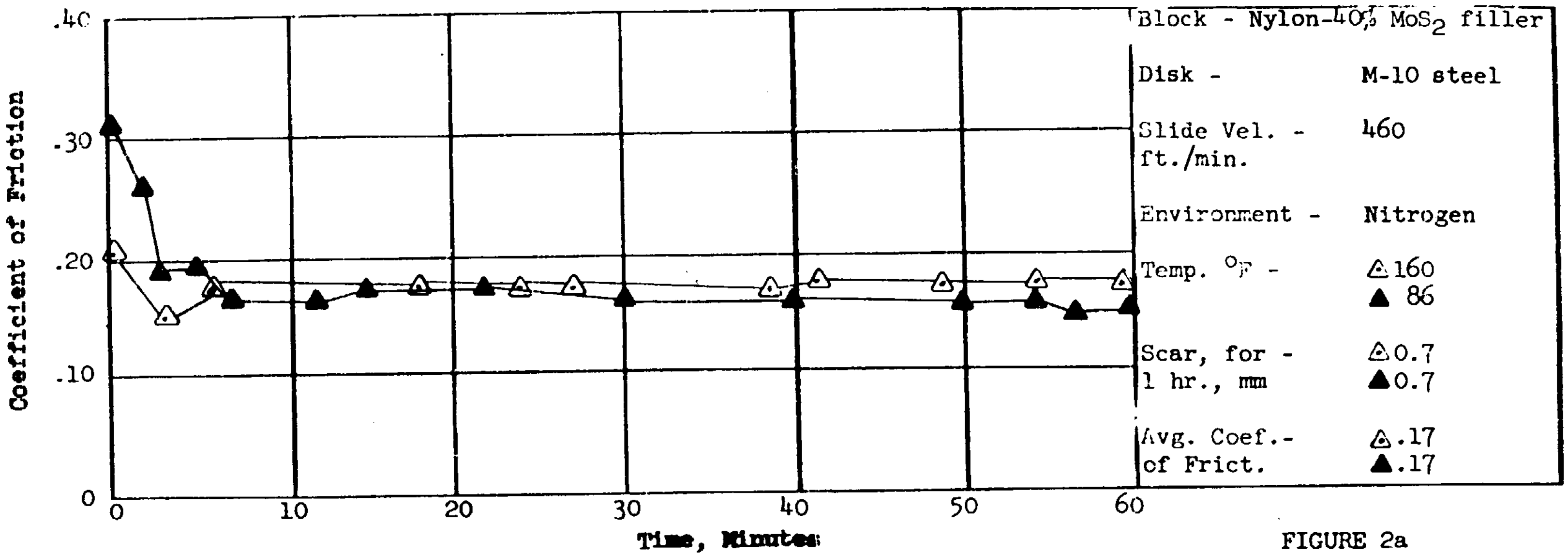

FIGURE 2a

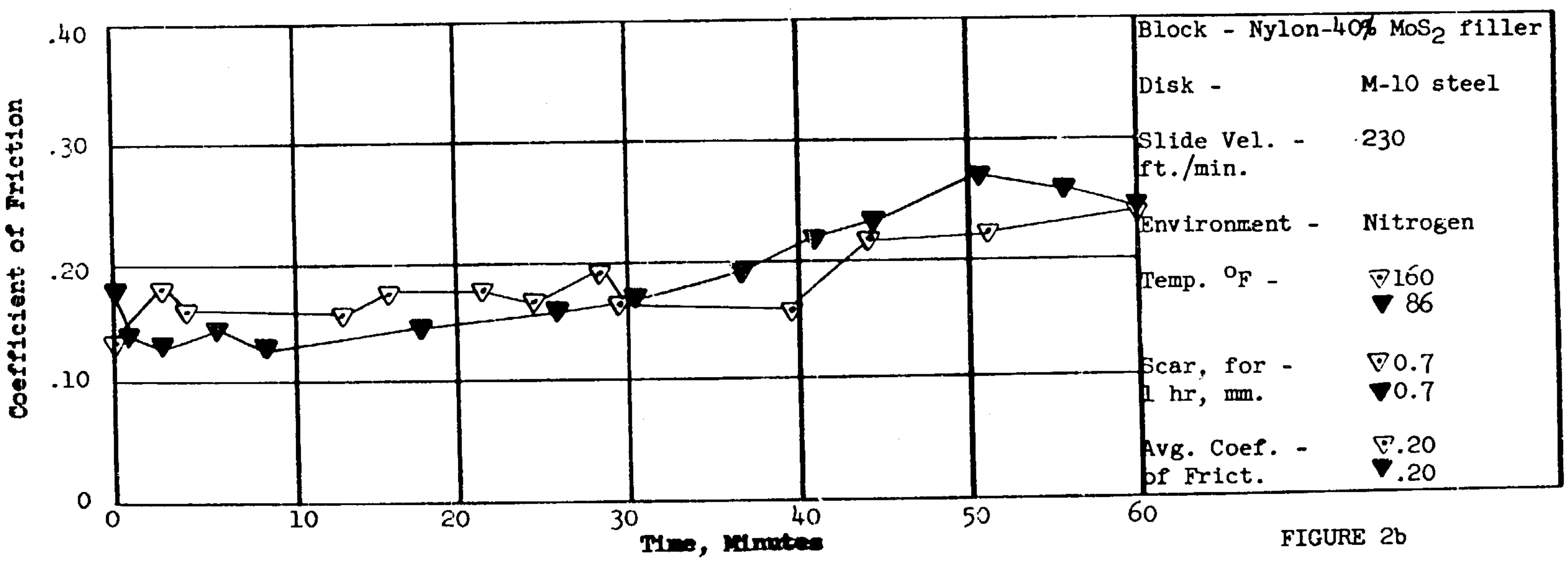

FIGURE 2b

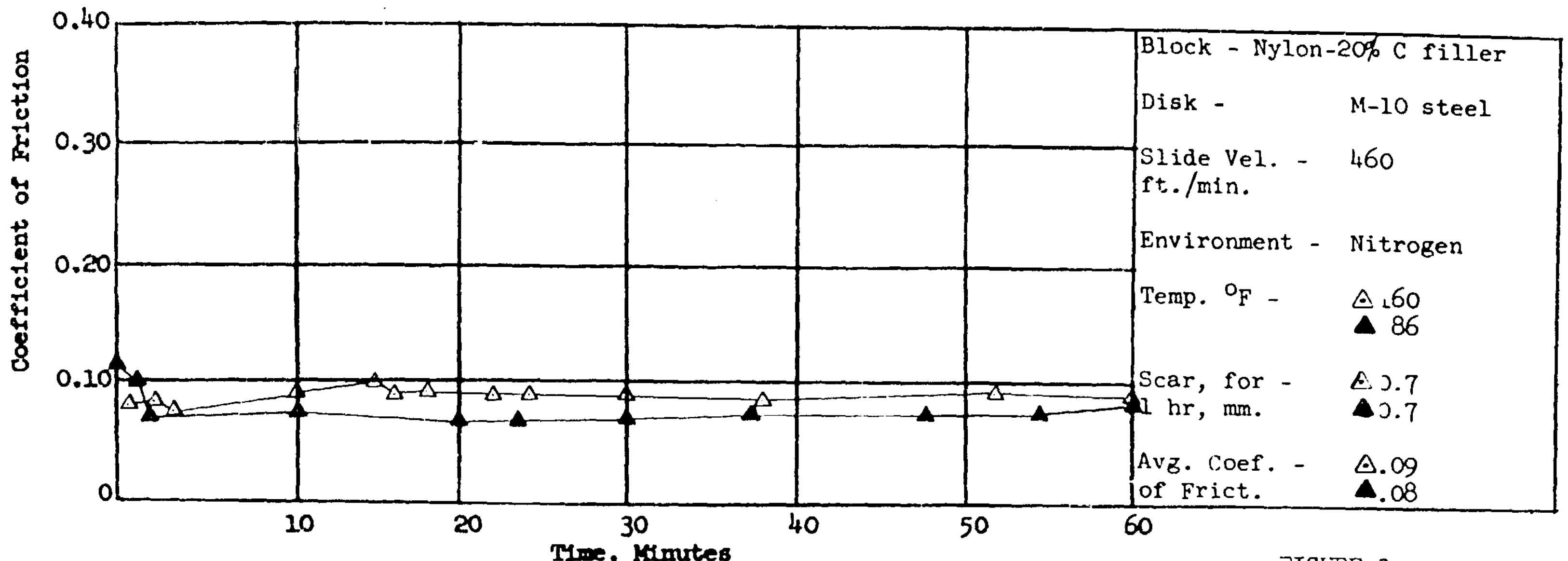

FIGURE 3a

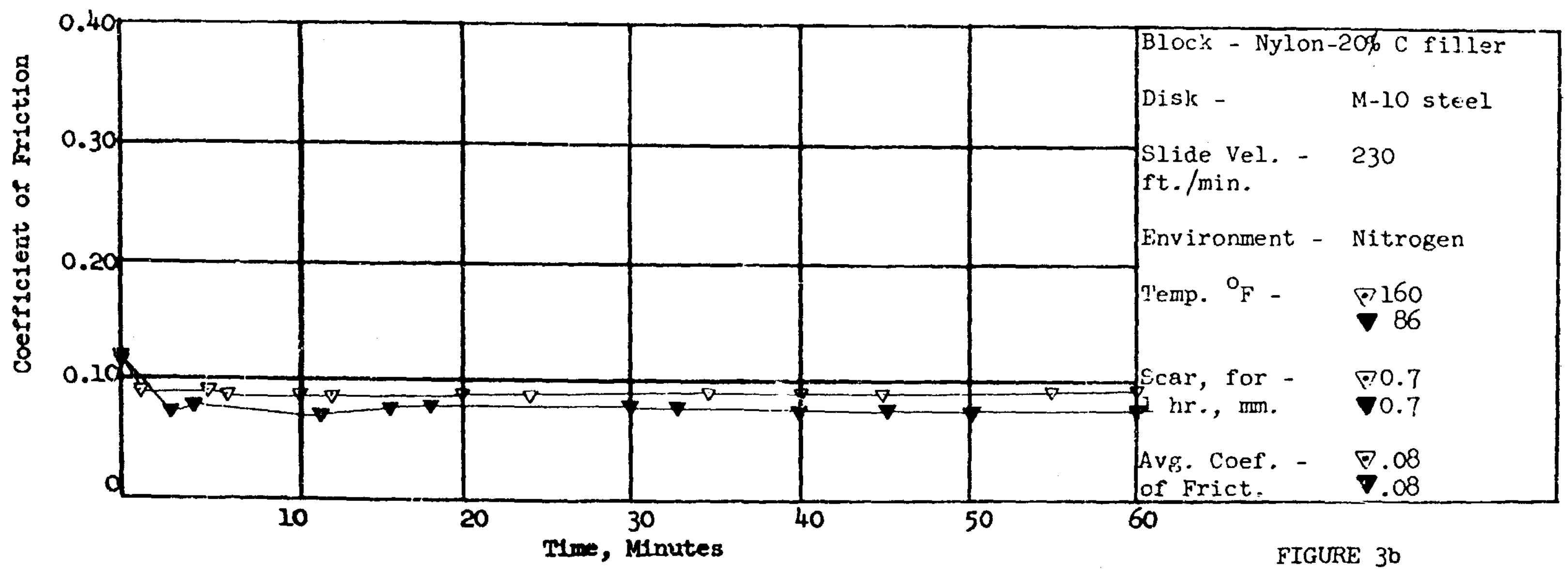

FIGURE 3b

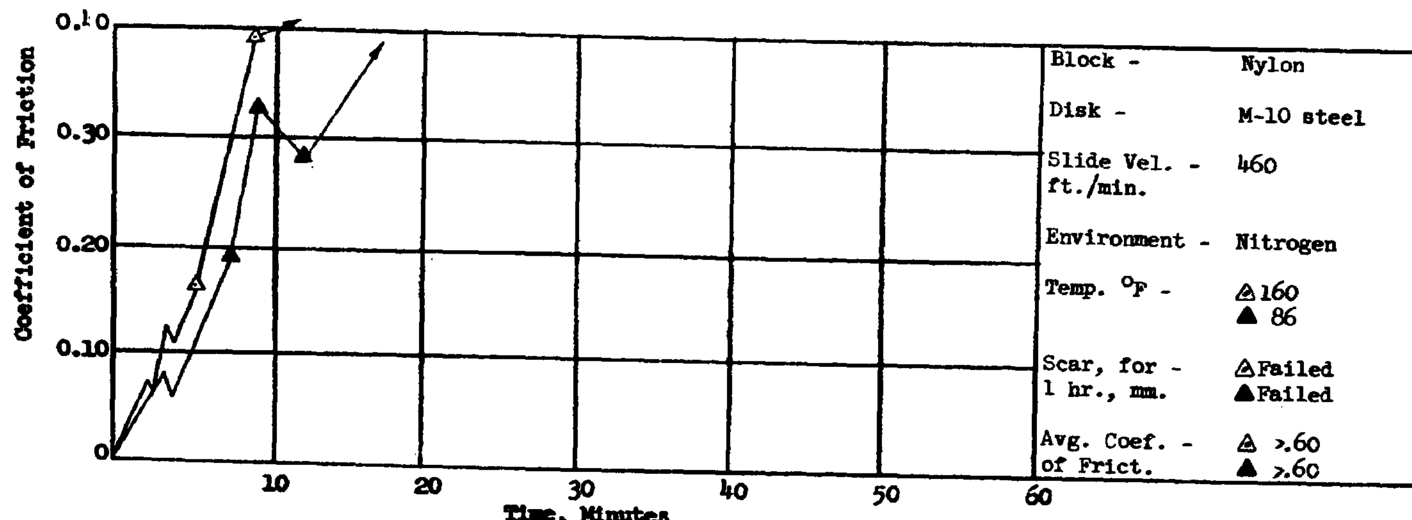

FIGURE 4a

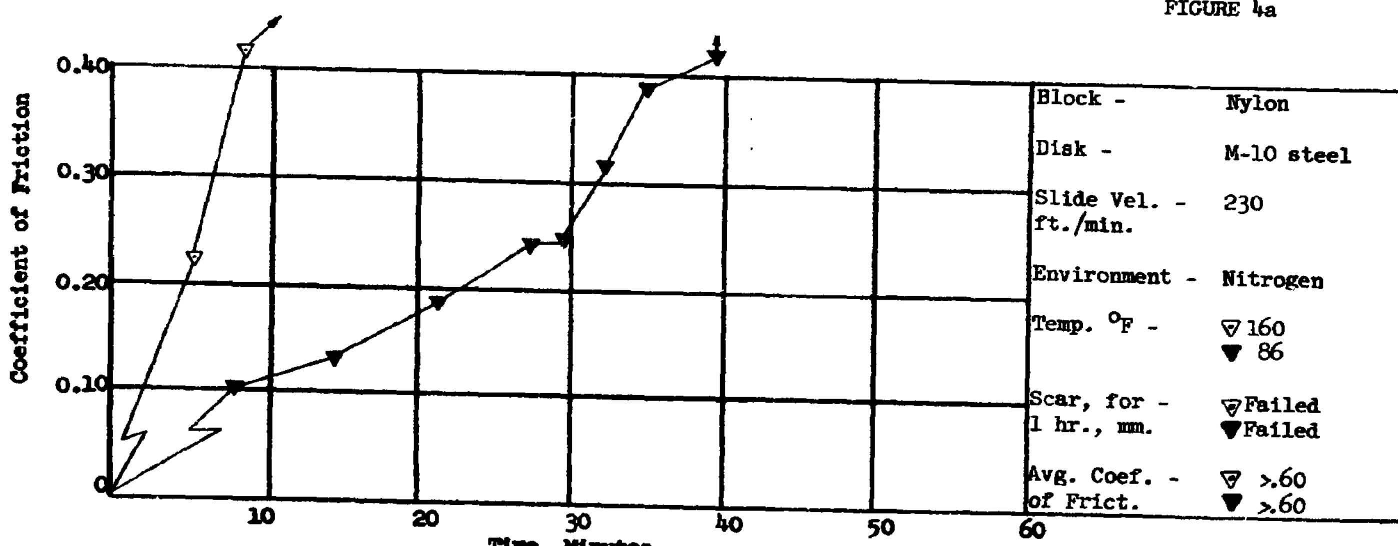

FIGURE 4b

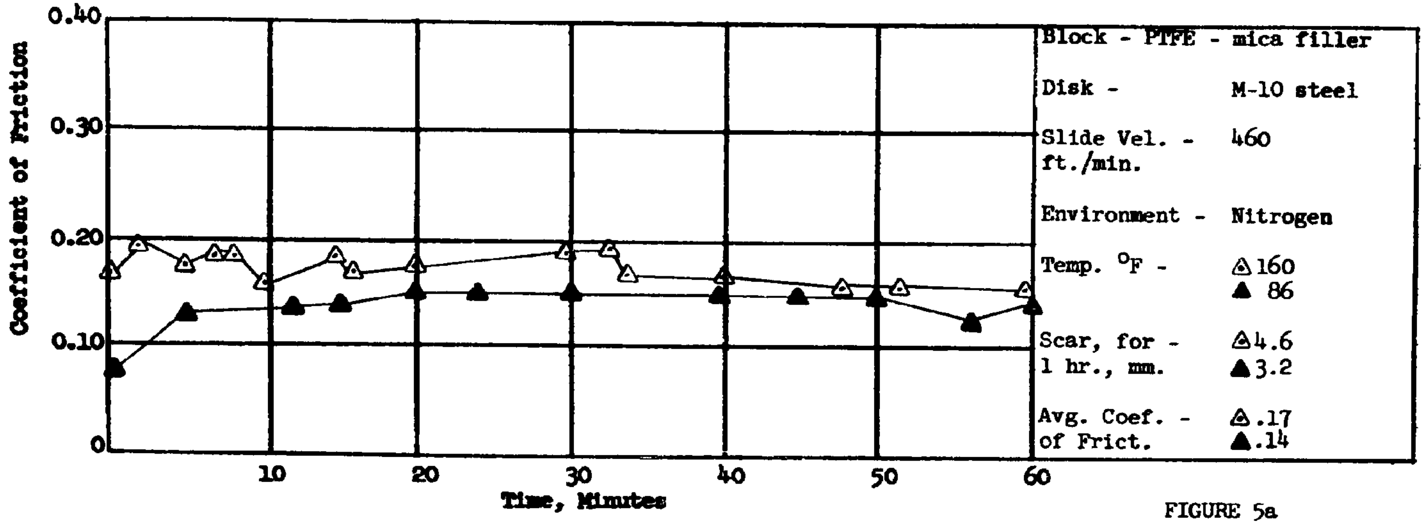

FIGURE 5a

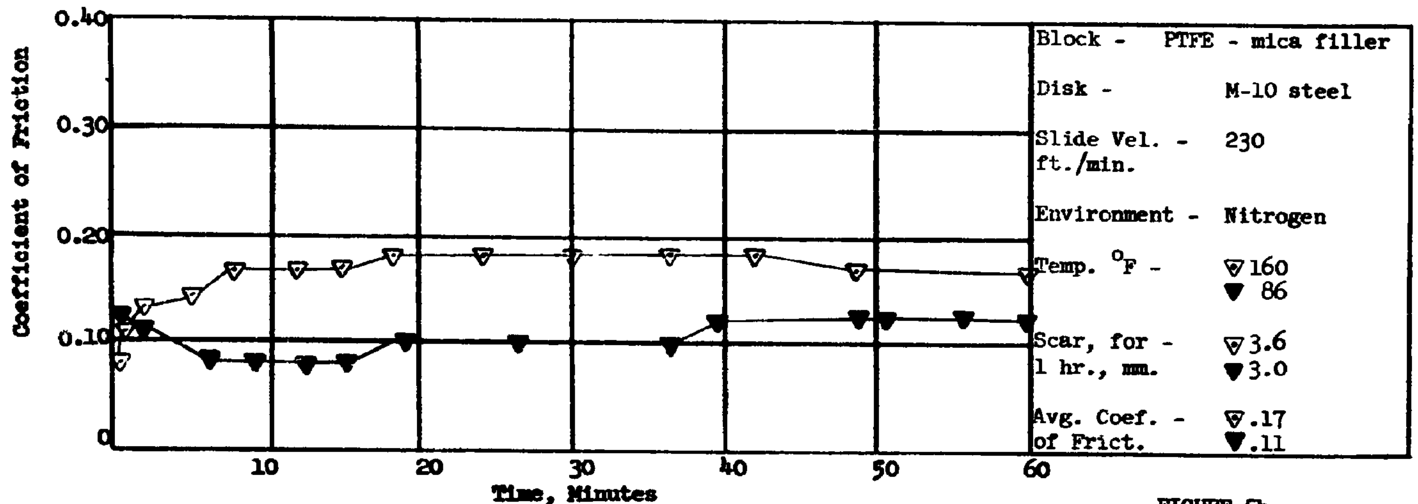

FIGURE 5b

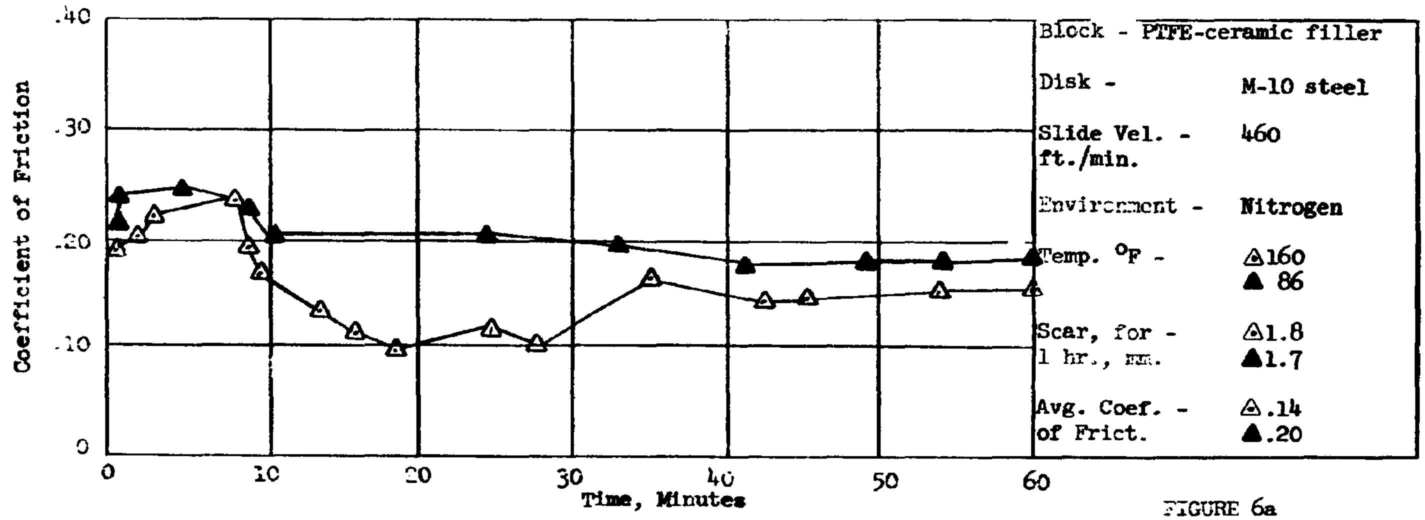

FIGURE 6a

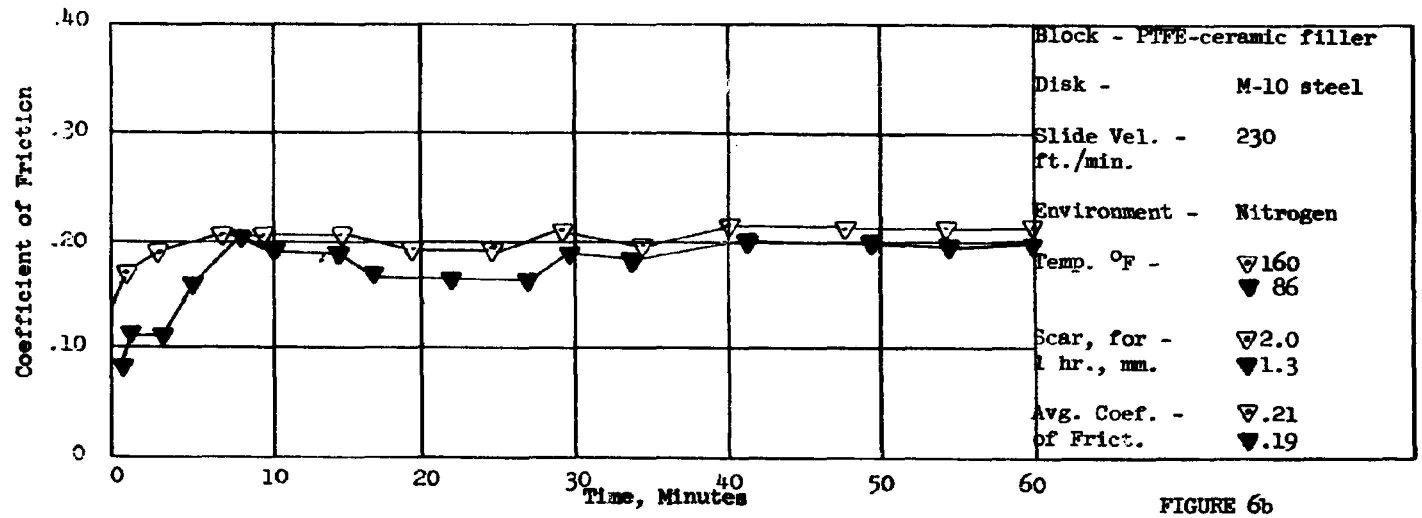

FIGURE 6b

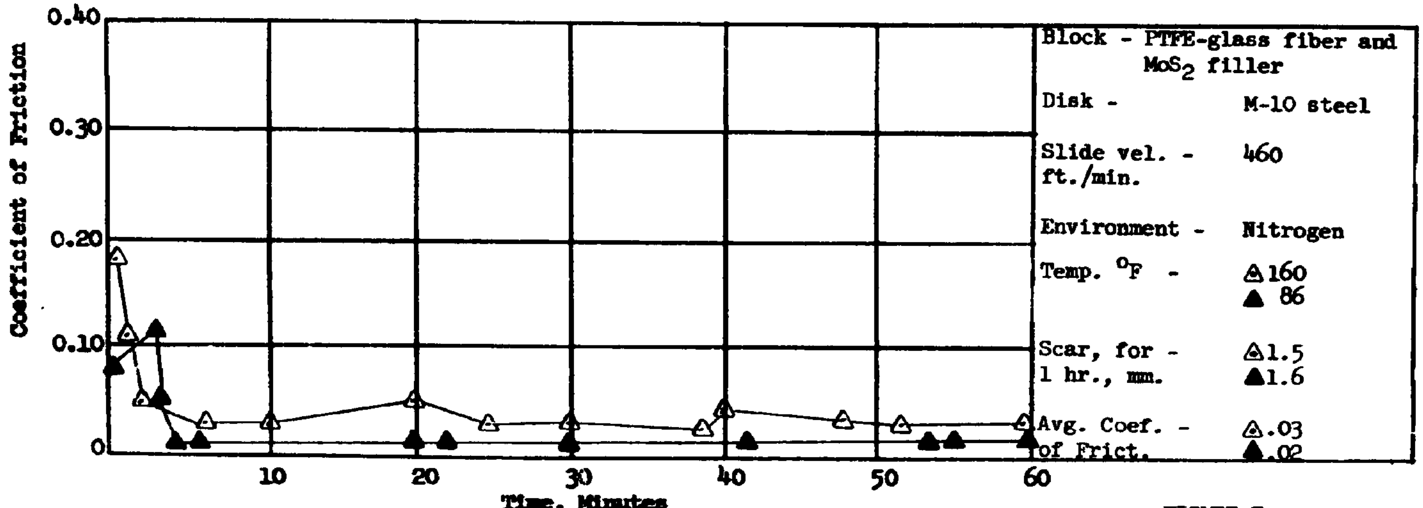

FIGURE 7a

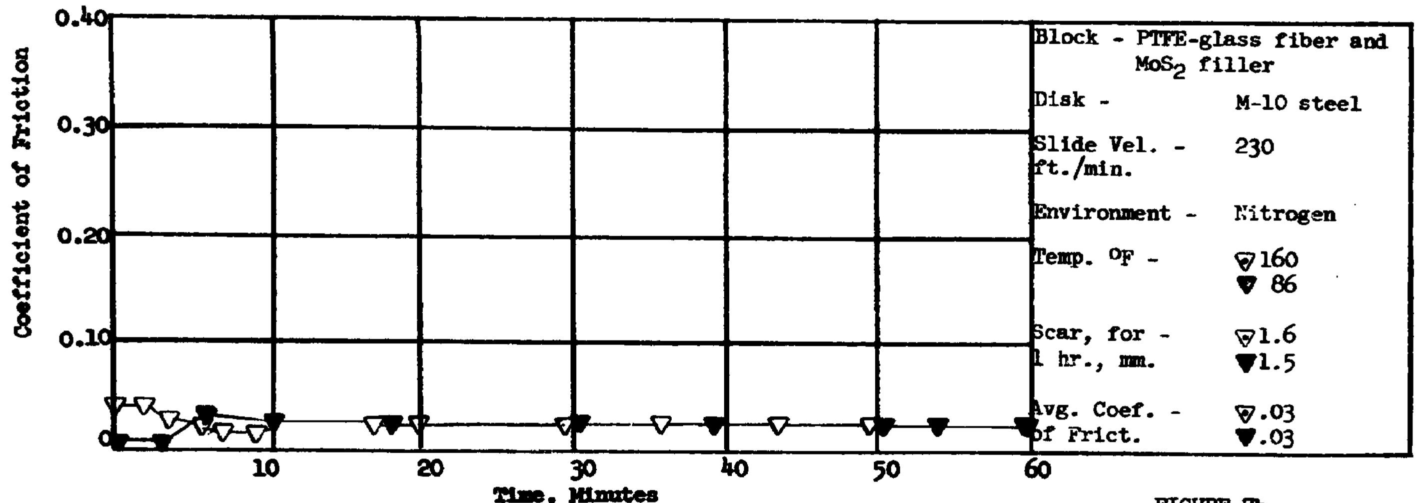

FIGURE 7b

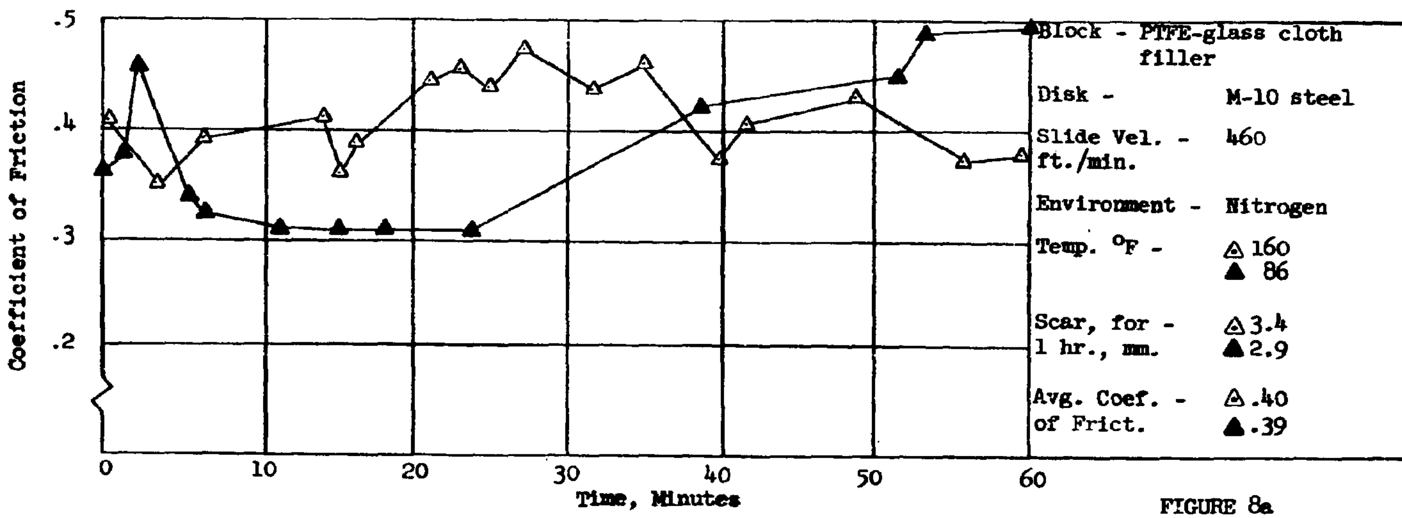

FIGURE 8a

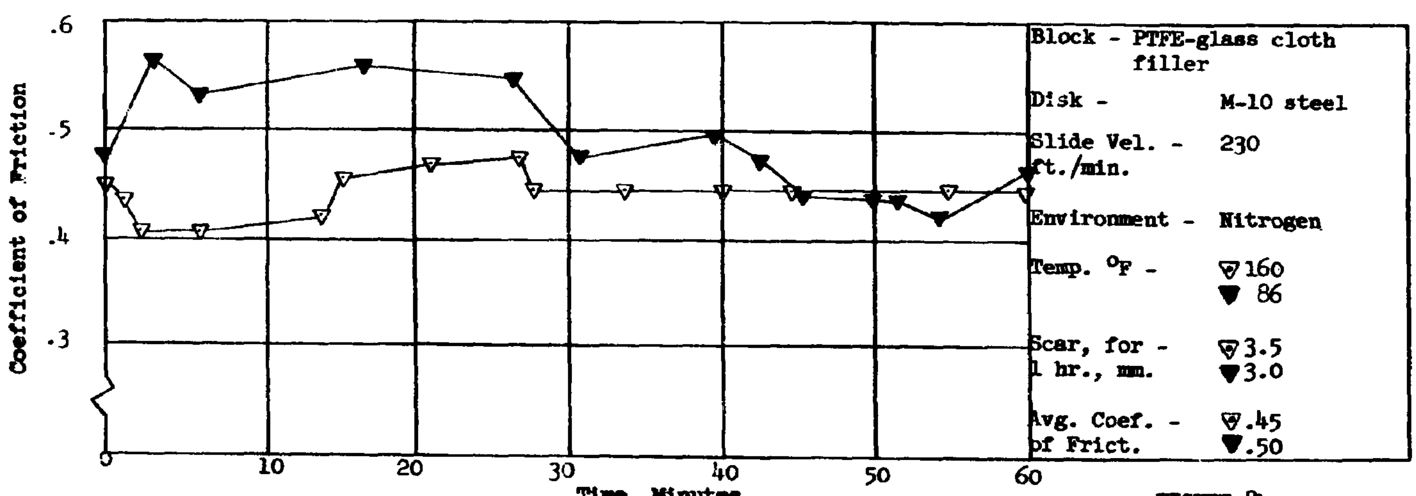

FIGURE 8b

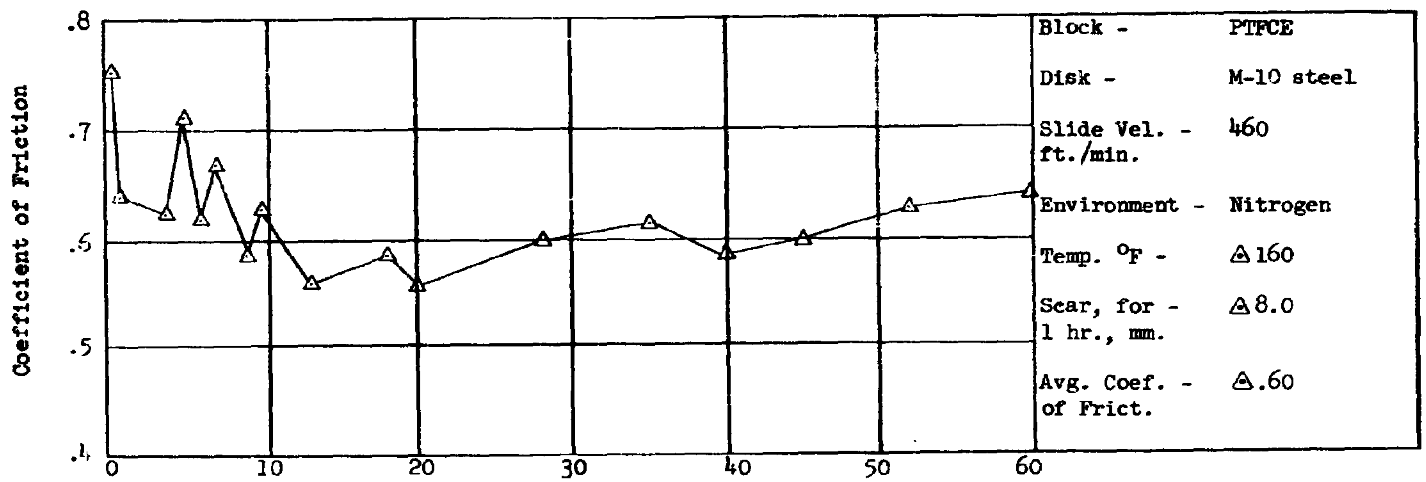

FIGURE 9a

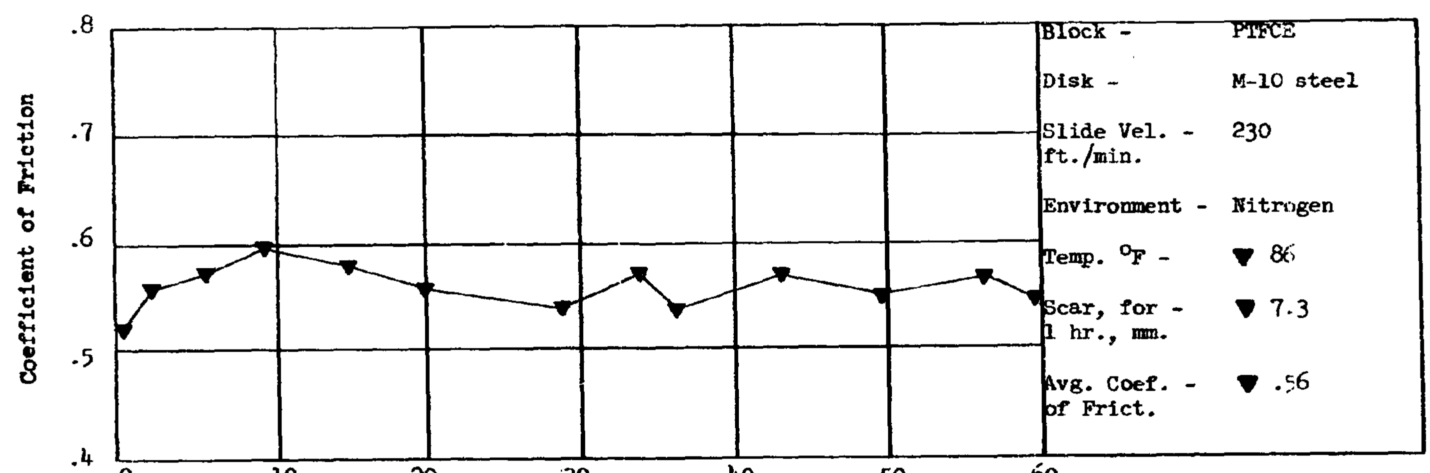

FIGURE 9b

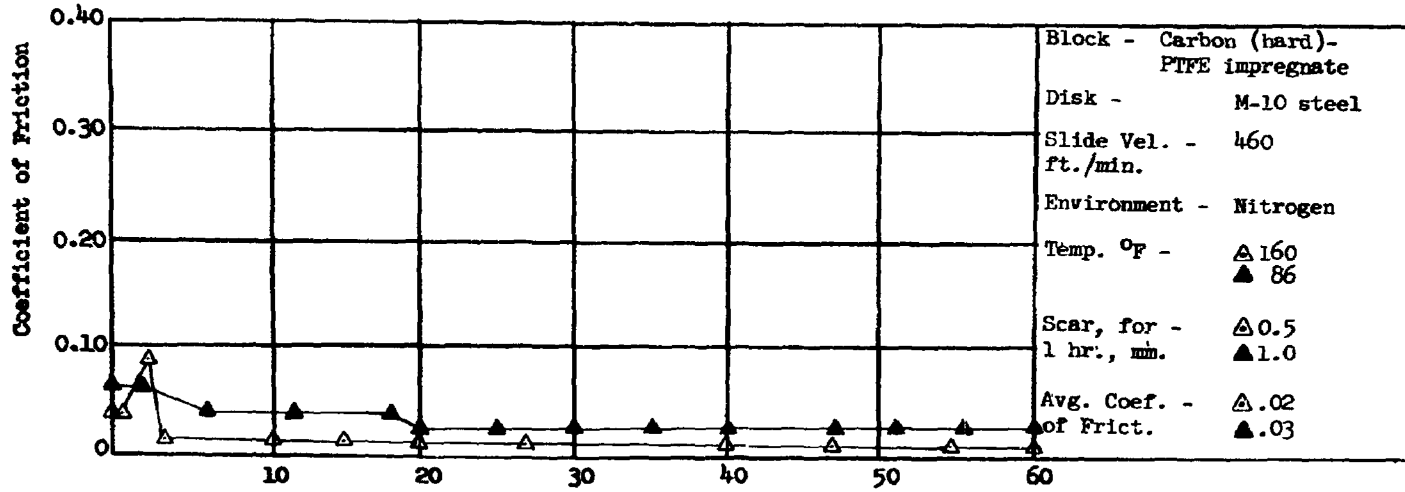

FIGURE 10a

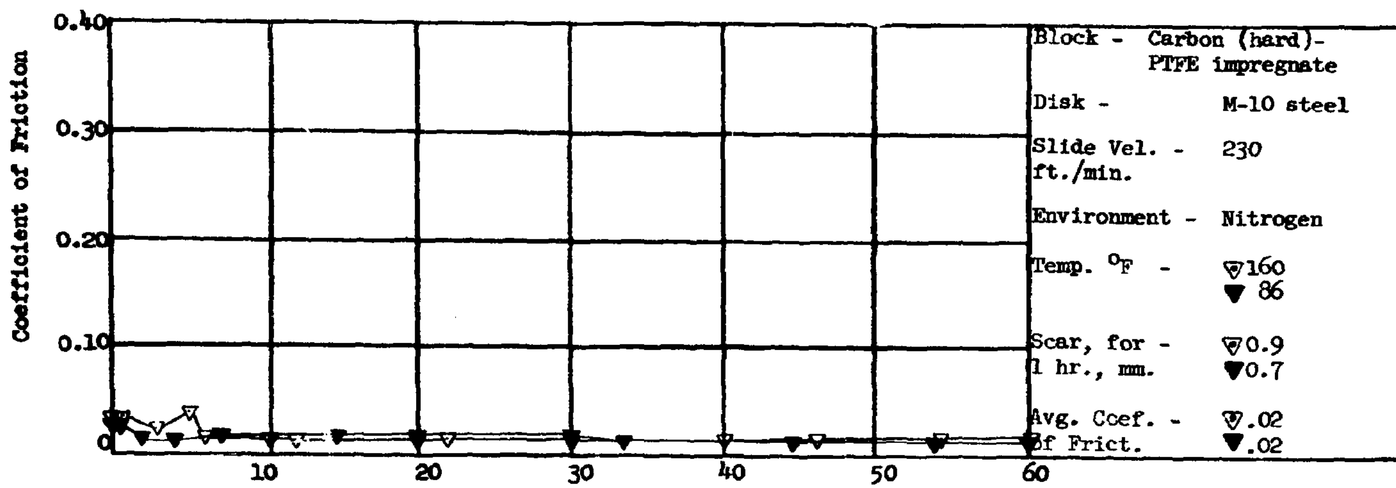

FIGURE 10b

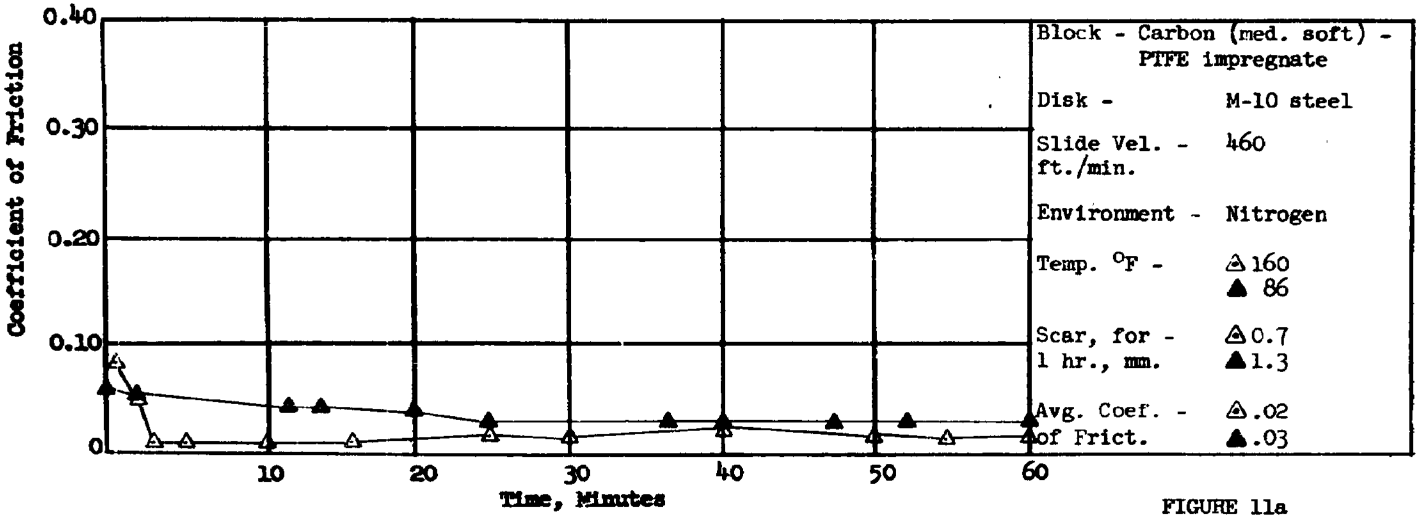

FIGURE 11a

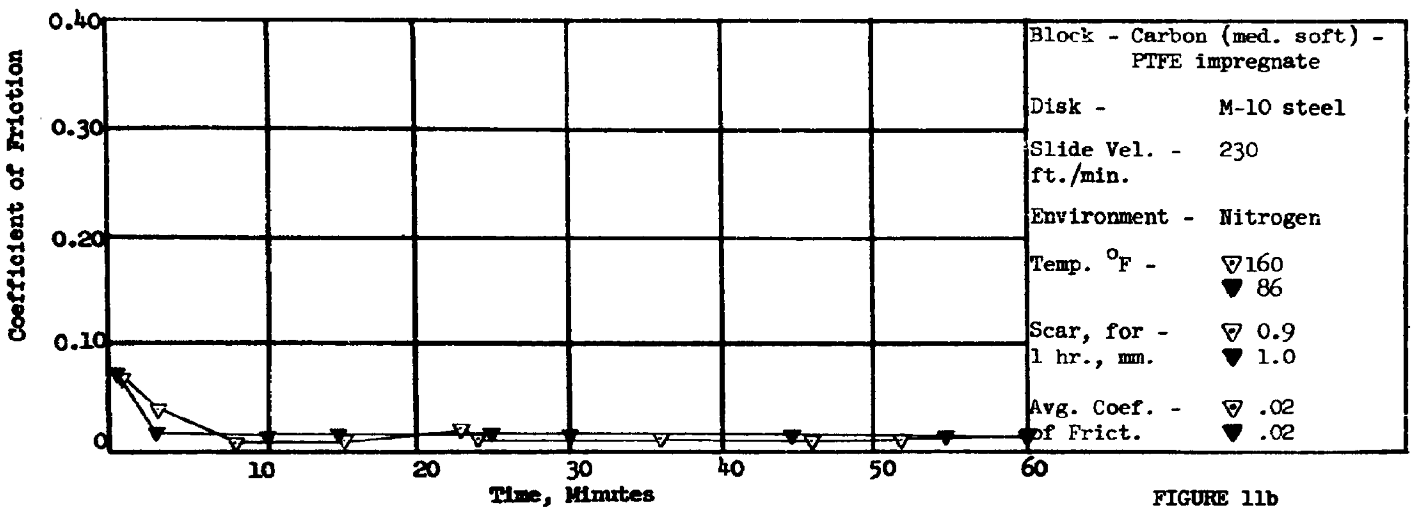

FIGURE 11b

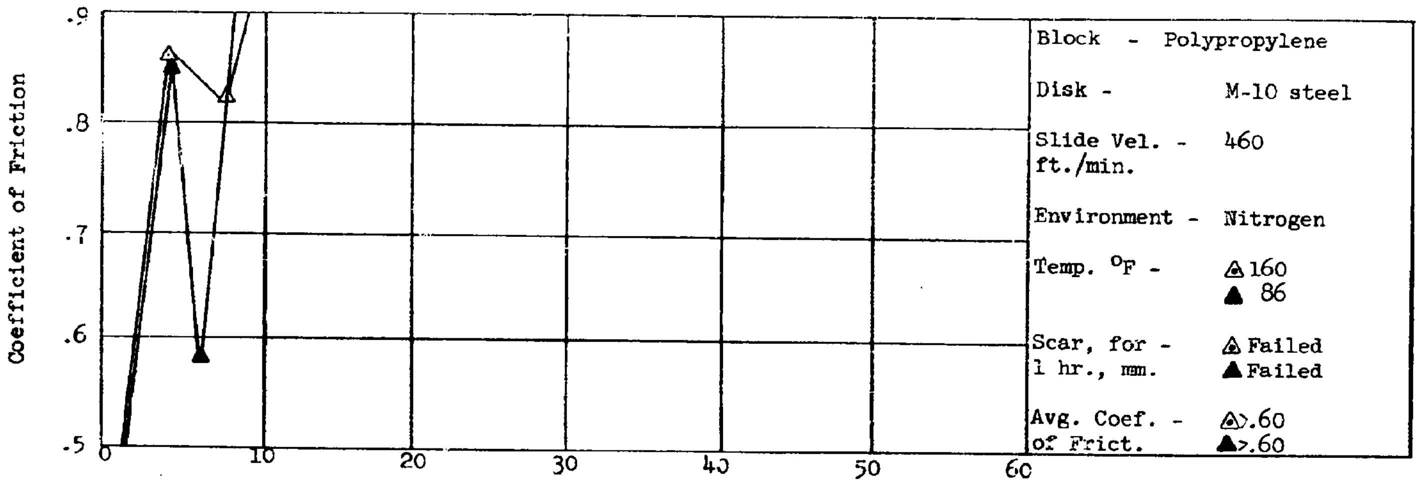

FIGURE 12a

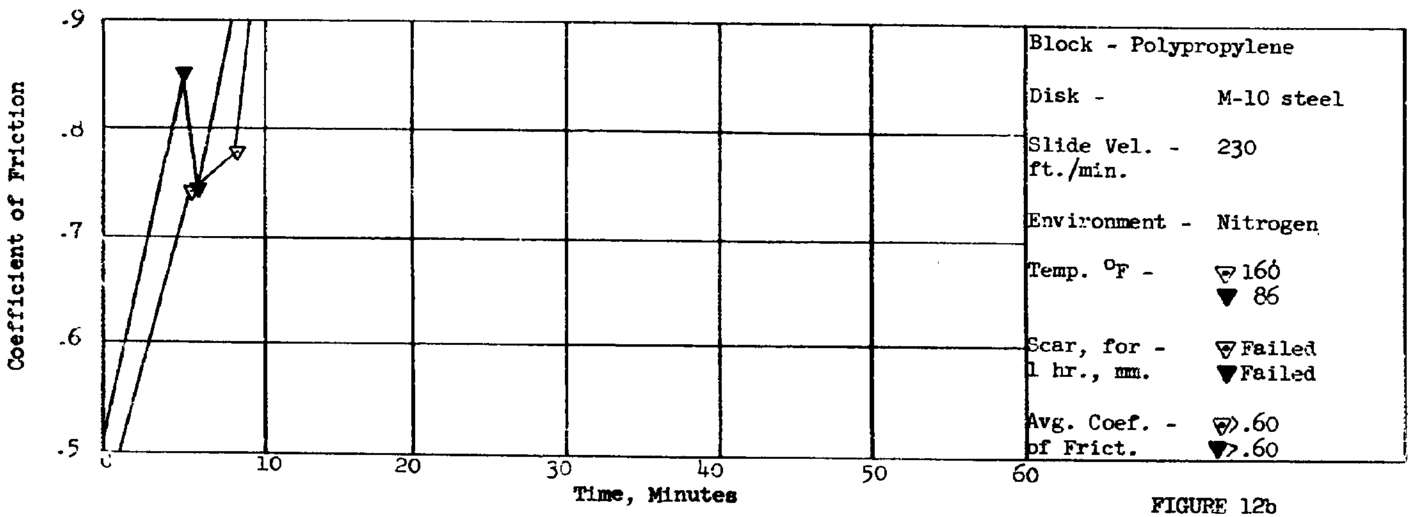

FIGURE 12b

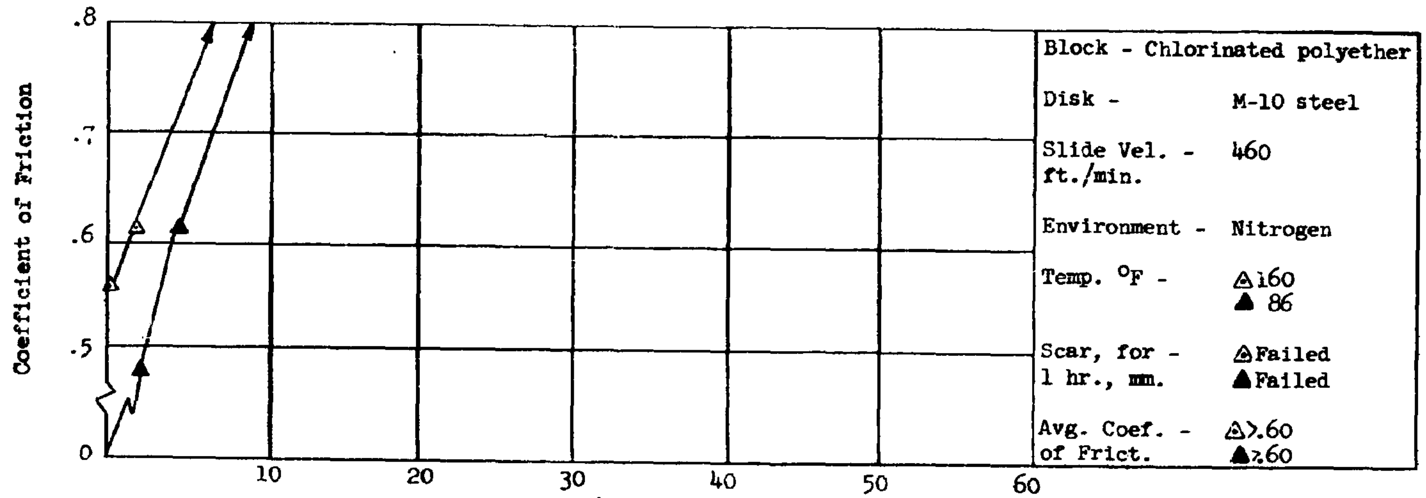

FIGURE 13a

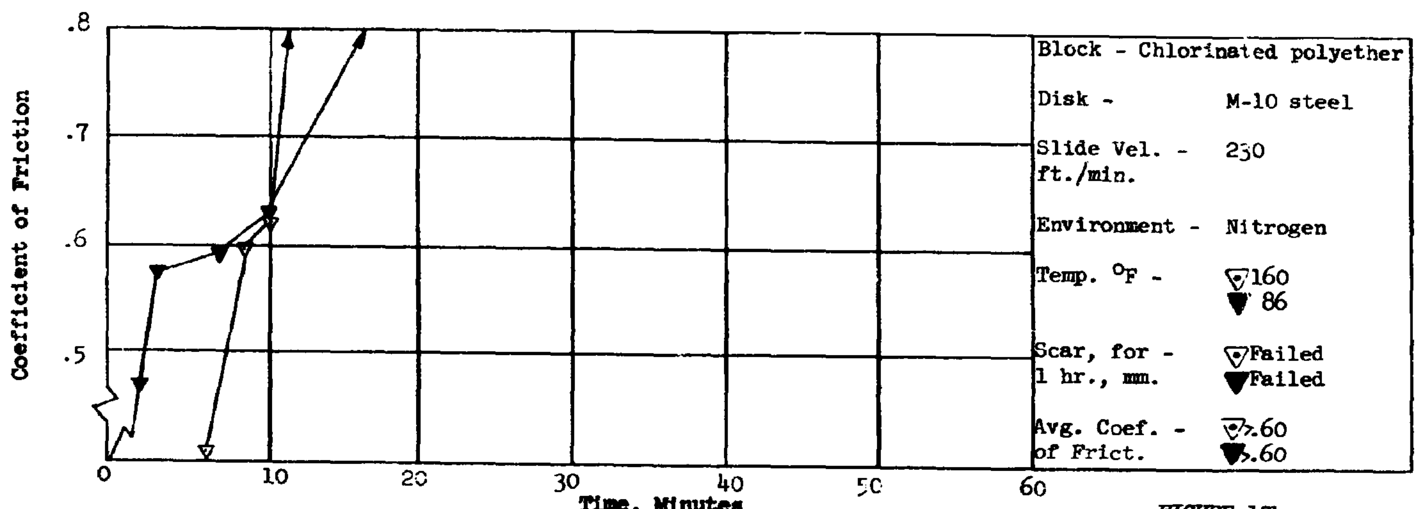

FIGURE 13b

SUMMARY OF WEAR AND FRICTION DATA ON PLASTICS

Plastics evaluated as test blocks rubbing against a rotating M-10 tool steel disk in a dry nitrogen atmosphere.

Curve Ref. (Fig. No.)	Test Material	Test Temp. °F	Sliding Vel. (ft./min.)	Coefficient of Friction (0 .1 .2 .3 .4 .5)	Average Wear/mm (0 1.0 2.0 3.0 4.0)
2a	Nylon + 40% MoS_2	160	460		
2a	Nylon + 40% MoS_2	86	460		
2b	Nylon + 40% MoS_2	160	230		
2b	Nylon + 40% MoS_2	86	230		
3a	Nylon + 20% C	160	460		
3a	Nylon + 20% C	86	460		
3b	Nylon + 20% C	160	230		
3b	Nylon + 20% C	86	230		
4a	Nylon	160	460	>.6	Failure
4a	Nylon	86	460	>.6	Failure
4b	Nylon	160	230	>.6	Failure
4b	Nylon	86	230	>.6	Failure
5a	PTFE* + Mica	160	460		4.6
5a	PTFE + Mica	86	460		
5b	PTFE + Mica	160	230		
5b	PTFE + Mica	86	230		
6a	PTFE + Ceramic	160	460		
6a	PTFE + Ceramic	86	460		
6b	PTFE + Ceramic	160	230		
6b	PTFE + Ceramic	86	230		
7a	PTFE + GF** + MoS_2	160	460		
7a	PTFE + GF + MoS_2	86	460		
7b	PTFE + GF + MoS_2	160	230		
7b	PTFE + GF + MoS_2	86	230		
8a	PTFE + Glass Cloth	160	460		
8a	PTFE + Glass Cloth	86	460		
8b	PTFE + Glass Cloth	160	230		
8b	PTFE + Glass Cloth	86	230		
9a	PTFCE***	160	460	.6	8.0
9b	PTFCE	86	230	.56	7.3
10a	C (Hard) + PTFE	160	460		
10a	C (Hard) + PTFE	86	460		
10b	C (Hard) + PTFE	160	230		
10b	C (Hard) + PTFE	86	230		
11a	C (Med. S) + PTFE	160	460		
11a	C (Med. S) + PTFE	86	460		
11b	C (Med. S) + PTFE	160	230		
11b	C (Med. S) + PTFE	86	230		
12a	Polypropylene	160	460	>.6	Failure
12a	Polypropylene	86	460	>.6	Failure
12b	Polypropylene	160	230	>.6	Failure
12b	Polypropylene	86	230	>.6	Failure
13a	Chlor. polyether	160	460	>.6	Failure
13a	Chlor. polyether	86	460	>.6	Failure
13b	Chlor. polyether	160	230	>.6	Failure
13b	Chlor. polyether	86	230	>.6	Failure

*PTFE designates polytetrafluoroethylene.
**GF designates glass fiber.
***PTFCE designates polychlorotrifluoroethylene.

FIGURE 14

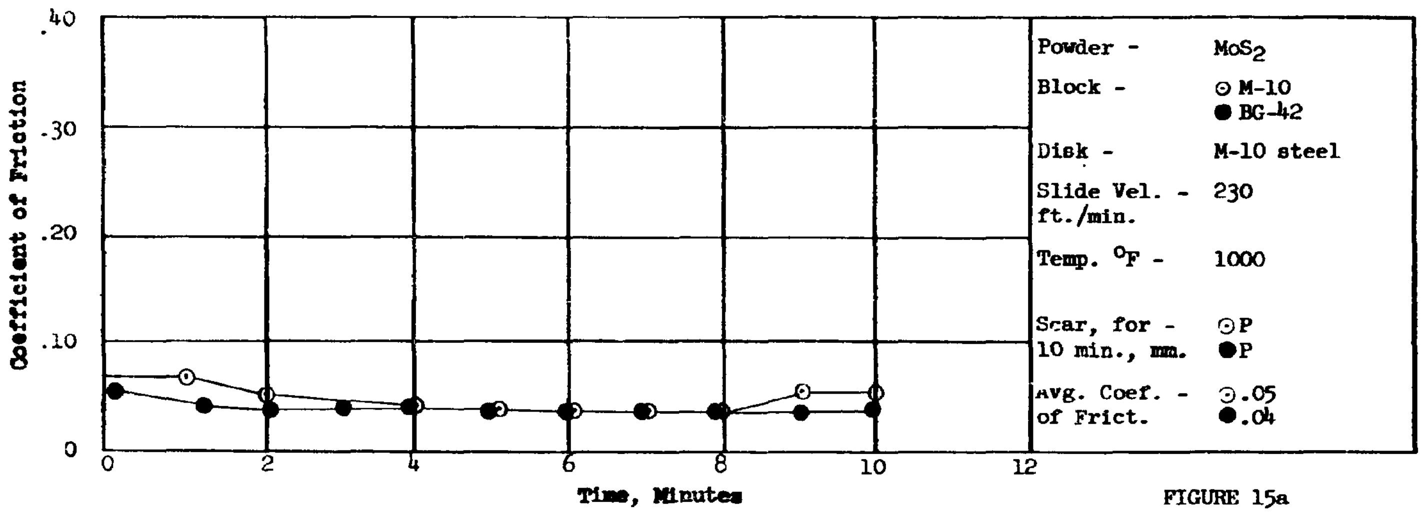

FIGURE 15a

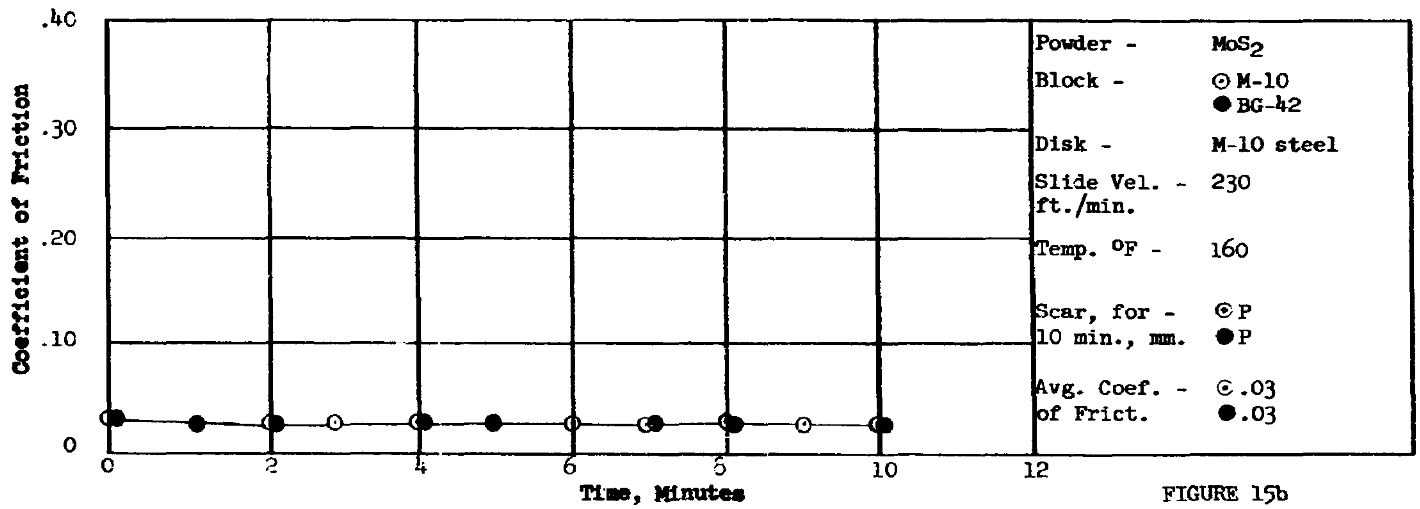

FIGURE 15b

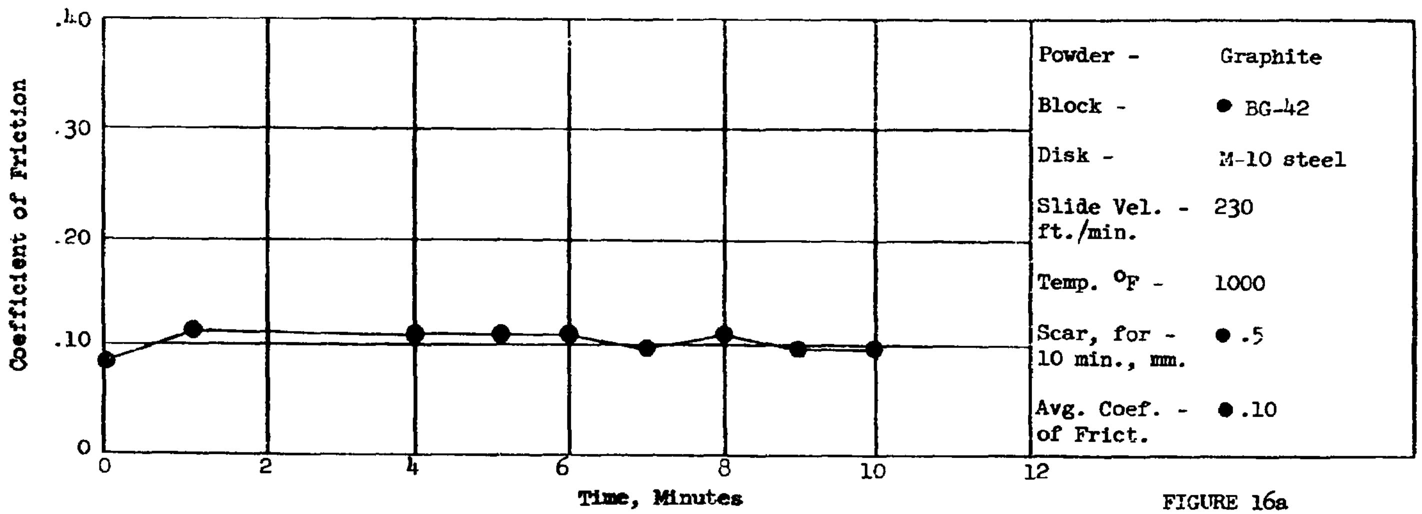

FIGURE 16a

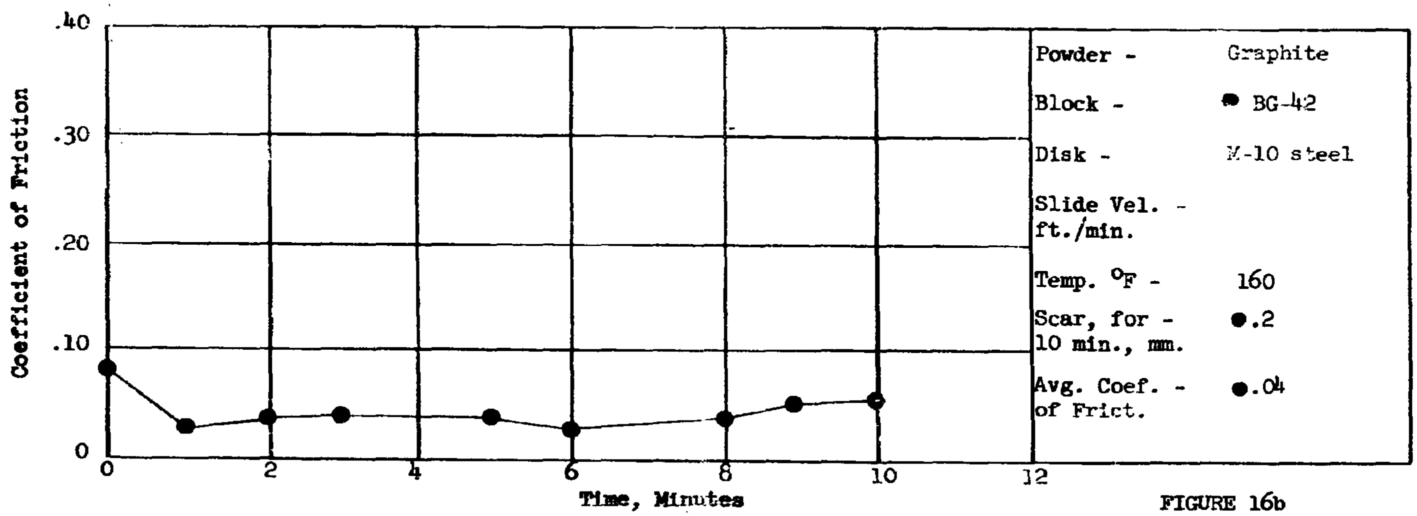

FIGURE 16b

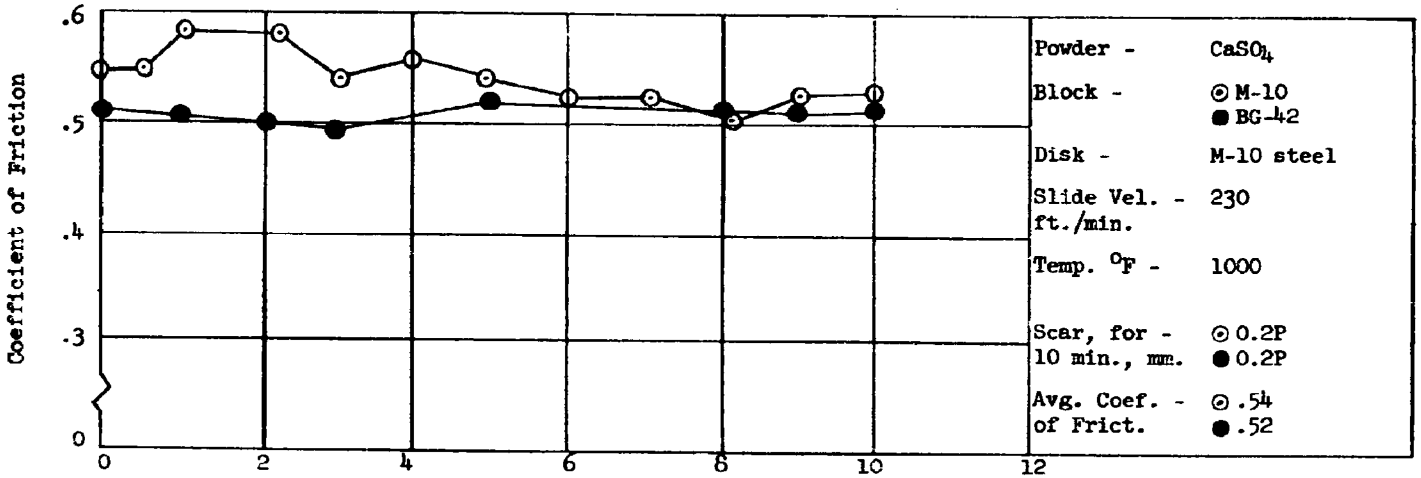

FIGURE 17a

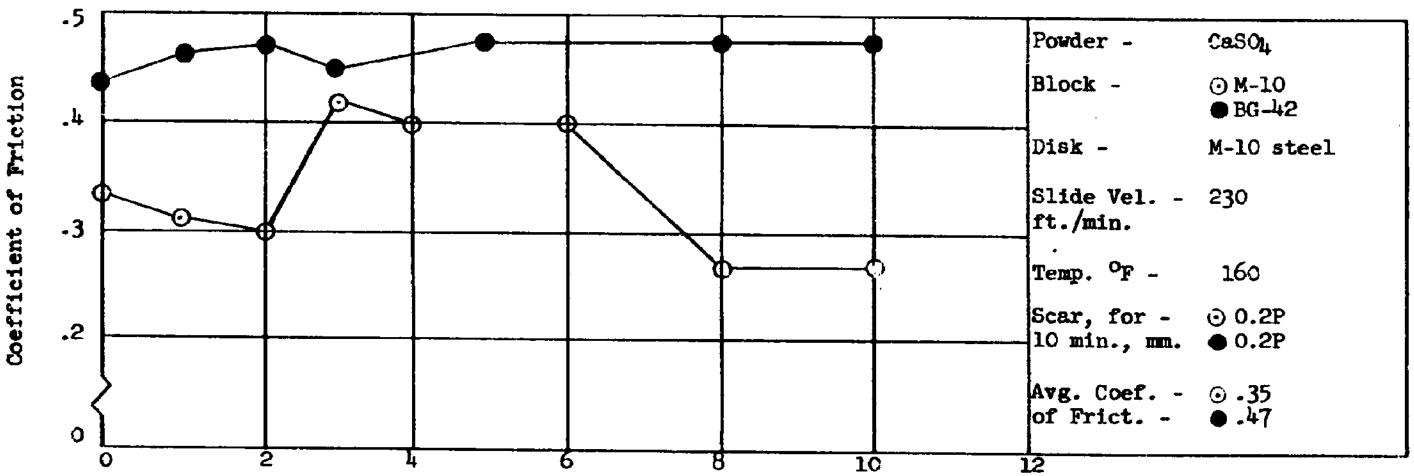

FIGURE 17b

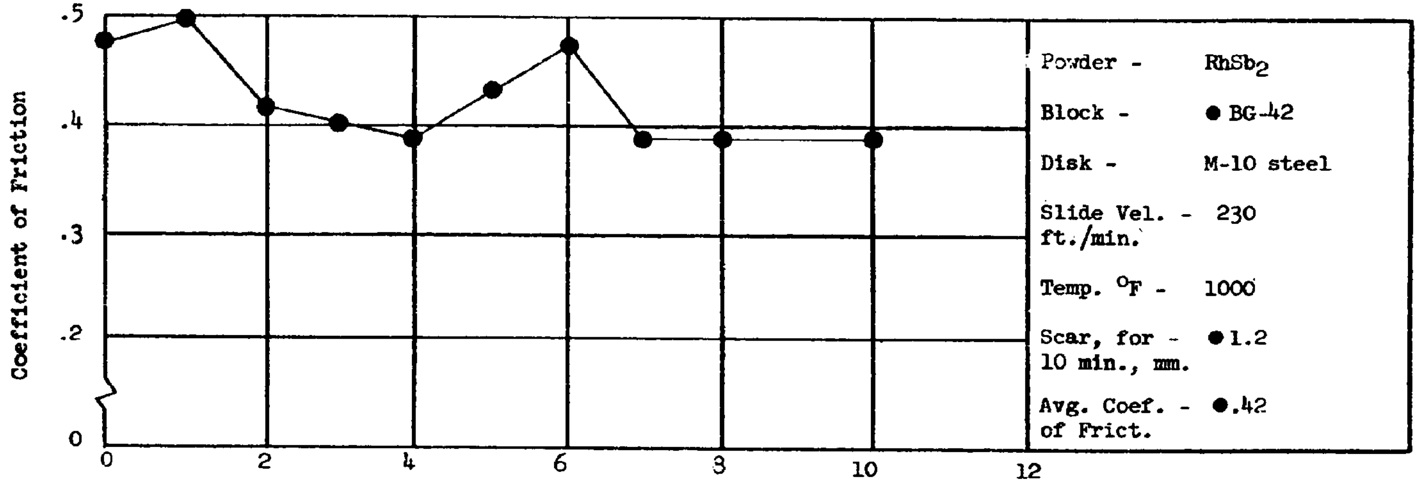

FIGURE 18a

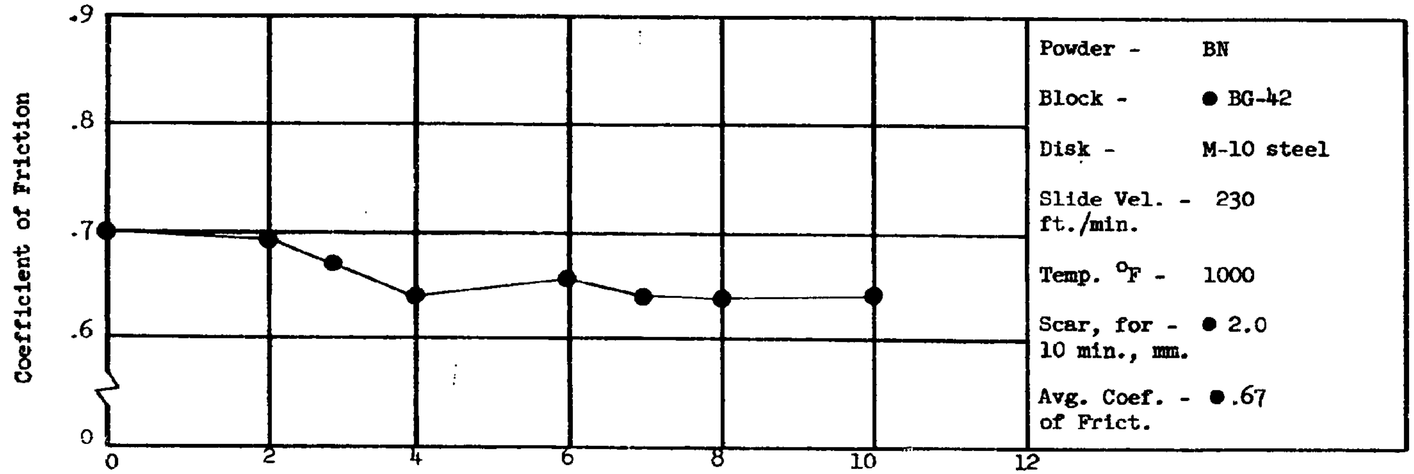

FIGURE 18b

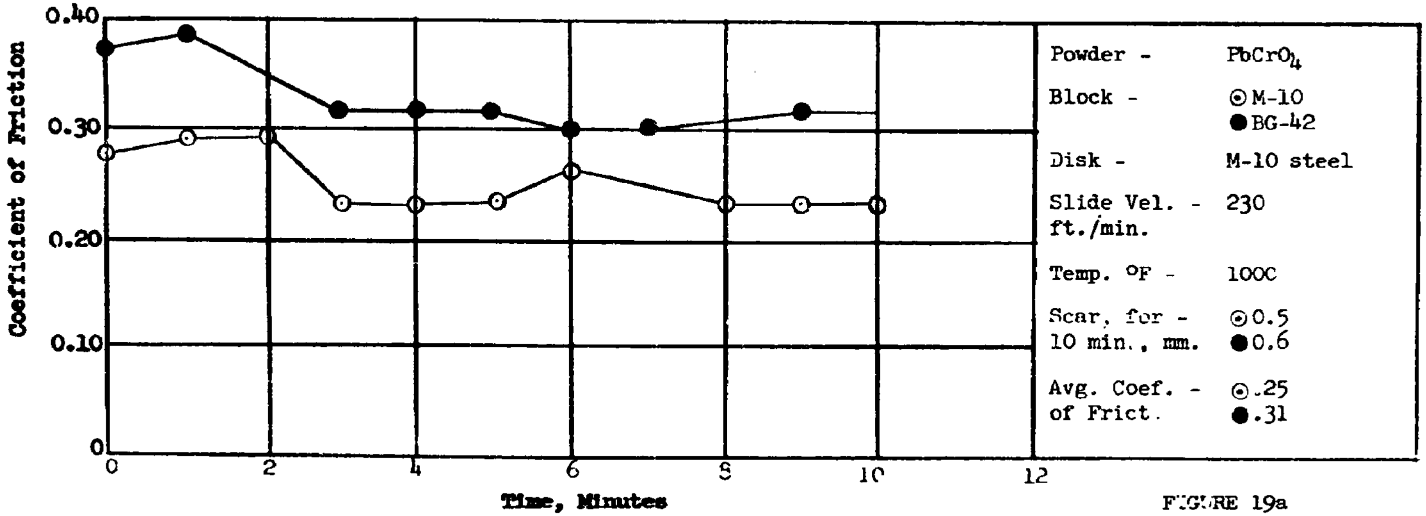

FIGURE 19a

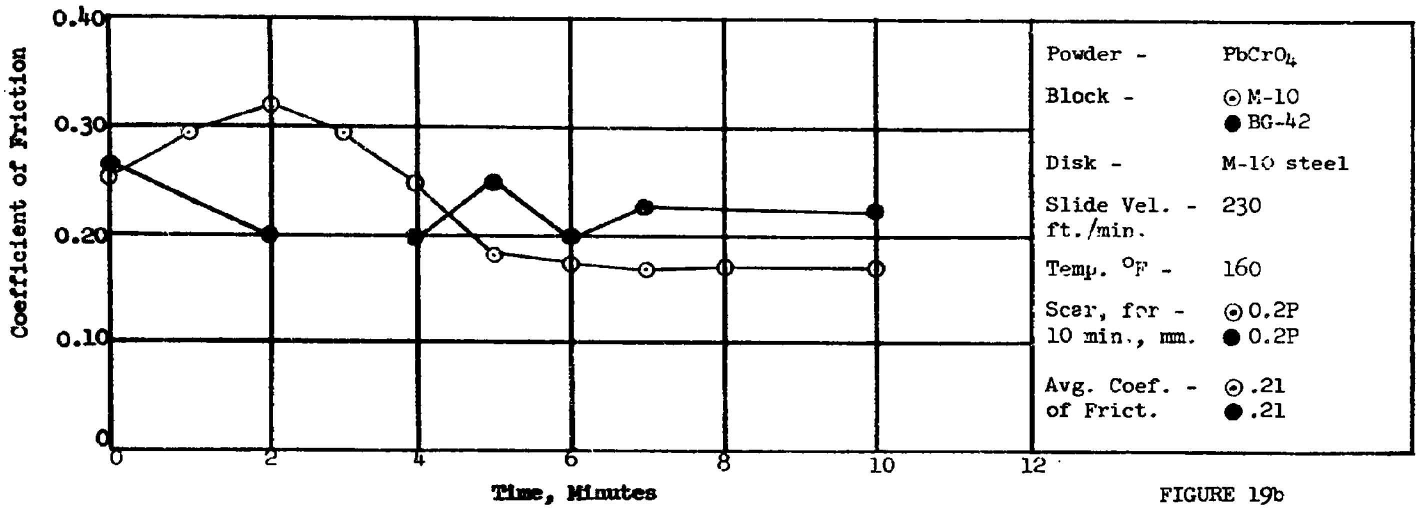

FIGURE 19b

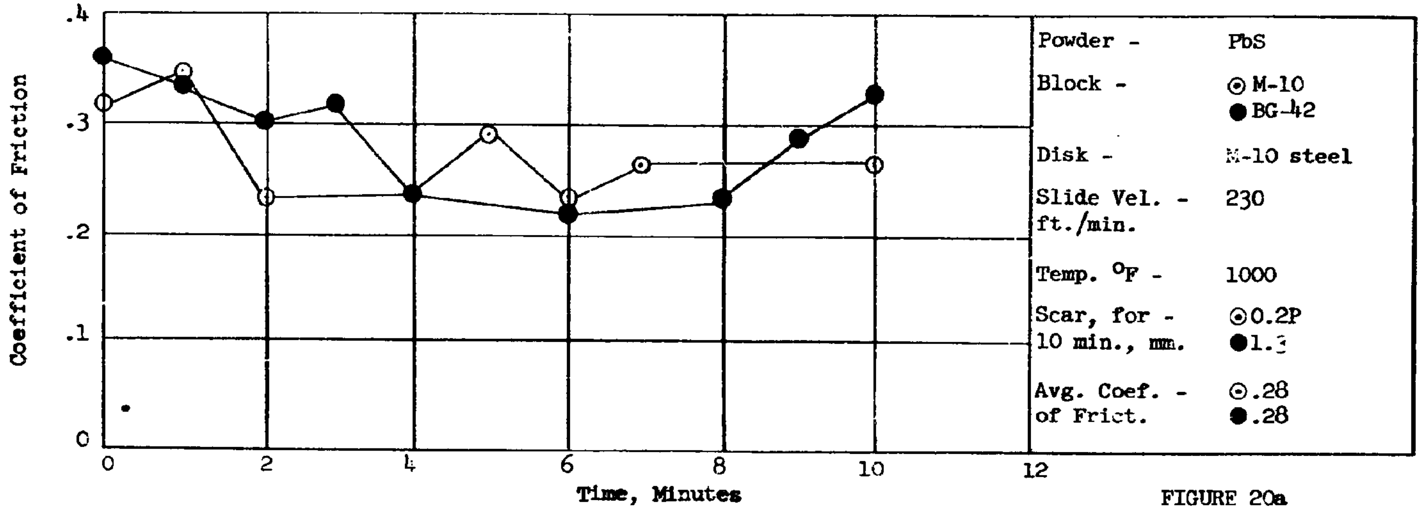

FIGURE 20a

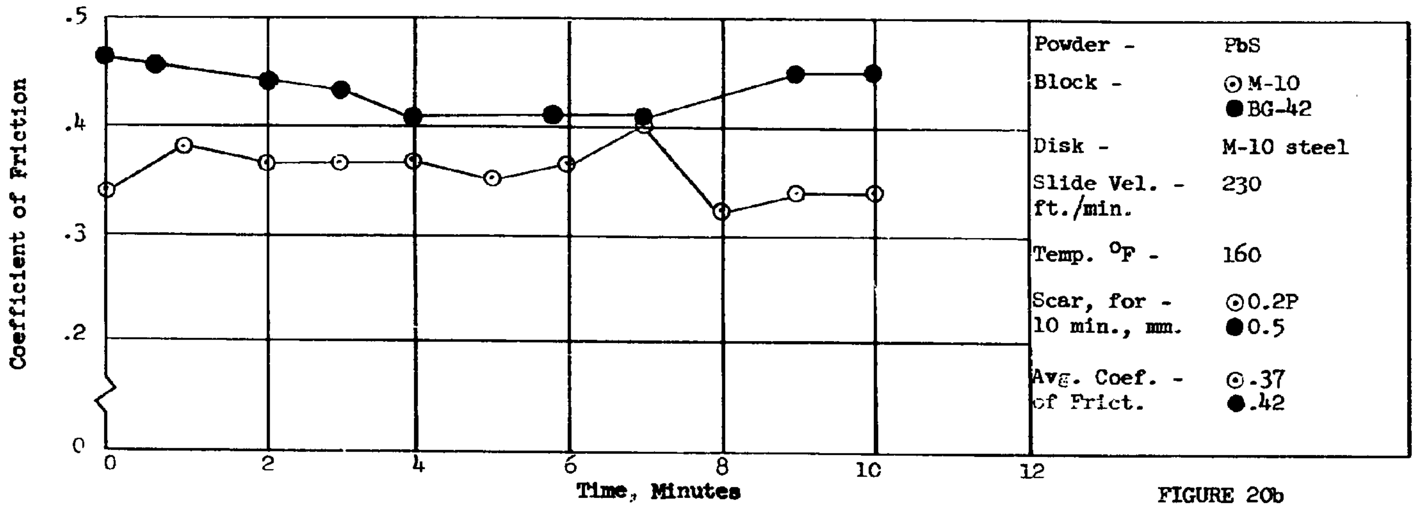

FIGURE 20b

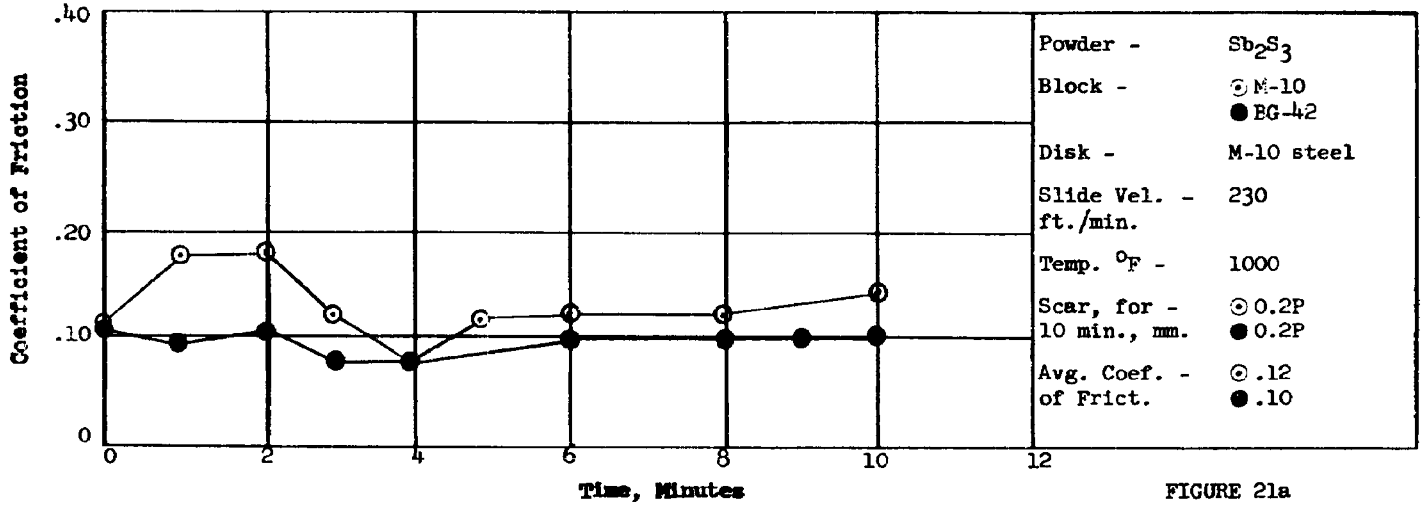

FIGURE 21a

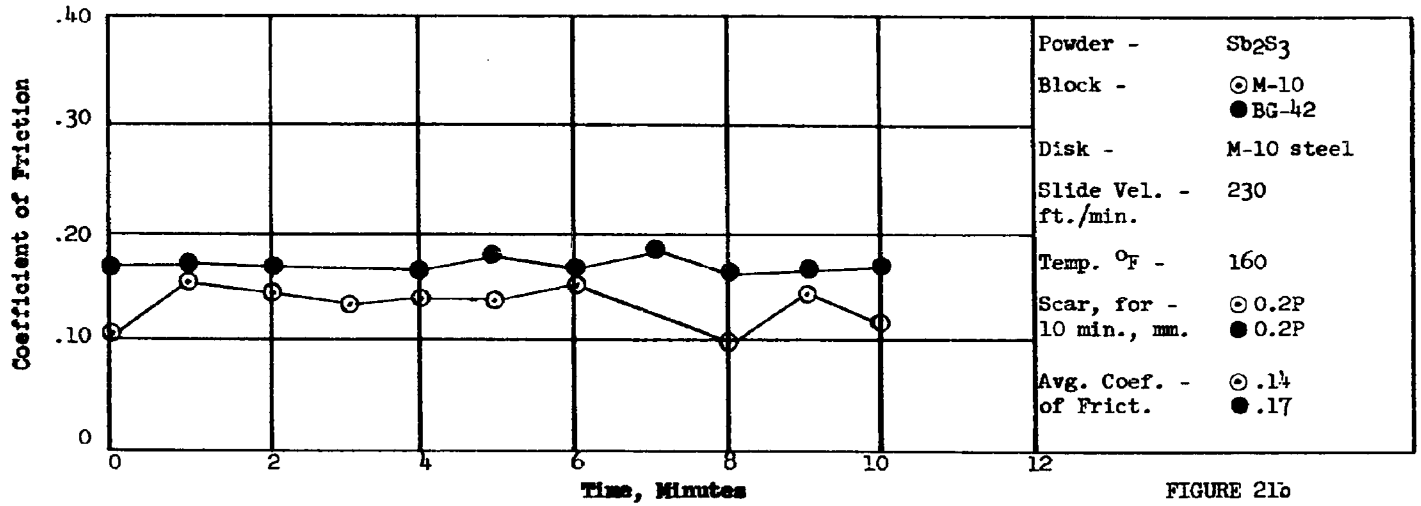

FIGURE 21b

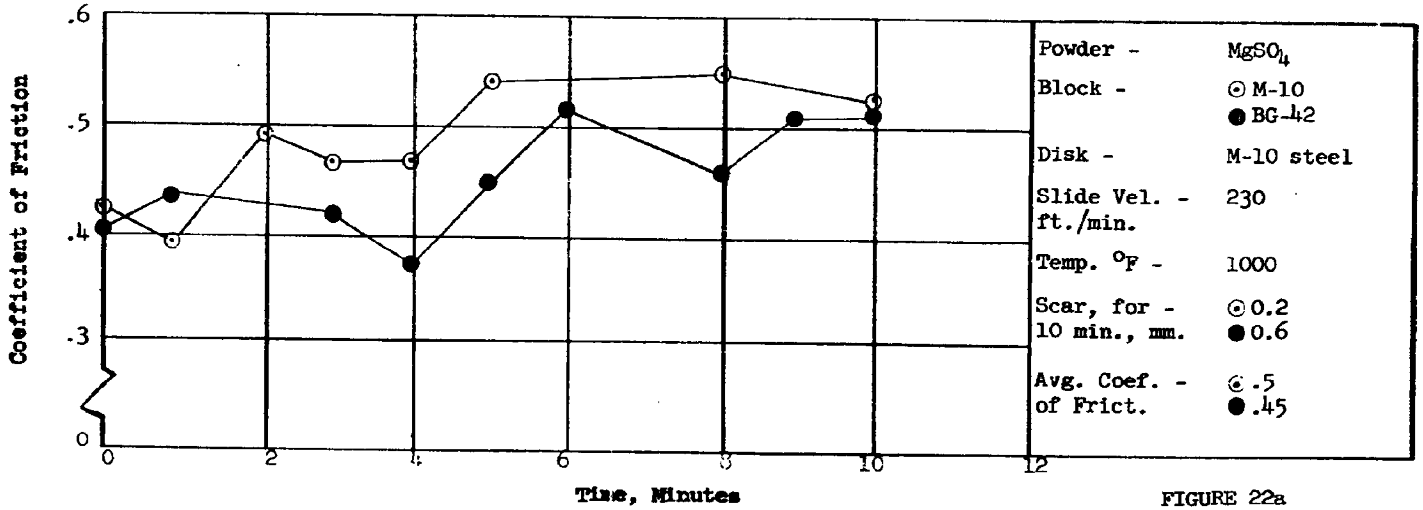

FIGURE 22a

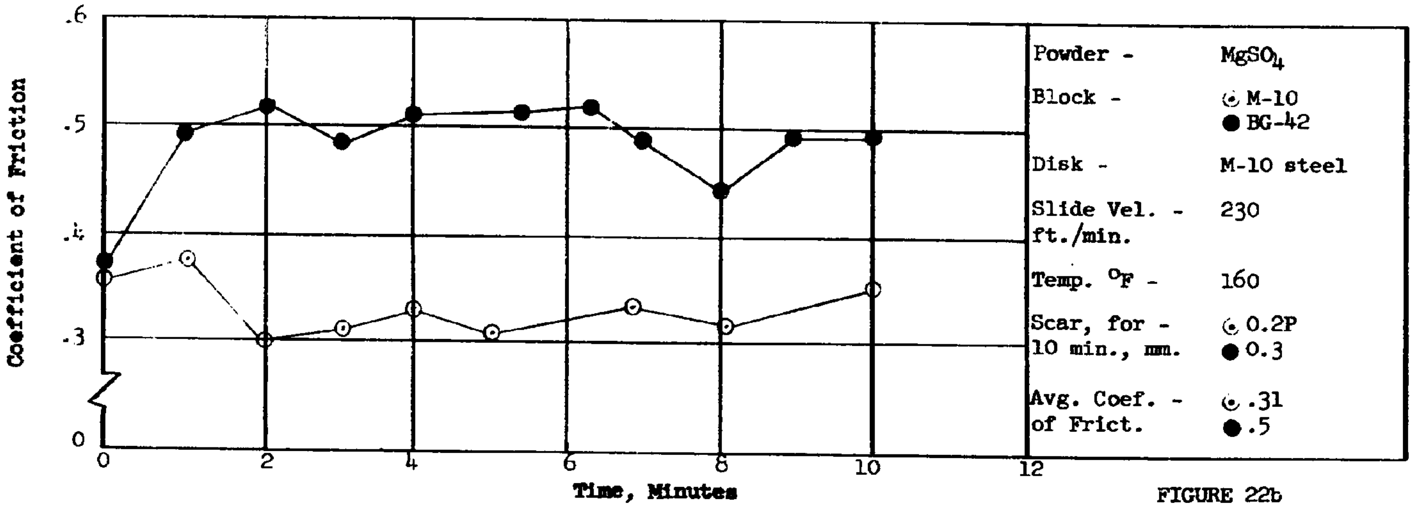

FIGURE 22b

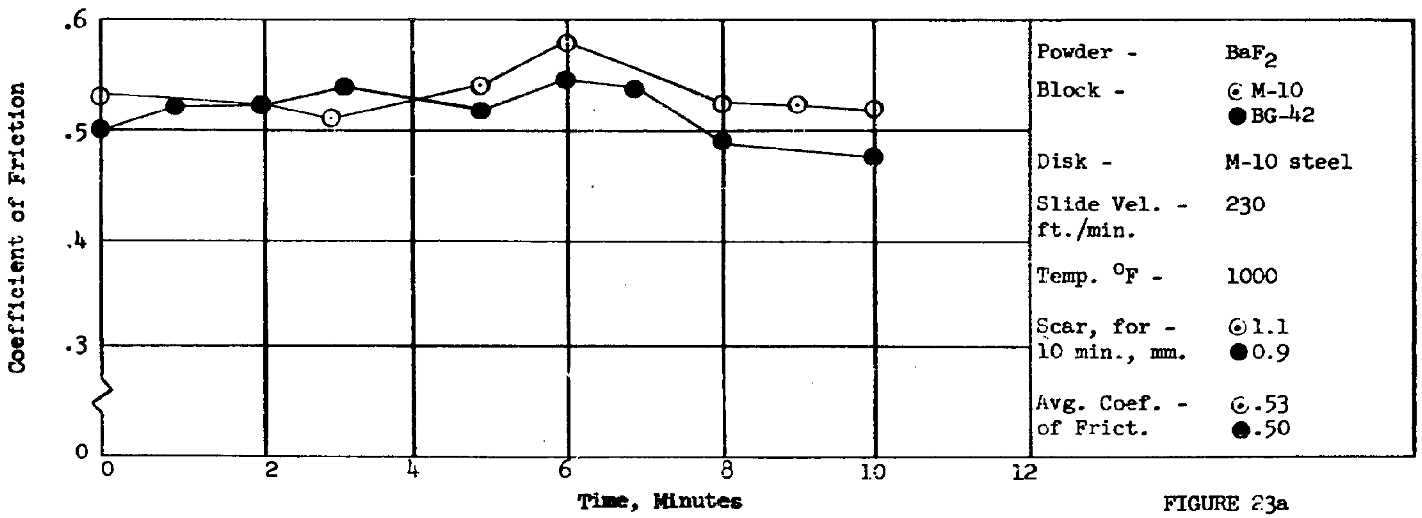

FIGURE 23a

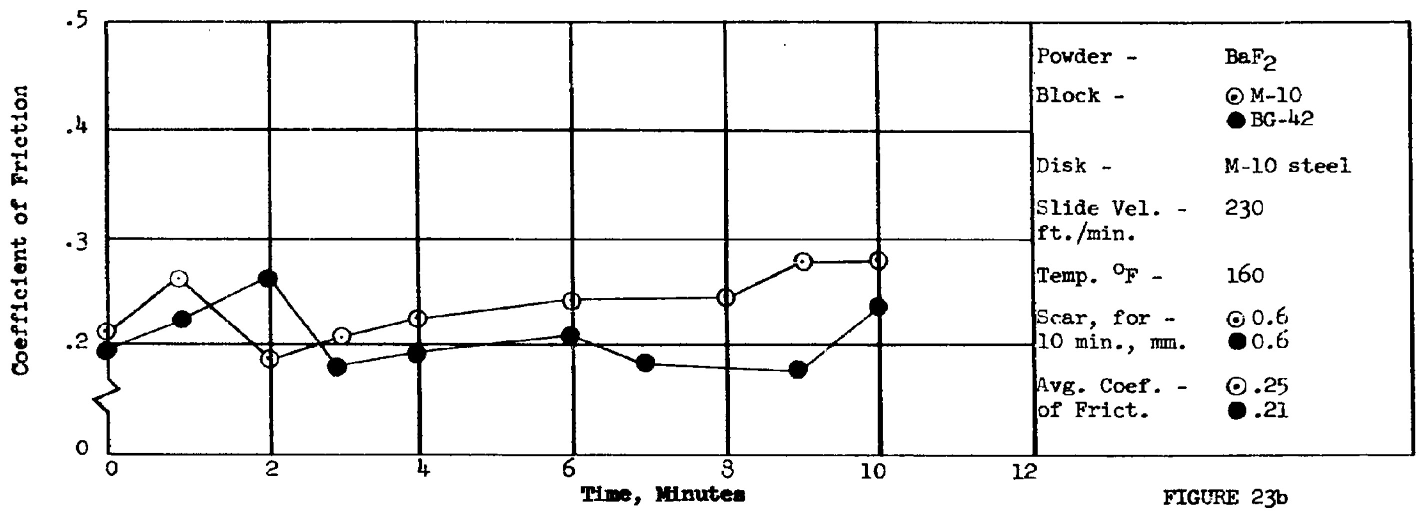

FIGURE 23b

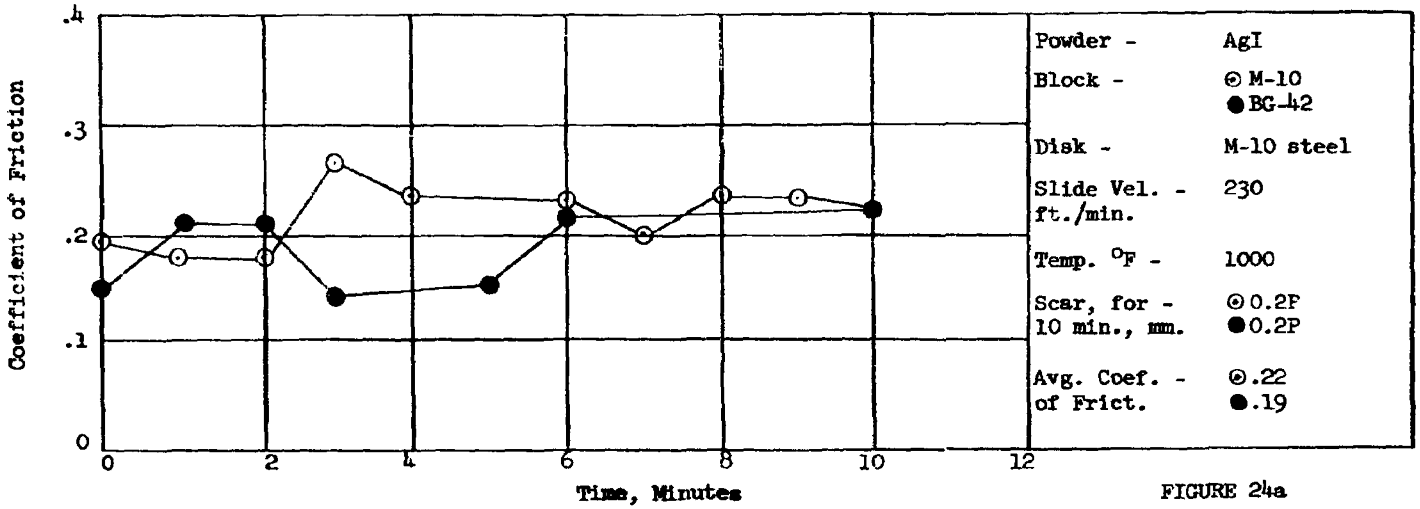

FIGURE 24a

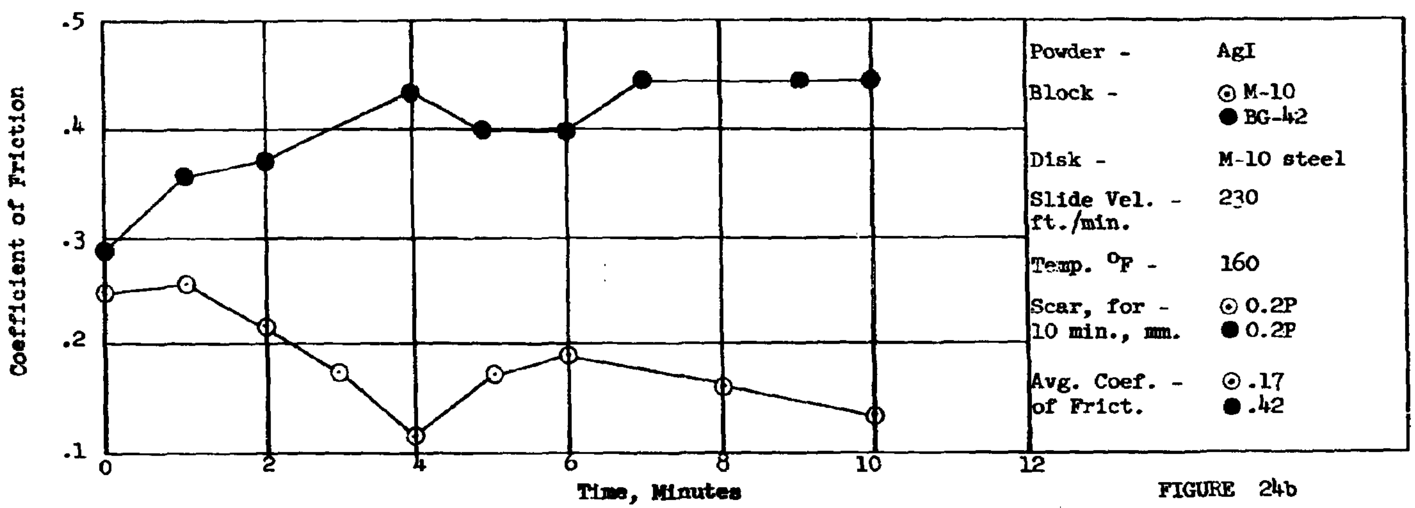

FIGURE 24b

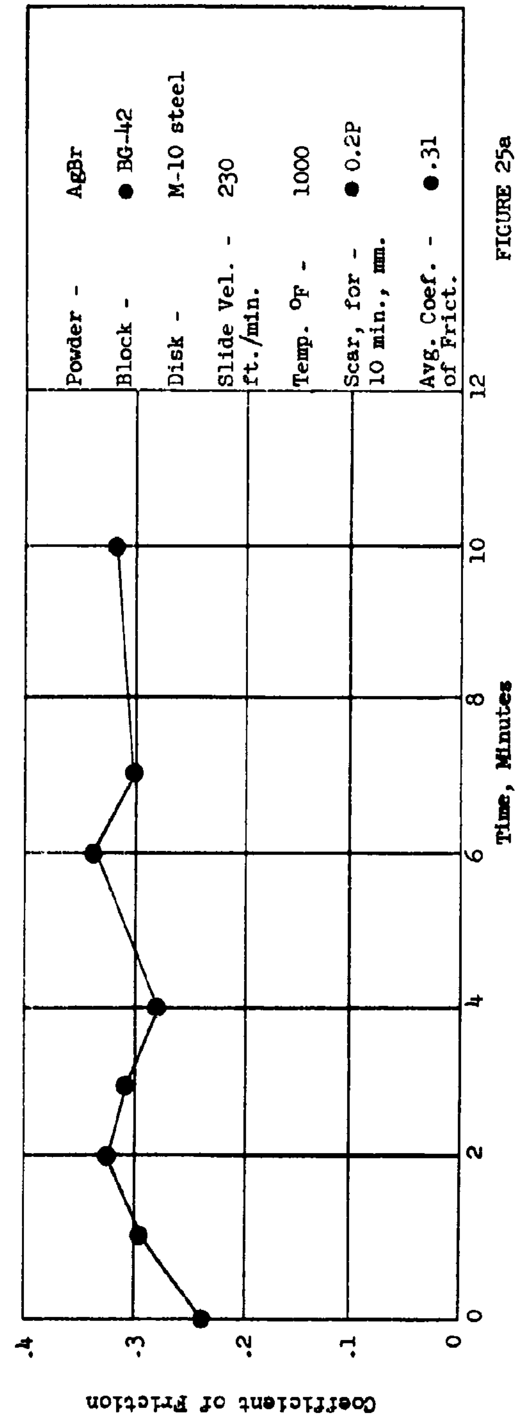

FIGURE 25a

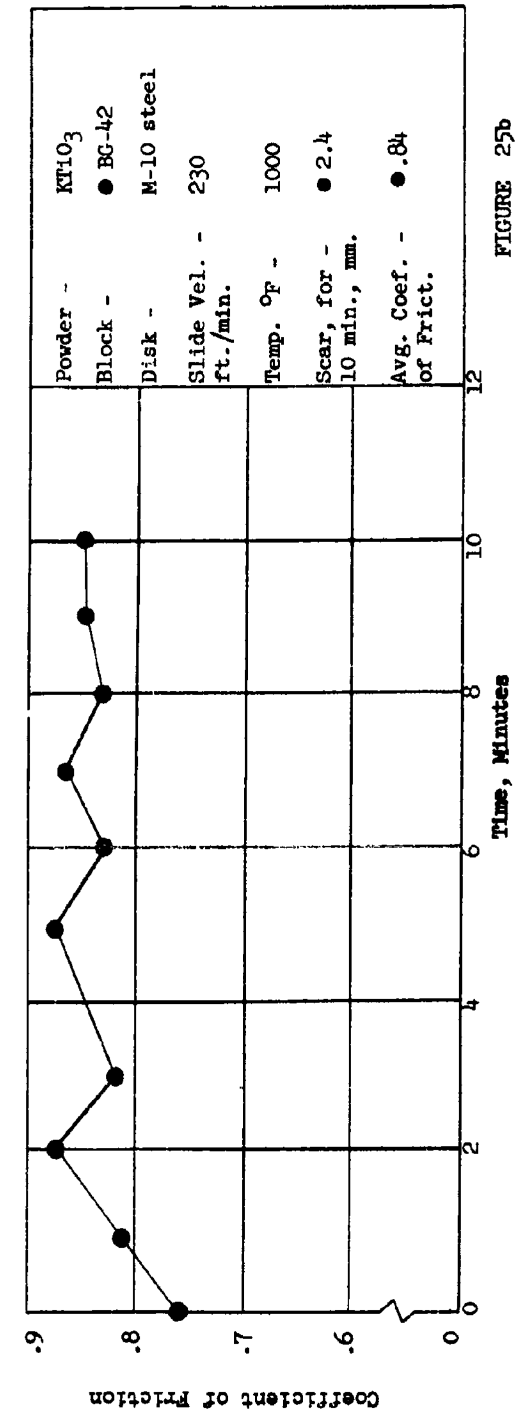

FIGURE 25b

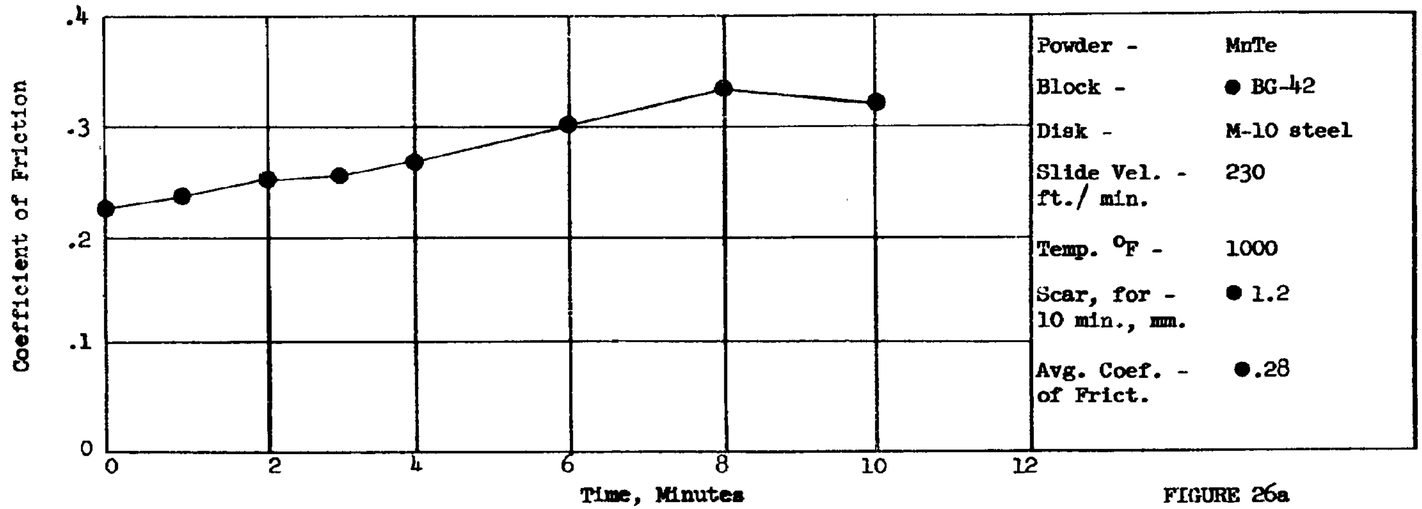

FIGURE 26a

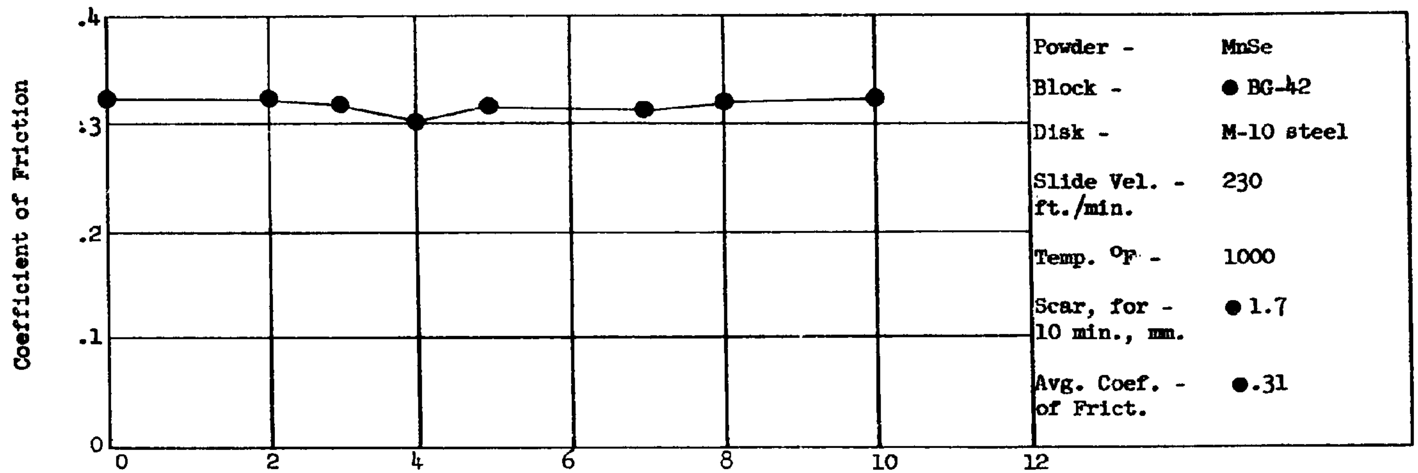

FIGURE 26b

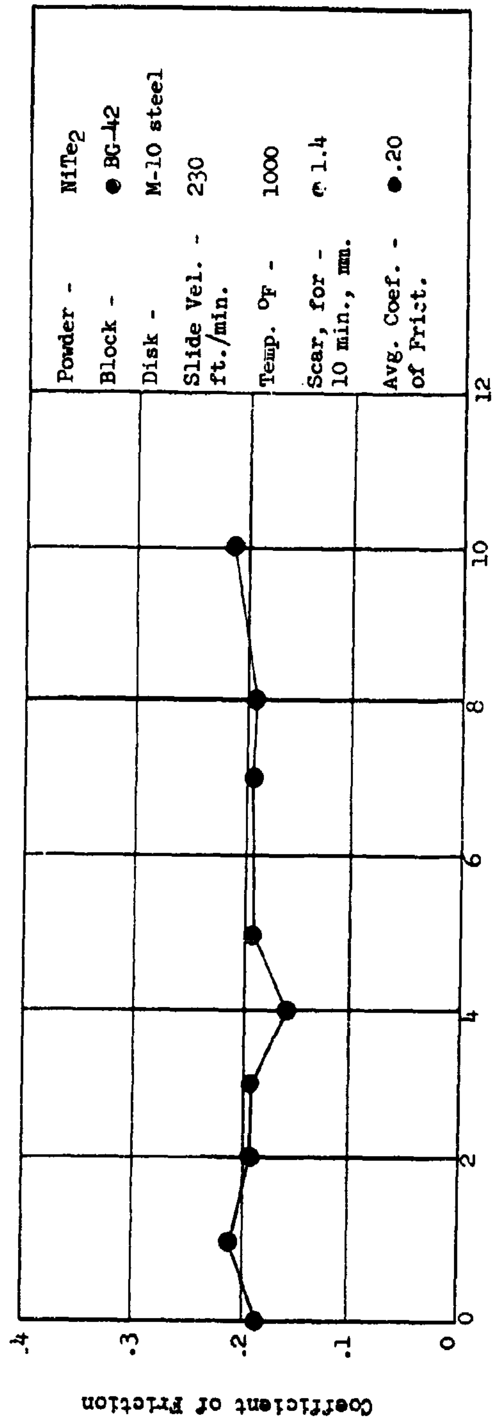

FIGURE 27a

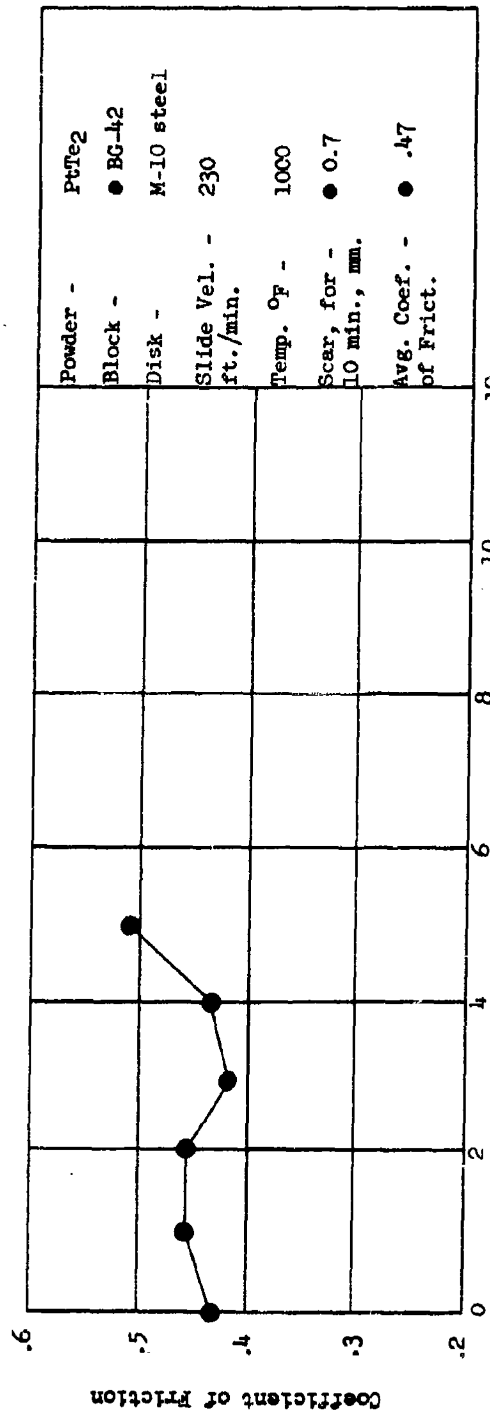

FIGURE 27b

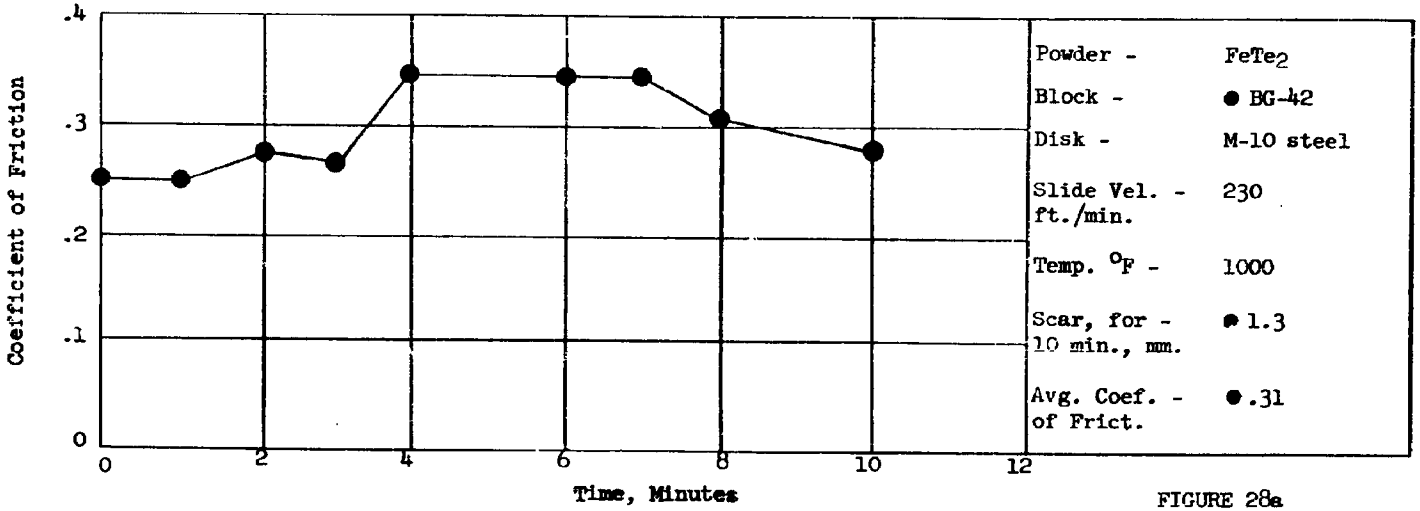

FIGURE 28a

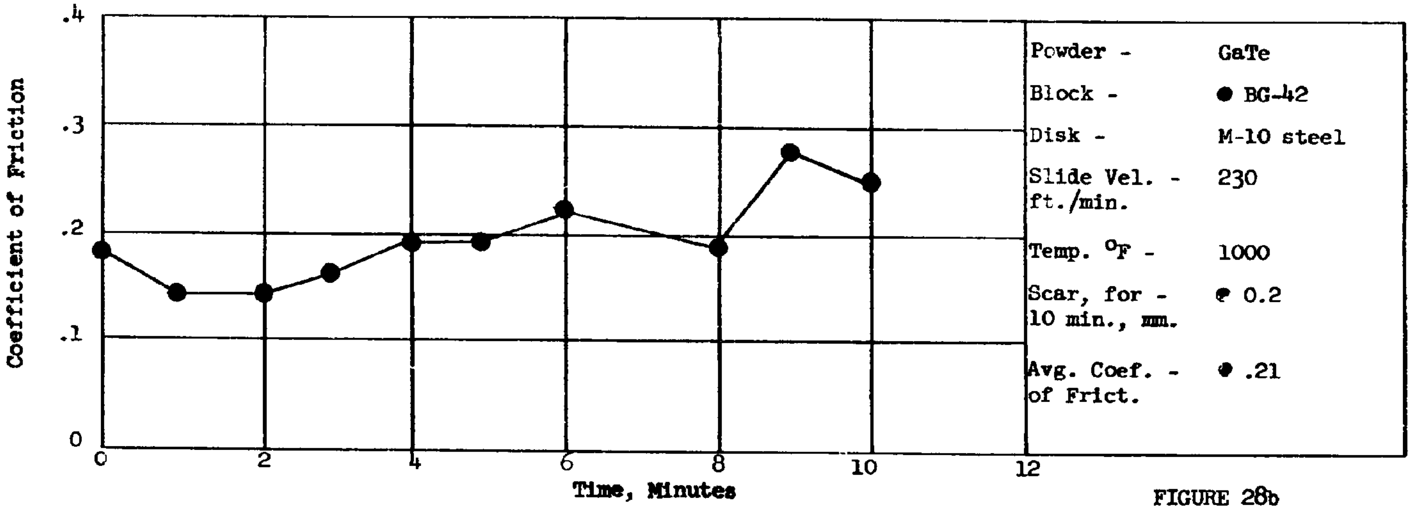

FIGURE 28b

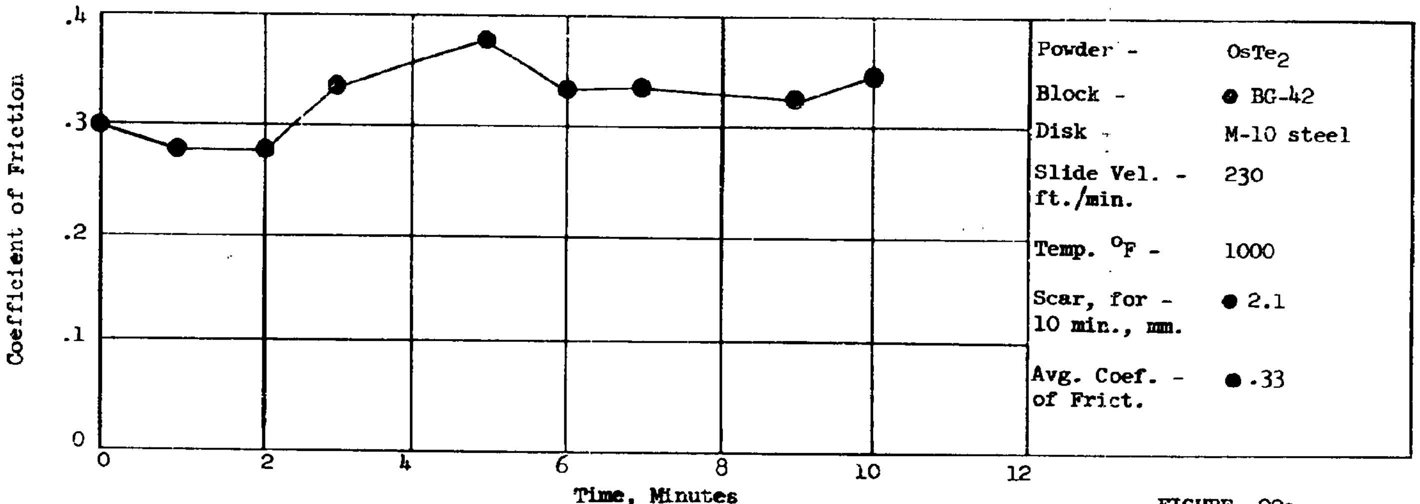

FIGURE 29a

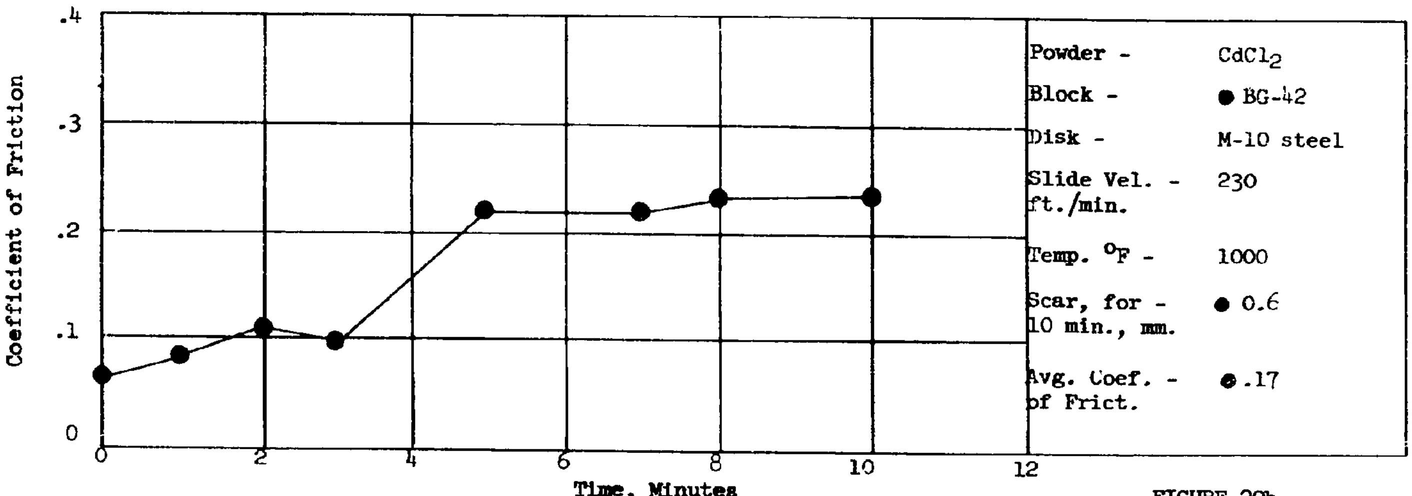

FIGURE 29b

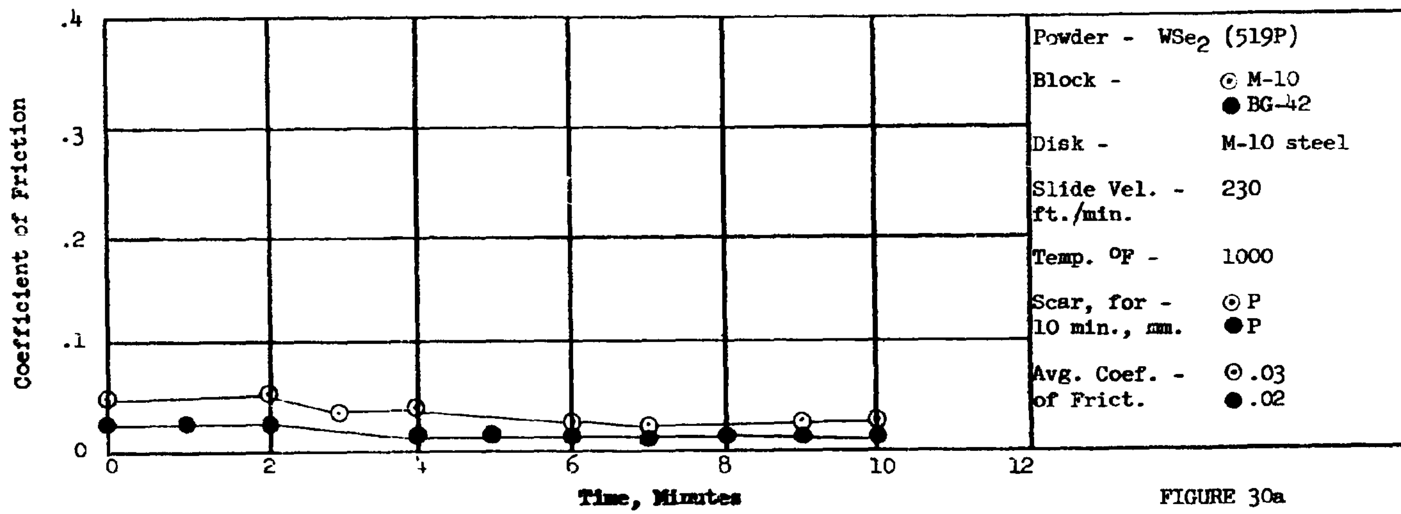

FIGURE 30a

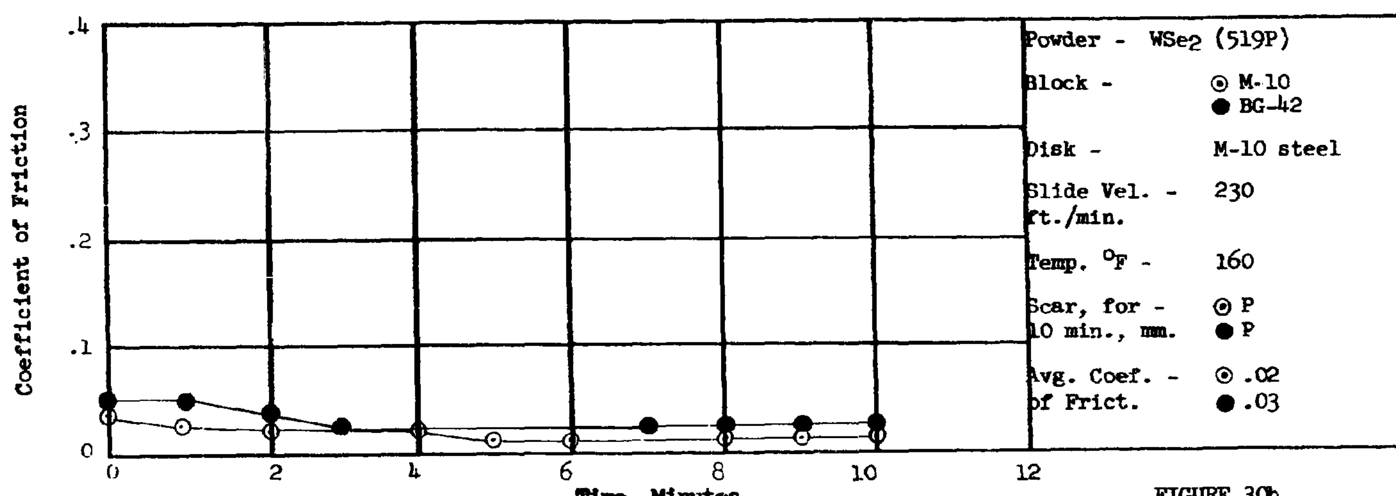

FIGURE 30b

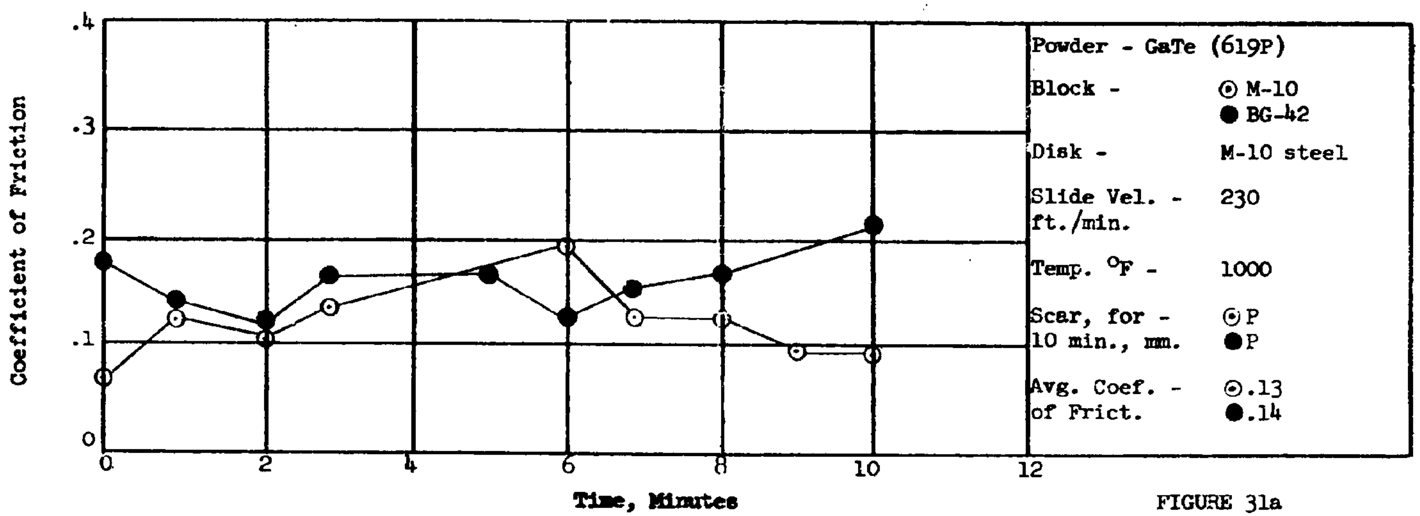

FIGURE 31a

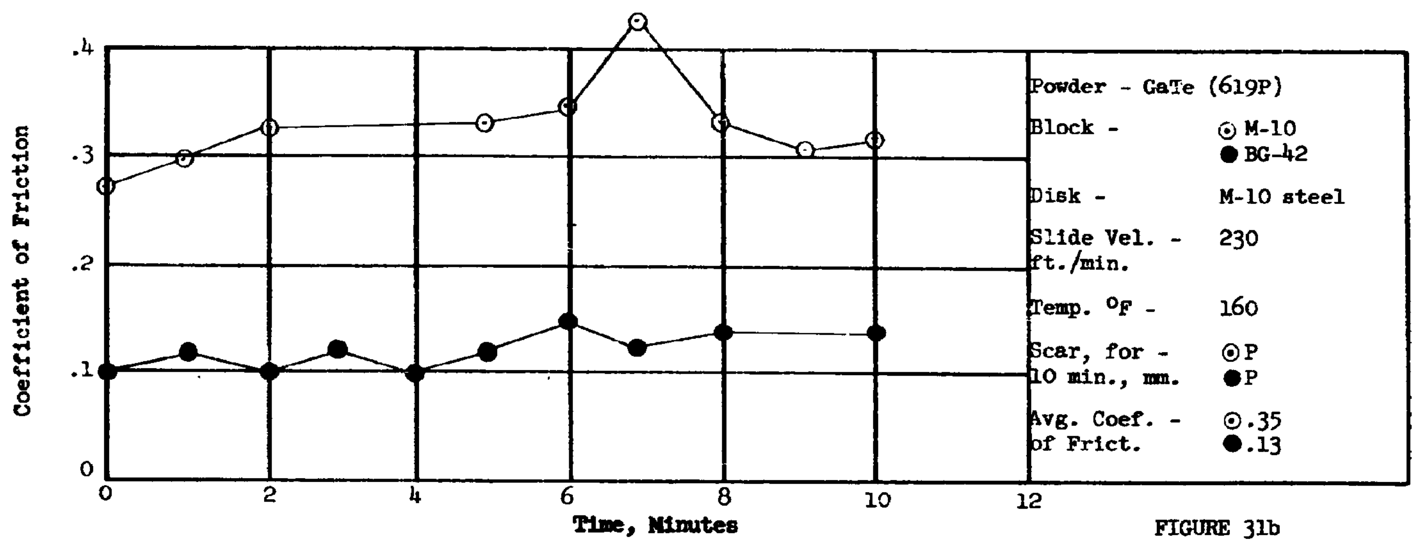

FIGURE 31b

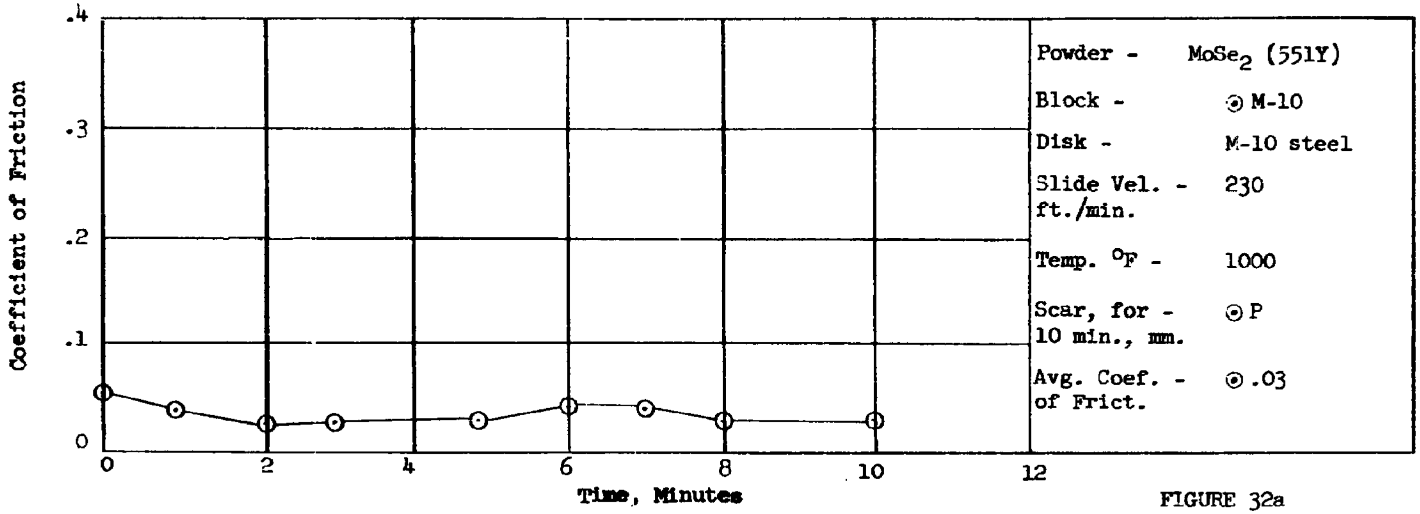

FIGURE 32a

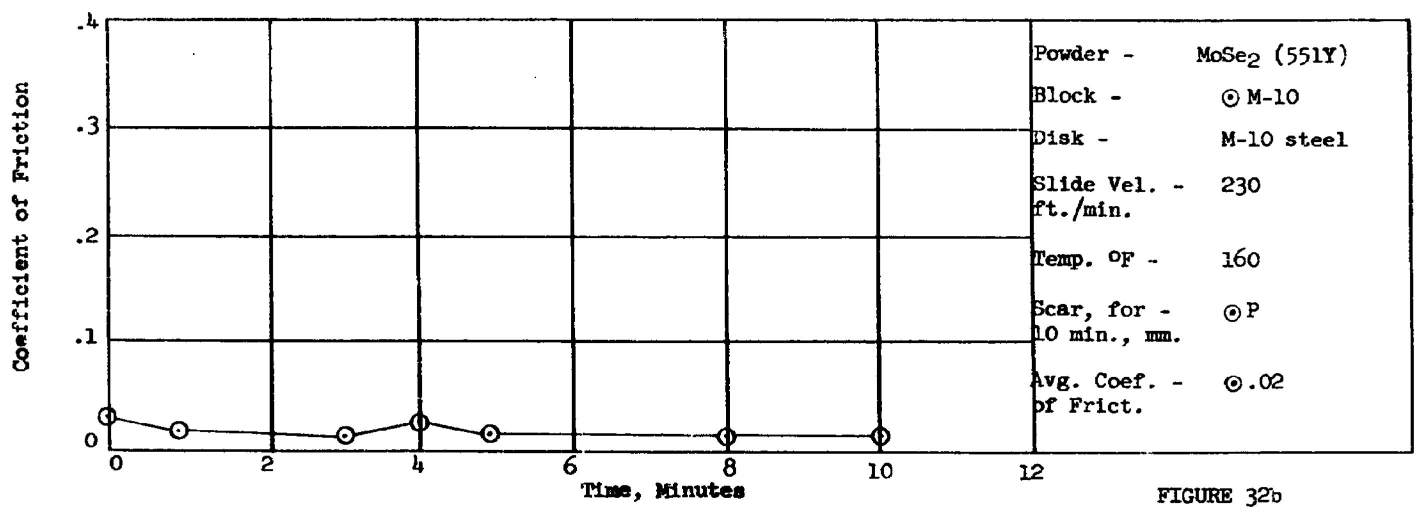

FIGURE 32b

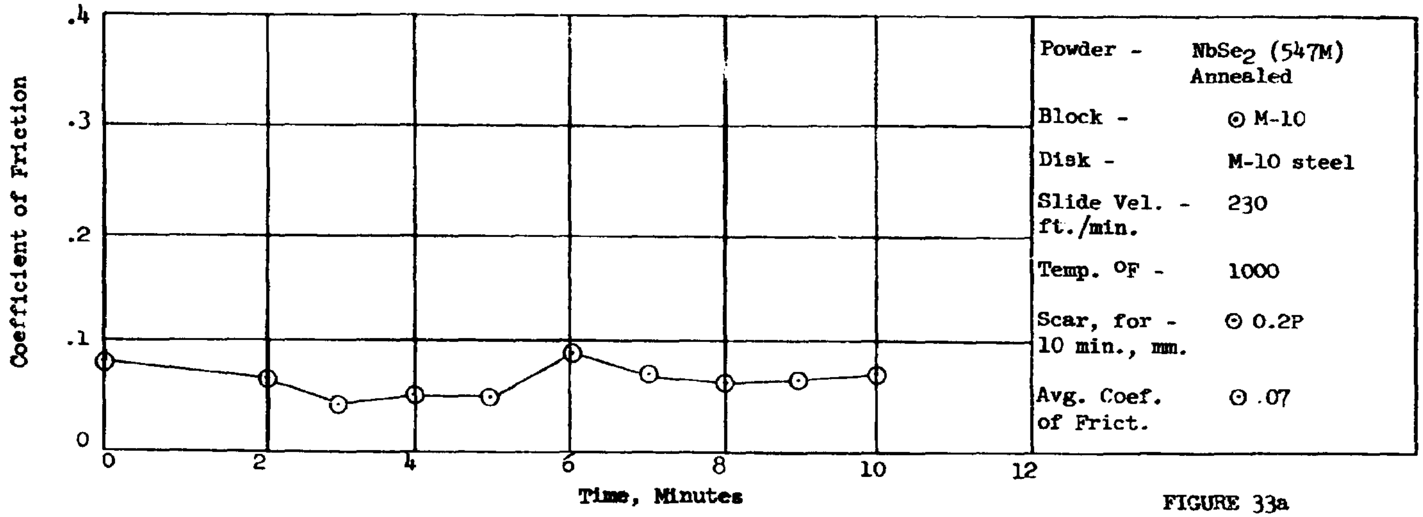

FIGURE 33a

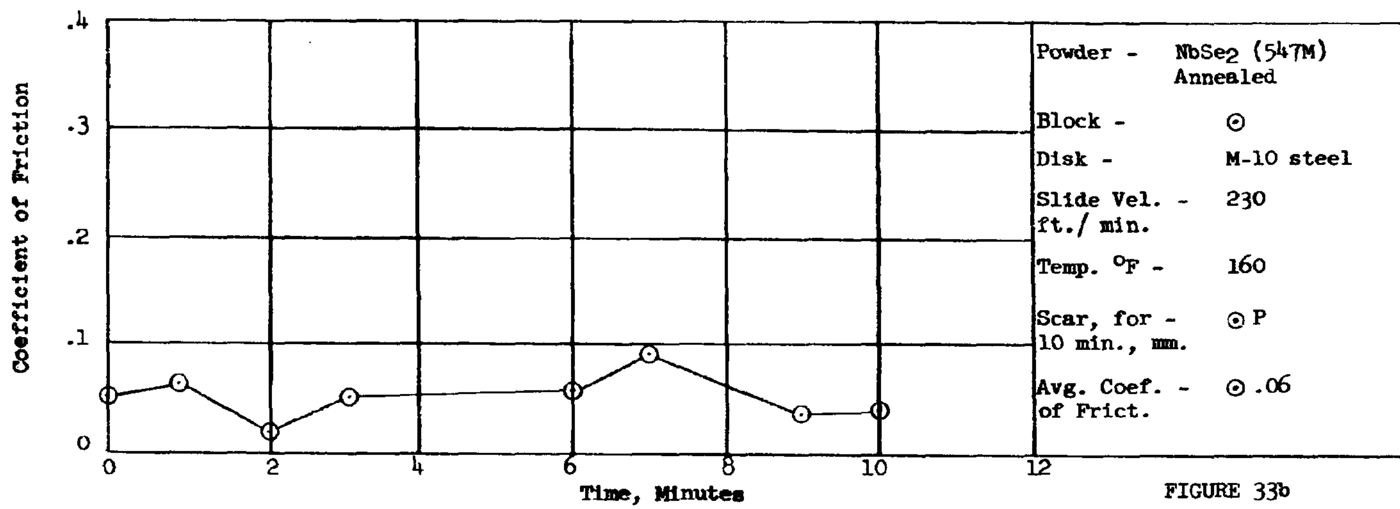

FIGURE 33b

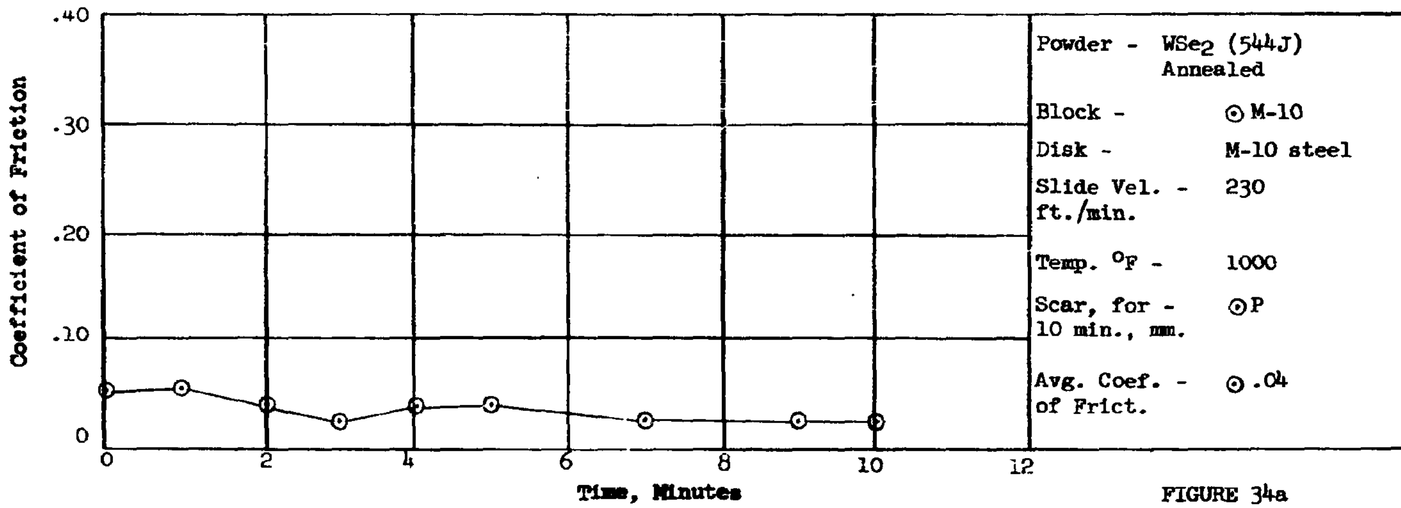

FIGURE 34a

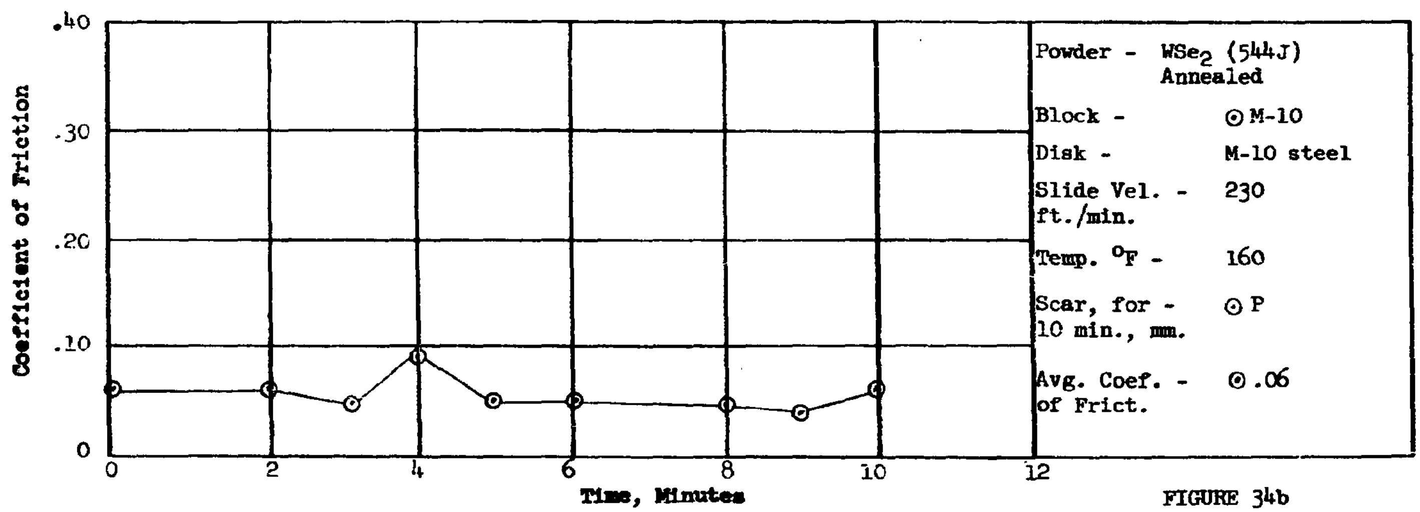

FIGURE 34b

SUMMARY OF WEAR AND FRICTION DATA WITH DRY POWDERS

Powders were evaluated as lubricants rubbing against various block materials and an M-10 tool steel disk at a sliding velocity of 230 ft./min. in a dry nitrogen atmosphere.

Curve Reference (Fig. No.)	Test Material	Test Temp. °F	Block Material	Coefficient of Friction (0 .1 .2 .3 .4 .5)	Average Wear/mm (0 0.4 0.8 1.2 1.6 2.0 2.4)
15a	MoS_2	1000	BG42		P
15a	MoS_2	1000	M10		P
15b	MoS_2	160	BG42		P
15b	MoS_2	160	M10		P
16a	Graphite	1000	BG42		
16b	Graphite	160	M10		P
17a	$CaSO_4$	1000	BG42	.54	P
17a	$CaSO_4$	1000	M10	.52	P
17b	$CaSO_4$	160	BG42		P
17c	$CaSO_4$	160	M10		P
18a	$RhSb_2$	1000	BG42		
18b	BN	1000	BG42	.67	
19a	$PbCrO_4$	1000	M10		
19a	$PbCrO_4$	1000	BG42		
19b	$PbCrO_4$	160	M10		P
19b	$PbCrO_4$	160	BG42		P
20a	PbS	1000	M10		P
20a	PbS	1000	BG42		
20b	PbS	160	M10		P
20b	PbS	160	BG42		
21a	Sb_2S_3	1000	M10		P
21a	Sb_2S_3	1000	BG42		P
21b	Sb_2S_3	160	M10		P
21b	Sb_2S_3	160	BG42		P
22a	$MgSO_4$	1000	M10		
22a	$MgSO_4$	1000	BG42		
22b	$MgSO_4$	160	M10		P
22b	$MgSO_4$	160	BG42		
23a	BaF_2	1000	M10	.53	
23a	BaF_2	1000	BG42		
23b	BaF_2	160	M10		
23b	BaF_2	160	BG42		
24a	AgI	1000	M10		P
24a	AgI	1000	BG42		P
24b	AgI	160	M10		P
24b	AgI	160	BG42		P
25a	AgBr	1000	BG42		P
25b	$KTiO_3$	1000	BG42	.84	
26a	MnTe	1000	BG42		
26b	MnSe	1000	BG42		
27a	$NiTe_2$	1000	BG42		
27b	$PtTe_2$	1000	BG42		
28a	FeTe	1000	BG42		
28b	GaTe	1000	BG42		
29a	OsTe	1000	BG42		
29b	$CdCl_2$	1000	BG42		
30a	WSe_2	1000	M10		P
30a	WSe_2	1000	BG42		P
30b	WSe_2	160	M10		P
30b	WSe_2	160	BG42		P
31a	GaTe	1000	M10		P
31a	GaTe	1000	BG42		P
31b	GaTe	160	M10		P
31b	GaTe	160	BG42		P
32a	$MoSe_2$	1000	M10		P
32b	$MoSe_2$	160	M10		P
33a	$NbSe_2$	1000	M10		P
33b	$NbSe_2$	160	M10		P
34a	WSe_2	1000	M10		P
34b	WSe_2	160	M10		P

FIGURE 35

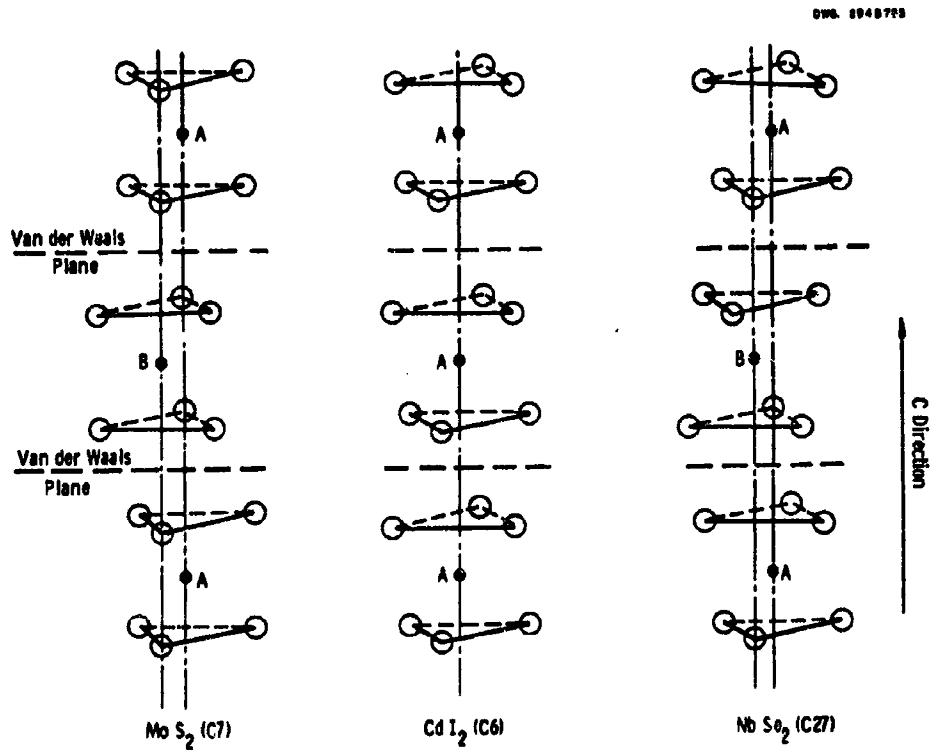

SCHEMATIC REPRESENTATION OF CRYSTAL STRUCTURES OF MoS_2, CdI_2, AND $NbSe_2$

● METAL

○ NON METAL

FIGURE 36

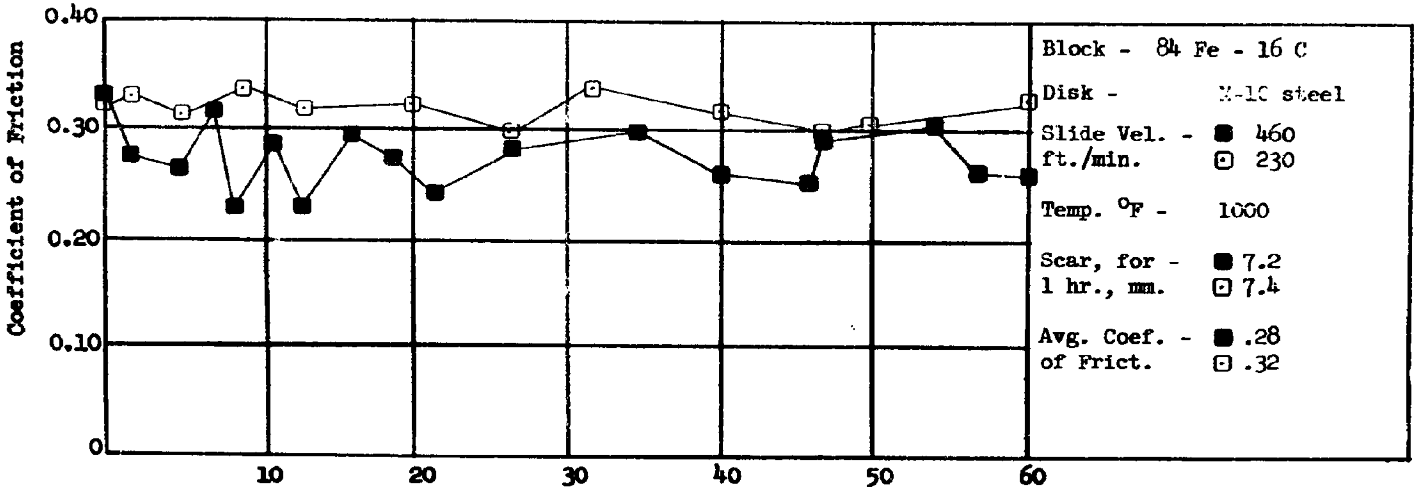

FIGURE 37a

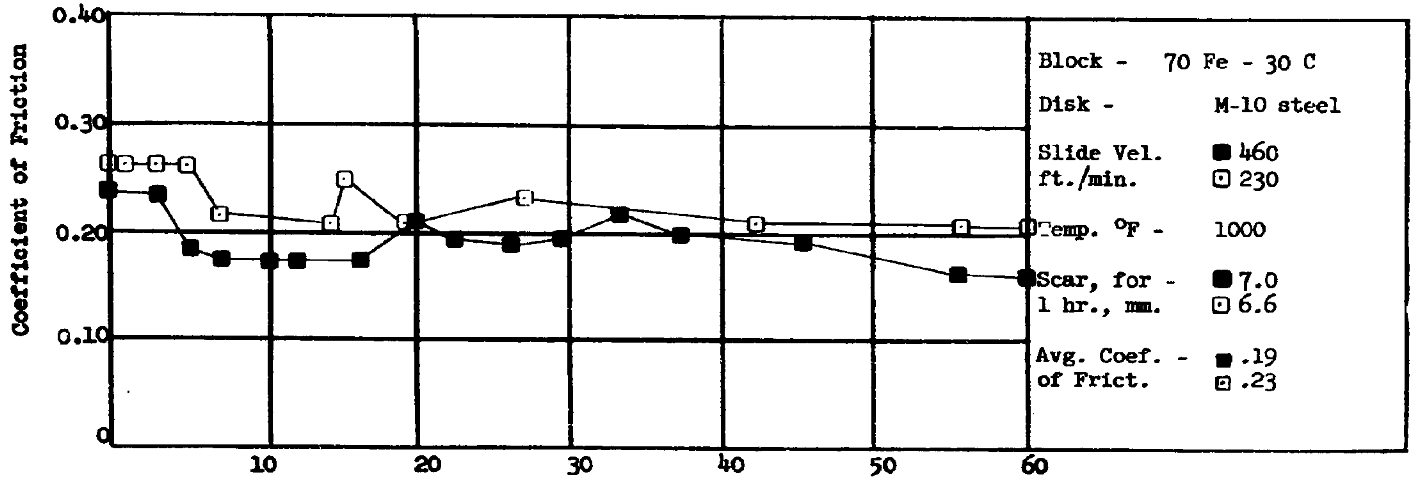

FIGURE 37b

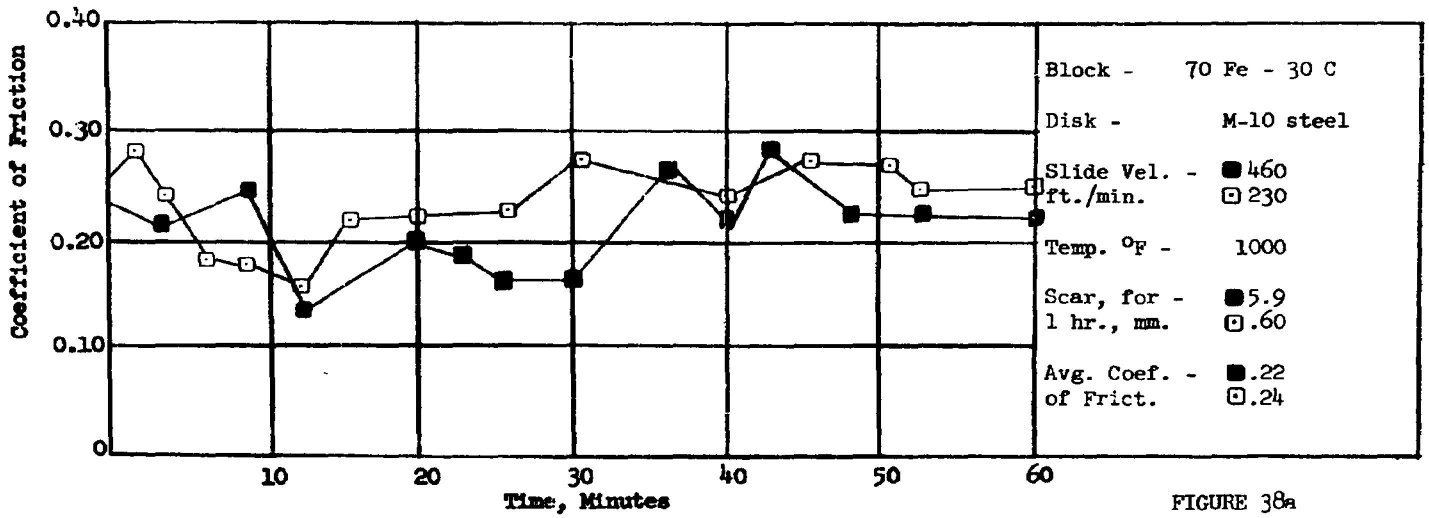

FIGURE 38a

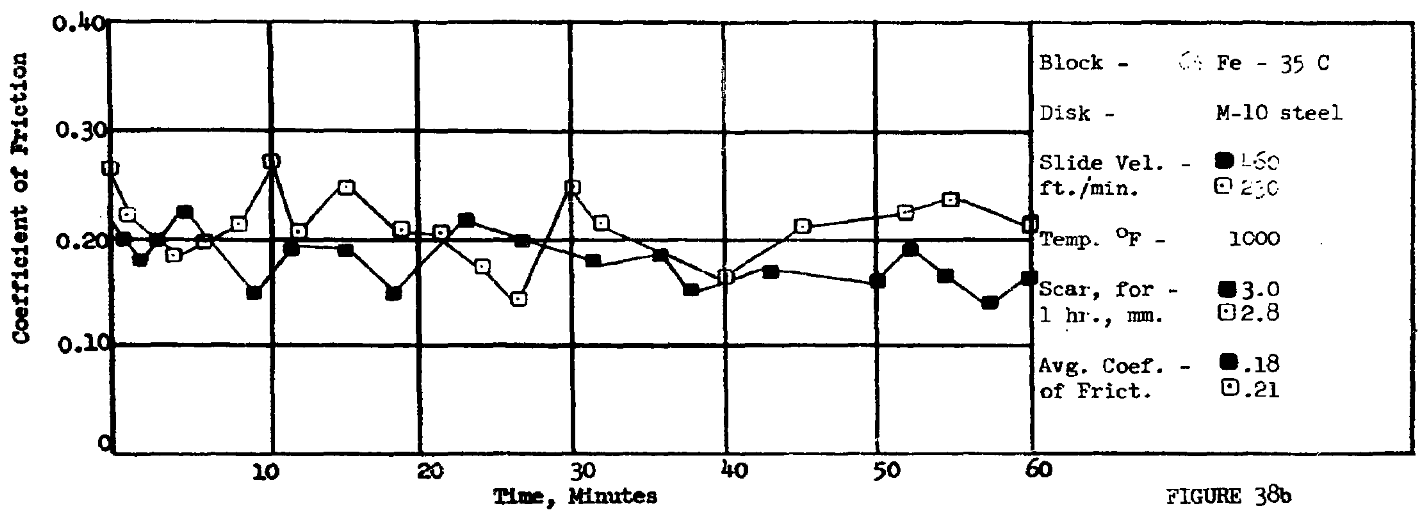

FIGURE 38b

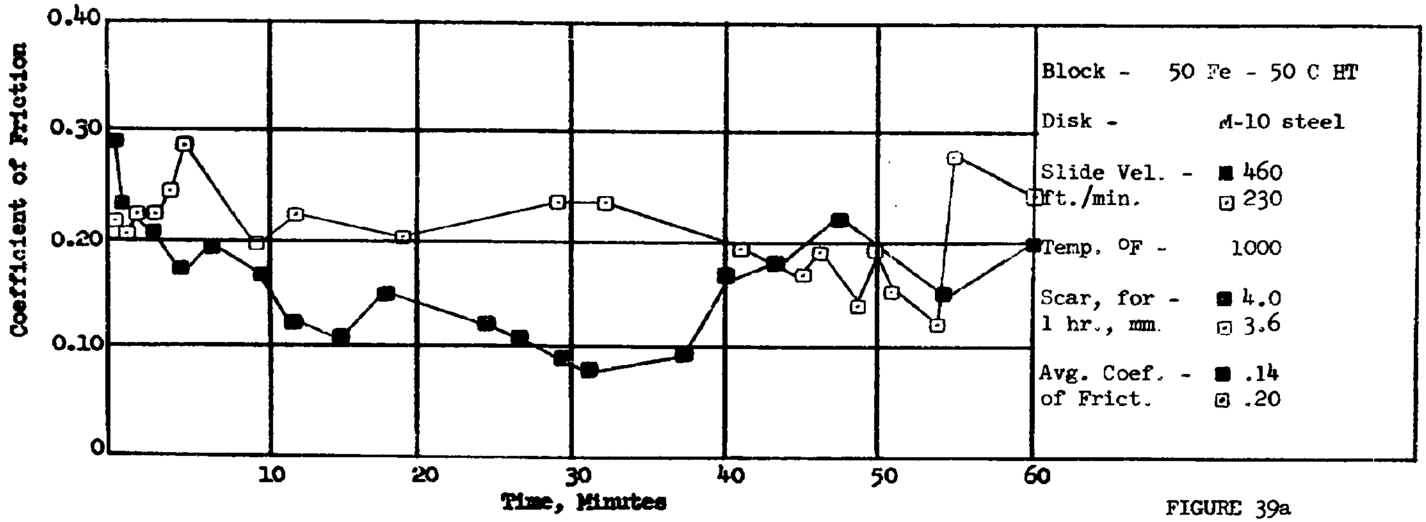

FIGURE 39a

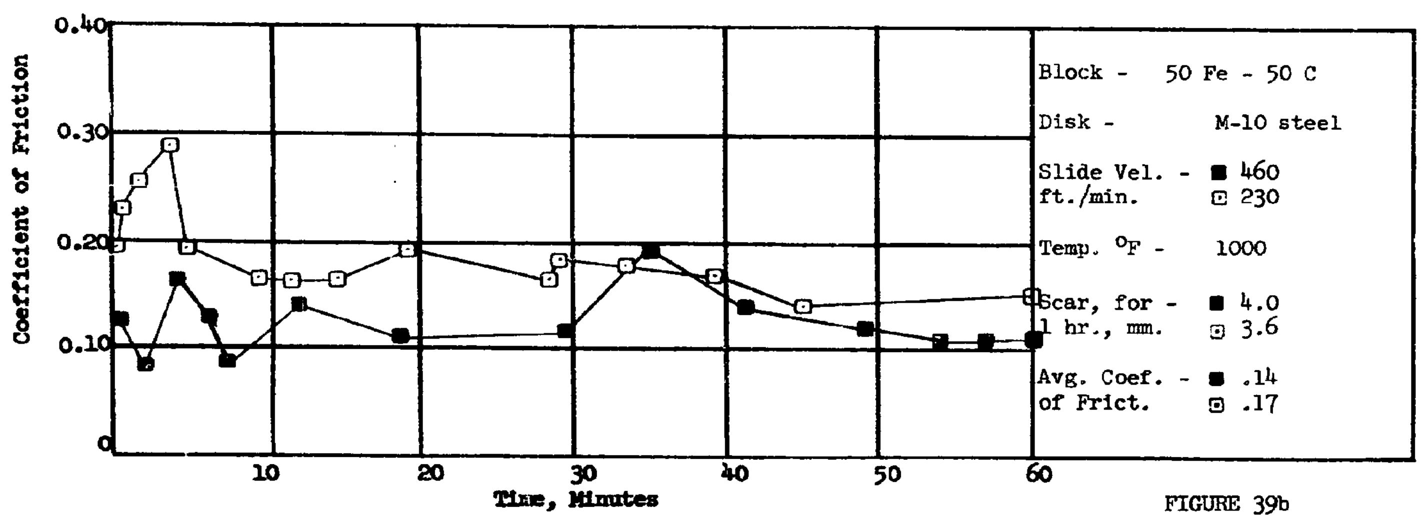

FIGURE 39b

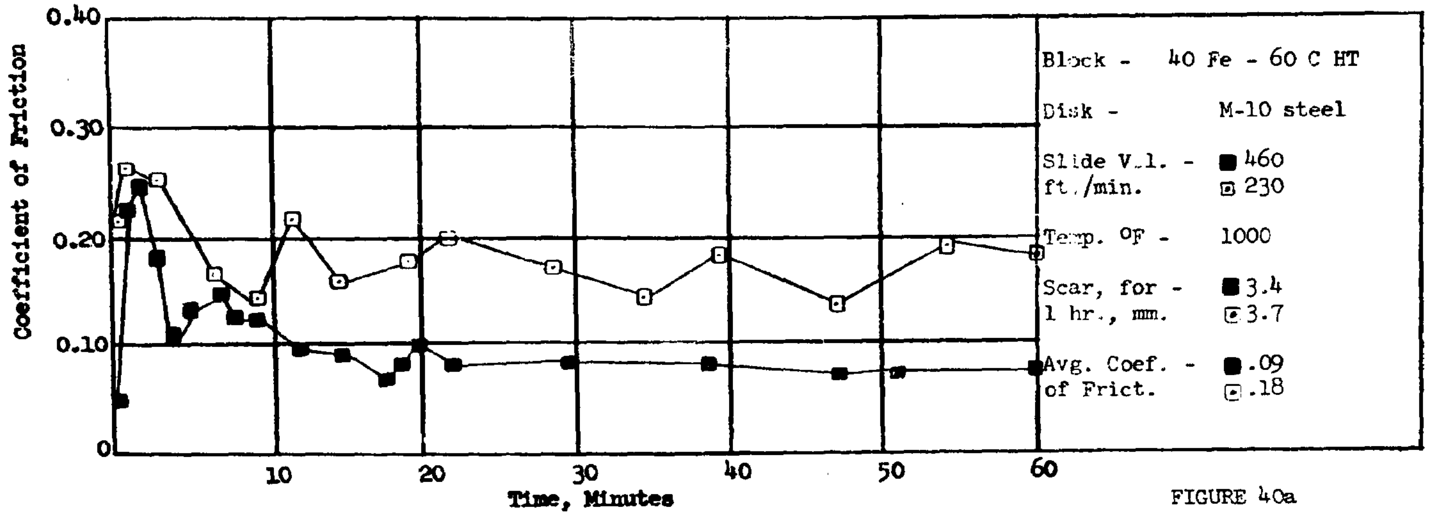

FIGURE 40a

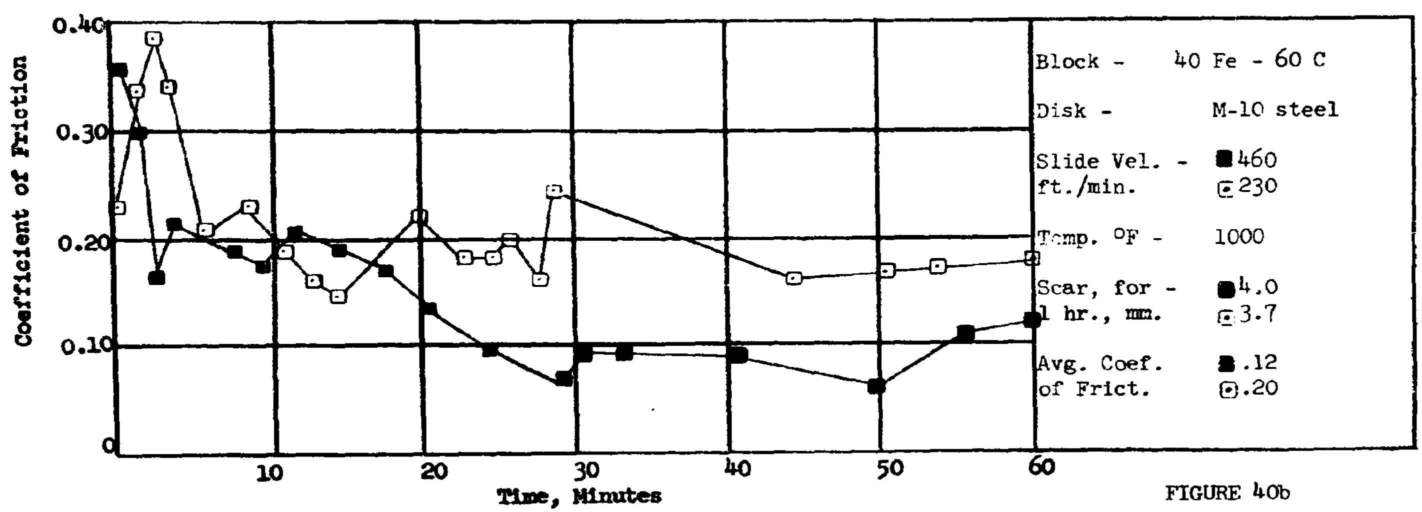

FIGURE 40b

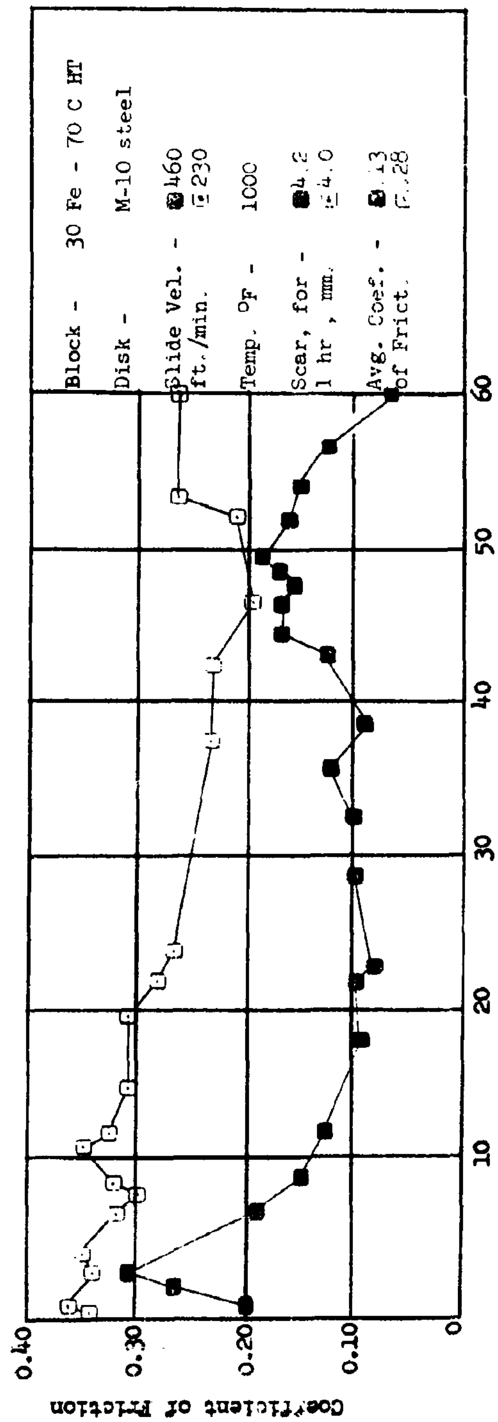

FIGURE 41a

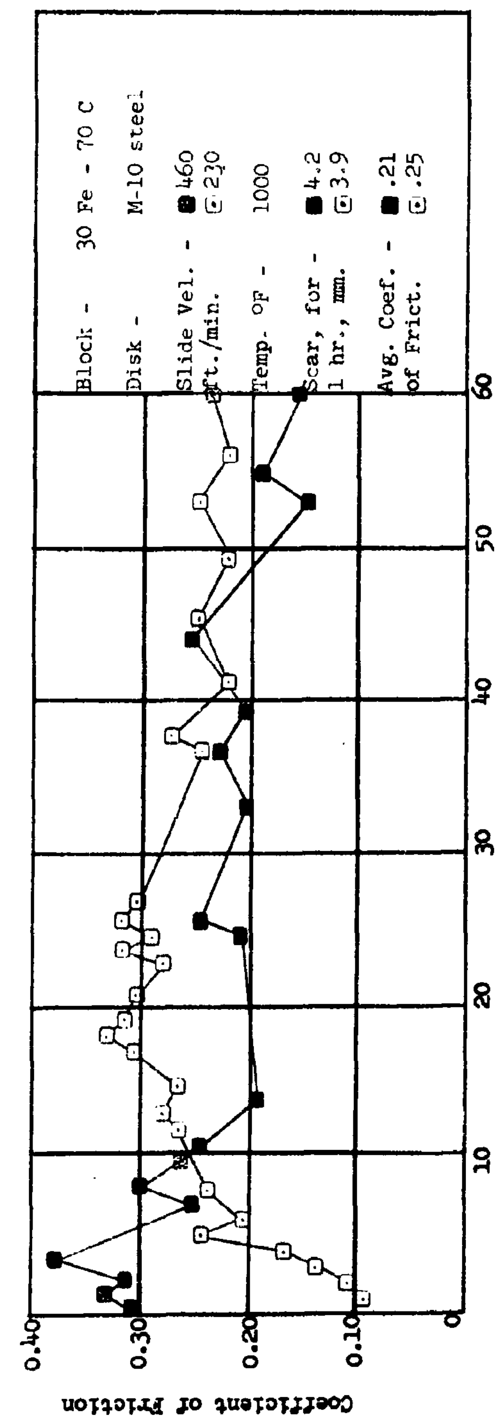

FIGURE 41b

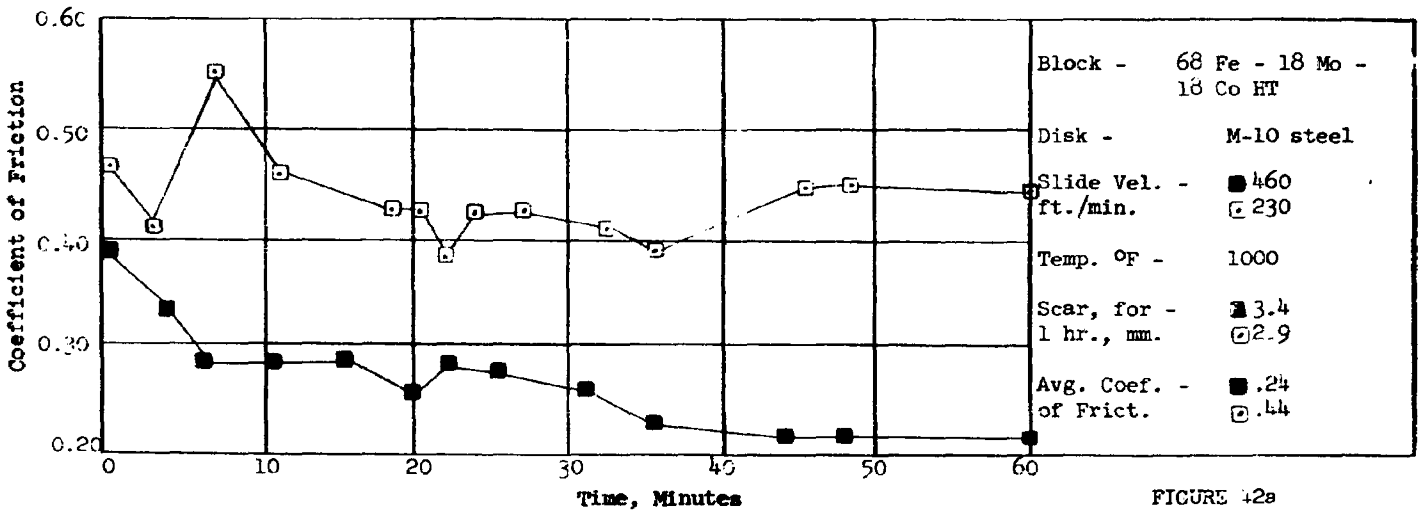

FIGURE 42a

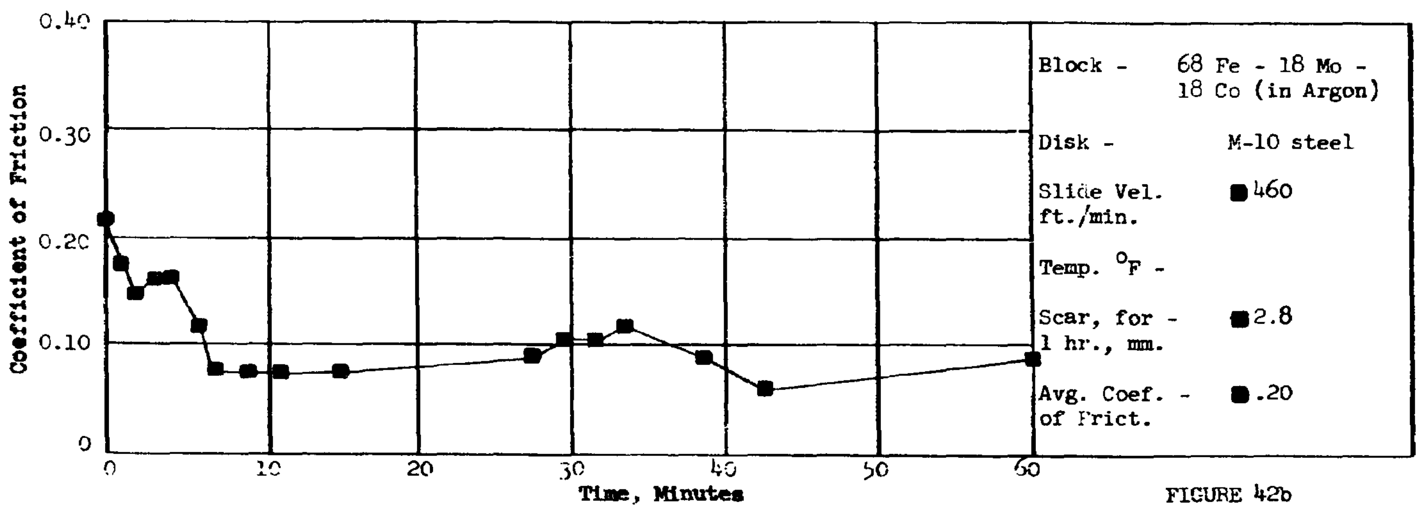

FIGURE 42b

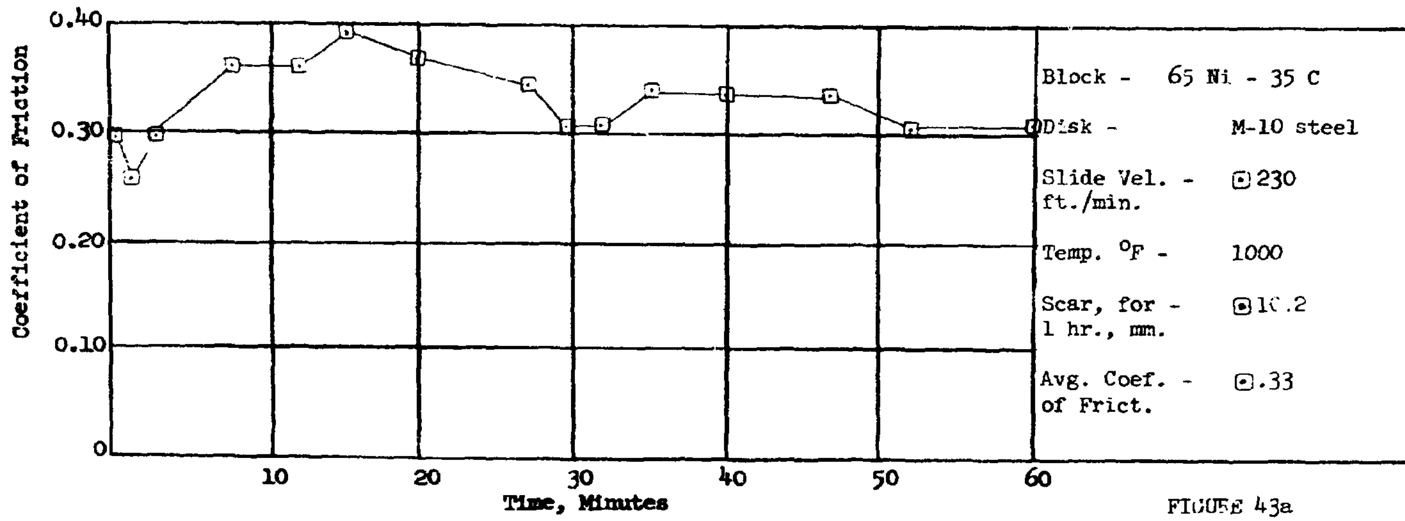

FIGURE 43a

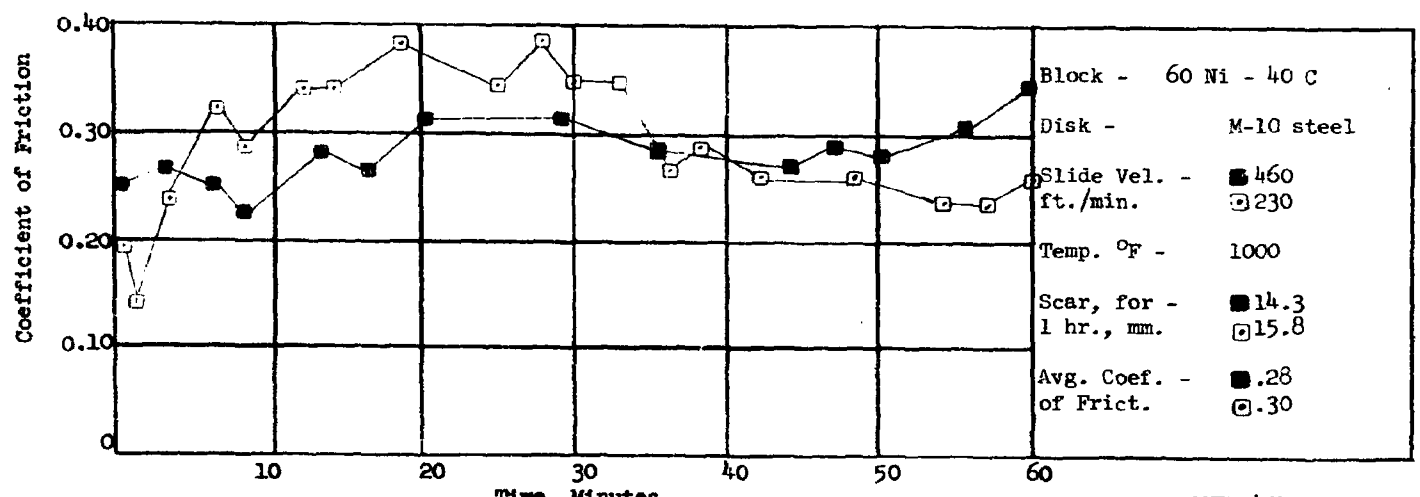

FIGURE 43b

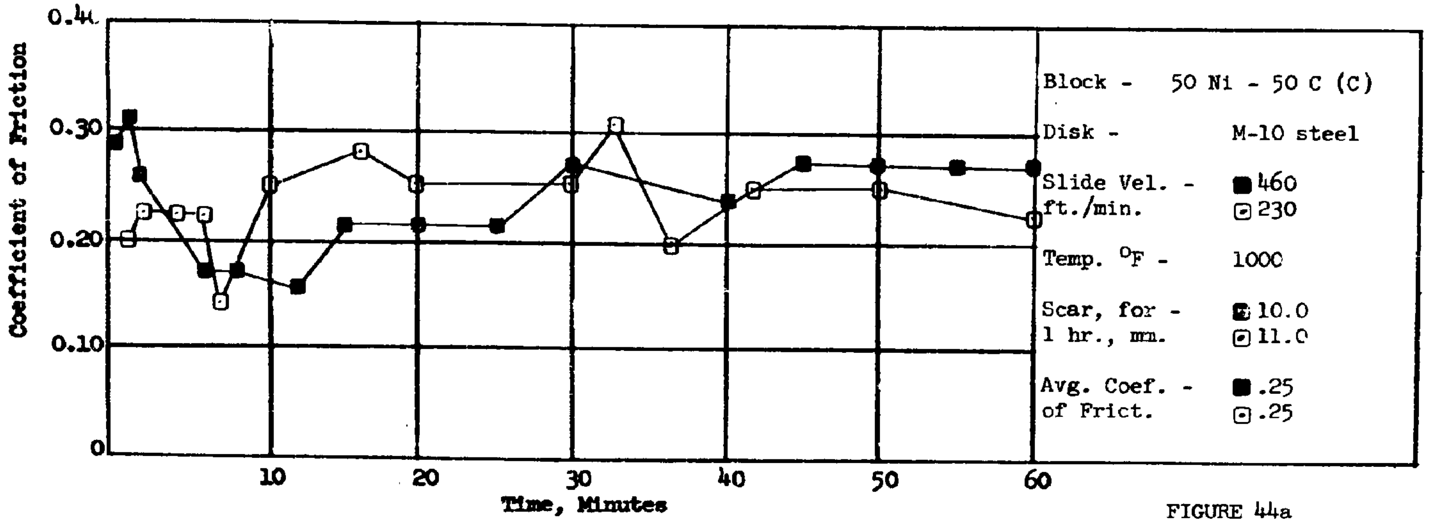

FIGURE 44a

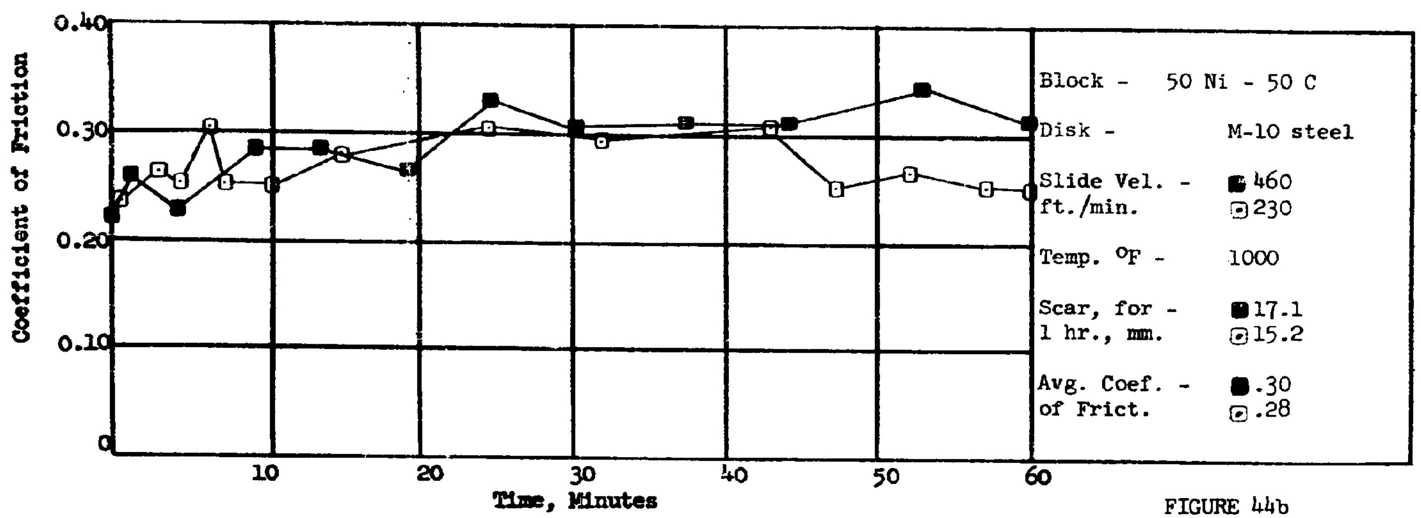

FIGURE 44b

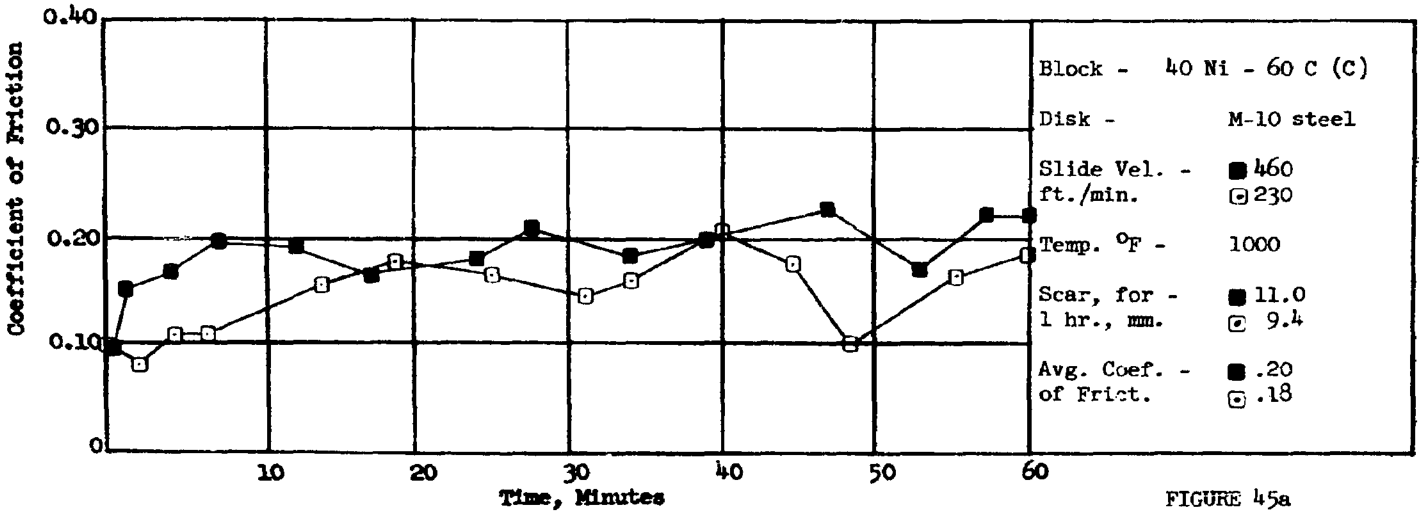

FIGURE 45a

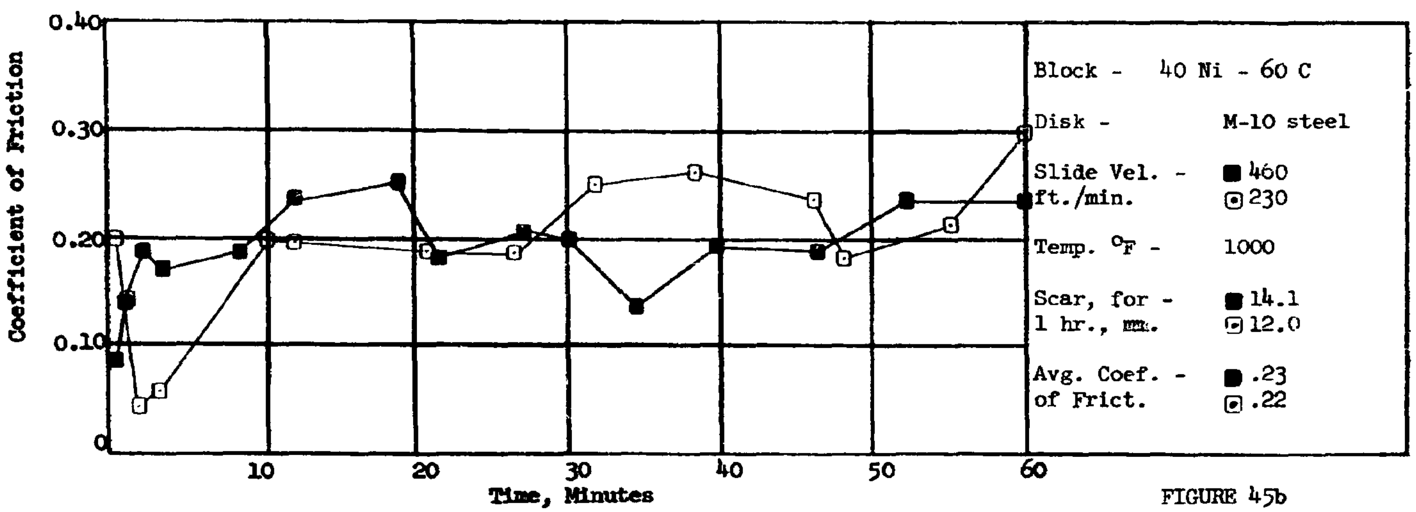

FIGURE 45b

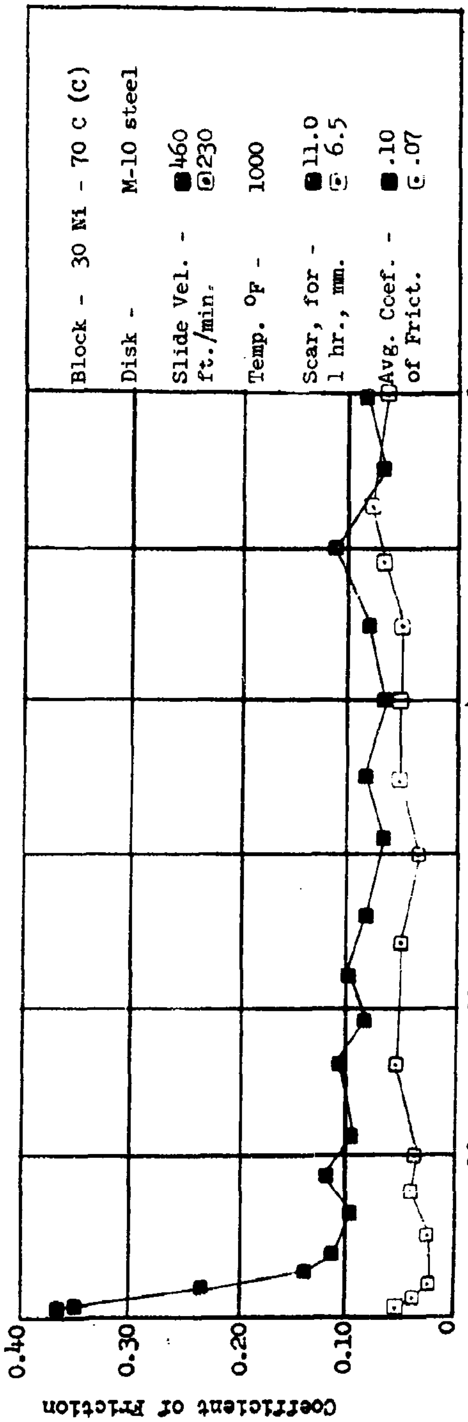

FIGURE 46a

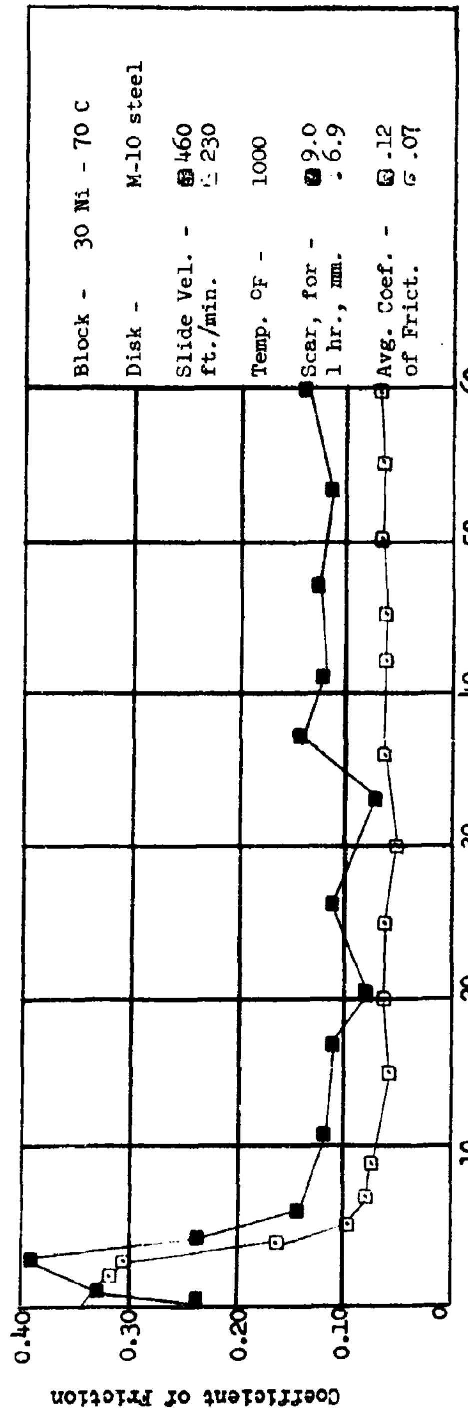

FIGURE 46b

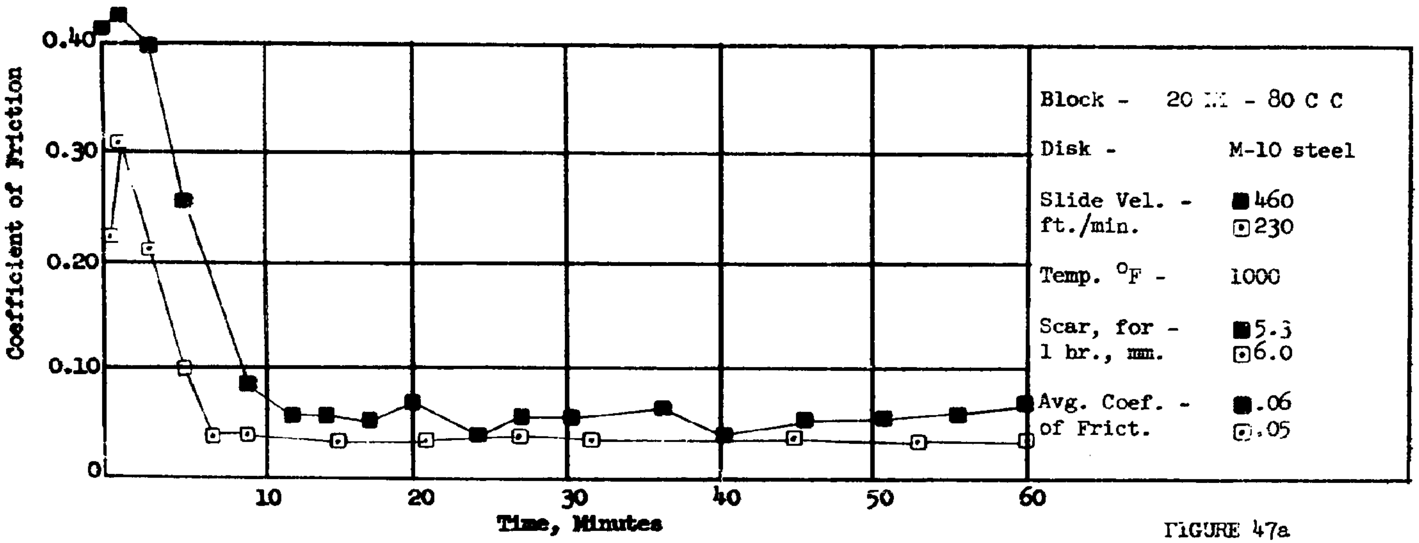

FIGURE 47a

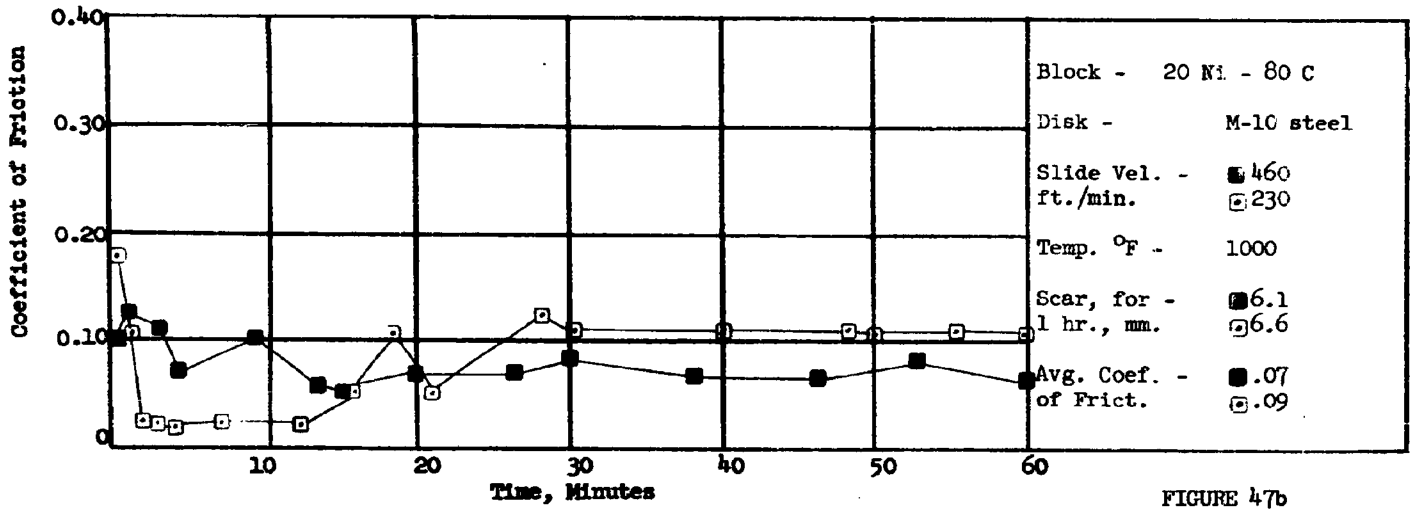

FIGURE 47b

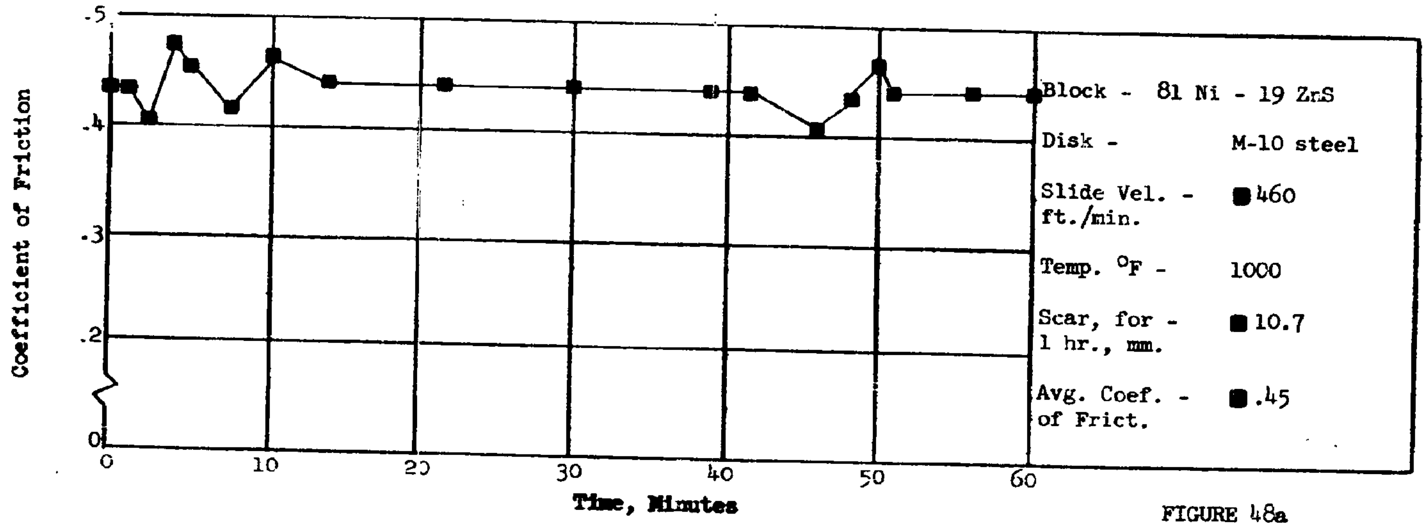

FIGURE 48a

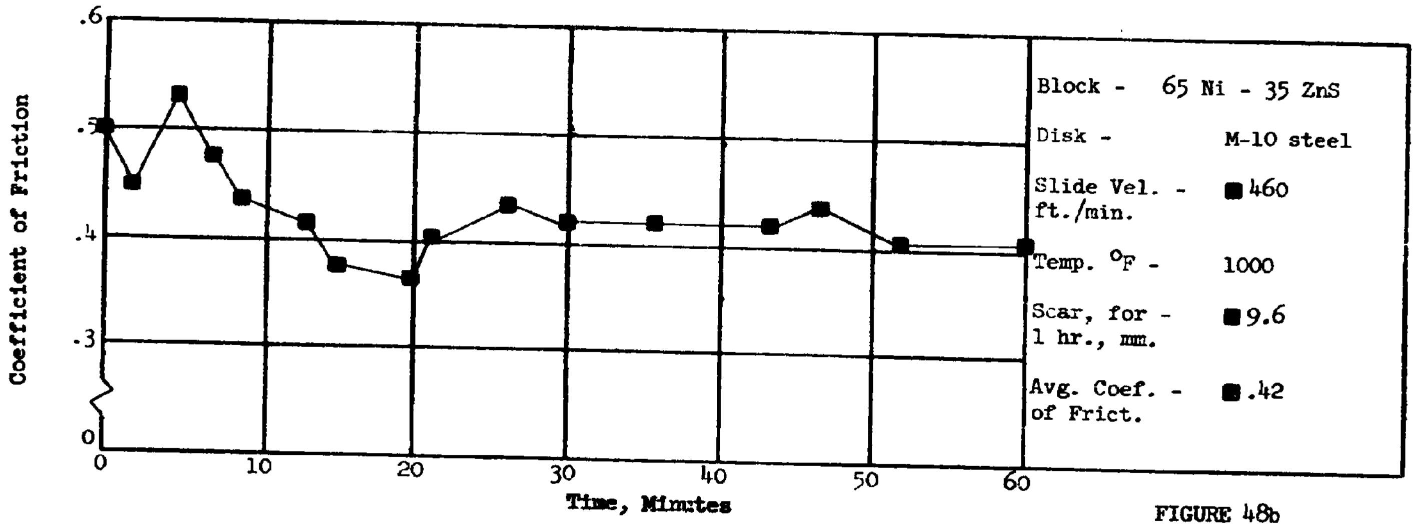

FIGURE 48b

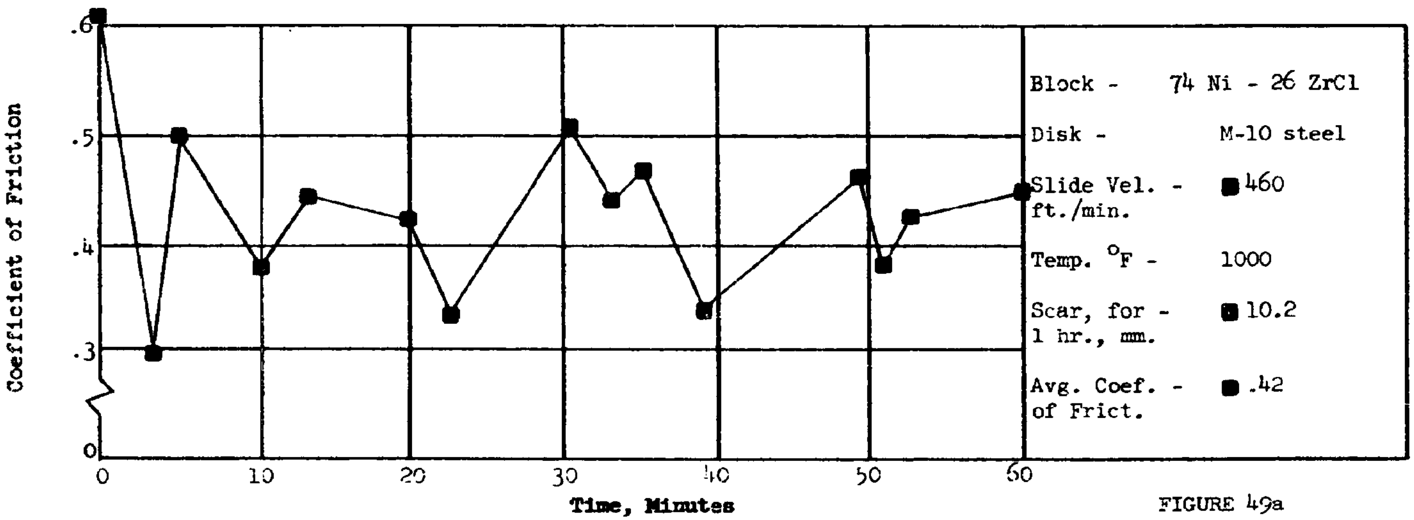

FIGURE 49a

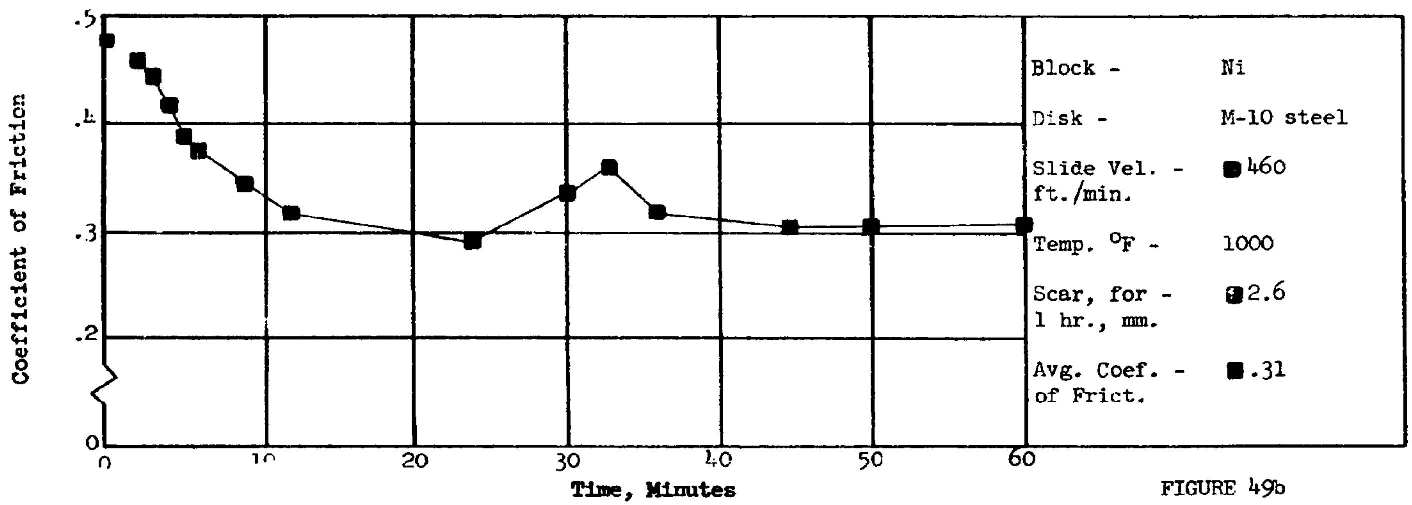

FIGURE 49b

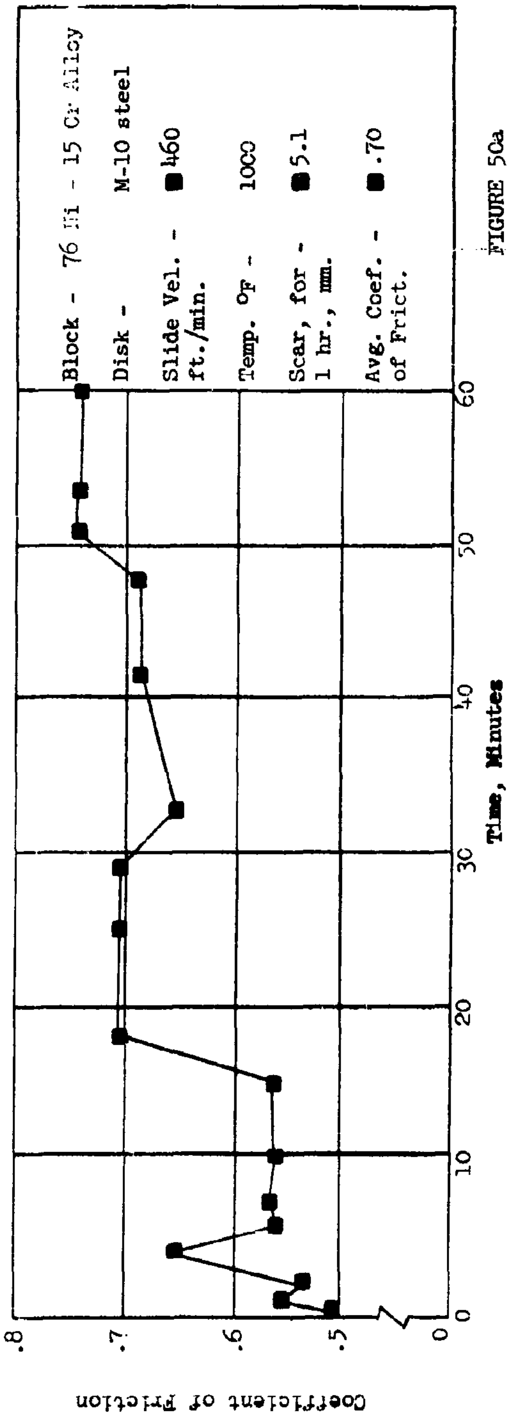

FIGURE 50a

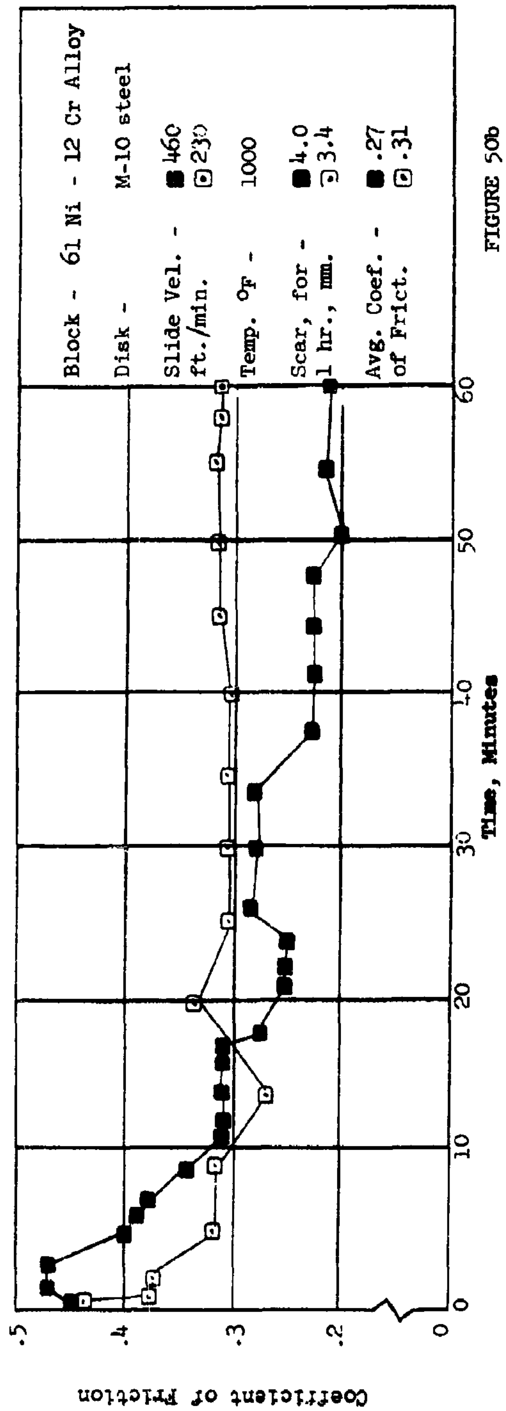

FIGURE 50b

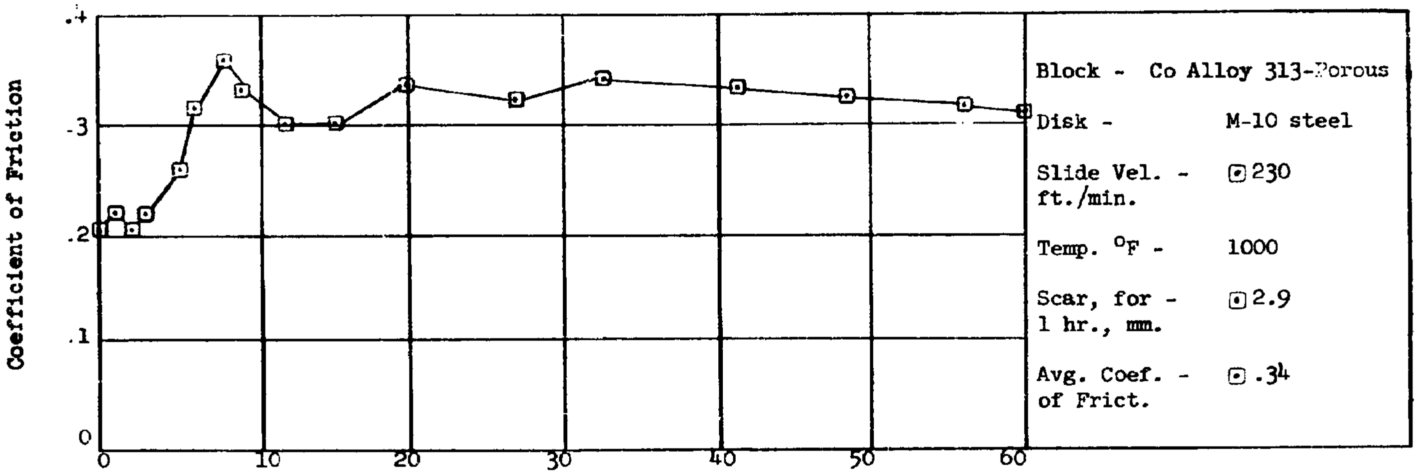

FIGURE 51a

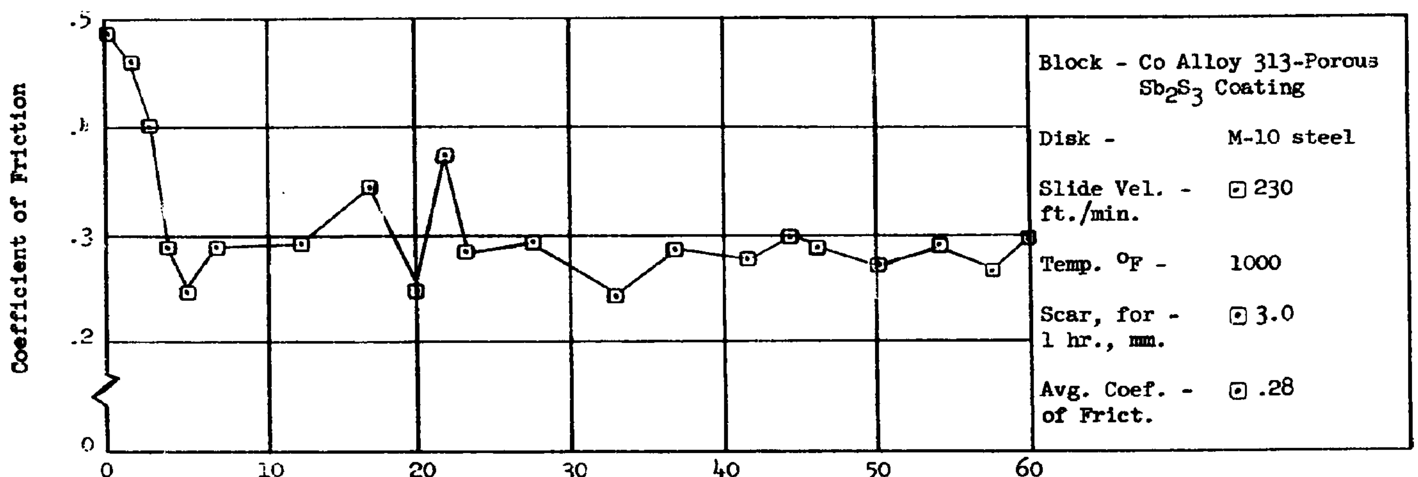

FIGURE 51b

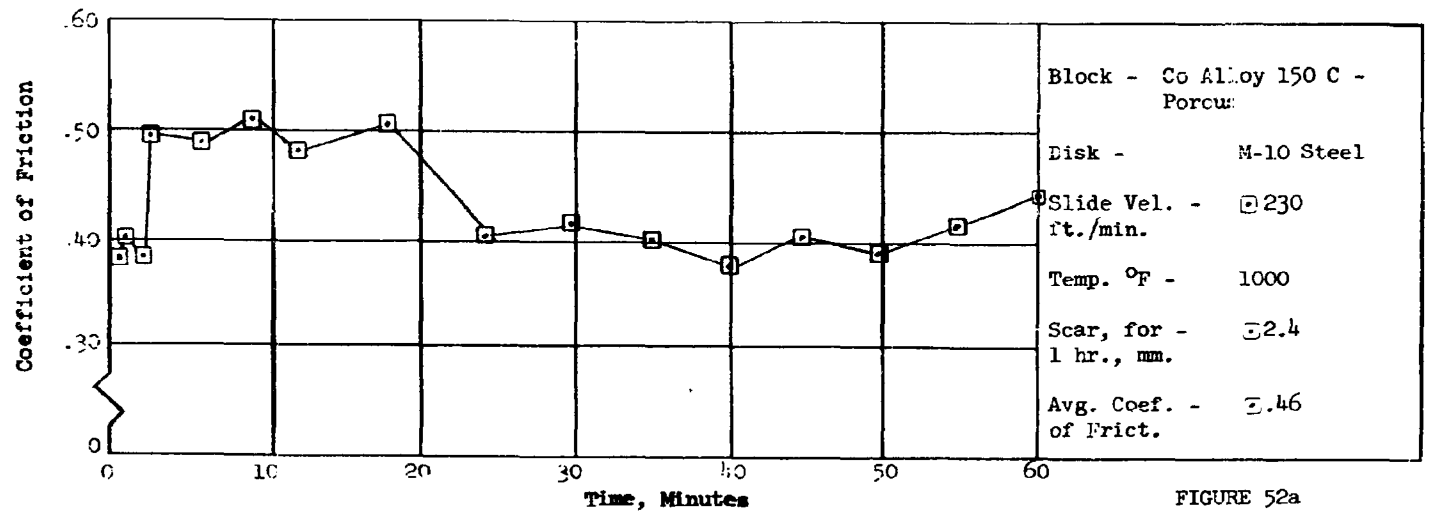

FIGURE 52a

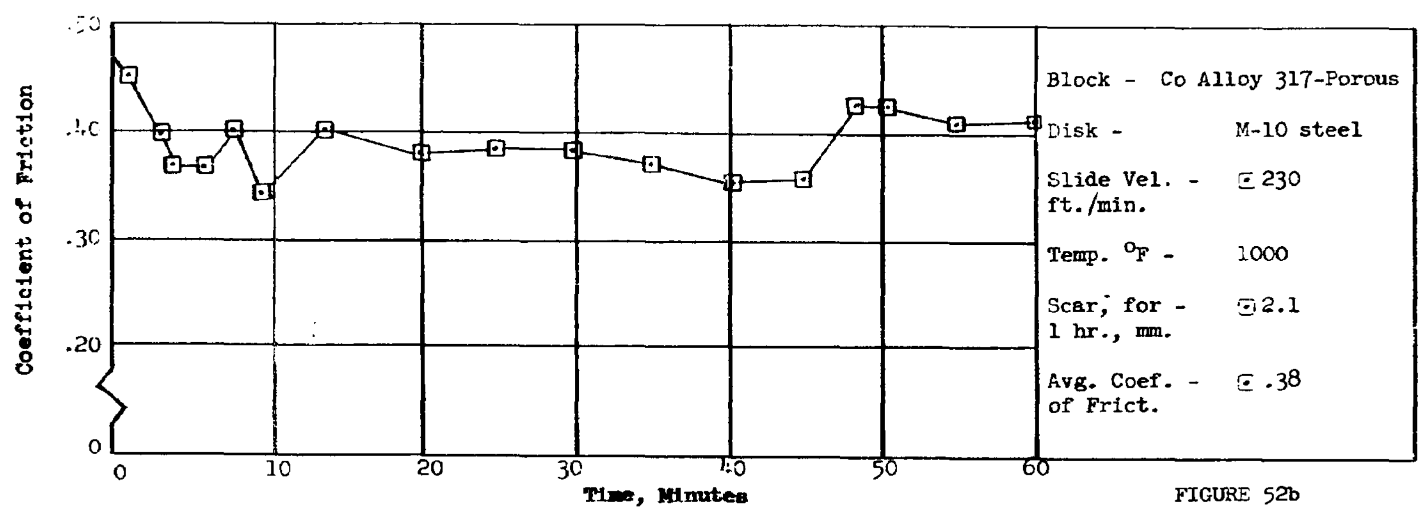

FIGURE 52b

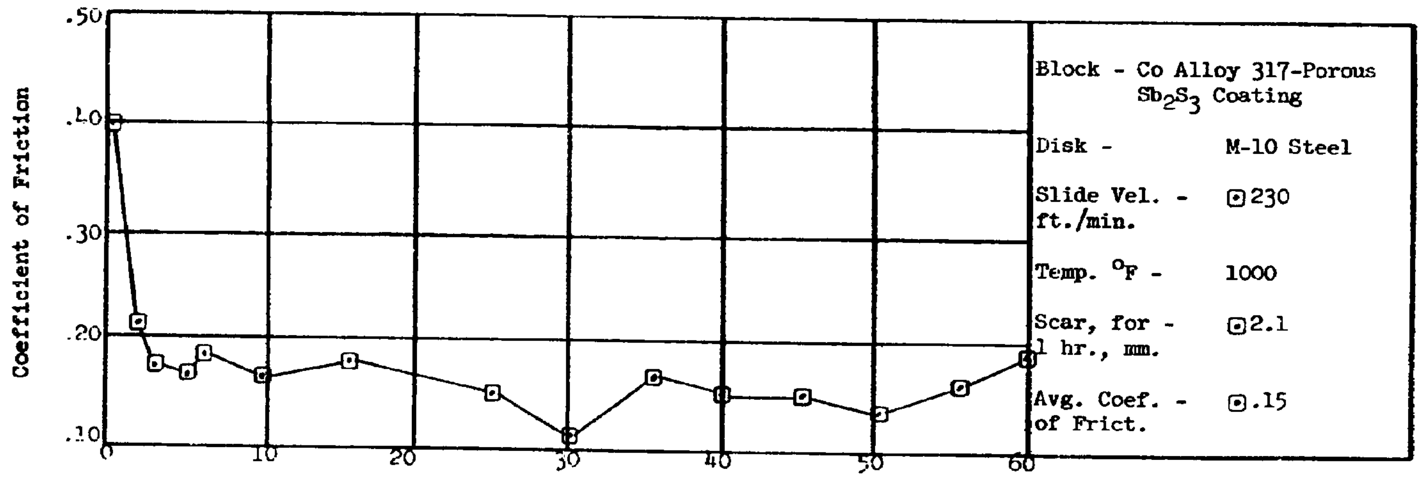

FIGURE 53a

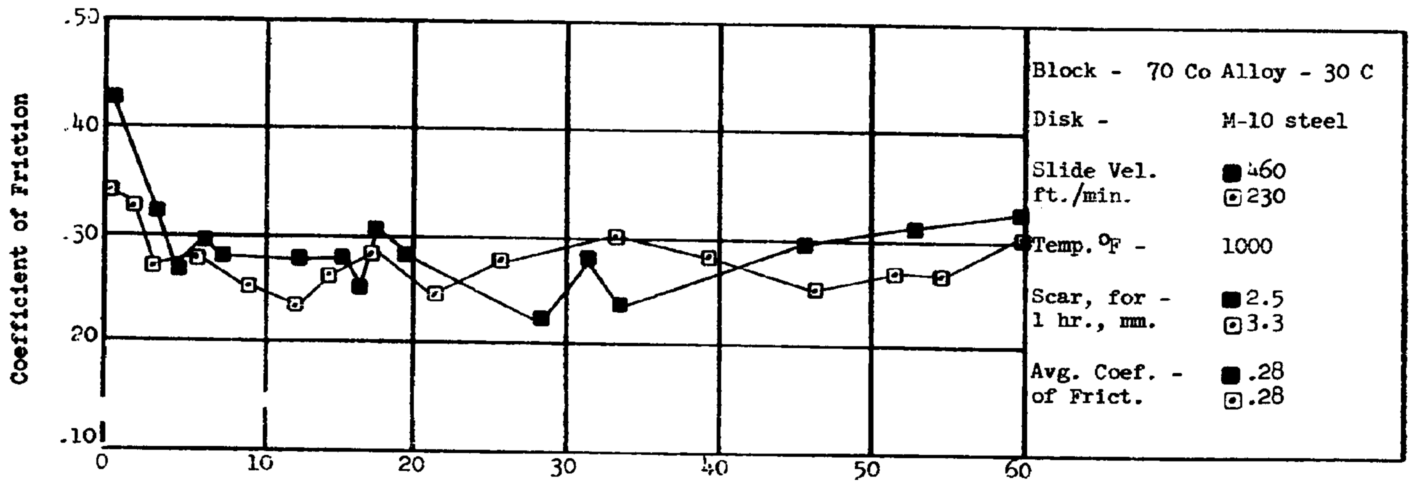

FIGURE 53b

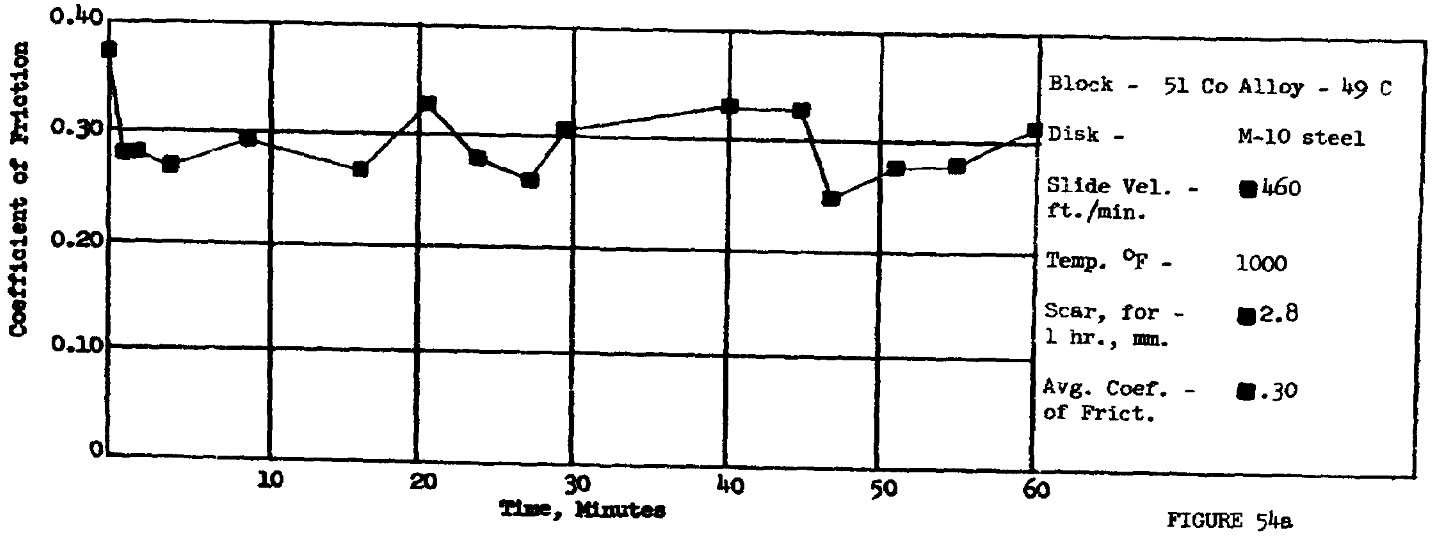

FIGURE 54a

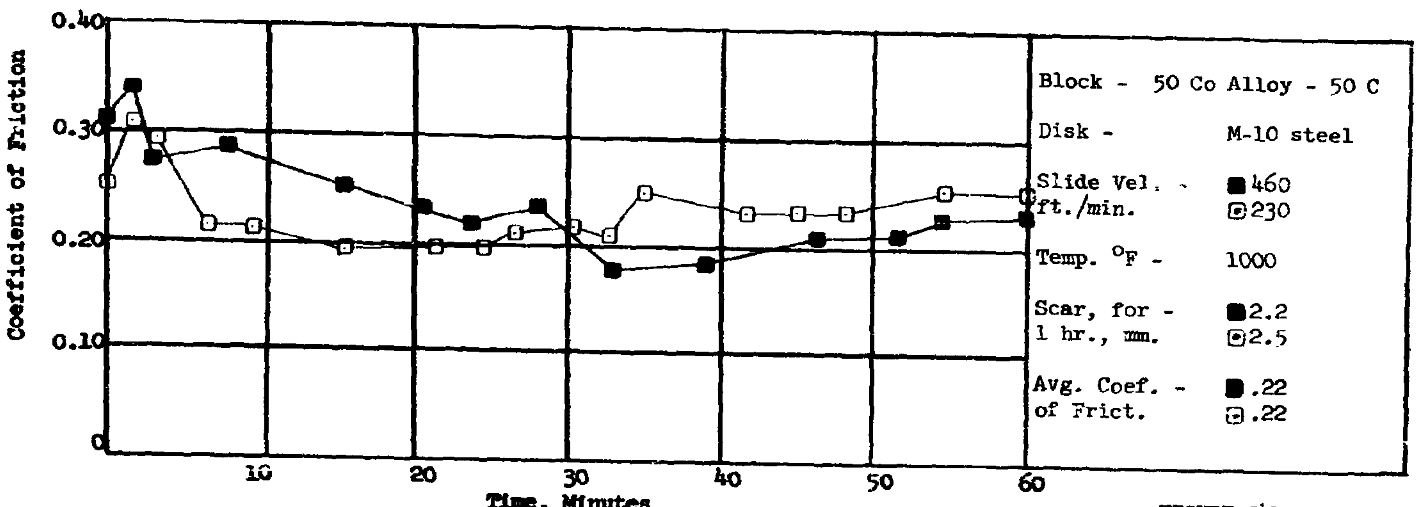

FIGURE 54b

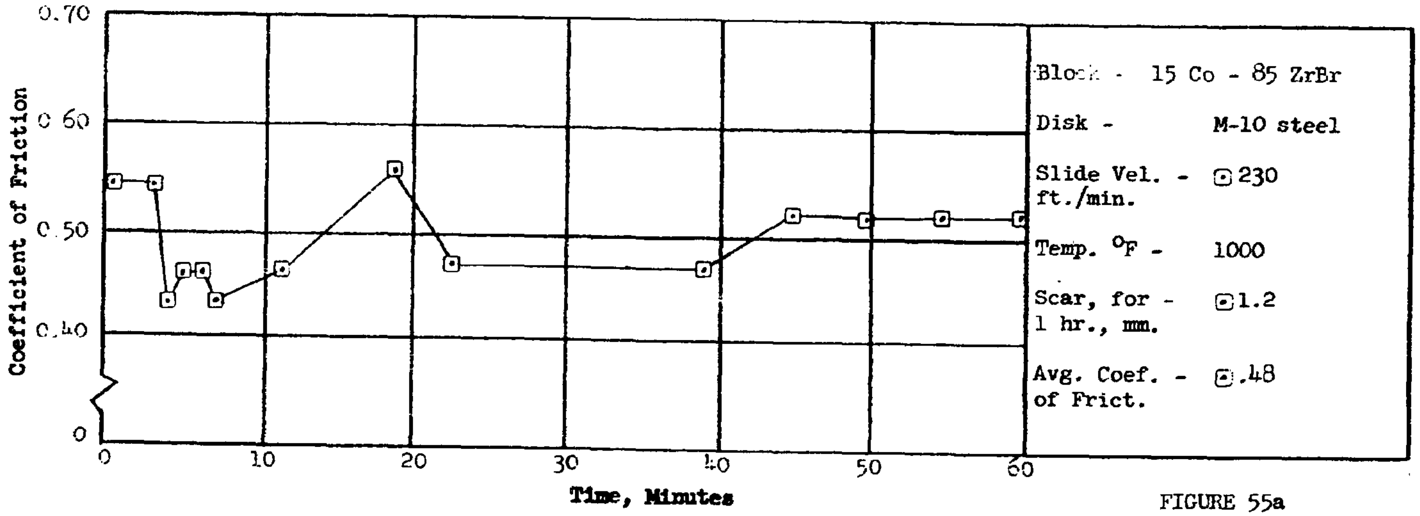

FIGURE 55a

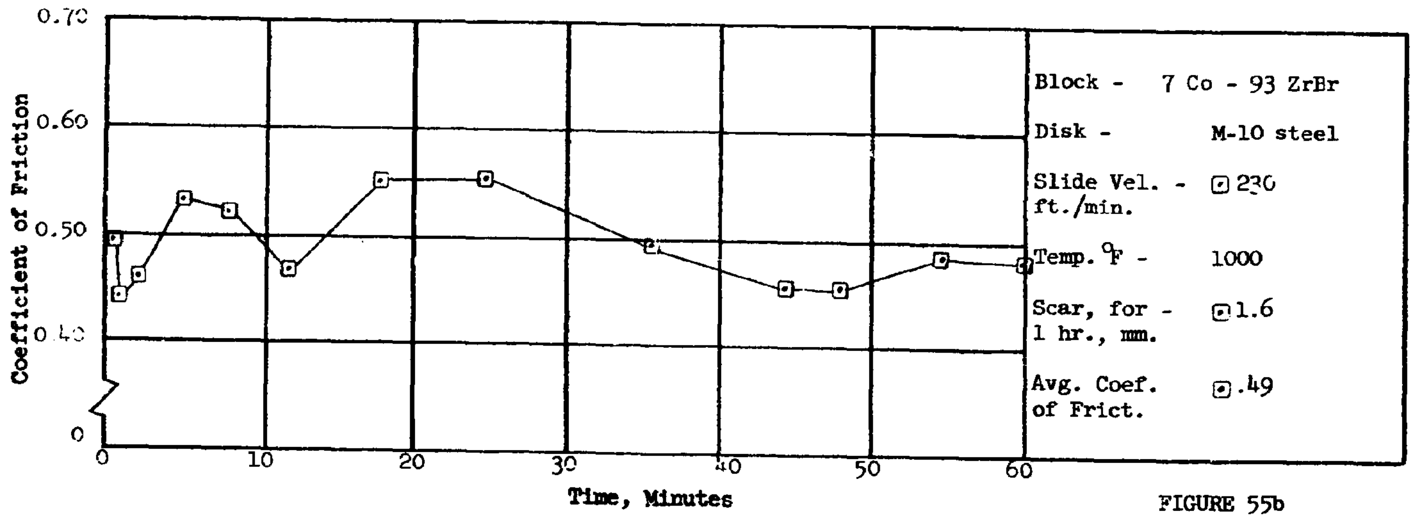

FIGURE 55b

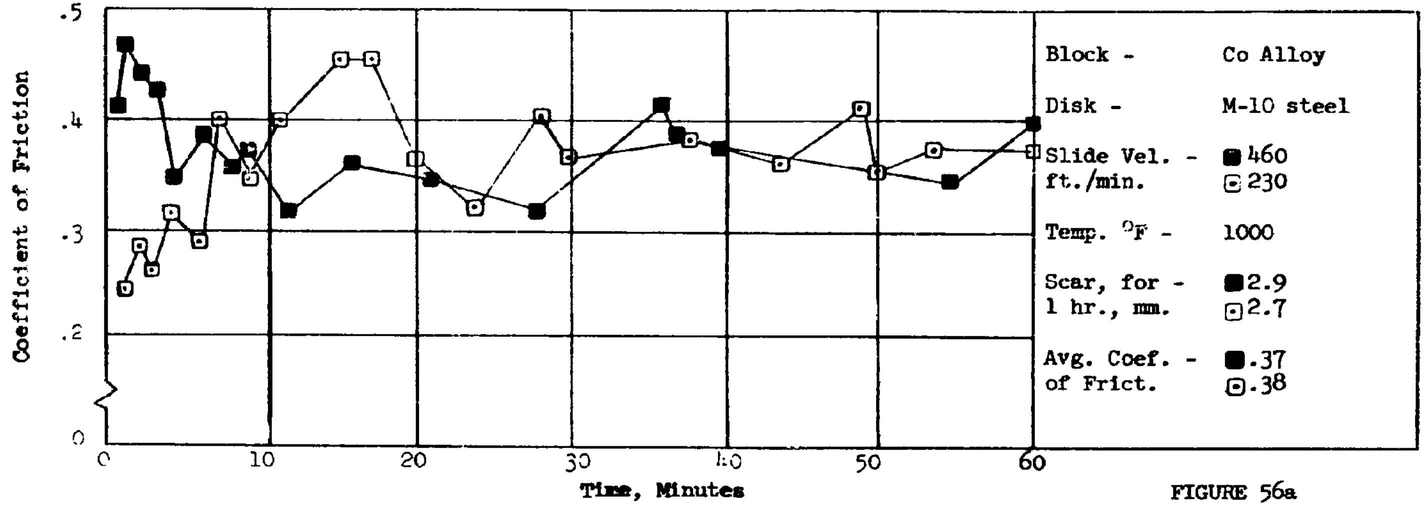

FIGURE 56a

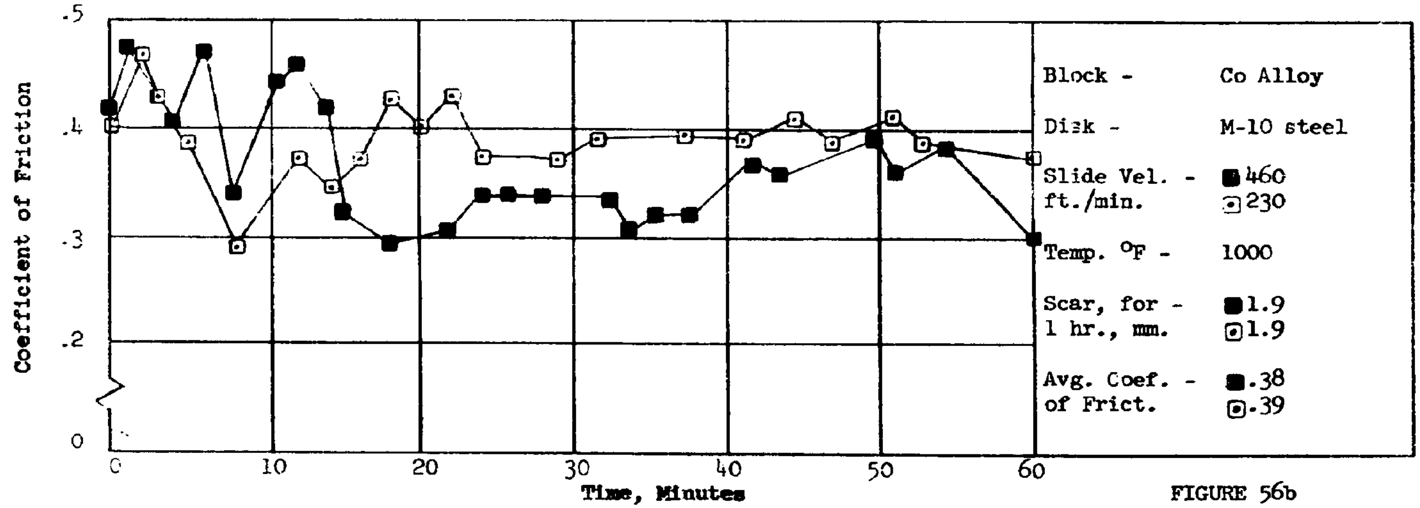

FIGURE 56b

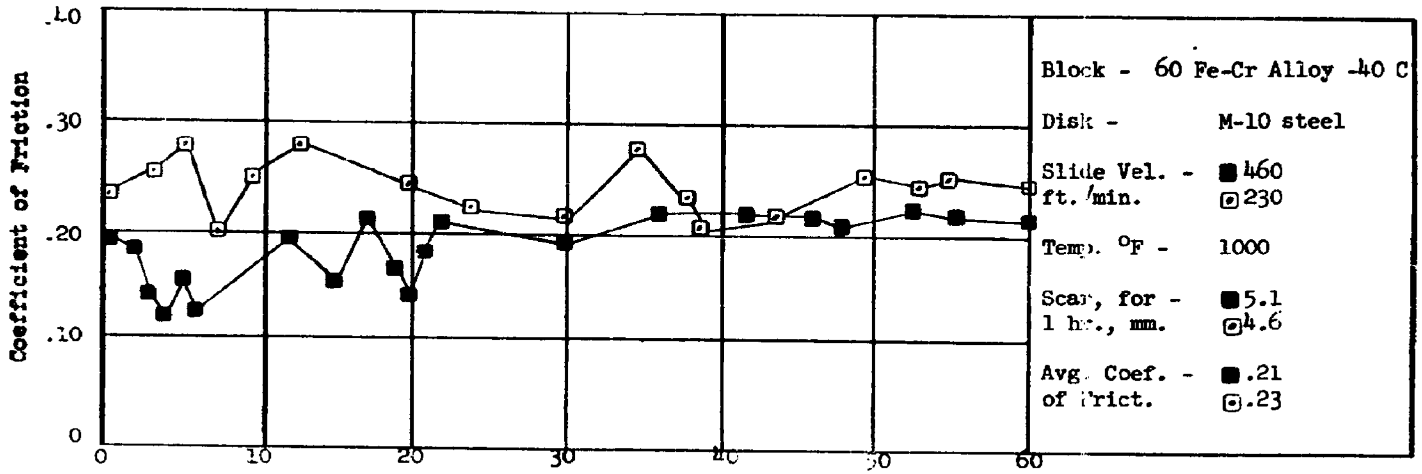

FIGURE 57a

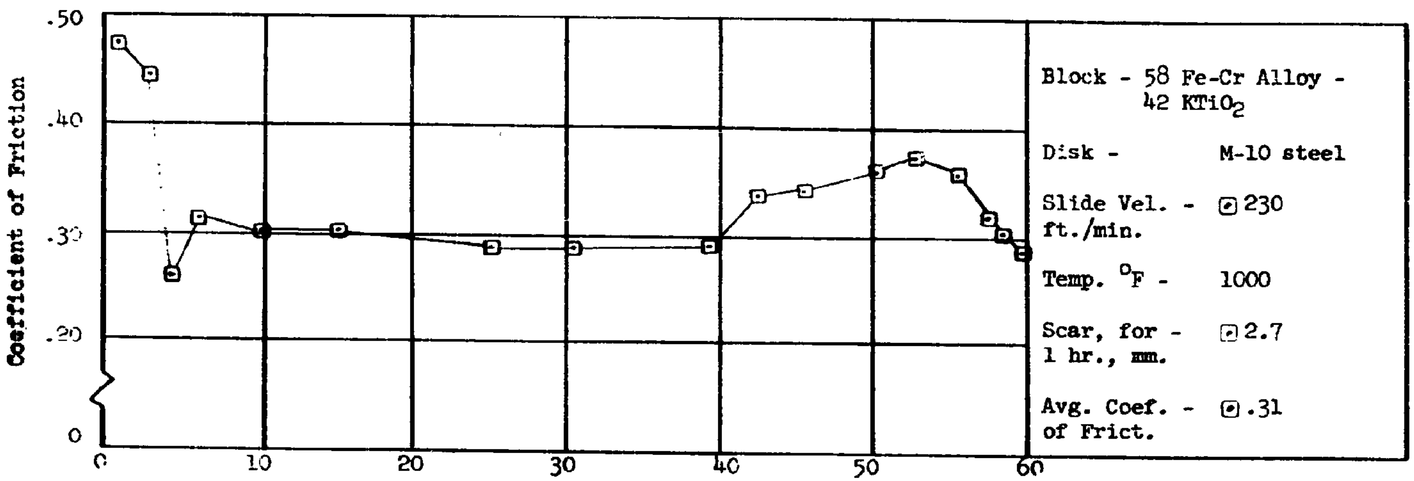

FIGURE 57b

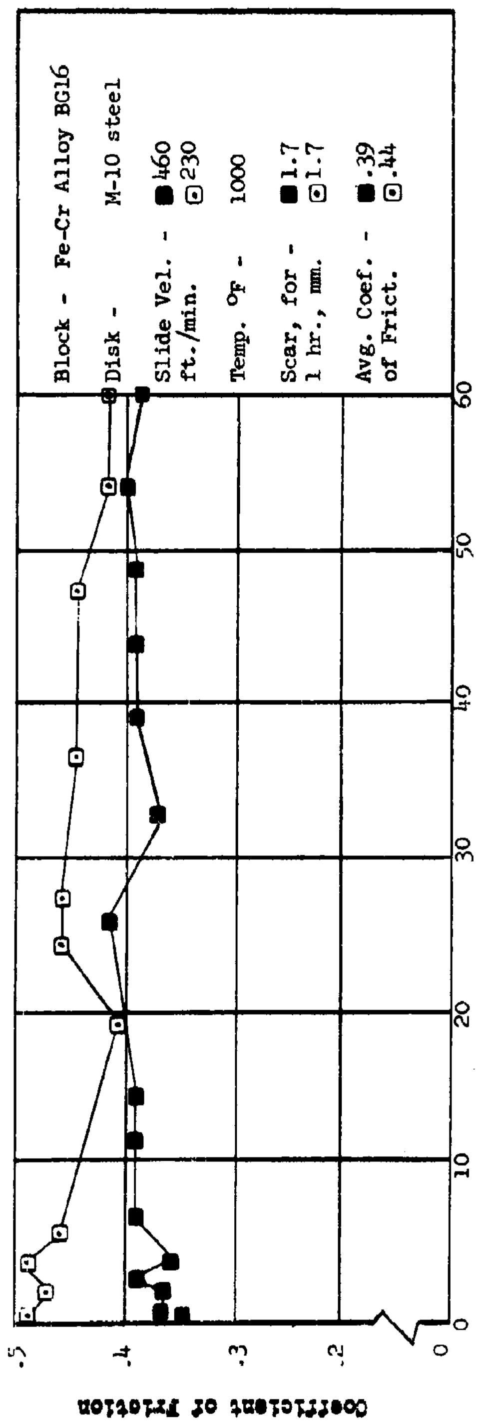

FIGURE 58a

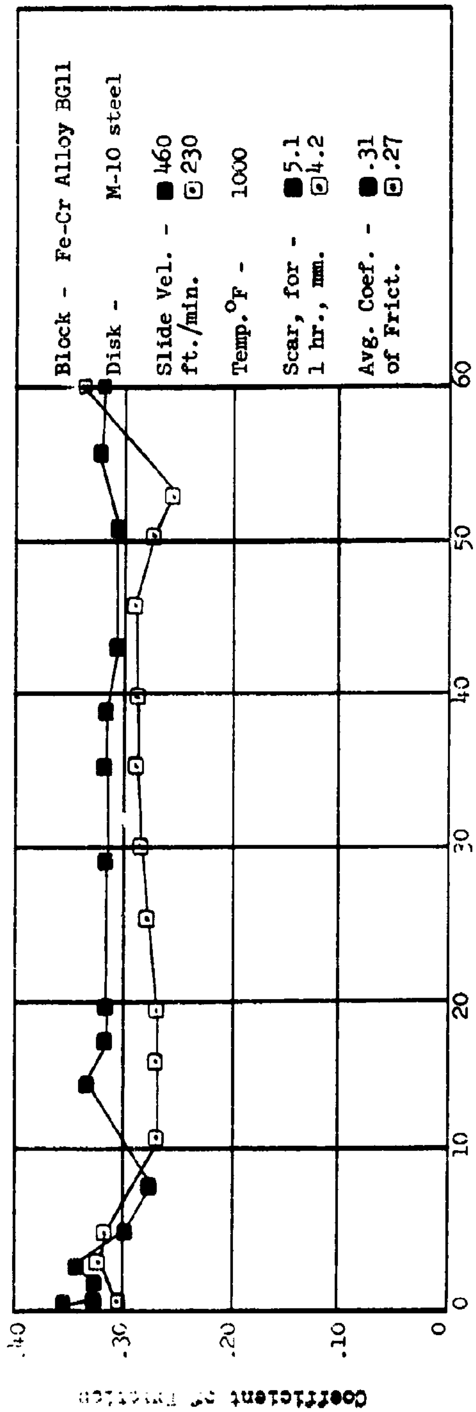

FIGURE 58b

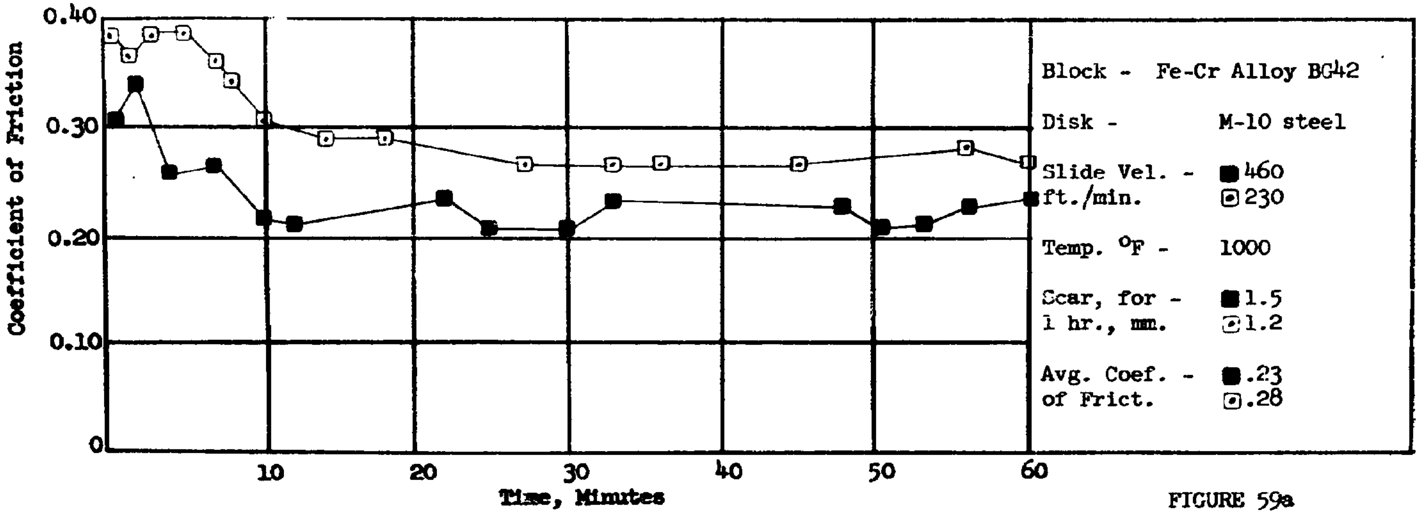

FIGURE 59a

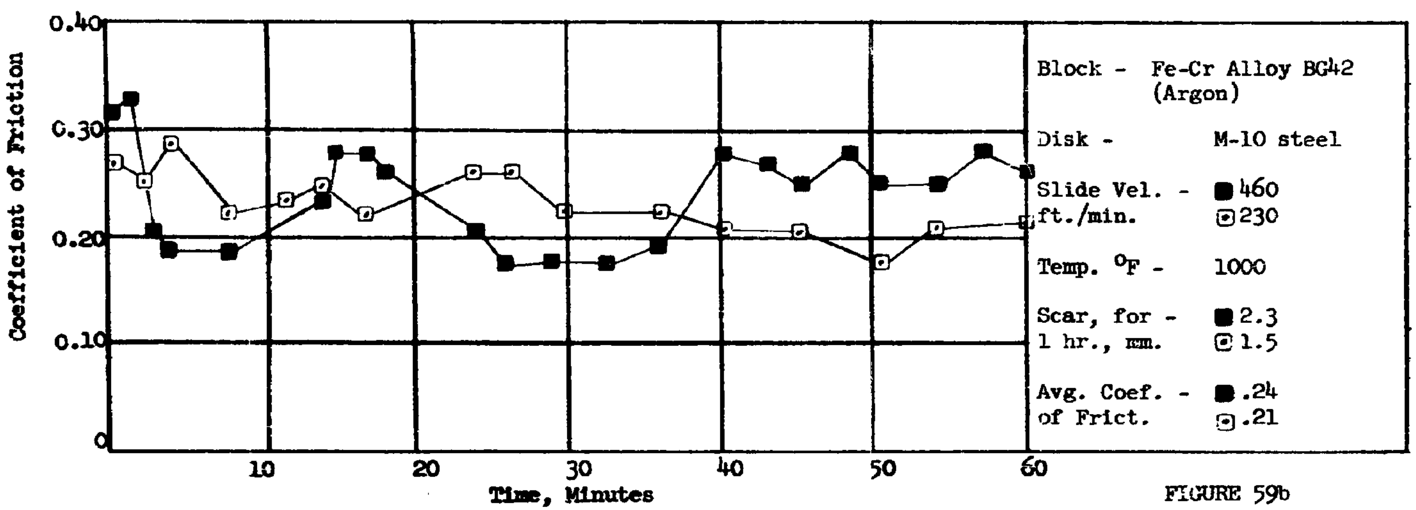

FIGURE 59b

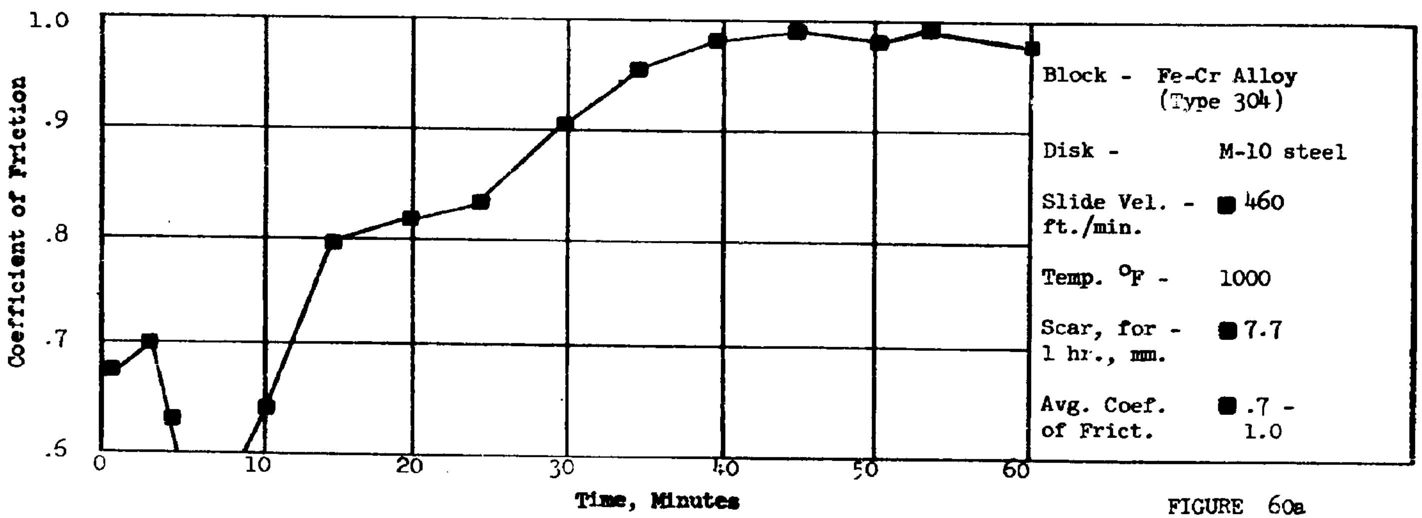
1.0
.9
.8
.7
.6
Coefficient of Friction
0
10
20
30
40
50
60
Time, Minutes
Block - Fe-Cr Alloy (Type 304)
Disk - M-10 steel
Slide Vel. - ft./min. 460
Temp. °F - 1000
Scar, for - 1 hr., mm. 7.7
Avg. Coef. of Frict. .7 - 1.0

FIGURE 60a

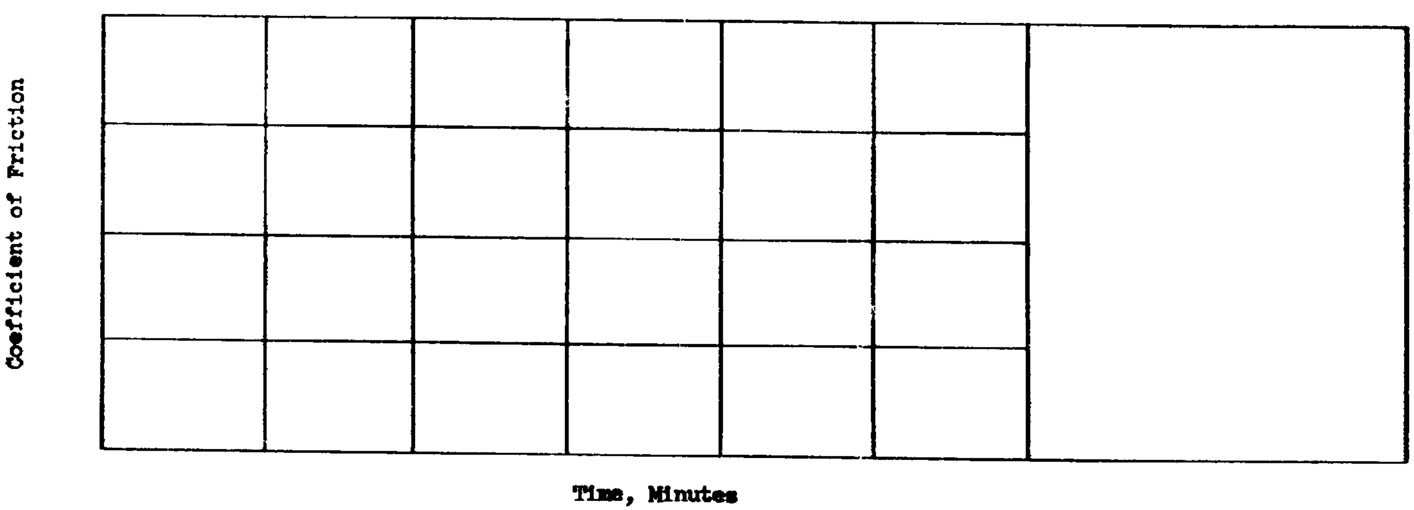
Coefficient of Friction
Time, Minutes

SUMMARY OF WEAR AND FRICTION DATA ON COMPOSITES AND ALLOYS

Materials evaluated as test blocks rubbing against a rotating M-10 tool steel disk in a dry nitrogen atmosphere at 1000°F.

Curve Reference (Fig. No.)	Test Material (% Vol.)	Sliding Vel (ft./min.)	Coefficient of Friction (0 – .5)	Average Wear/mm (0 – 1.0)
37a	84 Fe - 16 C	460		
37a	84 Fe - 16 C	230		
37b	70 Fe - 30 C	460		
37b	70 Fe - 30 C	230		
38a	70 Fe - 30 C	460		
38a	70 Fe - 30 C	230		
38b	65 Fe - 35 C	460		
38b	65 Fe - 35 C	230		
39a	50 Fe - 50 C HT	460		
39a	50 Fe - 50 C HT	230		
39b	50 Fe - 50 C	460		
39b	50 Fe - 50 C	230		
40a	40 Fe - 60 C HT	460		
40a	40 Fe - 60 C HT	230		
40b	40 Fe - 60 C	460		
40b	40 Fe - 60 C	230		
41a	30 Fe - 70 C HT	460		
41a	30 Fe - 70 C HT	230		
41b	30 Fe - 70 C	460		
41b	30 Fe - 70 C	230		
42a	68 Fe - 18 Mo - 18 Co HT	460		
42a	68 Fe - 18 Mo - 18 Co HT	230		
42b	68 Fe - 18 Mo - 18 Co (Argon)	460		
43a	65 Ni - 35 C	230		10.2
43b	60 Ni - 40 C	460		14.3
43b	60 Ni - 40 C	230		15.8
44a	50 Ni - 50 C C	460		
44a	50 Ni - 50 C C	230		11.0
44b	50 Ni - 50 C	460		17.1
44b	50 Ni - 50 C	230		15.2
45a	40 Ni - 60 C C	460		11.0
45a	40 Ni - 60 C C	230		
45b	40 Ni - 60 C	460		14.1
45b	40 Ni - 60 C	230		12.0
46a	30 Ni - 70 C C	460		11.0
46a	30 Ni - 70 C C	230		
46b	30 Ni - 70 C	460		
46b	30 Ni - 70 C	230		
47a	20 Ni - 80 C C	460		
47a	20 Ni - 80 C C	230		
47b	20 Ni - 80 C	460		
47b	20 Ni - 80 C	230		
48a	81 Ni - 19 ZnS	460		10.7
48b	65 Ni - 35 ZnS	460		
49a	74 Ni - 26 ZrCl	460		10.2
49b	Ni	460		
50a	76 Ni - 15 Cr alloy**	460	7.0	
50b	61 Ni - 12 Cr alloy**	460		
50b	61 Ni - 12 Cr alloy**	230		
51a	Co alloy (313) Porous	230		
51b	Co alloy (313) Porous Sb_2S_3	230		
52a	Co alloy 150-1	230		
52b	Co alloy 317	230		
53a	Co alloy (317) + Sb_2S_3	230		
53b	70 Co alloy - 30 C	460		
53b	70 Co alloy - 30 C	230		
54a	51 Co alloy - 49 C	460		
54b	50 Co alloy - 50 C	460		
54b	50 Co alloy - 50 C	230		
55a	15 Co - 85 ZrBr	230		
55b	7 Co - 93 ZrBr	230		
56a	Co alloy	460		
56a	Co alloy	230		
56b	Co alloy X	460		
56b	Co alloy X	230		
57a	60 FeCr alloy - 40 C	460		
57a	60 FeCr alloy - 40 C	230		
57b	58 FeCr alloy - 42 K_2TiO_3	230		
58a	Fe-Cr alloy BG16**	460		
58a	Fe-Cr alloy BG16**	230		
58b	Fe-Cr alloy BG11**	460		
58b	Fe-Cr alloy BG11**	230		
59a	Fe-Cr alloy BG42**	460		
59a	Fe-Cr alloy BG42**	230		
59b	Fe-Cr alloy BG42 (Argon)**	460		
59b	Fe-Cr alloy BG42 (Argon)**	230		
60a	Fe-Cr alloy (Type 304)**	460		

*Compositions on a per cent by weight basis
**Deposited, cast or wrought alloy

FIGURE 61

ANALYTICAL AND EXPERIMENTAL STUDY OF ADAPTING BEARINGS FOR USE IN AN ULTRA-HIGH VACUUM ENVIRONMENT

Phase II

Outgassing Determination of Plastics, Dry Powders, and Composites

By

P. H. Bowen
Materials Laboratories
Westinghouse Electric Corporation
East Pittsburgh, Pennsylvania

(The reproducible copy supplied by the author was used in the reproduction of this report.)

February 1962
Contract AF 40(600)-915

I. INTRODUCTION

Handling facilities are required in the positioning and testing of space vehicles and other equipment in the large ground vacuum chambers contemplated for the Arnold Air Force Station, Tennessee. This program concerns the study of bearings and lubricant systems for use in electric hoist motors operating in these ground vacuum chambers under vacuum conditions similar to those of space operation.

The initial program was divided into three phases. In Phase I the wear and friction characteristics of various dry powders and dry self-lubricating materials suitable for use in ball bearing components were evaluated in a dry inert atmosphere. In Phase II the selected materials from Phase I were subjected to a vacuum environment to determine the rate of outgassing of each material. In Phase III the most promising self-lubricating materials of Phase II will be fabricated into retainers and evaluated along with dry powders in 20 mm ball bearings operating in a vacuum chamber at pressures in the range of 1×10^{-6} to 1×10^{-9} mm of Hg. Starts will be made at -60°F with actual bearing operation at temperatures ranging from ambient to 1000°F. All tests will be made with a radial bearing load of 75 lbs. and an axial bearing load of 5 lbs.

At the extremely low pressure levels encountered in space and also contemplated for simulation in a ground test facility, conventional bearing lubricants evaporate or sublime causing lubricating films to disappear with a resultant tremendous increase in surface friction and wear of the ball bearings. Under such conditions, clean surfaces when rubbing on one another in laboratory tests with apparently the last monomolecular film layer removed have been known to cold weld. In addition, in an ultra-high vacuum environment, the only natural mechanisms of heat dissipation from a bearing are by radiation or conduction to contacting surfaces. This heat reservoir effect compounds the problem, as lubricant evaporation is accelerated at higher bulk temperatures. Some bearing materials have poor heat transfer characteristics and will not dissipate the thermal energy over the entire bearing surface but retain it at the localized areas where the asperities of each material make contact.

In selecting satisfactory dry self-lubricating materials and dry lubricants for use in ball bearings, a knowledge of the vapor pressures or outgassing characteristics is often of great importance. It is especially important to know the outgassing characteristics of lubricating materials that may find possible use in bearings over a wide temperature range in ground space chambers where the vacuum environment must be produced to simulate ultra-high vacuums that exist beyond the earth's recognized atmosphere. To be useful, the outgassing rate of the materials must not exceed the provided pumping speed of the chamber at the desired operating pressure.

II. TEST PROCEDURE

The object of the outgassing study was not only to find the rate of gas evolution of the materials but also to determine both the molecular structure and quantity of each gas evolved. The data was obtained over the known useful temperature range for the materials and also at temperatures at which some of the materials exhibited large thermal degradation rates. Several groups of materials were tested in the "as received" state and again immediately after a twenty-four hour "bake out" in vacuum at an elevated temperature.

The outgassing tests were carried out in a zirconia-quartz vacuum furnace tube in which the sample was heated. The gases evolved from the sample were collected in a three liter flask, cooled to standard conditions and then measured. After determining the total gas volume, the gases were transferred to a mass spectrometer. The outgassing data output from the spectrometer was processed through a Datatron computer to provide the calculated mol % of each gas for the gases evolved from each material. Figure 1 is a photograph showing the mass spectrometer cubical housing containing the electronic components, the spectrometer magnet and tube, and the sample pumping system. Figure 2 shows the zirconia-quartz tube with the vacuum valve.

To conduct each test the sample was placed in the quartz end of the vacuum furnace tube. The tube was evacuated to a pressure of 1×10^{-5} mm of Hg and the zirconia end was placed in the furnace. The zirconia tube was heated to 1200°F-1300°F while pumping continued until a negligible background was observed during periodic sampling of gases from the tube. By containing the sample in the cool quartz end of the tube and by heating only the zirconia end, all background contamination of the tube could be removed. After a satisfactory background determination, the zirconia end of the tube was cooled and the sample was transferred to the zirconia end by tipping the tube. The tube was again placed in the furnace and the furnace adjusted to the test temperature. The sample was held at temperature in the furnace for 20 minutes. The gas build-up in the zirconia tube at the end of a 20 minute period was transferred to the three liter flask, measured and then analyzed using the mass spectrometer. In conducting the outgassing run at the next higher temperature, the sample was returned to the quartz end of the vacuum tube, and the zirconia end again heated to 1200°F-1300°F until the background was brought below the sensitivity of the mass spectrometer. The tube was removed from the furnace, cooled and the test sample moved to the zirconia end and heated to the next higher temperature and the outgassing of the sample at that temperature was determined. The temperature level at each outgassing test was increased in increments of 100°F to 300°F until the maximum test temperature was reached or the sample decomposed as evidenced by relatively large amounts of outgassing.

Selected plastic materials, dry powders and metal composites were also evaluated in the outgassing tests to determine what gases would be evolved from these materials after extended soaking periods in a vacuum. The materials were given a "pre-bake out" at a specified temperature for a period of 24 hours in the zirconia tube prior to obtaining the outgassing data.

III. OUTGASSING DETERMINATION OF PLASTICS

1. Selection of Materials

Most of the plastic materials screened in Phase I to determine their respective friction and wear characteristics were selected for further evaluation in the outgassing tests. The materials evaluated in Phase II are listed in Table I. Two materials not run in Phase I were included in the outgassing studies. The first material, unfilled PTFE, was selected to give a comparison with that of the filled PTFE material. The 56HT carbon-graphite material (containing no PTFE) was selected because of the possible indirect improvement in wear and friction properties that the impregnants were known to add to the carbon-graphite. The test temperatures selected for the studies ranged from 160°F to 1260°F or a value where the thermal degradation of the material occurred.

2. Test Results

Large amounts of gases were evolved from all the plastic materials that were studied in the "as received" condition. The test data is shown in Table II. Each of the gases is reported in mol % of the total gas evolved at each of the different temperatures. The total quantity of gases evolved at 160°F from each of the materials was below 0.03 cc/gram of sample for all except ceramic filled PTFE, glass fiber-MoS_2 filled PTFE, and impregnated carbon-graphite. As the temperature increased, contaminant gases were evolved in sufficient quantity to mask the normal outgassing expected of the material during prolonged exposure to a vacuum.

Significant amounts of water vapor were evolved from each of the materials except PTFCE. This is especially true of the filled PTFE and the filled and unfilled nylon materials, where the mol % of water ranged between 90% and 99% at temperatures up to 360°F. The PTFE, carbon-graphite, and polypropylene had a mol % of water vapor ranging between 1% and 70% at temperatures up to 360°F.

All of the materials evolved carbon dioxide or carbon monoxide gas. Only PTFE, PTFCE, graphite filled nylon and glass filled PTFE contained nitrogen and/or oxygen. All of the materials except unfilled PTFE exhibited traces of one or more gases that were entrapped in the material during processing (molding of shapes). In the ceramic filled PTFE, traces of sulfur dioxide, sulfur fluoride and methane were found. A trace of unidentified hydrocarbons was found during outgassing at 760°F and 860°F. Glass fiber filled PTFE evolved traces of SO_2, nitrogen and unidentified hydrocarbons. PTFCE evolved a significant amount of nitrogen with traces of oxygen, argon & unidentified hydrocarbons. The Carbon-graphite material evolved nitrogen, oxygen and unidentified hydrocarbons. Polypropylene released unidentified hydrocarbon and possibly nitrogen. A second Purecarbon material containing an impregnant, released traces of hydrogen, unidentified hydrocarbons, sulfur dioxide and possibly nitrogen.

More meaningful outgassing measurements were obtained on the plastic materials after they were degassed or "prebaked out" prior to the outgassing determination. In each of the tests for which data is shown in Table III, the materials were baked in a vacuum at a pressure of 1×10^{-6} mm of Hg for 24 hours at temperatures of 360°F, 560°F or 760°F. The nylon materials were baked at 360°F to prevent thermal degradation prior to the outgassing tests. The glass cloth filled PTFE was degassed at a temperature of 760°F. All other materials were degassed at 560°F.

The volume of gases evolved from each of the selected plastic and carbon-graphite materials in the degassed condition was extremely low. As noted in Figure 3, the rate of evolution of gas over the temperature range of 160°F to 360°F for any of the six materials did not exceed 0.0020 cc/gram of sample. At temperatures up to 560°F the outgassing rate was still less than 0.0090 cc/gram for each material.

In a comparison of the outgassing rate of the unfilled PTFE with the filled PTFE materials, the filled materials had lower outgassing rates at 160°F and 360°F. The best self-lubricating filled PTFE material, which contained glass fiber and molybdenum disulfide, had the highest outgassing rate of all the materials tested at temperatures of 560°F and above. The unfilled PTFE and the glass cloth filled PTFE, were stable at 760°F and did not show evidence of thermal degradation until outgassed at the next higher temperature of 960°F. The graphite filled nylon material appeared to be stable at 760°F but showed evidence of thermal degradation at 860°F. The carbon-graphite material evolved large quantities of gases at 760°F.

The gases evolved from the plastic materials were mostly water vapor with varying amounts of carbon dioxide or carbon monoxide in all with the possible exception of PTFCE which evolved carbon monoxide and nitrogen gas.

All materials, including the carbon-graphite, released unidentified hydrocarbons at a temperature where thermal degradation of the plastic materials occurred.

IV. OUTGASSING DETERMINATION OF DRY POWDERS

1. Selection of Materials

Ten of the original twenty-seven powders evaluated in Phase I for wear and friction characteristics were selected for outgassing studies. Most of the powders selected had low wear rates. However, the coefficient of friction was not considered as critical and as a result, several of the powders selected had friction values as high as 0.4 when rubbing between steel surfaces. The powders selected were:

No.	Material		No.	Material	
12	Molybdenum disulfide	MoS_2	17	Silver iodide	AgI
13	Graphitic-carbon	C	18	Gallium telluride	GaTe
14	Lead chromate	$PbCrO_4$	19	Tungsten diselenide	WSe_2
15	Lead sulfide	PbS	20	Tungsten diselenide (purified)	WSe_2
16	Antimony trisulfide	Sb_2S_3	21	Molybdenum diselenide	$MoSe_2$

The range of temperatures selected for outgassing tests of the dry powders was 160°F to 1160°F. All powders except molybdenum diselenide were studied in the "as received" condition. Only the following six powders were studied in a degassed or "Pre-baked out" condition.

No.	Material		No.	Material	
12	Molybdenum disulfide	MoS_2	18	Gallium telluride	GaTe
15	Graphitic-carbon	C	20	Tungsten diselenide	WSe_2
16	Antimony trisulfide	Sb_2S_3	21	Molybdenum diselenide	$MoSe_2$

2. Test Results

Nine different "as received" dry powder lubricants were studied for outgassing characteristics. The test results are shown in Table IV. Two samples of tungsten diselenide were subjected to outgassing tests. One sample was "purified" for the "as received" tests. These two conditions reflect the worst and average amount of contamination that might be found in powders considered as candidate lubricants. The method of reporting the results in mol % of the total gas evolved is similar to that used in the study of plastic materials.

All of the "as received" powders evolved a major amount of water vapor and varying minor amounts of carbon dioxide and carbon monoxide. In addition, molybdenum disulfide, graphite, lead chromate, antimony trisulfide and gallium telluride evolved a small amount of sulfur dioxide gas. Small amounts of hydrogen and unidentified hydrocarbon gases were released from the graphite, lead chromate, antimony trisulfide, lead sulfide, gallium telluride and tungsten diselenide. Other gases evolved from only one or a few of the powders included: acetic acid from lead sulfide, nitric oxide from silver iodide, and methane from tungsten diselenide. The "purified" tungsten selenide powder exhibited a significantly lower outgassing rate than the "as made" powder. The outgassing of the purified powder was only one-third that of the uncleaned powder over the range of 160°F to 560°F. Of the other powders only tungsten diselenide and silver iodide appeared to be "clean" powders without significant contamination. In general the contamination in the form of gases released from materials were apparently in the powders from the time of their original processing.

Test results of the degassed powders are shown in Table V. All these powders that were degassed exhibited low outgassing rates at 760°F except for the antimony trisulfide. Antimony trisulfide apparently underwent a physical change. At the higher temperatures the outgassing rate was significantly lower than the rate at 760°F. Molybdenum disulfide exhibited an extremely low outgassing rate at a temperature of 760°F but increased rapidly at 960°F and 1160°F. The tungsten diselenide had a consistently low outgassing rate at temperatures of 760°F, 960°F and 1160°F. The tungsten exhibited a lower outgassing rate than molybdenum when each was evaluated as a selenide compound. A review of the vapor pressure data for metals indicated that tungsten at a pressure of 1×10^{-7} mm of Hg has a higher vaporization temperature (2480°K) than molybdenum (1970°K).

At a temperature of 1160°F only tungsten diselenide, gallium telluride, antimony trisulfide and molybdenum diselenide exhibited low outgassing rates. All of the composites evolved carbon dioxide gas. All but gallium telluride evolved carbon monoxide gas. Graphite evolved water vapor at only one temperature (960°F). Hydrogen gas was released from the graphite, antimony trisulfide, gallium telluride and molybdenum diselenide. At the high temperatures, both of the sulfide compounds and molybdenum diselenide evolved sulfur dioxide gas.

V. OUTGASSING DETERMINATION OF COMPOSITES

1. Selection of Materials

The six composites and alloys that exhibited the most desirable properties of low wear and low friction when rubbing against metal in Phase I tests were selected for outgassing study. A description of each material is given in Table VI. The 84% Fe - 16% C and the 20% Ni - 80% C composites were the only materials of the group not subjected to heat treating or annealing by the supplier.

All of the test samples were given a 24 hour "bake out" immediately prior to the outgassing tests. The "bake out" and test procedure was similar to the procedure used in evaluating the dry powders. Gas evolution from the composites was determined over a twenty minute period for each of three temperatures: 760°F, 960°F and 1160°F. One material, 84% Fe - 16% C was heated for one hour at temperature rather than 20 minutes.

2. Results of Tests

The results of outgassing of the composite materials are shown in Table VII. The outgassing rates in general of these materials were low at 760°F and 960°F, but significantly higher at the temperature of 1160°F. All of the composite materials evolved a major amount of hydrogen, carbon monoxide and carbon dioxide gases. Water vapor, which was released in copious quantities by the plastic and powder materials, was not evolved from the composite materials except for the 20% Ni - 80% C composite at 960°F. The 84% Fe - 16% C composite evolved unidentified hydrocarbon gases at all three temperatures. The 50% Fe - 50% C heat treated composite evolved some unidentified hydrocarbon gas. These hydrocarbon gases were probably the result of heavy waxes or other petroleum products used as binders in green pressing the composites.

Although the outgassing rate of 50% Fe - 50% C and 20% Ni - 80% C materials was low at a temperature of 760°F, large amounts of carbon monoxide and carbon dioxide gases were released at 960°F. The rate of hydrogen gas released increased with temperature of all the composites except the 20% Ni - 80% C composite. At 1160°F the rate of outgassing was low for only the 40% Ni - 60% C composite.

No correlation was found regarding the amount of lubricant or type of metal in the composite and the rate of outgassing at the three test temperatures.

The hydrogen gas was evolved from both the metal and lubricant. The amount of nitrogen evolved from the graphite powder at 960°F was .007 cc/gram of sample. This is a significant amount when compared to the nitrogen gas released from each of the composites at 960°F. At a temperature of 1160°F, the outgassing rate is high for all materials except the 40% Ni - 60% C carburized material. However, this method of making the material was similar to that of 30% Ni - 70% C carburized. No relationship existed between the method of making the composite or the amount of graphite incorporated in each material.

VI. DISCUSSION

The vapor pressure of the materials had little or no effect on their outgassing rates because the gases that were observed were primarily contaminants or decomposition products. It was important to determine what contaminants were evolved from the materials and the mol % of each fraction. In the plastic materials, the Nylasint yielded carbon monoxide, carbon dioxide and ammonia along with the other heavy molecular weight materials. The water, although tightly associated with the nylon, hydrolized the nylon to form carboxylic acid and an amine. The end product of this breakdown reaction would give carbon monoxide, carbon dioxide and ammonia gas. The polytetrafluoroethylene did not fractionate but appeared to start to depolymerize. If decomposition of the low molecular weight polymer occurred, fluorine gas would be formed. In the outgassing tests of plastic materials, a distillate was generally formed from all the samples at an elevated temperature.

Contaminants were also found during the outgassing of powders and, in addition, metallic films were deposited in the cooler part of the quartz tube which indicated fractionation of the material had occurred. Most noticeable was the film formed during the outgassing of antimony trisulfide.

Other variables could also influence the rate of outgassing of the candidate lubricant materials. Such variables include porosity, particle size, surface area, and density.

A comparison of outgassing rates was made on all the materials at 760°F. The bar chart, Figure 6, shows the outgassing rate of the materials after a 24 hour bake out. Unfilled PTFE had outgassing rates similar to that of most of the metal composites. Nylasint containing 20% graphite had an outgassing rate similar to that of graphite powder. The outgassing of Duroid 5813, glass fiber MoS_2 filled PTFE, is not due to the PTFE or the MoS_2 powder as noted by each of the materials in separate tests. Since glass is not believed to have a high outgassing rate, the gas must have been evolved because of a reaction of the materials during the molding process. Additional pretreatment of Duroid 5813 may further reduce evolution of water vapor, carbon monoxide, carbon dioxide, and sulfur dioxide gases.

The fact that plastic materials do not have a true vapor pressure make them desirable for use in a vacuum environment where temperature and strength requirements permit. Tensile strength tests of the glass fiber molybdenum disulfide filled PTFE in accordance with ASTM D638-58T, show that the material retains approximately 66% of the room temperature lengthwise and crosswise strength at 250°F and 33% of the room temperature strength at 500°F. The strength of unfilled PTFE would be slightly less at all temperatures.

With regard to radiation, PTFE has been shown to be stable in a vacuum when exposed to ultraviolet radiation equivalent to 2-1/2 times the solar constant (4 or 5 calories per cm^2 per min.) for periods up to approximately 100 hours. Additional tests made in Materials Laboratories show that PTFE can be used in applications in a vacuum where the material is exposed to ionizing radiation dosages as high as 10^6 to 10^7 rads.

The data from the mass spectrometer was programed into the Datatron 205 computer to identify and obtain the mol % of each of the gases evolved from the candidate lubricating materials.

The mass spectrum of the gases evolved during each outgassing test was represented in the mass spectrometer by a peak intensity of the ion current at each mass to charge (m/e) value. The relative intensities of the ion current were used in the computational procedure with the Datatron 205. A calibration record of spectrum from a large number of known pure compounds, expressed in terms of pattern and sensitivity coefficients computed for each m/e value, was obtained and used as the basis for the calculation of the mixture spectrum. The record consisted of pure compounds related to the expected gases that might be evolved from the test materials in these and previous tests.

The mixture spectrum was the sum, or linear superposition, of the spectra contributed by its components. The pattern and sensitivity coefficients obtained in the calibration runs could be applied to a component whether it was alone or in the mixture.

Mass spectral data was obtained by solving simultaneous linear equations. It was necessary to use one equation for each unknown in the mixture of gases.

After the simultaneous equations were solved, the partial pressures were obtained. Mol percentage composition was determined by dividing each partial pressure by the total pressure, which was the sum of the partial pressures.

VII. CONCLUSIONS

1. Candidate dry lubricants and self-lubricating materials were evaluated for outgassing properties at various temperatures. The outgassing data were determined for materials in the "as received" condition and for materials which had been degassed prior to the outgassing determination.

2. Most of the materials in the degassed condition are more suitable for use in a vacuum than is generally believed. The gases evolved were from contaminants and were not the result of evaporation of the lubricant materials.

3. The major gas constituents evolved from the plastic and dry powder materials were water vapor, carbon dioxide and carbon monoxide. Duroid 5813, the best candidate plastic self-lubricating material from Phase I, exhibited a low outgassing rate at temperatures from 160°F to 360°F. Molybdenum disulfide and tungsten diselenide exhibited low outgassing rates at a temperature of 760°F.

4. The major gas constituents evolved from the composite materials were hydrogen, carbon monoxide and carbon dioxide. The 40% Ni - 60% C carburized composite material exhibited the lowest outgassing rate at 760°F.

Prepared By P H Bowen
P. H. Bowen
Project Engineer

Supervised By E S Bober
E. S. Bober
Supervisory Engineer

Approved By Harry R Sheppard
H. R. Sheppard, Mgr.
Chemical Appl. Sec.

TABLE I

DESCRIPTION OF PLASTICS

No.	Material	Trade Name	Supplier
1	Nylon	Nylatron GS	Polymer Corp. of Pennsylvania
2	Nylon - 20% C filler	Nylasint 2G	Polymer Corp. of Pennsylvania
3	Polytetrafluoroethylene	Teflon	E.I. Dupont de Nemours & Co.
4	Polytetrafluoroethylene with mica filler	Fluorosint	Polymer Corp. of Pennsylvania
5	Polytetrafluoroethylene with ceramic filler	Duroid 5613	Rogers Corporation
6	Polytetrafluoroethylene with glass fiber and MoS_2 filler	Duroid 5813	Rogers Corporation
7	Polytetrafluoroethylene with glass cloth filler	Armalon	E.I. DuPont de Nemours & Co. Fabrics & Finishes Department
8	Polychlorotrifluoroethylene	Halon TVS	Allied Chemical Corporation Plastics Coal & Chemicals Dept.
9	Carbon graphite (hard) with polytetrafluoroethylene impregnate	P5TF (hard)	Purecarbon Company
10	Polypropylene	Profax Type 6513	Hercules Powder Company Cellulose Products Department
11	Carbon graphite with chemical salt impregnate for high temperature	56HT	Purecarbon Company

TABLE II

OUTGASSING CHARACTERISTICS OF PLASTICS

No.	Material	Wt. of Sample Grams	Temp. °F	Mol % of Gases Evolved H_2O	CO	CO_2	SO_2	N_2	O_2	CO and/ or N_2	SiF_4	Uniden- tified*	Miscel- laneous	Vol.**of Gases Evolved cc/gm.
1	Nylon	0.6421	160	97.19	-	-	-	-	-	2.81	-	-	-	0.0175
			360	97.21	-	1.82	-	-	-	0.97	-	-	-	1.0723
			460	96.99	-	1.96	-	-	-	1.05	-	-	-	0.4513
2	Nylasint 2G	0.8023	160	87.33	-	-	-	9.49	3.18	-	-	-	-	0.0289
			360	98.30	-	1.13	-	0.57	-	-	-	-	-	1.5216
			560	93.96	-	5.54	-	-	-	-	-	0.50	-	0.9098
			760	-	-	84.17	-	-	-	-	-	2.00	13.82a	41.3285
3	PTFE	0.9010	160	12.07	-	-	-	62.51	25.42	-	-	-	-	0.0067
			360	14.10	-	-	-	64.64	21.26	-	-	-	-	0.0164
			560	6.28	-	1.78	-	72.88	19.06	-	-	-	-	0.0172
			760	64.37	-	14.14	-	-	-	21.49	-	-	-	0.0052
			960	1.36	-	12.19	-	-	-	4.85	-	81.60	-	0.0672
			1060	-	-	0.87	-	-	-	0.40	-	98.73	-	2.0262
4	PTFE - mica filler	0.8513	160	99.99	-	-	-	-	-	-	-	-	-	0.0056
			360	96.76	0.96	1.49	-	-	-	-	-	-	0.79b	0.0615
			460	92.27	2.03	4.18	-	-	-	-	-	-	1.52b	0.0262
			560	81.06	3.84	10.52	-	-	-	-	-	-	4.58b	0.0199
			560***	80.32	4.32	10.03	-	-	-	-	-	-	5.33b	0.0199
			760	42.76	10.16	29.39	-	-	-	-	-	1.00	16.69b	0.0178
			860	20.91	9.73	27.40	-	-	-	-	-	10.00	31.96b	0.0368
			960	7.28	6.98	13.94	-	-	-	-	-	23.45	48.35b	0.1172
			1060	0.93	4.78	5.34	-	-	-	-	-	60.02	28.93b	2.1769

*Gases were unidentified hydrocarbons
**Total volume of gases was measured at STP
***PTFE - mica filled material heated for additional 90 min. @ 560°F

a - NH_3 b - C_6H_6

TABLE II (Continued)

OUTGASSING CHARACTERISTICS OF PLASTICS

No.	Material	Wt. of Sample Grams	Temp. °F	Mol % of Gases Evolved										Vol.** of Gases Evolved CC/gm.
				H_2O	CO	CO_2	SO_2	H_2	O_2	CO and/or N_2	SiF_4	Unidentified*	Miscellaneous	
5	PTFE ceramic filler	0.9573	160	99.99	-	-	-	-	-	-	-	-	-	0.0796
			260	98.12	0.42	0.62	0.84	-	-	-	-	-	-	0.4005
			360	91.33	0.97	4.20	3.50	-	-	-	-	-	-	0.1942
			460	84.18	2.13	8.13	5.51	-	-	-	-	-	-	0.0767
			560	59.88	4.02	15.40	20.09	-	-	-	0.41	0.20	-	0.2061
			560+	37.61	5.29	17.61	38.[illegible]	-	-	-	0.73	-	-	0.0419
			660	27.53	5.54	23.19	41.81	-	-	-	1.20	0.73	-	0.1664
			760	38.32	9.01	25.17	25.19	-	-	-	1.65	0.67	-	0.3974
6	PTFE - glass fiber + MoS_2 filler	0.9591	160	98.92	0.48	0.21	0.39	-	-	-	-	-	-	0.1165
			360	97.03	0.62	1.17	1.18	-	-	-	-	-	-	0.1094
			560	97.44	0.52	1.06	0.98	-	-	-	-	-	-	0.2459
			760	89.46	5.68	1.69	2.67	-	-	-	-	0.50	-	0.9117
			860	27.62	55.57	7.19	9.52	-	-	-	-	0.10	-	2.3885
7	PTFE - glass cloth filler	0.9385	160	99.99	-	-	-	-	-	-	-	-	-	0.0006
			360	99.99	-	-	-	-	-	-	-	-	-	0.0010
			560	99.99	-	-	-	-	-	-	-	-	-	0.0010
			760	89.00	11.00	-	-	-	-	-	-	-	-	0.0030
			860	38.14	19.72	37.88	1.48	0.53	-	-	-	2.25	-	0.0470
			960	11.82	15.96	33.13	2.12	1.78	-	-	-	35.19	-	0.0787
			1060	-	2.96	4.26	-	2.38	-	-	-	90.40	-	15.[illegible]
8	PTCFE	1.0553	160	-	-	-	-	70.84	29.13	-	-	-	-	0.0008
			360	-	-	4.82	-	67.88	26.13	-	-	-	1.33c	0.0101
			560	-	-	9.59	-	58.20	12.34	10.45	-	8.45	0.97c	0.0211
			760	-	-	21.10	-	-	-	24.20	-	54.70	-	0.0102
			860	-	-	-	-	-	-	-	-	99.99	-	3.5158

+ PTFE - ceramic filled material heated for additional 20 min. @ 560°F
c = Argon
*Gases were unidentified hydrocarbons
**Total volume of gases was measured at STP

TABLE II (Continued)

OUTGASSING CHARACTERISTICS OF PLASTICS

No.	Material	Wt. of Sample Grams	Temp. °F	Mol % of Gases Evolved										Vol.** of Gasses Evolved CC/gm.
				H_2O	CO	CO_2	SO_2	N_2	O_2	CO and/ or N_2	SiF_4	Uniden- tified*	Miscel- laneous	
9	Carbon-graphite (hard)-PTFE Impregnated	0.3767	160	35.09	-	-	-	52.94	11.97	-	-	-	-	0.0030
			360	25.72	57.93	16.35	-	-	-	-	-	-	-	0.0020
			560	36.25	1.54	39.97	-	22.24	-	-	-	-	-	0.0128
			760	40.15	-	59.65	-	-	-	-	-	0.20	-	0.0250
			960	7.24	-	3.53	-	-	-	-	-	89.23	-	0.4673
10	Poly-propylene	0.7231	160	31.72	-	18.15	-	-		50.13	-	-	-	0.0051
			360	45.21	-	-	-	-	-	-	-	54.79	-	0.1220
			460	18.25	-	-	-	-	-	-	-	81.75	-	0.0632
11	Carbon-graphite with salt for high temperature	0.3767	160	99.99	-	-	-	-	-	-	-	-	-	0.0380
			360	99.79	-	0.06	-	-	-	0.15	-	-	-	0.4192
			560	99.25	-	0.31	0.07	-	-	0.37	-	-	-	1.4992
			760	99.46	-	0.24	-	-	-	0.30	-	-	-	1.0571
			960	98.77	-	0.45	-	-	-	0.59	-	0.10d	0.09e	0.2210
			1160	92.55	-	2.53	-	-	-	2.92	-	0.37d	1.63e	0.2250
			1160++	52.65	-	15.97	-	-	-	17.06	-	1.50d	12.82e	0.0081
			1260	-	-	33.43	-	-	-	34.25	-	-	32.32e	0.0025

++ = Carbon-graphite material heated for additional 20 min. @ 1160°F
d = Believed to be H_2S
e = Hydrogen

*Gases were unidentified hydrocarbons
**Total volume of gases was measured at STP

TABLE III

OUTGASSING CHARACTERISTICS OF PLASTICS AFTER 24 HR. BAKE OUT

No.	Material	Wt. of Sample Grams	Temp. °F	Mol % of Gases Evolved								Vol.** of Gases Evolved CC/gm.
				H_2O	CO	CO_2	SO_2	CO and/ or N_2	SiF_4	NH_3	Uniden- tified*	
2	Nylon + carbon filler	0.6968	160	88.19	-	-	-	11.81	-	-	-	0.0019
			360	81.13	-	-	-	18.87	-	-	-	0.0020
			560	86.90	-	-	-	13.10	-	-	-	0.0026
			660	99.99	-	-	-	-	-	-	-	0.0021
			760	99.99	-	-	-	-	-	-	-	0.0024
			860	38.29	-	41.29	-	-	-	2.85	17.57*	0.6800
3	PTFE	0.9344	160	99.99	-	-	-	-	-	-	-	0.0012
			350	99.99	-	-	-	-	-	-	-	0.0016
			560	99.99	-	-	-	-	-	-	-	0.0017
			760	99.99	-	-	-	-	-	-	-	0.0009
			960	3.33	3.96	11.89	-	-	-	-	30.82+	0.0608
5	PTFE - Glass fiber + MoS_2 filler	0.9063	160	99.99	-	-	-	-	-	-	-	0.0006
			360	99.99	-	-	-	-	-	-	-	0.0007
			560	91.99	-	-	-	8.01	-	-	-	0.0039
			760	45.75	36.86	6.06	10.13	-	-	1.20	-	0.2106
7	PTFE - Glass cloth filler	1.1691	160	99.99	-	-	-	-	-	-	-	0.0010
			360	99.99	-	-	-	-	-	-	-	0.0015
			560	99.99	-	-	-	-	-	-	-	0.0013
			760	68.59	14.30	17.11	-	-	-	-	-	0.0024
			960	0.63	7.51	15.92	1.29	-	2.67	-	71.98+	0.1621
8	PTFCE	1.2254	160	99.99	-	-	-	-	-	-	-	0.0008
			360	No gases detected in spectrometer				-	-	-	-	-
			560	70.36	-	-	-	29.64	-	-	-	0.0017
			760	-							99.99++	0.0235
11	Carbon-graphite (hard) - PTFE impregnated	0.8428	160	99.99	-	-	-	-	-	-	-	0.0003
			360	99.99	-	-	-	-	-	-	-	0.0011
			650	99.99	-	-	-	-	-	-	-	0.0028
			760	68.60	-	31.40	-	-	-	-	-	0.0044
			960	9.00	-	6.15	-	-	-	-	84.85++	0.1866

*Gases were unidentified hydrocarbons
**Total volume of gases was measured at STP

+Gases were unidentified carbon-fluorine compounds
++Gases were unidentified compounds

TABLE IV

OUTGASSING CHARACTERISTICS OF DRY POWDERS

No.	Material	Wt. of Sample Grams	Temp. °F	Mol % of Gases Evolved: H_2O	CO	CO_2	SO_2	N_2	H_2	CO and/ or N_2	Unident-* ified	Misc.	Vol.** of Gases Evolved CC/Gm.
12	MoS_2	0.1916	160	99.99	-	-	-	-	-	-	-	-	0.0556
			360	98.12	-	0.73	1.15	-	-	-	-	-	0.1338
			560	87.52	1.72	2.34	8.42	-	-	-	-	-	0.4410
			760	7.75	3.22	7.94	81.08	-	-	-	-	-	1.1317
13	Graphitic carbon	0.1114	160	99.99	-	-	-	-	-	-	-	-	0.0065
			360	71.03	-	3.32	3.84	-	-	-	-	-	0.0927
			560	60.84	5.54	21.93	2.45	-		-	-	-	0.2830
			760	54.43	10.86	25.39	2.85	-	0.88	-	-	-	0.5925
			960	60.05	15.01	19.47	-	-	4.44	-	-	-	3.4279
14	$PbCrO_4$	0.2863	160	82.46	-	2.48	-	-	15.06	-	-	-	0.0414
			360	92.42	-	3.13	0.39	2.60	-	-	-	-	0.1586
			560	53.32	2.31	22.47	0.71	10.70	-	-	-	-	0.1026
			760	49.68	2.12	13.89	0.34	2.86	-	-	-	3.54a	0.2775
			960	19.98	2.56	2.01	0.06	-	-	-	-	1.05b	1.2109
15	PbS	0.6497	160	97.41	0.84	1.75	-	-	-	-		-	0.0410
			360	86.44	0.15	10.13	-	-	-	-	0.50d	2.78c	0.7310
			560	18.04	-	50.75	-	-	-	-	17.55d	13.66c	3.5386
16	Sb_2S_3	0.3616	160	58.57	2.13	5.12	-	25.56	2.03	-	-	6.59e	0.0506
			360	83.46	0.70	6.54	1.60	6.26	-	-	-	1.44e	0.1002
			560	45.83	4.43	36.52	7.03	4.94	0.28	-	-	0.94e	0.1420
			760	34.49	6.14	43.02	6.78	8.70	-	-	-	0.87f	0.0572
			960	3.44	2.71	60.06	30.60	2.64	-	-	-	0.55f	0.1573
17	AgI	0.3530	160	-	-	-	-	-	-	-	-	-	-
			360	51.08	-	25.31	-	-	-	23.61	-	-	0.0014
			560	12.05	-	35.23	-	-	-	14.42	-	38.30g	0.0085
			760	7.27	-	31.79	-	-	-	15.46	-	45.48g	0.0157
			960	7.16	-	34.93	-	-	-	19.93	-	37.89g	0.0100
			1160	-	-	31.69	-	-	-	31.19	-	37.12g	0.0025

*Gases were unidentified hydrocarbons
**Total volume of gases was measured at STP

a = HCl
b = Oxygen
c = Acetic acid
d = Believed to be hydrocarbons and sulfur compounds
e = Oxygen
f = Methane
g = NO

TABLE IV (Continued)

OUTGASSING CHARACTERISTICS OF DRY POWDERS

No.	Material	Wt. of Sample Grams	Temp. °F	Mol % of Gases Evolved									Vol.** of Gases Evolved CC/Gm.
				H_2O	CO	CO_2	SO_2	N_2	H_2	CO and/ or N_2	Unident-* ified	Misc.	
18	Gate	0.1265	392	99.85	-	0.15	-	-	-	-	-	-	0.9084
			572	96.29	0.18	0.42	0.14	-	2.84	-	-	0.13f	0.3181
			752	66.45	0.90	2.94	1.10	-	28.18	-	-	0.43f	0.1611
			932	25.38	3.77	12.17	1.05	-	56.34	-	-	1.29f	0.0507
			1112	2.28	3.24	6.18	0.65	-	86.36	-	-	1.29f	0.0700
19	WSe_2	0.3123	160	49.62	-	-	-	-	-	50.38	-	-	0.0030
			360	56.16	-	19.39	-	-	-	12.66	11.79	-	0.0081
			560	41.66	25.31	21.84	-	-	-	-	11.19	-	0.0353
			760	39.37	39.87	12.33	-	-	1.47	-	6.96	-	0.1310
			960	22.00	6.35	3.20	-	-	63.46	-	0.50	4.49f	0.2736
20	WSe_2 Purified	0.9611	392	44.97	-	33.07	-	-	-	21.96	-	-	0.0008
			572	38.11	-	24.11	-	-	-	37.78	-	-	0.0044
			752	65.94	-	16.17	-	-	-	17.89	-	-	0.0027
			932	30.97	-	23.91	-	-	23.05	23.07	-	-	0.0016
			1112	29.99	44.58	17.07	-	-	7.42	-	0.94	-	0.0556

*Gases were unidentified hydrocarbons
**Total volume of gases was measured at STD
f=Methane

TABLE V

OUTGASSING OF DRY POWDERS AFTER 24 HRS. BAKEOUT

No.	Material	Wt. of Sample Grams	Temp. °F	Mol % of Gases Evolved: H_2O	CO	CO_2	SO_2	H_2	CO and/or N_2	Vol* of Gases Evolved cc/gm.
12	MoS_2	0.1916	760	-	-	-	-	-	-	<0.0005
			960	-	23.27	60.11	16.62	-	-	0.0073
			1160	-	24.74	66.82	8.44	-	-	0.1691
13	Graphitic Carbon	0.1346	760	-	30.76	69.24	-	-	-	0.0024
			960	18.96	18.96	33.42	-	28.66	-	0.0241
			1160	-	21.43	75.05	-	3.53	-	0.1499
16	Sb_2S_3	0.6945	760	-	2.47	3.84	-	93.69	-	0.0121
			960	-	18.52	81.48	-	-	-	0.0003
			1160	-	7.81	74.03	18.16	-	-	0.0110
18	GaTe	0.4256	760	-	-	-	-	-	-	<0.0005
			960	-	-	26.29	-	46.43	27.28	0.0042
			1160	-	-	5.39	-	89.22	5.39	0.0139
20	WSe_2	0.7198	760	-	-	-	-	-	-	<0.0004
			960	-	73.66	26.34	-	-	-	0.0015
			1160	-	60.90	39.10	-	-	-	0.0082
21	$MoSe_2$	0.5112	760	-	10.44	83.16	6.40	-	-	0.0031
			960	-	27.36	64.46	2.78	5.40	-	0.0163
			1160	-	28.20	65.61	2.60	3.59	-	0.0232

*Total volume of gases was measured at STP

TABLE VI

DESCRIPTION OF COMPOSITES

No.	Material Compositions (% by Vol.)	Remarks	Supplier
37a	84 Fe - 16 C	Hot coined	SKC Research Associates, Deva Metal Division
39a	50 Fe - 50 C HT	Contained $CaSi_2$, LPS*, heat treated	Ford Motor Company, Scientific Laboratory
40a	40 Fe - 60 C HT	Contained $CaSi_2$, LPS*, heat treated	Ford Motor Company, Scientific Laboratory
45a	40 Ni - 60 C**	Contained $CaSi_2$, LPS*, heat treated	Ford Motor Company, Scientific Laboratory
46a	30 Ni - 70 C**	Contained $CaSi_2$, LPS*, heat treated	Ford Motor Company, Scientific Laboratory
47a	20 Ni - 80 C	Contained $CaSi_2$, LPS*, heat treated	Ford Motor Company, Scientific Laboratory

*LPS - Liquid Phase Sintered
**C - Carburized

TABLE VII

OUTGASSING CHARACTERISTICS OF COMPOSITES AFTER 24 HOURS BAKEOUT AT 760°F

No.	Material	Wt. of Sample Grams	Temp. °F	Mol % of Gases Evolved						Vol.** of Gases Evolved CC/Grms.
				H_2	CO	CO_2	CH_4	H_2O	Hydro-carbons	
22	84% Fe - 16% C*	4.7520	760	89.97	-	5.03	-	-	5.00	.0014
			960	97.18	-	1.42	-	-	1.40	.0088
			1160	51.07	10.20	11.26	-	-	27.47	.0249
23	50% Fe - 50% C HT	2.6442	760	89.31	10.69	-	-	-	-	.0008
			960	94.58	4.11	1.31	-	-	-	.0040
			1160	57.51	30.24	4.28	-	-	7.97	.0477
24	40% Fe - 60% C HT	1.8572	760	-	46.25	53.75	-	-	-	.0006
			960	56.78	11.78	31.28	-	-	-	.0016
			1160	11.98	40.40	41.62	-	-	-	.0284
25	40% Ni - 60% C C	2.2451	760	-	99.99	-	-	-	-	<.0001
			960	86.02	13.98	-	-	-	-	.0003
			1160	91.16	4.03	4.81	-	-	-	.0021
26	30% Ni - 70% C C	1.4621	760	63.09	36.91	-	-	-	-	.0005
			960	87.34	12.66	-	-	-	-	.0027
			1160	71.25	22.97	4.07	1.71	-	-	.0145
27	20% Ni - 80% C	3.1350	760	26.33	61.81	11.86	-	-	-	.0015
			960	17.75	14.11	56.12	1.50	10.52	-	.0115
			1160	15.40	54.97	29.42	0.21	-	-	.2990

*Gases were unidentified hydrocarbons

**Total volume of gases measured at STP

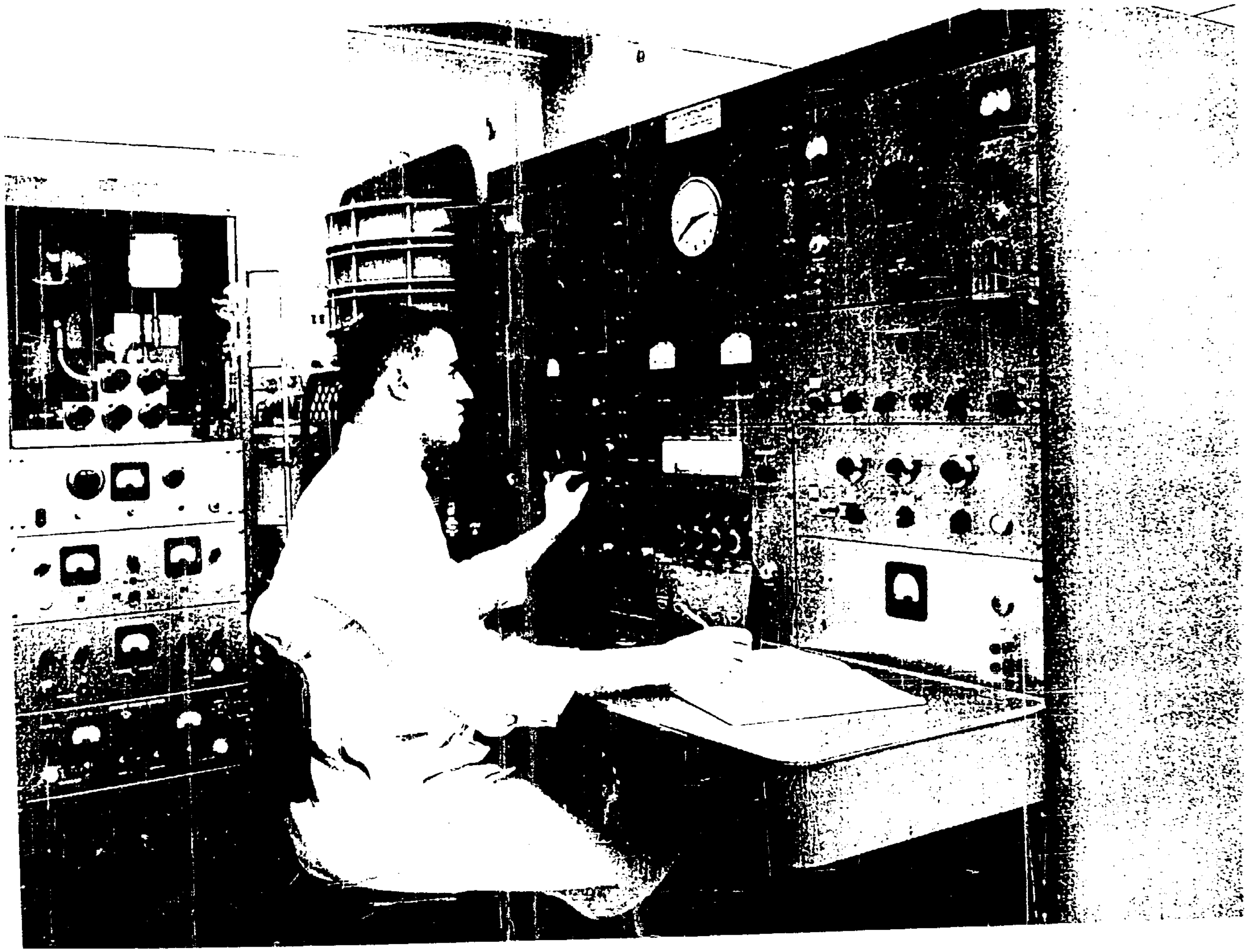

MASS SPECTROMETER AND SAMPLE PUMPING SYSTEM
FIGURE 1

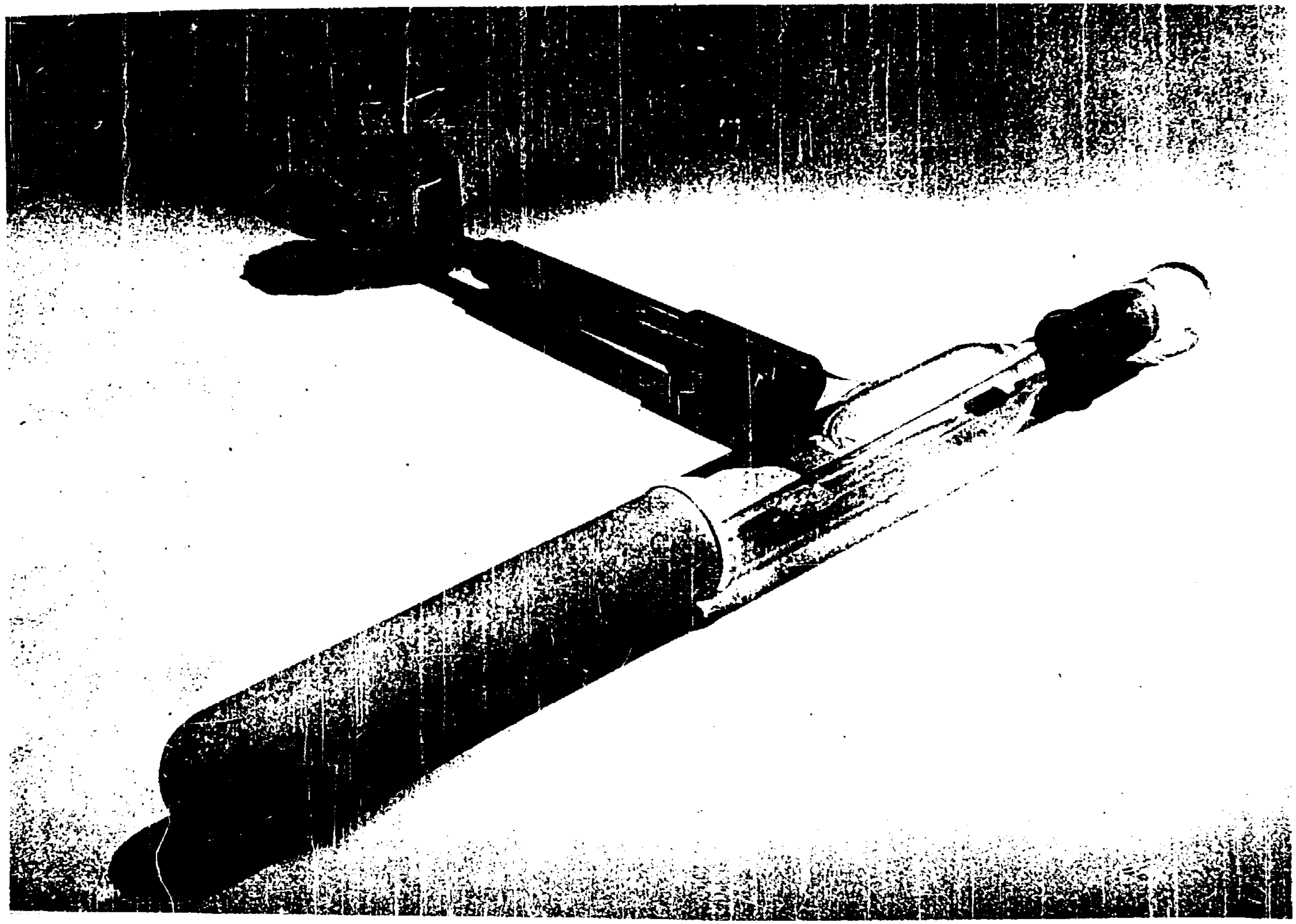

ZIRCONIA–QUARTZ TUBE WITH VACUUM VALVE
FIGURE 2

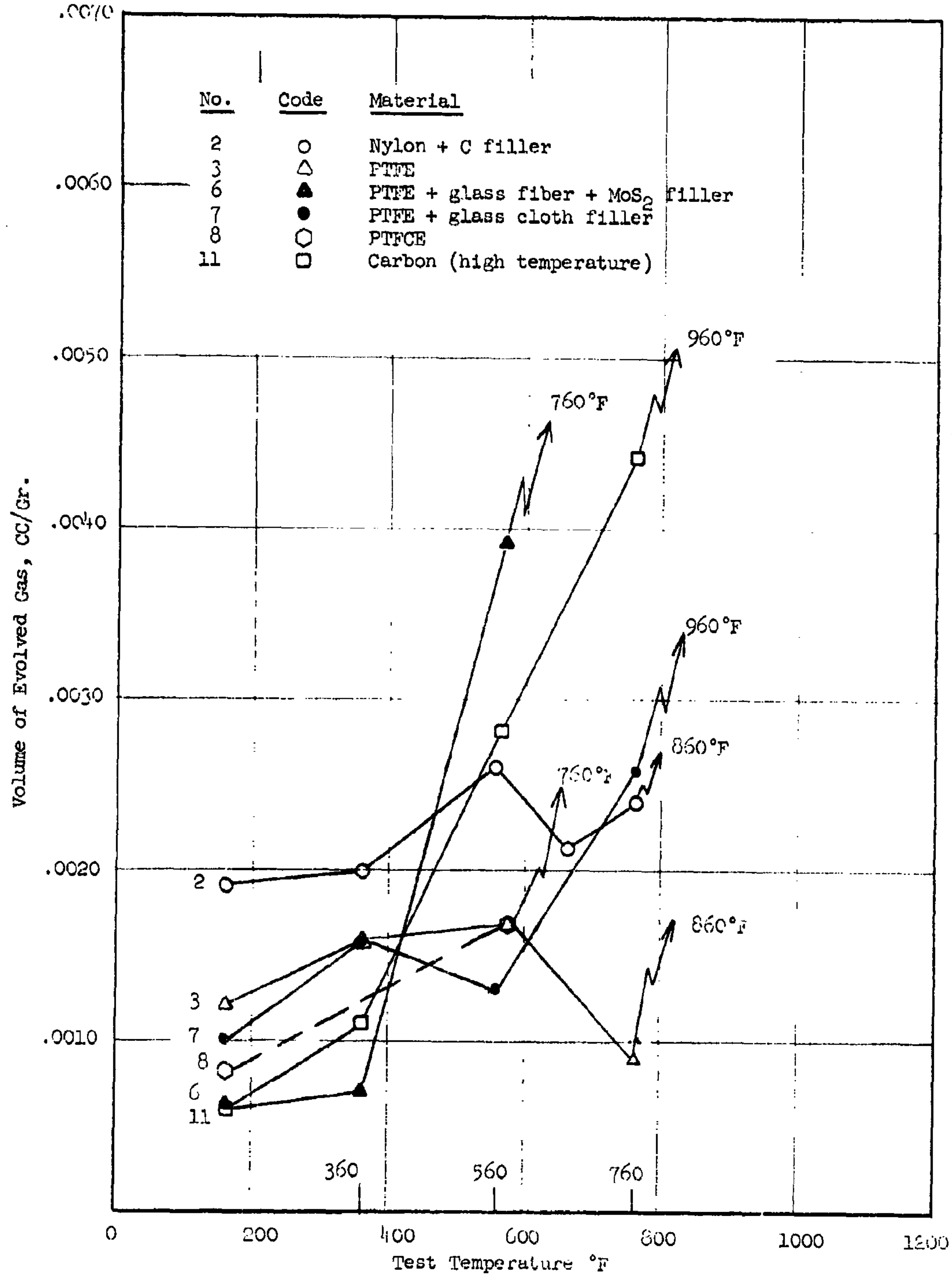

FIGURE 3

OUTGASSING OF DEGASSED PLASTIC MATERIALS

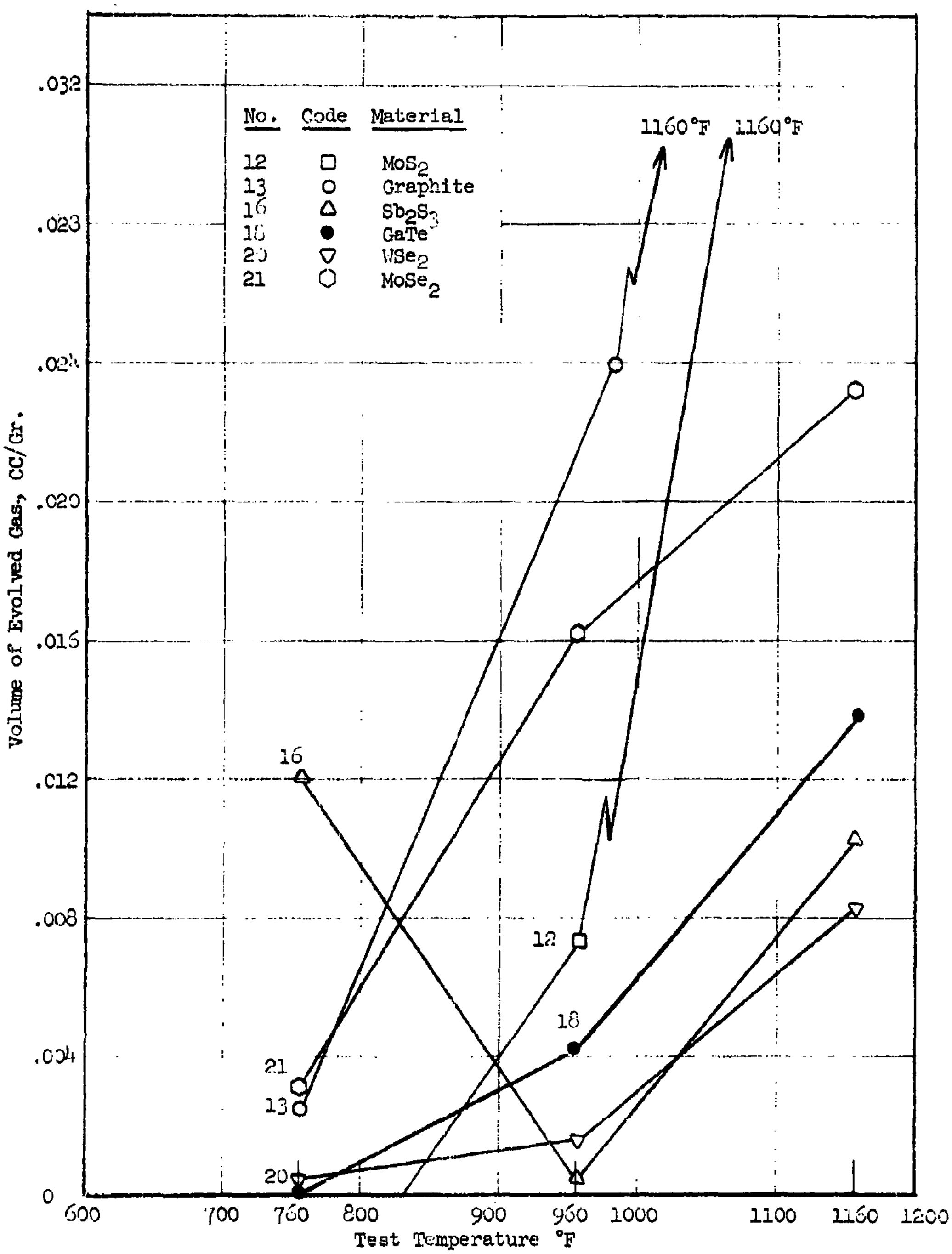

FIGURE 4

OUTGASSING OF DEGASSED POWDER MATERIALS

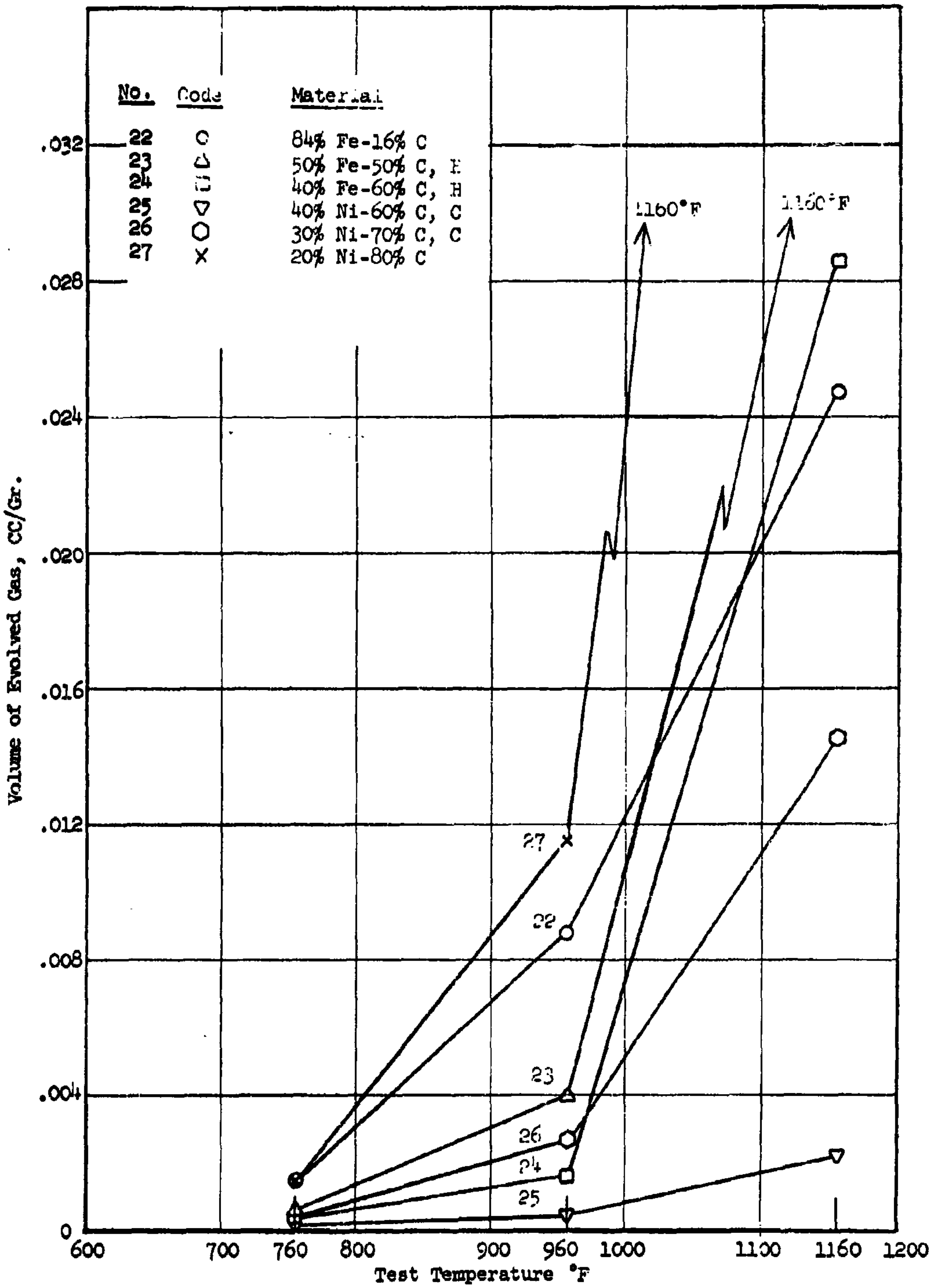

FIGURE 5
OUTGASSING OF DEGASSED COMPOSITE MATERIALS

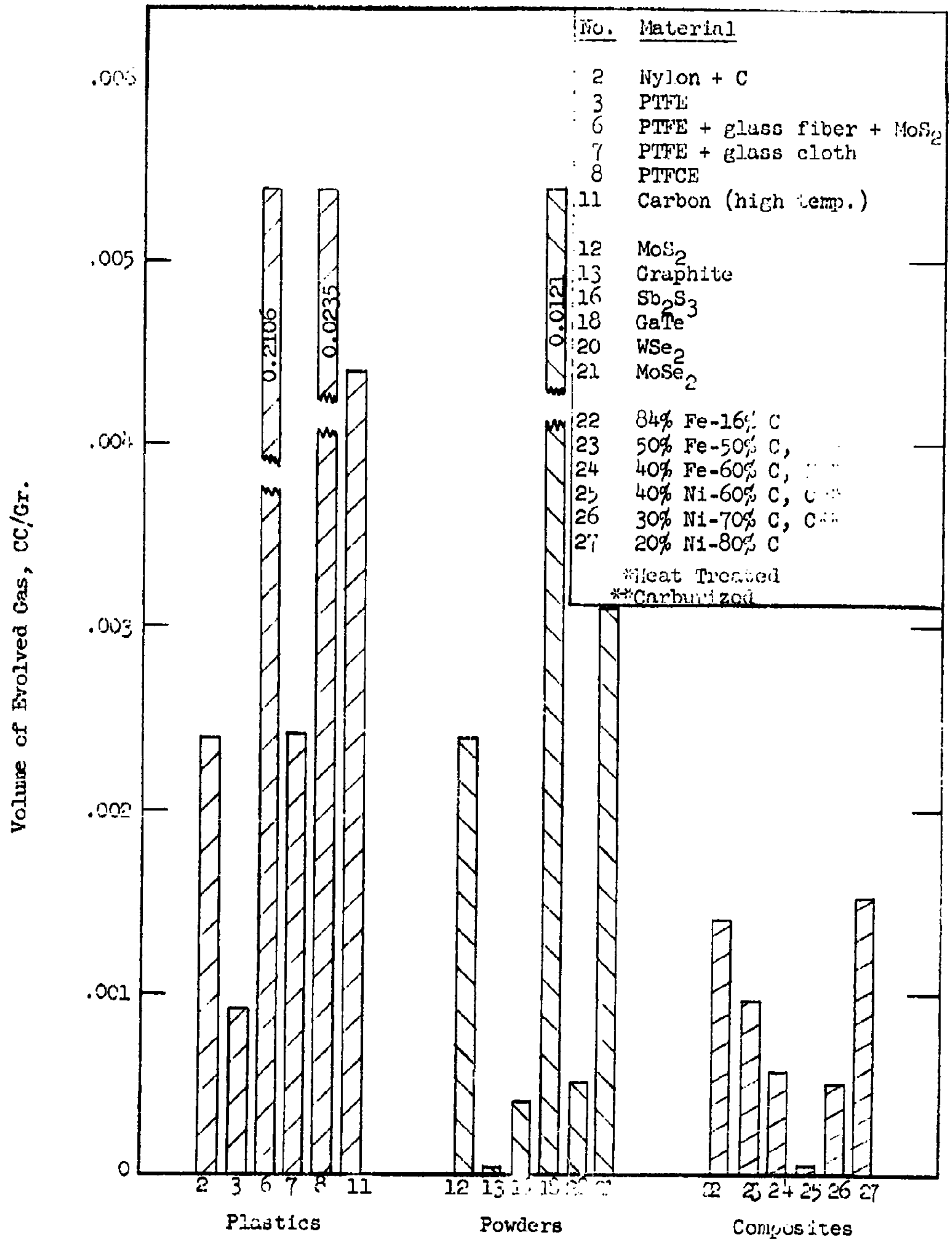

FIGURE 6

COMPARISON OF GAS EVOLUTION OF PLASTICS, POWDERS AND COMPOSITES

ANALYTICAL AND EXPERIMENTAL STUDY OF ADAPTING BEARINGS FOR USE IN AN ULTRA-HIGH VACUUM ENVIRONMENT

Phase III

Evaluation of Dry Powder Lubricants and Self-Lubricating Materials in Ultra-High Vacuum Bearing Tests

By

P. H. Bowen
Materials Laboratories
Westinghouse Electric Corporation
East Pittsburgh, Pennsylvania

(The reproducible copy supplied by the author was used in the reproduction of this report.)

February 1962

Contract AF 40(600)-915

I. INTRODUCTION

Handling facilities are required for use in positioning and testing space vehicles and other apparatus in the large space environment test chambers contemplated for the Arnold Air Force Station, Tennessee. Many items of rotating equipment will be required to operate in the chamber prior to and during the test of each space vehicle. The program reported herein concerns the study of lubricants in bearings for use in electric hoist motors, large gimbal mounts and rail cars, as well as lubricants for both gears and bearings of 100 ton overhead travelling cranes. It is required that these lubricated gear and bearing systems be capable of operation in an environment where the pressures are in the range of 1×10^{-6} to 1×10^{-9} mm of Hg and the temperatures range from -300°F to 300°F. In addition, some of the hoist motor bearings may be operated under certain conditions at temperatures up to 1000°F. The stress on the test bearings and gears in this study will be of the same order of magnitude as that which will be experienced in the actual equipment.

The initial program was divided into three phases but was later extended to include seven phases. In Phase I the wear and friction characteristics of various dry powders and dry self-lubricating materials suitable for use in ball bearing components were evaluated in a dry inert atmosphere. In Phase II selected materials from Phase I were subjected to a vacuum environment to determine the rate of outgassing of each material. In Phase III the most promising self-lubricating materials of Phase II were fabricated into retainers and were evaluated in 20 mm ball bearings operating in a hard vacuum at temperatures from -60°F up to 450°F with limited operation at temperatures above 1000°F. Tests were made with a radial bearing load of 75 pounds and an axial load of 5 pounds.

In the forthcoming Phases IV through VII, the program will cover wear and friction studies of improved self-lubricating materials for use at higher bearing loads, additional outgassing studies, additional screening evaluation of wear and friction characteristics in a vacuum, and tests on dry lubricated, heavily-loaded, prototype gears and bearings operating in a hard vacuum.

At the extremely low pressure levels encountered in space and also contemplated for simulation in a ground test facility, conventional bearing lubricants evaporate or sublime causing lubricating films to disappear with a resultant tremendous increase in surface friction and wear of the ball bearings. Under such conditions clean surfaces, when rubbing on one another in laboratory tests with apparently the last monomolecular film layer removed, have been known to cold weld. In addition, in an ultra-high vacuum environment, the only natural mechanisms of heat dissipation from a bearing are by radiation or conduction to contacting surfaces. This heat reservoir effect compounds the problem, as lubricant evaporation is accelerated at higher bulk temperatures. Some bearing materials have poor heat transfer characteristics and will not dissipate the thermal energy over the entire bearing surface but retain it at the localized areas where the asperities of each material make contact.

In the ball bearing tests of Phase III, rubbing occurred between the ball surface and ball pockets of the retainer and between the retainer surface and the corresponding guide lands of the inner race. Self lubricating materials were used as retainers or as lubricating rings to lubricate the bearings. Dry powders were also used as lubricants. To accomplish satisfactory operation in an ultra-high vacuum it was necessary that the dry materials provide a film on the rubbing and rolling surfaces of the bearing to prevent galling or abrasive wear.

II. LUBRICANT SELECTION

The lubricant materials selected for evaluation in actual bearing tests were those that appeared promising on the basis of the results from Phases I and II. In addition, several new materials were also considered for evaluation in bearings. A description of the dry powders, self-lubricating plastic composites and alloy materials evaluated in this Phase is contained in Table I.

A. Plastic Materials

Duroid 5813 (a molybdenum disulfide-filled, glass fiber-reinforced Teflon) exhibited the most satisfactory wear and friction characteristics of all the plastic compositions screened. Since Teflon was one of the lubricating materials in Duroid 5813, Armalon (Teflon impregnated glass cloth) and Fluorosint (mica filled Teflon) were then reconsidered for test in bearings. In addition, retainers were made of Nylasint M4 and Nylasint 2G even though it was recognized that they may not possess the required strength at the bearing operating temperature.

Several phenolic resin base materials containing molybdenum disulfide powder as a filler were used to fabricate specimens.

Carbon graphite was considered as a retainer material and also a material for fabrication of lubricating rings. These rings were used to evaluate a new lubricating device which could utilize good lubricating materials that in themselves did not possess sufficient strength for their use as a retainer. One carbon lubricating ring contained small quantities of molybdenum disulfide or various oxidation inhibitors and metallic salts in addition to carbon-graphite.

B. Powders

Molybdenum disulfide was used as a lubricant in two bonded dry films, M1284 and M-20, and as a slurry with a volatile carrier. The carrier was evaporated from the slurry before the bearing was placed in the test chamber.

C. Composite and Alloy Materials

Sinetex (Teflon-molybdenum disulfide impregnated sintered bronze) showed considerable promise as a candidate self-lubricating material in screening tests. None of the other sintered materials exhibited optimum lubricating properties. The BG42, M-10 and Inconel X alloy materials were used with their surfaces coated. Only Inconel X was tested as a retainer without a coating.

III. BEARING SELECTION CRITERIA

A. Configuration

Proper lubrication is essential to provide satisfactory bearing life. As the lubricants become marginal in their ability to provide a film between the rubbing surfaces, the configuration of the bearing components becomes more critical. Conventional ball bearings intended for use with oils or greases are not satisfactory for use with dry lubricants. The loads imposed by the centrifugal forces on the retainer and also the unpredictable loads resulting from thermal distortion, misalignment of the rolling elements and vibration all tend to rapidly destroy any dry lubricant film on the metallic parts and permit wear or metallic adhesion. All these factors serve to increase the severity of the retainer lubrication problem when using dry lubricants in a vacuum environment.

Several methods of reducing the severity of the lubrication problem are available. These include changes in bearing configuration, varying material of construction and imposing limitations on the speed and/or load performance of the bearing.

Although many ball bearing configuration changes can be considered, the changes with the most significant effects on life are those involving increase in radial clearance and retainer type used. The bearings used in this study were deep groove Conrad type 20 mm light series ball bearings of ABEC-3 grade. Standard bearings are made to tolerances outlined in Anti-friction Bearing Engineers Committee grade 1 (ABEC-1). Bearings of higher quality are manufactured with smaller tolerances and progressively better race finish, as well as less variation in ball size. The final design configuration of the bearing and retainer is shown as Figure 1. One land of the outer race was ground to provide a counterbore race shoulder and still retain a non-separable bearing. The shoulder height (depth of the race groove measured from the shoulder to the bottom of the groove) was 16% of the ball diameter. An inner-race riding, one-piece retainer was used. The rubbing velocity of the retainer on the OD of the inner race would be slightly higher for a 20 mm 204 size bearing than the rubbing velocity of the retainer on the ID of the outer race. However, it was decided to have the retainer rub on the inner race since that design offered more of a variety in retainer modifications and also permitted use of novel dry stick lubrication techniques. The rubbing velocity of the retainer on the inner race when the inner race is free to rotate is as follows:

$$V_e = 0.2618\ (V_a) \left[B_{od} - \frac{S_b}{2} \left(1 - \frac{d}{PD} \cos \mathcal{L}\right) \right]$$

Where V_e = linear velocity in FPM

V_a, velocity of inner race	=	1800 rpm
B_{od}, OD of inner race	=	1.065 inches
S_b, ID of retainer	=	1.080 inches
d, ball diameter	=	0.3120 inches
PD, pitch diameter	=	1.765 inches
$\mathcal{L}$, contact angle	=	3° 48'
Cos $\mathcal{L}$	=	0.9978
S_{od}, OD of retainer*	=	1.495 inches

$$V = 0.2618 \times 1800 \left[1.065 - \frac{1.080}{2} \left(1 - \frac{0.3120}{1.765} \times 0.9978\right) \right]$$

V = 292 in./min.

*Assumed (based on inner race riding designed retainer)

The formula for calculating the rubbing velocity of an outer race riding retainer would be:

$$V_e = 0.1309\ S_{od}\ (V_a) \left[1 - \frac{d}{PD} \cos \mathcal{L} \right]$$

V_e = 290 in./min.

B. Materials

The type of bearing material used for the balls and races greatly affects the stresses present at the ball and race contact point. The harder the material, the greater the stress. For a given load application the mean compressive stress in the contact area is approximately 60 per cent greater for materials having a modulus of elasticity of 60×10^6 lb./sq. in. (carbides) as compared to materials with a modulus of elasticity of 30×10^6 lb./sq. in. (steels). It was desirable to use a material having a relative low modulus of elasticity as the structural components of the bearing, provided good wear resistance still could be achieved. When the material is extremely hard and brittle, chipping and cracking can occur because of differences in coefficient of expansion and thermal distortion of the housing and shaft material used in the bearing system.

Four types of bearing construction materials were used for the bearing and lubricant tests in the vacuum chamber. A tool steel, M-10, was used in all tests run at temperatures up to 900°F. A cobalt-chromium-tungsten alloy, Haynes Stellite 19, was used for tests run in the temperature range of 1000°F to 1200°F. The balls for the high temperature tests were made of tungsten carbide and the races of Stellite 19. A nucleated glass ceramic material, Pyroceram 9606, was used in the exploratory tests at 1500°F. Properties of these materials are noted below.

Material	Coef. of Thermal Expansion	Mod. of Elasticity	Hardness
M-10	6.5×10^{-6} (78-400°F)	32.0×10^{6} psi	Rockwell C 66
Stellite 19	7.9×10^{-6} (67-1112°F)	36.6×10^{6} psi	Rockwell C 55
Tungsten Carbide	3.5×10^{-6} (1200°F)	80.0×10^{6} psi	Rockwell A 92
Pyroceram 9606	2.6×10^{-6} (68-600°F)	17.5×10^{6} psi	--

The hardness of the metals at elevated temperatures was also considered in selecting the candidate bearing material. For M-10 steel the hardness ranges from Rc 64 at room temperature to approximately Rc 52 at 900°F. For Stellite 19 the hardness ranges from Rc 55 at room temperature to Rc 42 at 1200°F. Tungsten carbide was selected over titanium carbide for the ball material because of its higher hardness. Oxidation of the tungsten carbide was not a problem since the bearings were to operate only in a high vacuum. The analysis of the tool steel and cobalt-chromium-tungsten alloy was as follows:

	Composition in Percent by Weight							
Material	C	Cr	Ni	V	W	Mo	Co	Fe
M-10 Steel	0.90	4.0	-	2.00	1.0 max.	8.00	-	Bal
Stellite 19	1.90	31.0	-	-	10.5	-	Bal	3.0 max.

C. Load Conditions

If the load on an oil or grease lubricated bearing is reduced, a significant increase in the life of the bearing will result. The life of the bearing is based on the following cubic relation:

$$L_n = \left(\frac{C}{W}\right)^3$$

Where: L_n = life, 1×10^6 revolutions
C = specific dynamic capacity*
W = load on bearing

*represents the load which a bearing can carry for one million revolutions with only a 10% failure rate.

Reducing the load on fluid lubricated bearings to one-half increases the life eight times. In the case of dry lubrication, a change in load would be expected to have even a greater effect on the life of the bearings, or on the wear of the self-lubricating component in the bearing.

A reduction of bearing speed will affect a corresponding linear increase in bearing life. For applications where speed varies considerably the life, in terms of number of revolutions, is the most practical one to consider.

The life-load and speed-life factors are approximations of complex relationships and depend on a certain extent upon the exact choice of configuration by each bearing manufacturer.

In this series of tests, ultimate bearing life was not determined but the rate of wear per unit time was established, and this rate of wear can provide an indication of expected bearing life.

IV. ULTRA-HIGH VACUUM TEST APPARATUS

The test apparatus used in this phase of the contract permits operation of bearing systems in a hard vacuum (down to 8×10^{-9} mm of Hg) at temperatures up to 1500°F under radial loads up to 75 pounds and axial loads up to 25 pounds. The loaded test bearing can be driven at speeds up to 15,000 rpm. The test bearing can be observed while under test; and frictional torque in the bearing can be measured and recorded during the test run. The test apparatus consists of the vacuum chamber, test spindle assembly, bearing loading device and torque-indicating system, drive motor, pumping system, leak detection system and pressure monitoring system. An overall view of the test apparatus and control consoles is shown in Figure 2.

A. Vacuum Chamber

The vacuum chamber housing the test spindle is roughly the shape of a cube approximately two cubic feet in volume. The chamber is constructed of stainless steel with all internal surfaces smooth and free from pits and scratches to facilitate removal of air from the surfaces. All blind holes inside the chamber are vented to eliminate virtual leaks. Gold wire seals are utilized at all flanges to permit the use of high temperature bake outs as well as high temperature operation of the chamber and test spindle assembly.

B. Test Spindle Assembly, Bearing Loading Device and Torque Indicating System

A cross section view of the test chamber showing the spindle assembly, test bearing, bearing loads, heater assembly and torque system is shown in Figure 3. The test bearing is mounted on the end of the spindle. The radial load is obtained with a 75 lb. weight, 12 inches in diameter and 3 inches thick, which surrounds the bearing and forms an integral part of the housing. A 5 lb. axial load is applied to the bearing by means of a wire fastened to the bearing housing and extending forward over a pulley on which the weight is supported. This wire, fastened by a set screw at the top of the pulley, also acts as a torsion member and restoring force for any rotational movement of the housing. The force of friction developed in the bearing causes the housing to rotate until the reactive torque in the wire is equal to the friction torque in the bearing. This degree of rotation can be observed through the sight port, and the values can be used to calculate the inch-ounces of frictional torque.

The test spindle assembly is supported in a pedestal that can be cooled with water or liquid nitrogen. The spindle assembly contains the spindle, three bearings and a housing tube. The rear bearing as well as the front-aft and front-forward bearings are 204 size 20 mm bearings with the same configuration as the test bearing. An exploded view of the test spindle assembly, test bearing in the housing weight, bearing heater assembly and torque indicating device is shown as Figure 4.

C. Drive Motor

The rotating source for the spindle is a canned-rotor electric motor. The bearings, rotor and shaft are located inside the can with the stator and field windings located outside the can. One end of the can has a flange that is bolted to a corresponding flange of the chamber, exposing the bearings and shaft assembly to the vacuum environment. A gold "O" ring is used as a seal in the bolted flange. An outer water cooled shell covers the stator and acts as a support for the thin wall can. The motor was designed to operate on either 60 cycle or 500 cycle current.

D. Pumping and Lead Detection System

The chamber pumping system consisted of three pumps; a gas ballast roughing pump, a small oil diffusion pump and a 1500 liters/sec. oil diffusion pump. Two traps were used; a dry trap of Zeolite pellets and a water cooled liquid trap. The pumping speed of the system was approximately 300 liters/second. The small diffusion pump was used to help prevent contamination by the mechanical pump oil of the large diffusion pump. The pellets of the dry trap, along with the liquid trap, prevented back streaming of the diffusion pump oil in the test chamber. The test chamber containing the facility equipment was capable of reaching pressures as low as 8×10^{-9} mm of Hg after a normal bake-out period.

The entire system could be checked for leaks using a helium-type mass spectrometer leak detector. The system was so designed that all of the gases from the chamber could be pumped through the detector. A mylar bag was made that provided an enclosure around the chamber and piping to contain the helium. The leak detector could with this system sense 100% of the helium tracer and provide sensitivity of 1×10^{-9} std. cc air/sec.

E. Pressure Monitoring System

The pressure sensing and indicating system consisted of two thermocouple vacuum gages, one ionization gage control and a Bayard-Alpert ionization gage.

The thermocouple vacuum gage was capable of measuring pressures from 1 mm of Hg to 1×10^{-3} mm of Hg. The ionization gage was capable of measuring pressures from 1×10^{-3} mm of Hg to 1×10^{-10} mm of Hg.

The ionization gage mounted on the top of the chamber was located near the test bearing. The connecting tubing was 8 inches long with an inside diameter of 0.62 inches. The time constant of the pressure measuring system was less than 1 second.

The thermocouple vacuum gage in conjunction with a meter relay was used to control the operation of the diffusion pump so that the pump would go on and stay on at pressures below 6×10^{-2} mm of Hg and would shut off when the pressure rose above 10×10^{-2} mm of Hg.

V. BEARING SCREENING TESTS

A. Test Procedure

Most of the retainer materials were screened in 20 mm ball bearings in a conventional MRC Bearing Tester under an inert atmosphere prior to being evaluated in tests in the vacuum chamber. Figure 5 is a cross-section view of the tester showing the test bearing, spindle, support bearing and housing structure.

The tester was operated at a speed of 1800 rpm with an axial load of 75 pounds on the test bearing unless otherwise noted. A flow of dry nitrogen was passed into the forward spindle area, through the test bearing and out the rear of the spindle through the oil lubricated support bearing. The duration of each test run was 100 hours.

Both the bearing components and retainer materials were cleaned, weighed and measured prior to assembly. The bearings were assembled by heating the outer race to approximately 300°F and at the same time forcing the race over the assembled inner race, balls and retainer. After the internal clearance on the bearing was measured, the bearing was again cleaned with alcohol and installed on the test spindle.

B. Results

The screening tests were used to evaluate retainers of self-lubricating materials that were considered questionable for use in the vacuum environment. The seven retainers eliminated from further tests by this type of screening are shown in Table II. The glass cloth fiber in the Armalon material was abrasive and not only prevented the formation of a Teflon film on the metal surfaces but also abraded the metal surface. Figure 6a is a photograph of the Armalon retainer before test. The two phenolic plastic retainers, EB1 and EB2, containing molybdenum disulfide did not have sufficient strength and broke during the screening test. Figure 6b is a photograph of one of the phenolic retainers before test.

The carbon-graphite retainer did not have sufficient strength. A metal retainer using carbon inserts in the ball pockets was also found unsatisfactory. Figure 6c is a photograph of the metal retainer after test and shows the broken inserts. A retainer of porous sintered Stellite No. 1 alloy was made. However, a crack was found in the retainer before being impregnated with a molten powder, and as a result it was not tested. Figure 6d is a photograph of the Stellite No. 1 alloy retainer.

The 2G Nylasint retainer ran successfully in the screening tests. A check of the strength and outgassing characteristics of

Phase II indicated the material may not be satisfactory at temperatures of 160°F to 200°F.

A series of screening tests at increasing loads were made to determine the bearing load that would cause a Duroid 5813 retainer to fail. One retainer completed a 100 hour test run under a 75 pound axial load, a second 100 hour test run under a 150 pound load and then operated for 56 hours under a 225 pound load before it broke.

In addition to the above tests at ambient temperature, a bearing utilizing Pyroceram 9606 races and tungsten carbide balls was assembled for initial tests. The assembled bearing was placed in a furnace with an inert atmosphere and was heated to 1500°F to determine if the bearing could still rotate at the high temperature. Although the bearing was in an inert atmosphere some oxidation of the balls did occur. Titanium carbide balls have greater oxidation resistance and would be used on any further high temperature tests at 1500°F.

VI. ULTRA-HIGH VACUUM BEARING TESTS

A. Test Procedure

Each bearing used in the tests was assigned a number and then was disassembled, inspected and cleaned. Both weight and linear measurements were made on all bearing components including the one piece retainer. The bearing and retainer were assembled following the same technique as that used during the screening tests.

The radial clearance of the bearing was measured in 12 different positions using a Sheffield gage. The values were averaged to obtain the nominal internal radial clearance. The assembled bearing after all the measurements were made was installed in the housing assembly. Information was also obtained on each of the facility bearings. The spindle and motor bearings were inspected, measured and assembled and then the radial clearance determined in a process similar to that used on the test bearing. (This operation was performed only when the facility bearings were changed.)

The components of the spindle unit and the drive motor were assembled and installed. The noise level, coasting time and drive motor power input were determined on the spindle assembly.

The test bearing and radial weight assembly were installed on the spindle shaft, the cover plate assembly was bolted in position and the torque wire connected. The thermocouple, heater assembly and electrical lead wires were installed and the spindle assembly checked to insure free movement of the bearing weight. After installation of the components was complete, the interior of the chamber was thoroughly cleaned with ethyl alcohol. In some of the tests, a stainless plate (check for oil back streaming) was installed in front of the pump outlet duct in the chamber. The lid with a new gold O ring gasket was placed in position and the lid bolts installed.

The test chamber was covered with an asbestos blanket and heat was slowly applied to the chamber. The temperature of the dry trap was controlled at 530°F. The temperature of the chamber was approximately 100°F lower. For the tests where metal retainers were to be evaluated, the bakeout temperature of the dry trap was held at 700°F and the chamber was 600°F. The chamber was cooled and the tests started when the pressure reached the 10^{-8} mm of Hg range with the exception of the last three tests. Immediately after the spindle started to rotate, the chamber pressure increased by 0.5 to 1 order of magnitude. This increase was not so pronounced during the tests using the metal retainers. In tests at elevated temperatures, the test bearing heater was used during the bakeout procedure.

During each test measurements of the chamber pressure, test bearing and spindle bearing temperatures, torque, test time, and motor power were made as well as the bearing heater current when the heater was used. Most of this data is recorded in Table III. The torque values were obtained by observing the angle through which the 75 lb. weight assembly rotated as the bearing was started and continued on test. Each time the test was stopped, the "zero" position of the rotating weight was checked to insure no shifting of the torque wire or housing connectors had occurred. The glass sight port on the chamber provided a good view of the weight assembly and heat source, which made rapid detection possible of any malfunction of the test bearing or facility equipment.

After test, the chamber lid was removed and the test assembly inspected. In tests where bearing operation was marginal, the motor drive shaft was slowly rotated by hand before and after the test bearing was removed to be sure that no malfunction of the test equipment had occurred. The test bearing was removed from the test weight assembly and the radial clearance determined. The bearing was disassembled, inspected, cleaned and weighed. Linear measurements of the components were also made. The bearing was then reassembled and a check of the radial clearance was again made.

The inspection procedure was modified so that additional operating time could be accumulated on the spindle and motor bearings. A visual observation determination of spindle coasting time and vibration analysis was sufficient to insure continued operation of the facility bearings.

During the test program, frequent inspections were made to insure no backstreaming of oil occurred in the chamber. A cleaned stainless steel specimen, whose surface was capable of being wetted with distilled water, was placed in the chamber and located in front of the dry trap. The method of inspection was to determine if the surface of the specimen was still capable of being wetted after the 100 hour bearing test. No oil backstreaming was observed during the program.

B. Results

The results of the 20 mm bore bearing runs in an ultra-high (hard) vacuum for 100 hours or less with various dry self-lubricating retainers and a new lubricating technique are shown in Table III and IV. The detailed data observed during each test are shown in Table III and include bearing temperature, bearing torque and chamber pressure measurements. The observed test data are plotted as curves and are included in this report. The bearing and retainer materials, test time, average conditions of test, along with weight change of bearing components, and calculated coefficient of friction for each of the fourteen tests are listed on summary Table IV.

Test No. 1

The first test was a preliminary test to check the operation of the facility bearings and facility bearing cooling system as well as the test bearing (Number 1). The forward heater assembly for the test bearing was not installed and it was possible to observe the bearing through the chamber sight port. The test run was started after the thermal insulation was removed from the chamber and the test bearing temperature cooled to approximately 150°F after the high temperature "bakeout". After 27 hours of test operation, water was circulated through the pedestal to cool the spindle bearings to approximately 85°F. The corresponding test bearing temperature was approximately 95°F. After 37 hours of operation, the test was stopped, the bearing removed for inspection and reinstalled. The bakeout cycle was rerun and then the test was resumed. Inspection of the bearing after the full 100 hours of test indicated that the amount of wear of the retainer was low (0.2373 grams) and that the bearing was capable of much longer operation. The 20 mm facility bearings, both the motor and spindle bearings, during this test run incorporated one piece plastic retainers of Fluorosint material.

Curves indicating the bearing temperature and chamber pressure during this test are shown as Figure 7. Torque was not measured.

Test No. 2

The bearing (Number 28) with the Duroid 5813 retainer successfully completed the 100 hour test run. Figure 8 is a photograph of the retainer and bearing disassembled after test showing each of the components. The bearing after the 100 hour test was in excellent condition and capable of much longer operation. Wear of the balls and races was not evident and wear of the Duroid retainer was only 0.1654 grams. The balls and races exhibited an increase in weight, indicating that a film existed on the surfaces of the bearing components which came in contact with the retainer. The average internal bearing clearance decreased 0.0007 inch over the 100 hour test period. If the film was evenly coated on the raceways and balls, it would average approximately 0.0001 inch in thickness.

The conditions of test are shown on the curves of Figure 9. The chamber pressure was slightly lower than that obtained in Test No. 1. The torque was higher but still comparable to that of an oil lubricated ball bearing. After two hours of operation, the test bearing was stopped for a period of 16 hours and then restarted to determine if the film would lubricate during a transient speed condition and after remaining in a static condition for a period of time. No increase in torque or noise level was noted and the test continued without incident.

The Fluorosint retainers of the spindle and motor bearings had been replaced with Duroid 5813 retainers prior to this test. In addition, the bearing heater and the torsion wire torque device were installed and were used during this test.

Test No. 3

Operation of the test bearing (18) with the Fluorosint retainer was terminated after 43.3 hours because of the fluctuation in torque, an increase in noise level, and a gradual increase in chamber pressure. Figure 10 is a photograph of the bearing components and the broken Fluorosint retainer after test. Four starts were made during the test to determine the degree of retainer malfunction. Wear not only of the retainer, but of the balls and both races had occurred. Based on an average increase of 0.0002 inch in radial clearance and an average loss of 0.0001 inch on the ball diameters, little or no wear occurred on each raceway surface and wear of approximately 0.00005 inch occurred on each ball surface for the 43.3 hour test period. An analysis of the wear debris using x-ray diffraction techniques indicated that it contained iron and a significant quantity of amorphous material, which appeared to be carbon. This large volume of carbon was formed only when mica was present in the PTFE. It did not form with the glass fiber-MoS_2 Duroid 5813 material. The high wear of the retainer in the test bearing was similar to the wear in the facility bearings when Fluorosint was used as the retainer in both the spindle and motor bearings. Although wear did occur on the test retainer, the torque values were low during the test.

The test conditions are shown as curves in Figure 11. The torque was erratic during the first 14.9 hours of test. The bearing was stopped three times during this period. After the last restart, the torque gradually increased along with the noise level and the bearing test was terminated after 43.4 hours.

Test No. 4

The test bearing (17) with the coated BG42 stainless steel retainer failed after 23.1 hours of operation. The coating on the retainer was Surf-Kote M1284. Figure 12 is a photograph of the disassembled bearing showing the galling that occurred on the retainer and the lands of the inner race. The mat finish on the balls and raceways indicated metallic wear had occurred. The average loss in ball diameter was 0.0037 inch and the average increase in radial clearance was 0.0098 inches. The average wear of the ball surface was 0.0018 inch and the raceway surface wear averaged 0.0006 inch.

Figure 13 is a curve showing the test conditions. The torque fluctuated throughout the test. The noise level was low during the first few hours of test but gradually increased as the test progressed. After 4.7 hours, the bearing temperature slowly increased from 158°F to 175°F. In an effort to reduce the noise level, heat was applied to the bearing until a temperature of 200°F was reached. The noise however continued. The test was stopped after 16.5 hours and the bearing was allowed to soak for a short period of time. When the test was resumed, the noise level continued to increase even though the bearing temperature was lowered by increasing the flow of cooling water in the pedestal. The torque fluctuated during the entire test. The sudden fluctuations did not appear to be related to the sudden and short "grinding" noises that occurred in the bearing. The frequency of the "grinding" noise continued to increase until the test was terminated.

Test No. 5

The bearing (3) with an uncoated Inconel X retainer and a special carbon-graphite lubricating (P5) ring was used in Test No. 5. The bearing seized after 0.1 hour of operation causing the torsion wire to break at the housing weld. Figure 14 is a photograph showing the bearing components and the broken P5 carbon ring after test. An exploded schematic of the lubricating ring device is shown in Figure 15 and discussed later in the report. The bearing failure was probably caused by the P5 ring breaking and becoming wedged between the race and the retainer. Slight galling occurred on the inner surface of the retainer and the lands of the inner race. No galling and little wear was observed on the surfaces of the balls or the pockets of the retainer. The wear and galling pattern indicated that rubbing of the retainer on the race lands is more critical than rubbing of the ball in the retainer pocket. The test conditions were not observed during this short test.

Test No. 6

The same combination of bearing, retainer and ring material that failed so quickly in Test No. 5 was again tested. However, in this test the Inconel X retainer was coated with a dry lubricant coating, Surf-Kote M1284. The operation of the bearing (22) with the coated retainer and lubricant ring combination was terminated after 71.0 hours because of a failure of the test bearing heater. Figure 16 is a photograph showing the bearing components and lubricating ring after test. Excessive wear of all the bearing components had occurred. An average increase of 0.0167 inch occurred in the radial clearance and an average reduction of 0.0009 inch occurred in the ball diameter. Average wear of each race surface was 0.0037 inch, while the ball wear was approximately 0.0004 inch for each surface. This indicated a much greater wear rate on the raceway than that which occurred on the balls.

The curves indicating the conditions of test are shown in Figure 17. The bearing temperature was 346°F at the start of the test but gradually dropped to approximately 275°F. The initial torque was high but began to decrease after 7 hours. The bearing noise gradually increased but after 24.5 hours of test the noise level was reduced and torque further lowered by increasing the bearing temperature to approximately 450°F. The noise level gradually increased and a stop and start were made at 55.5 hours to determine if any change would occur in the noise level or torque value. No change was noted. After 70.0 hours of test, the bearing temperature was to be increased to 900°F but the heater for the test bearing failed and the test was terminated. During this test, it was significant to note that although wear did occur in the bearing the torque was extremely low. The use of the coating on the retainer increased the bearing life some over that of the uncoated retainer but did not prevent excessive bearing wear.

Test No. 7

Operation of the bearing (24) with the M-20 coated races, M-20 coated BG42 steel retainer and the P2W lubricating ring was terminated after 1.0 hour of operation because of an equipment malfunction. A special ceramic insulator used as the hub of the disk weight assembly fractured. A 75 pound radial weight made of chromium plated copper was fastened to the insulator and was installed for this test so that the bearing could be tested at higher temperatures. This method of fastening the disk to the insulator was found unsatisfactory.

A photograph of the bearing after test is shown in Figure 18. The components were in excellent condition, however the M-20 coating had flaked in the raceway area, indicating poor adhesion to the raceway surface. This had been the first time that this coating had been applied to ball bearing surfaces. Perhaps with a refined processing technique, this coating may have satisfactory bonding characteristics. No data was recorded during this test.

Test No. 8

The test bearing (18) using Surf-Kote M-1284 coated races and BG42 retainer with an electrographic carbon P2W ring completed the 100 hour test. Figure 19 is a photograph showing the bearing components and lubricating ring after test. Wear of both the bearing and the retainer was excessive. The average increase in the radial clearance was 0.0220 inch and the average decrease in the ball diameters was 0.0064 inch. The average wear of each race surface was 0.0023 inch while the average wear of each ball surface was 0.0032 inch.

Lubrication of the bearing was provided not only by the lubricating ring but also by two P2W carbon lubricating sticks that were contained in two stagered holes in each inner race land. The holes were placed in such a position that they were in static and dynamic balance and also permitted the sticks to lubricate the retainer over the full width of each land.

The conditions of test are shown by the curves in Figure 20. The torque was extremely high at the start of the test and after 4 hours dropped to a low value and remained constant during the remaining period of test. The temperature at the beginning of test was 125°F, but was raised with the aid of the heater to approximately 170°F after 1 hour of test and then lowered to 140°F after 24 hours of test. The temperature was held at 140°F until the 100 hour test was completed. The chamber pressure remained constant at approximately 2.0×10^{-7} mm of Hg.

The original clearance on this bearing was small because of the M-1284 coating on both the inner and outer race. The coating was rather heavy, having an average thickness of 0.0007 inch on each metal surface. The normal thickness of coating would be approximately 0.0003 inch.

Test No. 9

The Sinetex retainer was operated in test bearing 12 for 100 hours. Figure 21 is a photograph of the bearing and retainer after test. The retainer broke into 4 pieces and apparently had operated for approximately 19 hours in the broken condition. Extremely light wear was noted on the outer race and balls with no wear occurring on the inner race. Light wear was noted on the retainer. A lubricating film was detected on the inner raceway and balls. This film will be discussed later in the report. The Sinetex retainer, even though broken sometime during the test, had lubricated the bearing without significant wear during the 100 hours.

The conditions of test are shown in the curves of Figure 22. The temperature of the test bearing was maintained between 130°F and 160°F during the entire test. The torque was rather high but dropped and remained constant at a value of 4 in. oz. after 4 hours of test. The pressure averaged 1.7×10^{-7} mm of Hg for the entire test. The bearing noise level was extremely low except for a small but significant increase after the 81st hour of test. The retainer may have broken during this period of time. No change in bearing torque or temperature was observed.

Test No. 10

The bearing (9) with a BG42 coated retainer and P2W lubricating ring was tested at temperatures above 400°F and was stopped after 72 hours of operation to determine wear at the three-quarter point of the test.

Figure 23 is a photograph showing the bearing and lubricating ring. The bearing components showed considerable wear and, except for the retainer, the amount of wear was proportional to the corresponding components of the bearing in Test No. 8. The average increase in the internal clearance was 0.0191 inch and the average loss in ball diameters was 0.0042 inch. The average wear on each raceway was 0.0027 inch, while wear of each ball surface was 0.0021 inch. Again the area of greatest wear on the retainer was the ball pockets. Abrasive wear could be observed on the bore of the retainer and corresponding outer lands of the inner race.

The conditions of test are shown in the curves of Figure 24. The bearing temperature at the start of the test was 200°F. Approximately 6 hours was required to reach the operating temperature of 400°F-450°F. The torque dropped from the original value but gradually rose again after the bearing reached the operating temperature. No change in torque was observed when the bearing was stopped and restarted after 17.5 hours of test. The average pressure of the chamber during the test was 6.0×10^{-7} mm of Hg.

Test No. 11

The Sinetex retainer, reinforced with a thin band of M-10 tool steel, completed the 100 hour test without incident. Figure 25 is a photograph which shows the bearing (5) components after test. Only slight wear can be seen in the ball pockets and the bore of the retainer. The average internal clearance of the bearing decreased 0.0003 inch, indicating an average film on the raceway and ball surfaces of approximately 0.00004 inch. This film resulted in a gain of weight for the outer race, inner race and balls. A better film was obtained in this test than that obtained with the unbanded Sinetex retainer (Test No. 9) as shown by a greater weight loss of the retainer and greater weight gain of the bearing components.

The conditions of test are shown in the curves of Figure 26. The bearing operated without noise or vibration during the entire test. No increase in the torque or noise level was noted when heat was supplied to the bearing to raise the operating temperature after 20 hours of test. Although the torque was steady, the retainer had a higher rubbing friction than that of the Duroid 5813 retainer bearings operating at a comparable load and speed. The average chamber pressure was 3.3×10^{-7} mm of Hg.

The expected life of a self-lubricated bearing with either Duroid 5813 or Sinetex retainer would be much greater than 100 hours. The operating temperature range of the Duroid 5813 material is approximately 160°F, while the Sinetex retainer operated satisfactory at a temperature of 450°F.

Test No. 12

Operation of the test bearing (11) using a coated BG42 steel retainer and a SK278 carbon lubricating ring containing a high percentage of MoS_2 was terminated after 33 hours. Figure 27 is a photograph of the bearing and lubricating ring. The bearing components exhibited excessive wear. The average increase in radial clearance was 0.0302 inch and the average decrease in ball diameters was 0.0117 inch. The average wear of the raceway surface was 0.0017 inch while the wear of each ball surface was 0.0058 inch. The major part of the wear occurred on the balls rather than on the retainer, a pattern different than that experienced in Test No. 8 and Test No. 10. This high wear of the balls may be attributed to the large amound of carbon-graphite particles worn from the soft lubricating ring material.

The conditions of test are shown in the curves of Figure 28. The bearing temperature was raised from 325°F at the start of the test to approximately 400°F in the first hour and held at that value for the remaining portion of the test period. The torque started at a low value and climbed at a rapid rate until reaching 9 in. oz. after 19.0 hours of test and then leveled off and remained constant for the remaining part of the test. The noise level gradually increased with the torque value during the first 20 hours and finally became severe after 30 hours of operation. The test was terminated 3 hours later.

Test No. 13

Operation of the test bearing (7) using a coated M-10 retainer and M-10 bearing with a P2W carbon ring was terminated after 6 hours of test because of a malfunction of the test equipment. Figure 29 is a photograph of the bearing and lubricating ring. The bearing components are in excellent condition but some wear was evident on the balls and raceways as indicated by the mat surfaces. All the bearing components lost weight apparently indicating wear, but the average increase in internal clearance was less than the average decrease on the diameter of the balls. The exact reason for this wear pattern is not known unless a film formed on the raceways faster than wear occurred in the balls.

The conditions of test are shown in the curves of Figure 30. The test was started at a temperature of 825°F and within two hours reached a value of 900°F. After 5 hours of operation, the 900°F temperature could not be maintained. The test was stopped and the temperature was lowered to 400°F. After 16 hours, the test was resumed but again stopped one hour later. The torque remained constant at a low value during the entire test.

This was the first bearing test scheduled for temperatures above 1000°F.

Test No. 14 and 14A

The test bearing (A) using a coated M-10 steel retainer, Stellite 19 races, tungsten carbide balls and 56HT lubricating ring was operated for 24.0 hours at a temperature of 1100°F (Test 14). Later in the same test, as both the test and facility bearing temperatures were decreased, the forward spindle bearing (25) using Sinetex retainers was operated at a temperature of -300°F for 3.6 hours (Test 14A).

Figure 31 is a photograph of the Stellite test bearing after 24.0 hours test at a temperature of 1100°F and 3.6 hours at temperatures below 200°F. Wear of the bearing components was low. The increase in the average radial clearance was 0.0002 inch and an average reduction in the ball diameters was 0.0001 inch. The wear of each raceway was extremely small with almost all wear occurring on each ball surface. Wear of the lubricating ring was small, indicating that having less carbon-graphite in the bearing than in previous tests may provide better lubrication. Some reduction in wear may be due to the composition of the carbon ring. The 56HT material contained a metallic salt and oxidation inhibitor. This same material when used as the retainer in a 204 bearing in another test program, provided excellent dry lubrication at a temperature of 972°F in a dry nitrogen atmosphere under a 5 lb. radial load.

The conditions of test for the Stellite high temperature bearing with the coated M-10 retainer is shown in the curve of Figure 32. The torque was low and uniform after an initial fluctuation period during the first several hours of test. The noise level was low and the bearing appeared to be capable of operating for a much longer period of time when the test bearing was stopped and all the bearings cooled for the low temperature start and operation.

In Test 14A, only the forward bearing of the two front spindle bearings was instrumented. The aft-front spindle bearing was probably at or near the same temperature as the forward bearing during most of the test. Figure 33 is a photograph of the spindle bearing with a banded Sinetex retainer after the 24.0 hour operation at temperatures above 100°F and the 3.6 hour operation at -300°F. The bearing components and retainer are in excellent condition. The average radial clearance decreased 0.0002 inch and the average diameter of the balls increased 0.0001 inch. This indicated that a film was on the balls but probably only a light film on the raceways. A weight increase of the inner and the outer race did indicate an extremely light film on the raceway. The spindle bearing was operated intermittantly as the liquid nitrogen was circulated through the pedestal to lower the temperature to -300°F. The bearing components and retainer are in excellent condition.

The bearing test conditions at the cryogenic temperature are shown in the curves of Figure 34. The bearing started and operated at -300°F without incident. Although the torque measurement could not be made at the low temperature, no surge of power or change in the low noise level was observed. The amperes drawn by the drive motor, as measured by a polyphase ammeter, remained relatively uniform for both the high temperature (14) and low temperature (14A) tests. The temperature of the motor and test bearing range from 0°F to 200°F. The approximate load on each of the two front spindle bearings was 50 lbs.

C. Facility Bearings

Test data was also obtained on the Duroid 5813 retainers used in the bearings of the drive motor and test spindle assembly. This information was used to prepare curves showing the relationship of load and retainer wear with bearing life. The bearings were in the chamber and operated at the same average pressure as the test bearings. The operating temperatures were controlled within the range of 86°F to 200°F. The location and calculated radial load for each bearing is shown below:

Bearing Location	Radial Load, Lbs.
Front Motor Bearing	1.8
Rear Motor Bearing	1.8
Rear Spindle Bearing	30.0
Front-Forward Spindle Bearing	51.0
Front-Aft Spindle Bearing	51.0

The test results of the motor and spindle bearings using the Duroid 5813 retainers are shown in Table V. Bearings No. 10, 20, 25 and 27 were removed, measured and reinstalled during the test program. The remaining bearings were only removed at the time of replacement. All of the bearings were in good operating condition when they were replaced during the test program.

Wear of the Duroid 5813 retainers in the facility bearings and the two test bearings is plotted as a function of operating time and load in the curves of Figure 35. The wear of the Sinetex retainers used in two test bearings is also included. Wear of the Duroid retainers in the test bearings (Test 1 and 2) although extremely low, was a larger wear per cent of total retainer weight than wear in any of the facility bearings. The Sinetex retainers, one banded the other unbanded, had a less wear (per cent of total retainer weight) than the Duroid 5813 retainers in the two test bearings. It appears that Sinetex retainers would give the longer life both at 160°F and 460°F as compared to the Duroid 5813 retainer which was tested at 130 to 160°F. Considerable spread in retainer wear was noted for the two front spindle bearings. This is understandable since the two bearings operated at different temperatures and different thrust loads. If both bearings evenly support the load in the test facility, the load on each would be 51 lb. Bearings, No. 15 and No. 23, operated at conditions less severe than bearings No. 25 and No. 27.

The retainer wear of the motor bearings was extremely low under their light loads. These bearings operated under almost constant conditions of temperature and load for all the tests.

D. Discussion

The measurement of wear of the bearing components by weight gain or loss is somewhat inaccurate. The retainers were inner land riding and if the self-lubricating retainer provided effective lubrication, as did only the Duroid 5813 and the Sinetex material, a film occurred not only in the ball path but also in the race land. If the retainer exhibited wear on the contact surface, a weight gain by galling or a weight loss by abrasion or a combination of weight gain and loss could occur on the inner race. Wear of the raceway of both races was considered as an average even though wear of the outer race was concentrated in the area of the load zone only.

The wear was calculated from the reduction in ball diameter and the increase in internal clearance as noted:

$$\text{Raceway wear of each surface} = \frac{(R_C - R_{C1}) - 2\,(d - d_1)}{4}$$

$$\text{Ball wear of each surface} = \frac{2\,(d - d_1)}{4}$$

R_C = Initial Radical Clearance in Inches

R_{C1} = Final Radical Clearance in Inches

d = Initial Ball Diameter

d_1 = Final Ball Diameter

Other methods were also used to determine effective lubrication of the two satisfactory self-lubricating material. Photo micrographs (20X) were taken of the raceways showing a "buildup" of the film. A view of a typical spot on the raceway of an unused inner race is shown in Figure 36a. The grinding marks are easily distinguishable running parallel to the race groove. The photograph on Figure 36b is of the inner race of the bearing used in Test 9 after 100 hours operation and shows the Teflon film formed. The thickness of this coating is more than sufficient to provide adequate bearing lubrication and may be as much as a thousand times the thickness of the film of an oil lubricated bearing. The photograph on Figure 37a is a view of the outer race of an unused bearing and the photograph on Figure 37b is a view of the outer race of the bearing used in Test 11 after 100 hours of operation. The coating on a ball used in Test 11 is shown in the photograph on Figure 38a. A light was directed at the ball in the center of the photograph. The dark area surrounding the center of the photograph is caused by the light reflection. The Teflon film covers the grinding marks and is streaked as if caused by weaving a paint brush along on a newly painted surface. The large dark spots are a mixture of Teflon, Molybdenum disulfide and bronze. The photograph shown on Figure 38b is a view of a Sinetex retainer pocket. At the bottom of the figure can be seen the edge of the steel band. Above the band is the wear area caused by rubbing of the ball in the pocket. Above the wear area is the surface of the porous filled Sinetex material.

No attempt was made to determine the life of the two types of self-lubricating retainers that provided satisfactory lubrication of 204 size 20 mm bore bearings operating in an ultra-high vacuum. Sufficient information has been obtained to indicate that life is much greater than the 100 hours that the materials were operated in the test chamber.

The test results of the facility bearings give some indication of wear vs. life for various bearing loads. Although a small weight loss of some of the races and balls was observed, no measureable wear of the ball or raceway diameters could be detected.

The unit (Hertz) stress has been calculated for the test bearing at various loads and plotted as a curve in Figure 39. Wear can be compared to various levels of unit stresses within the range of loads tested and should give some indication of wear of different size of bearings if the unit stress is held constant.

Some information was obtained with regard to bearing speeds. Test bearings with Sinetex retainers were operated in the vacuum chamber at DN values up to 220,000 for 50 hours at light loads of 1.8 lb.

The internal radial clearance of a bearing should not have an effect on bearing life if sufficient clearance is provided for the dry lubricant film. The motor bearings had an internal clearance of .0010 inches and operated satisfactory at light loads. The test and spindle bearings had an internal radial clearance of .0035 inches and operated satisfactory. It is recommended that .0010 inch be considered as the minimum internal clearance for 204 size 20 mm bore bearings.

It also became apparent during the tests of self-lubricating retainers in the bearings that no direct relationship existed between wear and friction. This was especially noted in the tests where the carbon graphite was used as a lubricant. The carbon proved to be an ineffective lubricant. An X-ray diffraction analysis of the wear debris removed from bearing tests No. 8, 12 and 13 were all alike and identified as a metallic carbide (opp M_7C_3) and a minor unidentified phase. The metallic carbide may have any combination of Fe, Cr, Mn, V and Mo and carbon.

VII. CONCLUSIONS

1. Conventional 204 size, 20 mm tool steel ball bearings have been adapted, with the aid of self-lubricating retainer materials, for use in an ultra-high vacuum environment.

2. Bearings incorporating dry lubricants were operated under a radial load of 75 pounds and an axial load of 5 pounds over a temperature range of 130 to 450°F in a vacuum environment of 1.7×10^{-7} to 3.7×10^{-7} mm of Hg pressure for 100 hours with no measurable wear occurring on the races or balls.

3. The feasibility of operating 20 mm bore bearings at temperatures above 1000°F in a vacuum environment was demonstrated.

4. A bearing incorporating a dry lubricant was successfully started and operated at a temperature of -300°F in a vacuum environment.

5. Sufficient test data has been obtained to verify that other bearing sizes in addition to 204, 20 mm bore bearings can be adapted for use in a vacuum environment where the maximum load, unit stress and speed for each bearing can be specified.

6. Of the two satisfactory self-lubricating retainer materials, Duroid 5813 (filled Teflon) exhibited slightly higher wear and lower friction than did the Sinctex (impregnated sintered bronze).

Prepared By

P. H. Bowen
Project Engineer

Supervised By

E. S. Bober
Supervisory Engineer

~~Approved By~~

H. R. Sheppard, Mgr.
Chemical Appl. Sec.

TABLE I

Description of Dry Powders and Self Lubricating Materials

Trade Name	Source	Description
P5	Purecarbon Co. Inc.	Hard grade of carbon graphite
P2W	Purecarbon Co. Inc.	Medium soft grade of carbon graphite
56HT	Purecarbon Co. Inc.	Medium hard grade of graphite impregnated with a metallic salt and anti-oxidant
SK278	Stackpole Carbon Co.	Carbon graphite containing MoS_2
M-20	Midwest Research Institute	An experimental bonded solid film lubricant containing MoS_2
M-1284	Hohman Plating and Mfg. Co.	A matrix bonded solid film lubricant containing MoS_2
Duroid 5813	Rogers Corporation	Teflon with glass fiber and MoS_2 filler
Armalon	E. I. DuPont de Nemours & Co.	Teflon with glass cloth filler
Fluorosint	Polymer Corp. of Pennsylvania	Teflon with mica filler
Nylasint 2G	Polymer Corp. of Pennsylvania	Nylon with carbon filler
Sinetex	Booker Cooper Inc.	Sintered bronze containing Teflon and MoS_2
Stellite No. 1	Haynes Stellite	Porous sintered alloy
XEB1	Westinghouse Elect. Corp.	Phenolic resin with MoS_2
XEB2	Westinghouse Elect. Corp.	Phenolic resin with MoS_2

TABLE II

SCREENING TESTS OF RETAINERS IN MRC BEARING TESTER
(Materials Not Further Evaluated in the Ultra-High Vacuum Environment)

Sample No.	Retainer Material	Test Time (Hours)	Axial Load (Lbs.)	Initial Wt. of Retainer	Wt. Loss (Grams)	Remarks
1	Armalon	100	75	10.1261	-0.0332	Wear of the bearing race and balls occurred.
2	Phenolic resin bonded MoS_2-EB6	100	75	8.0048	-0.0289	Retainer broken at end of test.
3	Phenolic resin bonded MoS_2-EB8	114	75	6.6292	-1.1832	Retainer broken at end of test.
4	Inconel X retainer with P2W carbon inserts	1	75	9.0398	-0.1998	Inserts broken and test stopped.
5	P2W Carbon	<1	75	--	--	Retainer broken and test stopped.
6	Sintered Stellite No. 1 alloy			Not Tested		Material cracked prior to bearing assembly.
7	2G Nylasint	100	75	5.7471	-0.0066	Results satisfactory: n excellent material: but not believed to have sufficient strength at 160-200°F.

TABLE III

ULTRA-HIGH VACUUM BEARING TEST DATA

Test 1 - Duroid 5813 Retainer

Time Hrs.	Pressure mm of Hg. X 1×10^{-7}	Bearing Temp. °F	Bearing Torque In.-Oz.
0.0	0.7	150	Data Not Observed During Test
1.0	5.4	160	
3.0	5.6	165	
10.0	6.5	160	
17.0	4.7	118	
27.0	4.5	95	
34.0	2.6	95	
37.0	2.5	95	
37.0*	0.8	175	
39.0	4.4	176	
54.5	4.2	120	
58.0	3.4	110	
63.0	3.5	100	
79.0	4.2	95	
83.6	3.4	90	
102.0	2.8	90	
Ave.	3.7		

Test 2 - Duroid 5813 Retainer

Time Hrs.	Pressure mm of Hg. X 1×10^{-7}	Bearing Temp. °F	Bearing Torque In.-Oz.
0.0	0.2	150	-
1.0	4.0	169	-
2.0	3.5	174	2.0
2.0*	0.3	123	-
4.5	3.6	126	-
6.6	6.0	127	2.5
8.0	4.0	120	2.0
24.0	3.4	134	2.0
29.4	5.0	132	2.0
48.0	2.2	128	-
54.0	2.4	131	2.0
64.0	2.2	130	2.0
79.0	3.4	135	2.0
100.0	2.0	135	2.0
Ave.	3.2		

Test 3 - Fluorosint Retainer

Time Hrs.	Pressure mm of Hg. X 1×10^{-7}	Bearing Temp. °F	Bearing Torque In.-Oz.
0.0	0.1	160	-
1.0	9.0	122	4.0
3.0	6.7	147	2.0
3.0*	0.2	150	-
4.0	5.1	150	1.0
7.3	7.5	136	1.0
7.3*	0.4	-	-
8.6	2.5	129	2.0
12.8	4.3	130	-
14.9	5.0	130	2.0
14.9*	0.4	-	2.0
16.0	4.1	122	2.0
39.0	6.9	125	3.0
43.3	7.0	127	3.5
Ave.	4.7		

Test 4 - BG-42 Steel Retainer

Time Hrs.	Pressure mm of Hg. X 1×10^{-7}	Bearing Temp. °F	Bearing Torque In.-Oz.
0.0	0.3	152	-
1.0	2.9	165	5.5
2.5	2.9	162	6.0
3.0	2.3	164	4.0
4.7	1.9	158	4.0
9.0	1.9	175	4.0
11.0	0.9	175	6.0
13.7	0.9	195	5.0
15.7	1.0	195	4.5
16.5	1.0	195	4.5
16.5*	0.6	160	-
19.0	2.0	175	4.0
21.0	2.8	175	4.0
23.0	2.8	175	4.0
Ave.	1.7		

TABLE III (Continued)

ULTRA-HIGH VACUUM BEARING TEST DATA

Test 5 - Data Not Observed

Test 6 - Coated Inconel X Retainer

Time Hrs.	Pressure mm of Hg. X 1×10^{-7}	Bearing Temp. °F	Bearing Torque In.-Oz.
0.0	0.8	346	-
1.0	7.0	310	4.0
2.0	2.3	275	4.5
10.0	2.2	267	2.0
20.0	2.6	260	2.0
24.5	3.7	260	2.0
24.5*	0.9	490	3.0
26.0	5.8	455	1.0
30.0	1.8	447	1.0
38.0	2.0	450	1.0
43.0	0.9	435	1.0
48.0	1.7	430	1.0
55.5	1.7	410	-
55.5*	0.2	420	1.0
58.0	2.0	417	1.5
64.0	2.5	430	1.5
70.0	2.1	420	1.0
Ave.	2.9		

Test 7 - Data Not Observed

Test 8 - Coated BG-42 Steel Retainer

Time Hrs.	Pressure mm of Hg. X 1×10^{-7}	Bearing Temp. °F	Bearing Torque In.-Oz.
0.0	0.7	125	-
1.0	2.3	172	8.0
2.0	2.9	170	7.0
4.0	2.7	178	-
24.0	1.8	140	3.0
57.0	2.0	140	-
67.0	2.0	135	2.0
72.0	2.3	142	-
73.0	2.3	145	2.0
77.0	2.3	142	-
91.0	2.3	145	2.0
93.0	1.5	145	-
96.0	1.6	145	2.0
99.0	1.7	145	-
100.0	1.6	145	2.0
Ave.	2.0		

Test 9 - Sinetex Retainer

Time No.	Pressure mm of Hg. X 1×10^{-7}	Bearing Temp. °F	Bearing Torque In.-Oz.
0.0	0.7	160	-
1.0	2.0	160	5.0
2.0	2.1	160	5.0
4.0	2.1	160	4.0
5.0	2.0	155	-
8.0	1.5	155	4.0
23.5	1.2	135	4.0
26.0	1.5	135	4.0
47.0	1.9	125	4.0
52.0	1.9	130	4.0
55.0	1.8	130	4.0
72.0	1.7	130	4.0
74.0	1.8	130	4.0
80.0	1.8	130	-
95.0	1.8	130	4.0
100.0	1.7	130	4.0
Ave.	1.7		

Test 10 - BG-42 Steel Retainer

Time Hrs.	Pressure mm of Hg. X 1×10^{-7}	Bearing Temp. °F	Bearing Torque In.-Oz.
0.0	0.5	200	-
2.0	6.8	275	4.0
3.0	7.0	310	-
4.5	8.8	380	2.0
6.0	9.0	400	-
7.5	9.3	450	-
16.0	4.0	450	3.0
17.5	4.2	420	-
17.5*	0.7	350	3.0
20.5	7.4	400	4.0
22.5	5.0	450	4.0
38.0	6.4	450	4.0
58.0	6.5	446	4.0
63.5	6.3	440	4.0
72.0	6.3	440	4.0
Ave.	6.0		

TABLE III (Continued)

ULTRA-HIGH VACUUM BEARING TEST DATA

Test 11 - Banded Sinetex Retainer

Time Hrs.	Pressure mm of Hg. X 1x10⁻⁷	Bearing Temp. °F	Bearing Torque In.-Oz.
0.0	0.9	370	-
1.0	1.8	375	2.0
2.5	1.8	370	-
18.0	2.0	375	4.5
20.0	6.0	400	-
23.5	6.0	420	4.0
26.0	5.0	430	4.0
27.0	3.5	400	-
50.0	2.9	390	4.0
67.0	3.1	390	4.0
100.0	2.8	390	4.0
Ave.	3.3		

Test 12 - Coated BG-42 Steel Retainer

Time Hrs.	Pressure mm of Hg. X 1x10⁻⁷	Bearing Temp. °F	Bearing Torque In.-Oz.
0.0	0.9	325	-
1.0	4.4	400	1.0
16.5	5.1	385	6.0
19.0	3.6	400	9.0
21.5	5.4	400	9.0
23.5	4.9	400	9.0
25.0	4.6	400	9.0
33.0	5.4	400	9.0
Ave.	4.7		

Test 13 - M-10 Steel Retainer

Time Hrs.	Pressure mm of Hg. X 1x10⁻⁷	Bearing Temp. °F	Bearing Torque In.-Oz.
0.0	2.0	825	-
1.0	9.3	830	1.0
2.2	28.0	935	1.0
3.0	20.0	940	1.0
5.0	15.0	900	1.0
5.0*	0.9	400	-
6.0	9.4	400	1.0
7.0	9.0	400	1.0
Ave.	15.3		

Test 14 - Coated M-10 Steel Retainer

Time Hrs.	Pressure mm of Hg. X 1x10⁻⁷	Bearing Temp. °F	Bearing Torque In.-Oz.
0.0	20.0	1050	2.0
0.9	26.0	1100	-
1.5	20.0	1100	1.0
2.0	20.0	1100	2.0
2.5	34.0	1100	-
6.0	34.0	1100	2.0
8.3	30.0	1100	2.0
20.1	20.0	1100	2.0
23.0	15.0	-	-
24.0	18.0	-	-
24.4	11.0	1070	2.0
Ave.	22.6		

Test 14A - Banded Sinetex Retainer - Ped. Brg.

Time Hrs.	Pressure mm of Hg. X 1x10⁻⁷	Bearing** Temp. °F	*Motor Brg*** Temp. °F	Ped. Brg. Temp. °F
0.0	38.0	250	-	-300
1.0	41.0	-	-	-300
2.0	27.0	185	-	-303
3.0	40.0	135	-10	-280
3.0*	16.0	130	5	-310
3.3	16.0	130	-	-310
3.6	22.0	150	13	-280
Ave.	28.5			

*Indicates Restart

**75 lb. Loaded Brg. Retainer Coated M10

***Motor Brg. Retainer Duroid 5813

TABLE IV

SUMMARY ULTRA-HIGH VACUUM BEARING TESTS

Test Identification No.	1	2	3	4	5	6	7
Bearing Speed, rpm	1800	1800	1800	1800	1800	1800	1800
Bearing Load, Radial Lb.	75	75	75	75	75	75	75
Bearing Load, Axial Lb.	5	5	5	5	5	5	5
Bearing Material	M-10	M-10	M-10	M-10	M-10	M-10	M-10
Bearing Number	1	23	18	17	3	22	24
Retainer Material	Duroid 5813	Duroid 5813	Fluorosint	BG42 + M1284	Inconel X	Inconel X + M1284	BG42+ + M-20
Lubricant Ring Material	-	-	-	-	P5	P5	P2W
Test Time Hours	104.0	100.0	42.0	23.1	0.1	71.0	1.0
Bearing Radial Clearance, In.	0.0033	0.0032	0.0033	0.0033	0.0034	0.0035	0.0033
Change in Radial Clearance, In.	-	-0.0007	0.0002	0.0098		0.0167	-
Initial Wt. of Retainer, Gms.	0.3122	0.3122	0.3122	0.3122		0.3122	
Ave. Change in Ball Dia. In.	NC++	NC	-0.0001	-0.0037		-0.0009	
Initial Wt. of Retainer Gms.	11.0103	11.1925	11.0495	35.9269		17.8513	
Change of Retainer Gms.	-0.2373	-0.1654	-0.3044	-0.1721	Data Not Recorded	-0.6464	Data Not Recorded
Initial Wt. of Outer Race Gms.	-	51.5954	51.8712	51.9151		51.8084	
Change of Outer Race, Gms.	-	0.0009	-0.0049	-0.0211		-0.0179	
Initial Wt. of Inner Race Gms.	-	25.4152	25.4730	25.4874		25.3669	
Change of Inner Race Gms.	-	0.0011	0.0018	-0.0161		-0.1779	
Initial Wt. of Balls Gms.	-	12.2754	12.2746	12.2766		12.2763	
Change of Balls (6) Gms.	-	0.0020	-0.0080	-0.4396		-0.1157	
Change of Lubricant Ring Gms.	-	-	-	-		-1.8164	
Wear of Retainer %	2.2	1.5	2.7	0.5		3.6	
Ave. Pressure mm of Hg 1 x 10^{-7}	3.7	3.2	4.7	1.7		2.9	
Ave. Bearing Temp. °F	100	130	130	175		275 & 440	
Ave. Torque In-Oz.	-	2.0	2.0	4.0		1.5	
Ave. Coef. of Friction	-	0.002	0.002	0.004		0.001	

+Inner Race Coated
++No Measurable Change in Diameter

TABLE IV (Continued)

SUMMARY ULTRA-HIGH VACUUM BEARING TESTS

Test Identification No.	8	9	10	11	12	13	14	14A
Bearing Speed, rpm	1800	1800	1800	1800	1800	1800	1800	1800
Bearing Load, Radial Lb.	75	75	75	75	75	75	75	75
Bearing Load, Axial Lb.	5	5	5	5	5	5	5	5
Bearing Material	M-10	M-10	M-10	M-10	M-10	M-10	Alloy 19**	M-10
Bearing Number	18	12	9	5	11	7	A	25
Retainer Material	BG42 +* M-1284	Sinetex	BG42 + M-1284	Sinetex Banded	BG42 + M-1284	M-10 + M-1284	M-10 + M-1284	Sinetex Banded
Lubricant Ring Material	P2W	-	P2W	-	SK278	P2W	56HT	-
Test Time Hours	100.0	100.0	72.0	100.0	33.0	6.0	24.0	3.6 + 24
Bearing Radial Clearance, In.	0.0006	0.0035	0.0036	0.0035	0.0036	0.0033	0.0024	0.0044
Change in Radial Clearance, In.	0.0220	0.0001	0.0191	-0.0003	0.0302	0.0001	0.0002	-0.0002
Initial Wt. of Retainer, Gms.	0.3122	0.3122	0.3122	0.3122	0.3122	0.3122	0.3124	0.3122
Ave. Change in Ball Dia. In.	-0.0064	NC	-0.0042	NC	-0.0117	-0.0003	-0.0001	-.0001
Initial Wt. of Retainer Gms.	17.1281	26.5139	17.9266	27.5882	14.8764	18.1360	18.2182	27.1000
Change of Retainer Gms.	-2.3993	-0.1935	-0.7758	-0.3303	-1.3722	-0.1097	-0.0167	-0.0700
Initial Wt. of Outer Race Gms.	51.9476	52.0082	51.3638	51.7647	51.8353	51.8710	56.3642	52.0705
Change of Outer Race, Gms.	-0.2832	-0.0028	-0.1903	0.0127	-0.1135	-0.0030	-0.0004	0.0006
Initial Wt. of Inner Race Gms.	24.9707	25.4738	25.4747	25.4962	25.4232	25.4055	27.3004	25.3843
Change of Inner Race Gms.	-0.3961	0.0001	-0.3297	0.0276	-0.3949	-0.0113	-0.0003	0.0004
Initial Wt. of Balls Gms.	12.2624	12.2784	12.2808	12.2585	12.2778	12.2694	13.4144	12.2793
Change of Balls (6) Gms.	-0.7574	-0.0017	-0.5091	0.0049	-1.3335	-0.0041	-0.0002	-0.0007
Change of Lubricant Ring Gms.	-1.3517	-	-1.0969	-	-1.3939	-0.2450	-	-
Wear of Retainer %	14.0	0.7	4.3	1.2	9.2	0.6	0.1	0.3
Ave. Pressure mm of Hg 1×10^{-7}	2.0	1.7	6.0	3.3	4.7	15.3	22.6	28.5
Ave. Bearing Temp. °F	150	135	440	390	400	900 & 400	1100	-300
Ave. Torque In-Oz.	2.5	4	4	4	9	1	2	-
Ave. Coef. of Friction	0.002	0.004	0.004	0.004	0.008	0.001	0.002	-

+Inner Race Coated
++No Measurable Change in Diameter
*Races Coated and Carbon Inserts in Inner Race Land
**Races Were of Alloy #19 and Balls Were of Tungsten Carbide

TABLE V

ULTRA-HIGH VACUUM FACILITY BEARING DATA

Bearing No.	10	10	20	20	15	25	25	23	27	27	30
Bearing Material	T-1	T-1	T-1	T-1	M-10	M-10	M-10	M-10	M-10	M-10	M-10
Retainer Material	Duroid*	Duroid	Duroid	Duroid	Duroid	Duroid	Duroid	Duroid	Duroid	Duroid	Duroid
Bearing Location and Position	Motor Rear	Motor Rear	Motor Front	Motor Front	Front Spindle Forward	Front Spindle Forward	Front Spindle Forward	Front Spindle Aft	Front Spindle Aft	Front Spindle Aft	Rear Spindle
Test Time Hours	238	678	338	778	405	100	238	405	100	238	405
Bearing Radial Clearance, In.	0.0010	0.0010	0.0010	0.0010	0.0035	0.0035	0.0035	0.0035	0.0035	0.0035	0.0035
Change Radial Clearance, In.	-0.0004	-0.0002	-0.0007	-0.0008	0.0001	0.0003	0.0005	-0.0003	0.0002	0.0002	-0.0005
Ave. Change in Ball Dia., In.	NC**	-0.0001	NC	NC	-0.0001	-0.0001	-0.0001	NC	NC	NC	-0.0001
Ball Diameter, Inches	0.3124	0.3124	0.3124	0.3124	0.3122	0.3122	0.3122	0.3122	0.3122	0.3122	0.3122
Initial Wt. of Retainer, Grams	10.6257	10.6257	11.0835	11.0835	10.5112	10.9930	10.9930	10.5848	10.6065	10.6065	10.6382
Change of Retainer Weight, Grams	-0.0173	-0.1153	-0.0582	-0.2046	-0.1532	-0.0861	-0.2223	-0.1311	-0.0444	-0.1657	-0.0379
Initial Wt. of Outer Race, Grams	56.2295	56.2295	55.7978	55.7978	51.5846	52.0792	52.0792	52.0557	52.0363	52.0363	52.2518
Change of Outer Race, Grams	-0.0020	-0.0032	-0.0006	-0.0004	0.0002	-0.0014	-0.0031	0.0015	-0.0010	-0.0035	-0.0008
Initial Wt. of Inner Race, Grams	28.8147	28.8147	28.4335	28.4335	25.4677	25.4047	25.4047	25.4439	25.4586	25.4586	25.4414
Change of Inner Race, Grams	-0.0011	-0.0033	-0.0005	0.0015	-0.0109	0.0062	-0.0080	0.0006	-0.0005	-0.0034	-0.0004
Retainer Loss, %	0.1	1.2	0.6	2.0	1.5	0.8	2.2	1.3	0.4	1.6	0.4

*Duroid 5813 material was used in all of the facility bearings
**NC - No measurable change in dimension

Bearing (MRC): 204 size 20 mm bore
Ball diameter: 0.3122" (6 Balls)
Outer race conformity: 52% of ball dia.
Inner race conformity: 51% of ball dia.
Inner race shoulder Ht: 16% of ball dia.

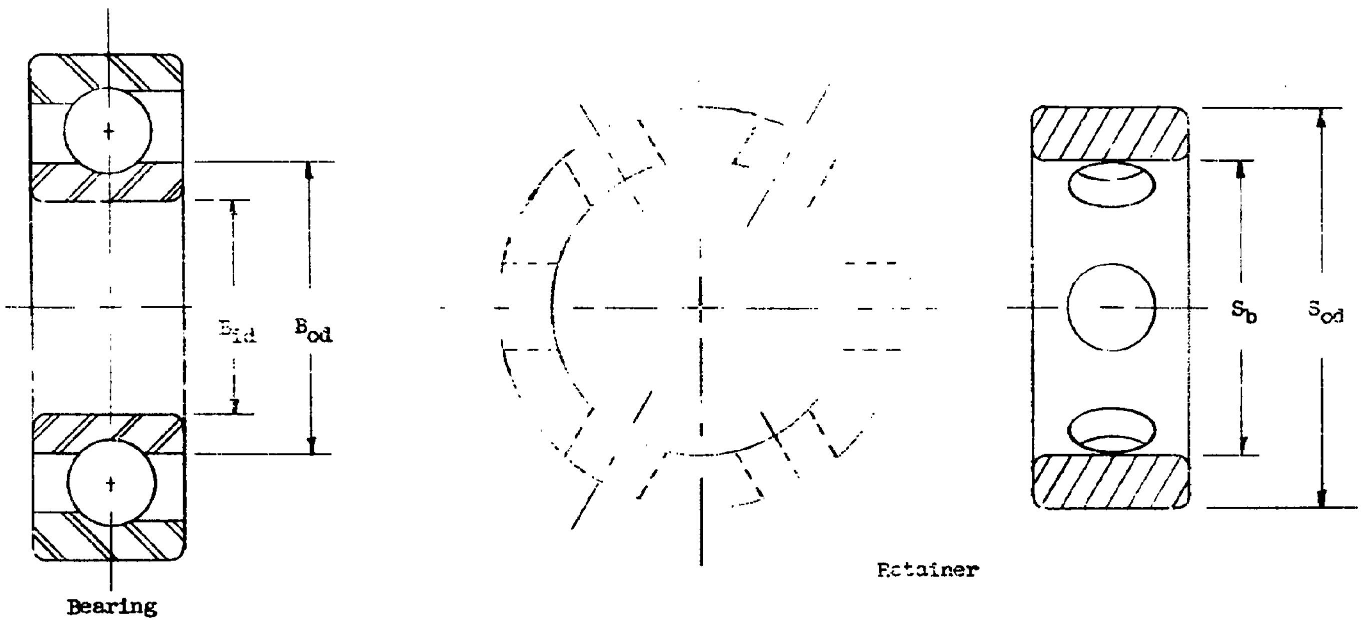

FIGURE 1

TEST BEARING DESIGN

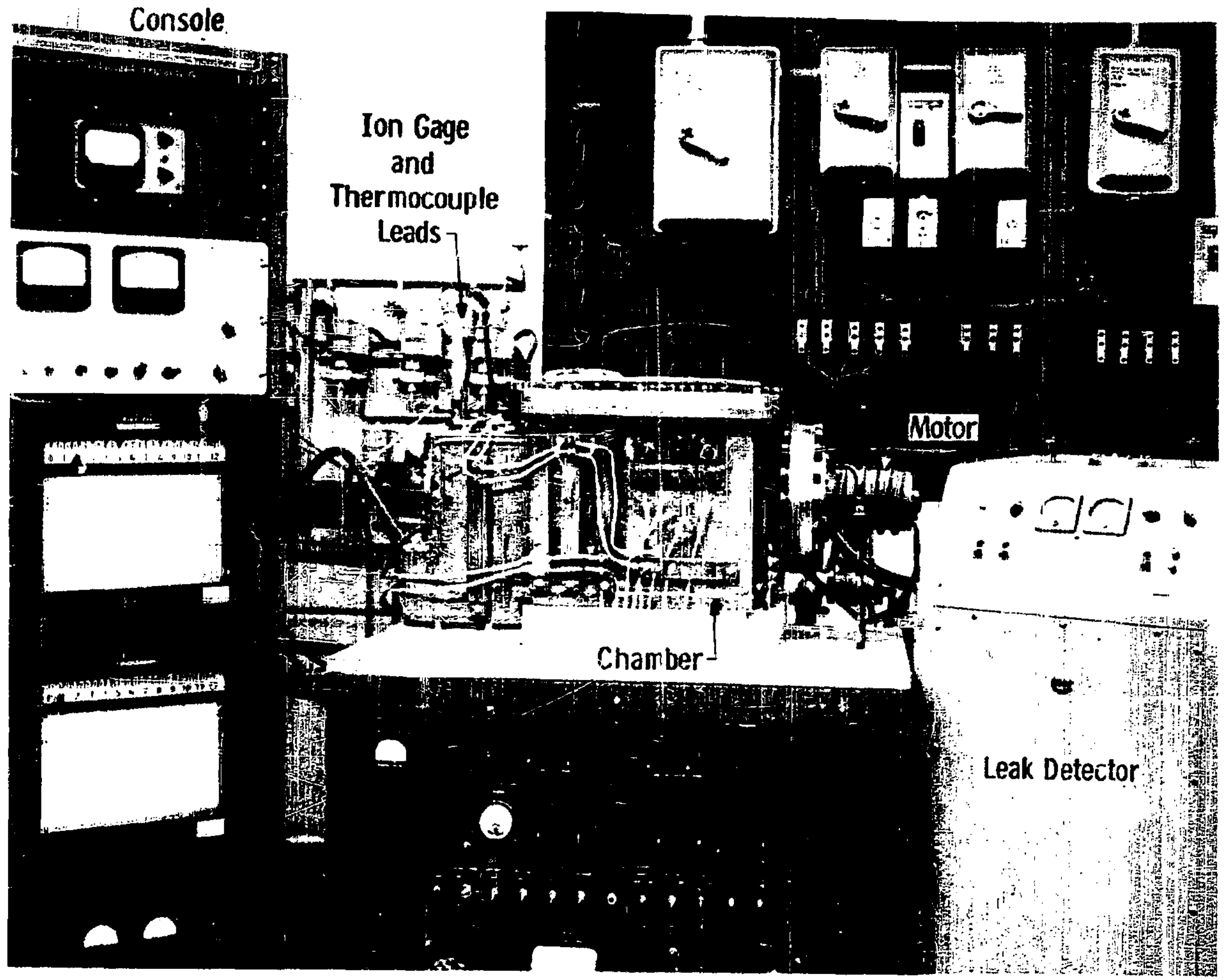

FIGURE 2

ULTRA–HIGH VACUUM BEARING AND LUBRICANT TEST APPARATUS

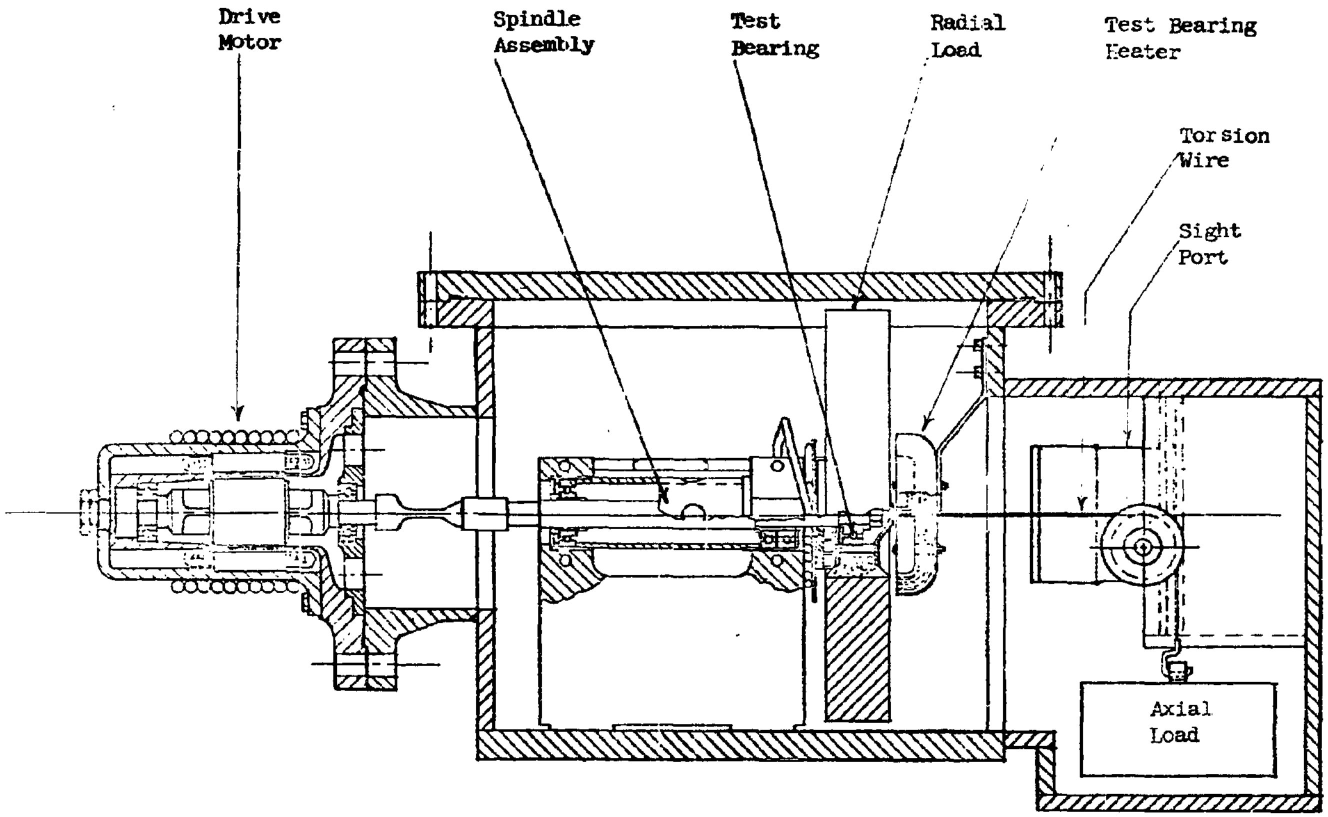

FIGURE 3 - CROSS-SECTIONAL VIEW OF ULTRA-HIGH VACUUM BEARING TESTER

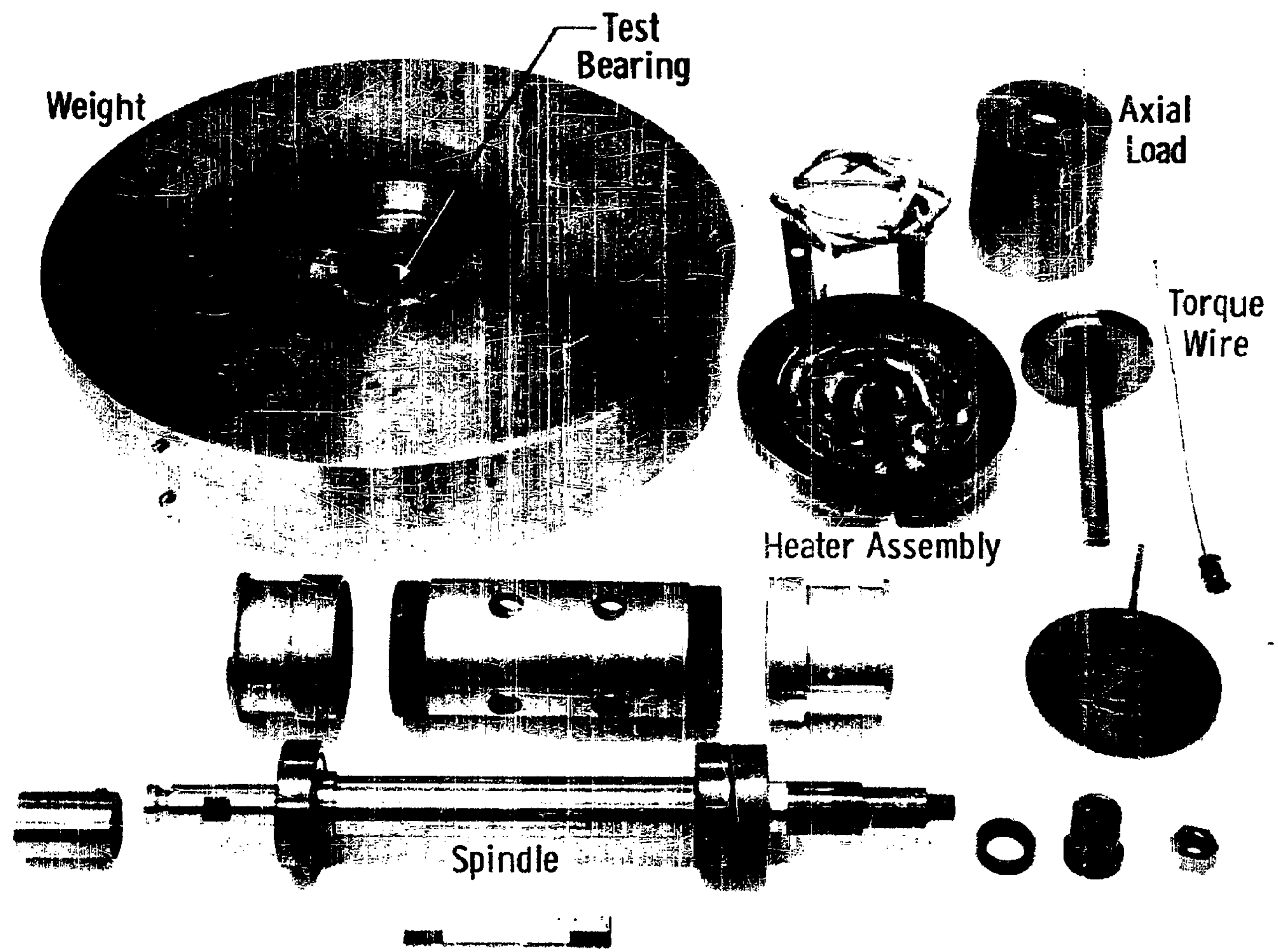

FIGURE 4

SPINDLE ASSEMBLY, LOAD AND TORQUE DEVICE

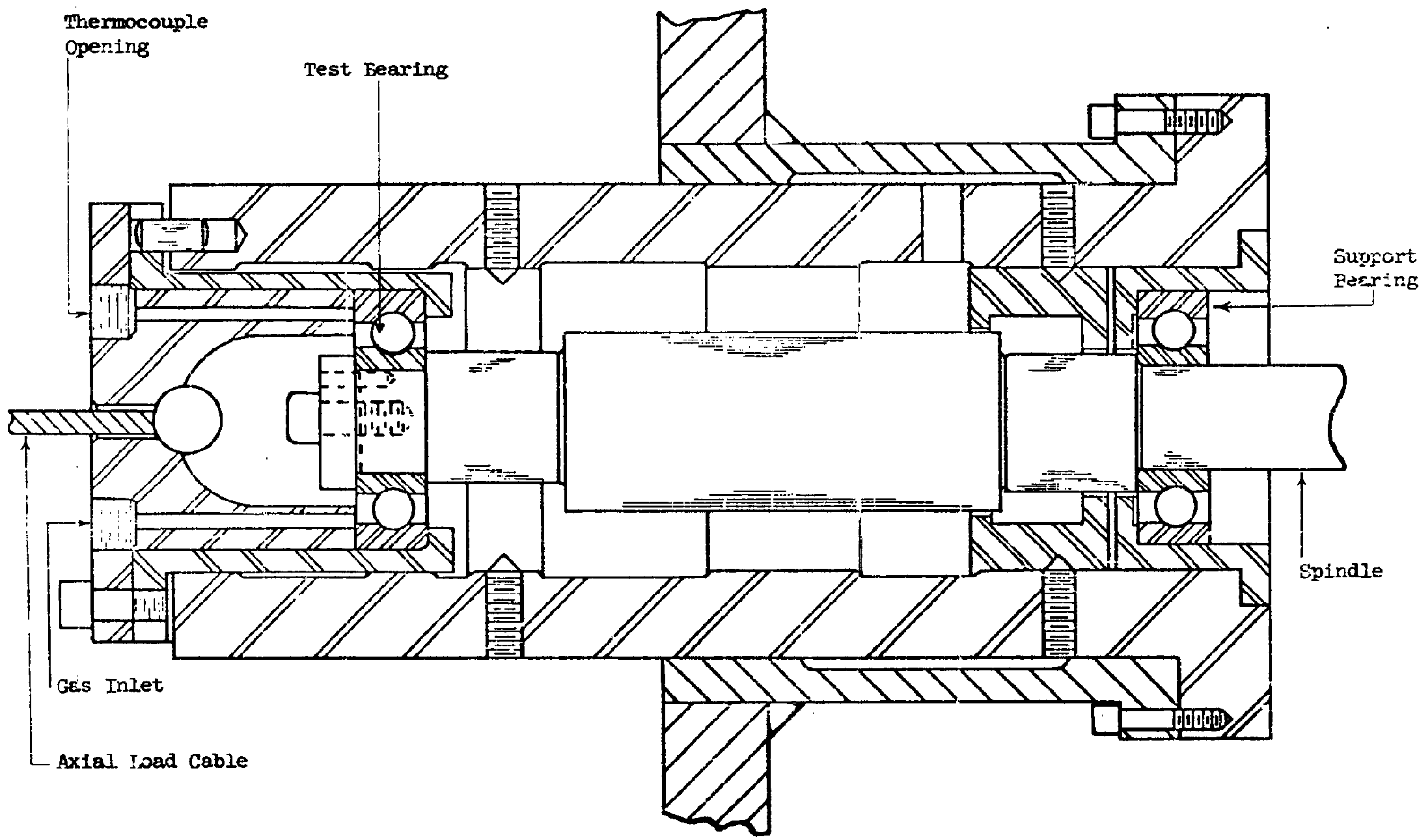

FIGURE 5

CROSS SECTION VIEW OF MRC BEARING TESTER

6A ARMALON

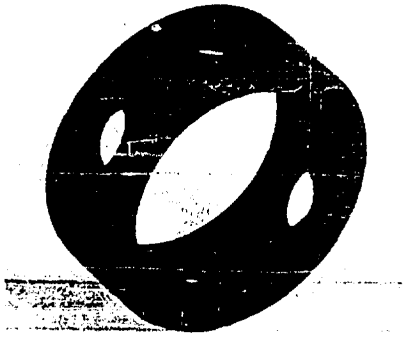

6B PHENOLIC BONDED MoS_2

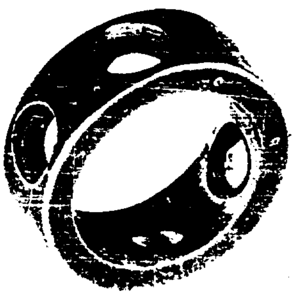

6C P2W INSERTS IN STEEL RETAINER

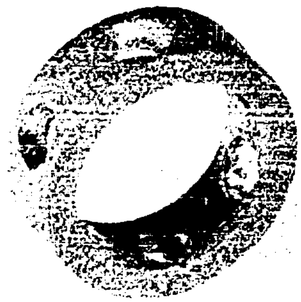

6D SINTERED STELLITE NO. 1 ALLOY

FIGURE 6

RETAINERS SCREENED IN MRC BEARING TESTER

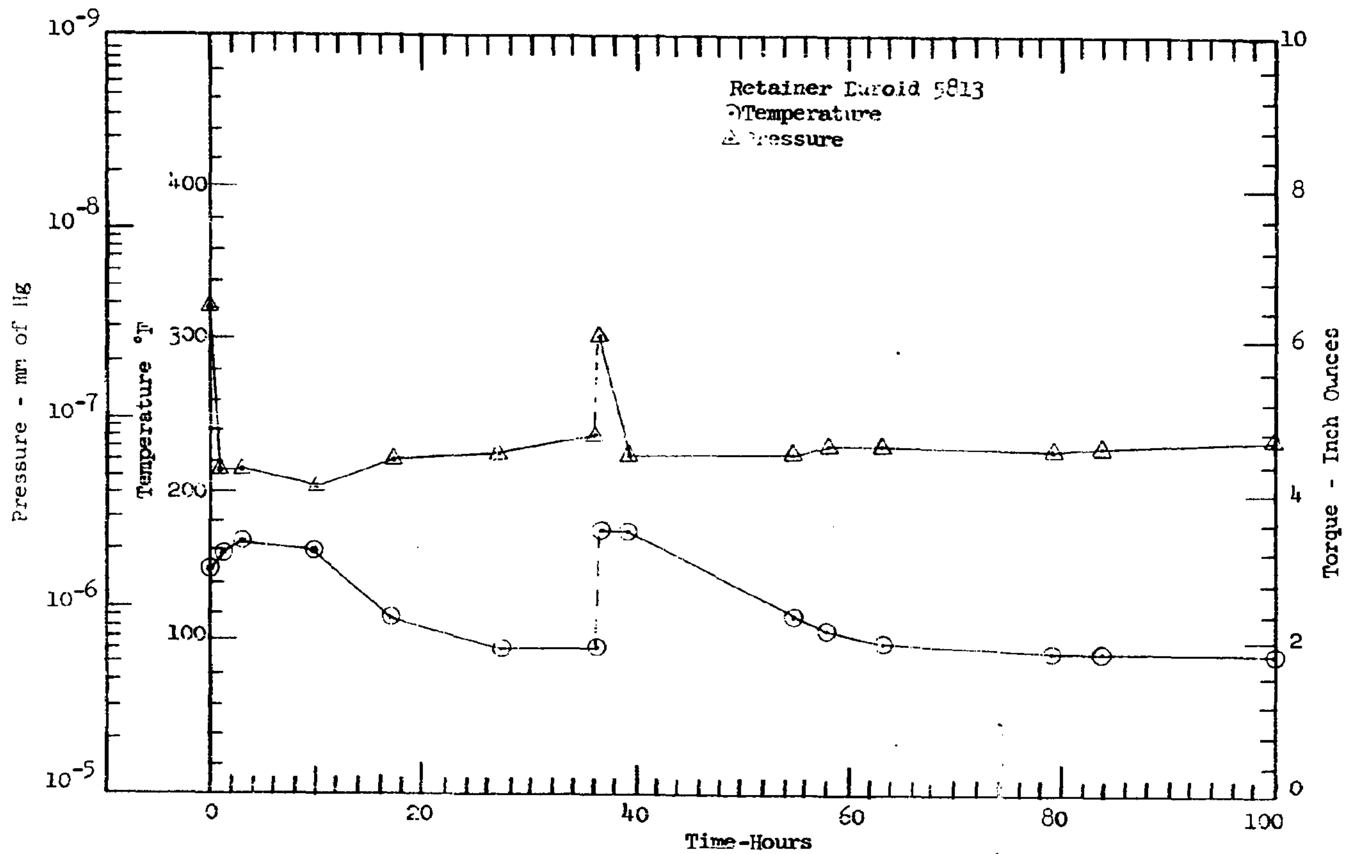

FIGURE 7

TEST CONDITIONS - BEARING TEST 1

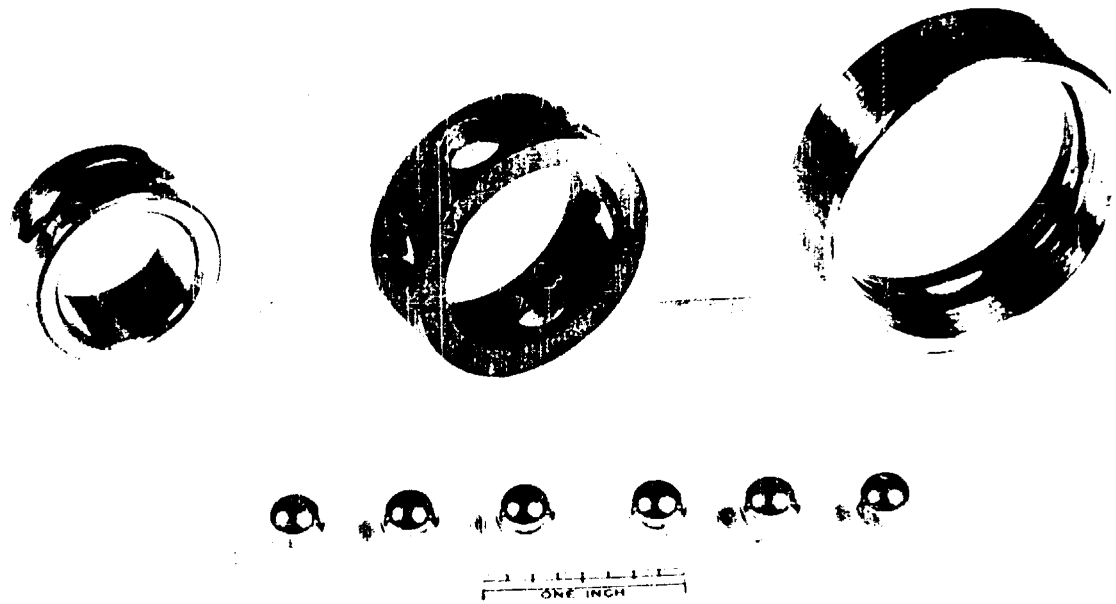

FIGURE 8

BEARING WITH DUROID 5813 RETAINER AFTER 100 HOURS OPERATION — TEST 2

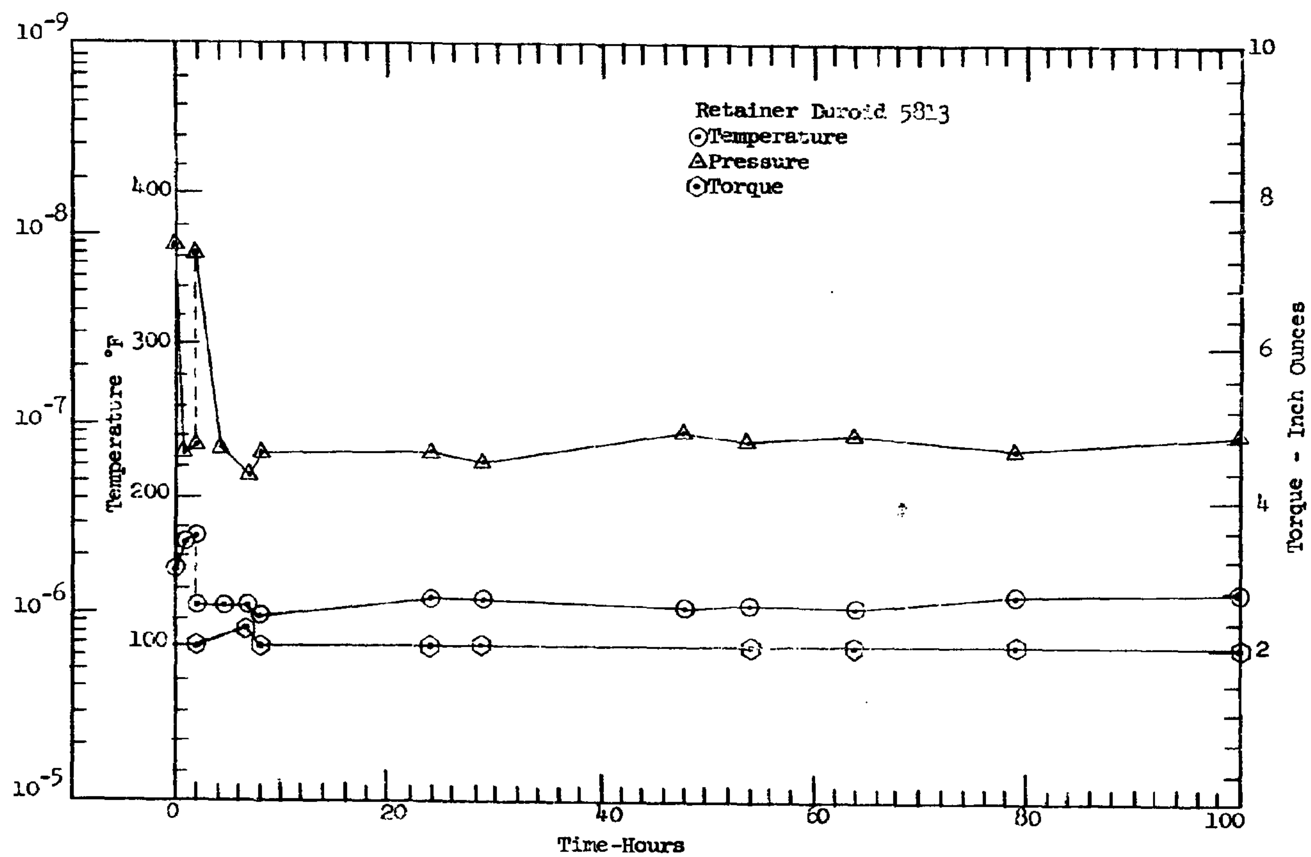

FIGURE 9

TEST CONDITIONS - BEARING TEST 2

FIGURE 10

BEARING WITH FLUOROSINT RETAINER AFTER 100 HOURS OPERATION —
TEST 3

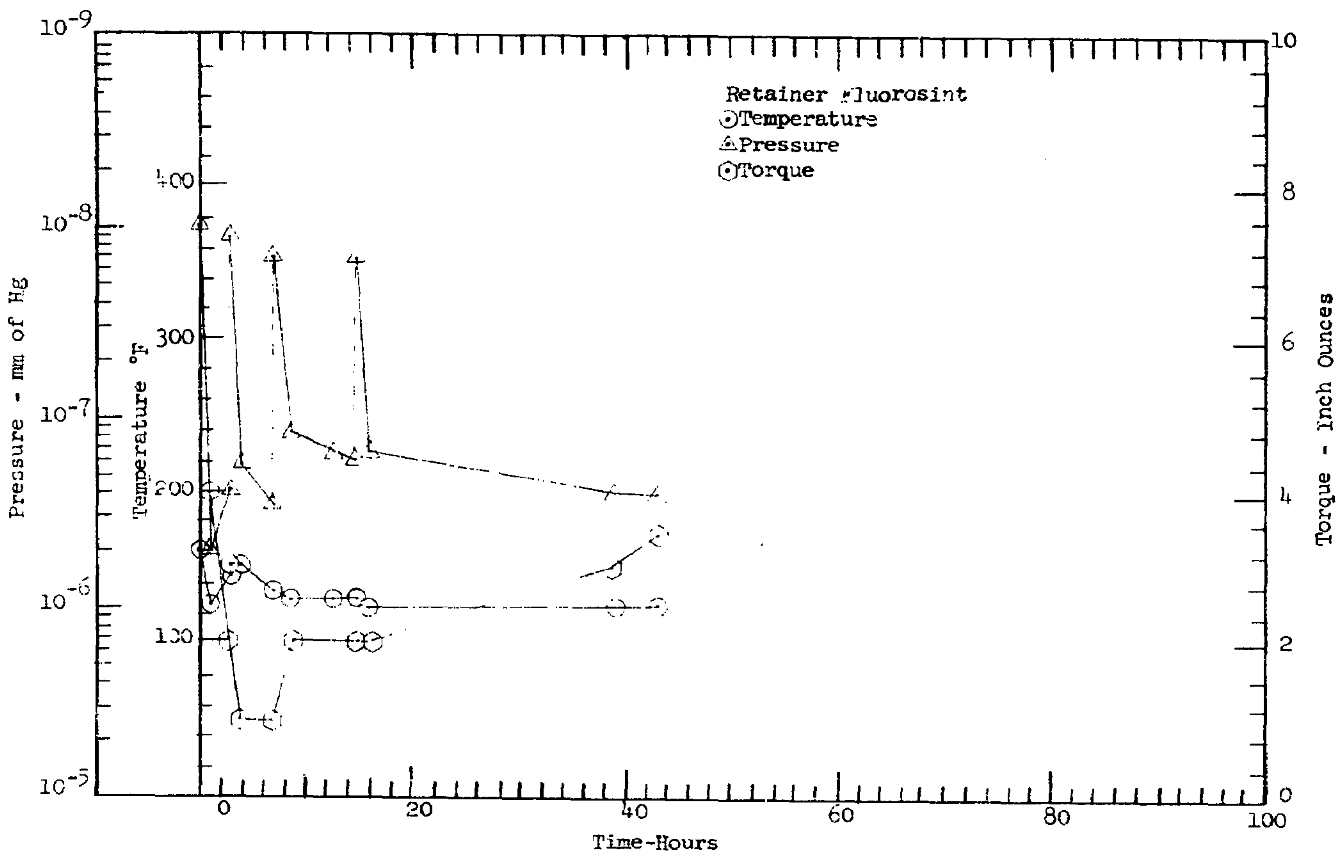

FIGURE 11

TEST CONDITIONS - BEARING TEST 3

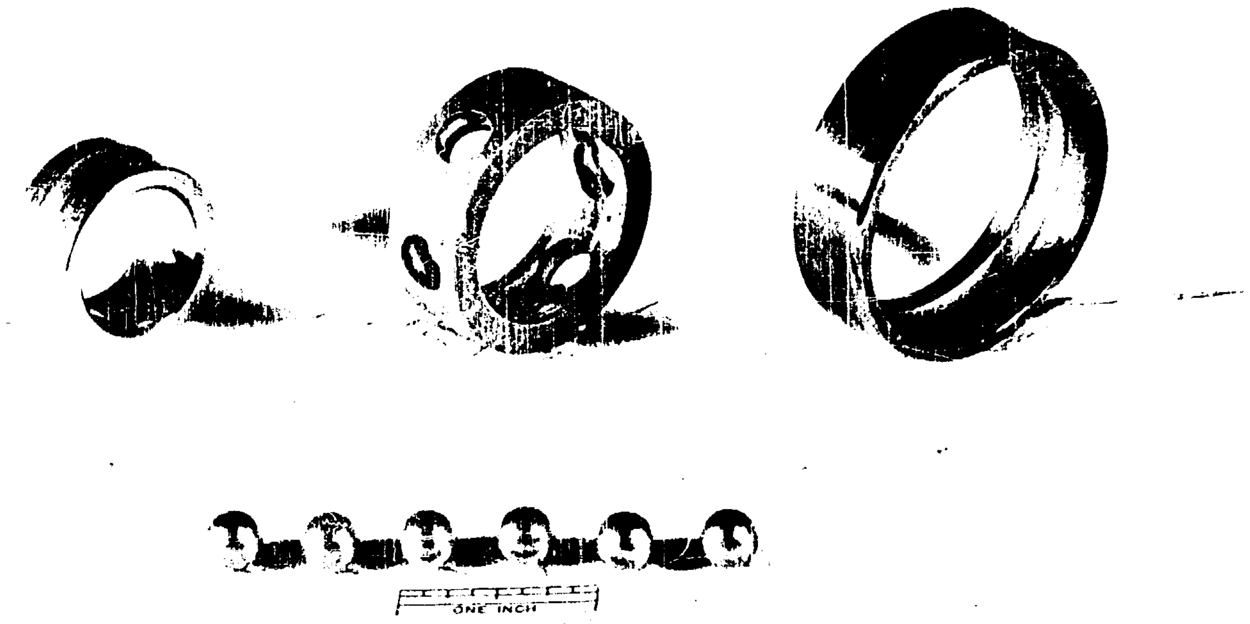

FIGURE 12

BEARING WITH COATED BG42 RETAINER AFTER 23.3 HOURS OPERATION — TEST 4

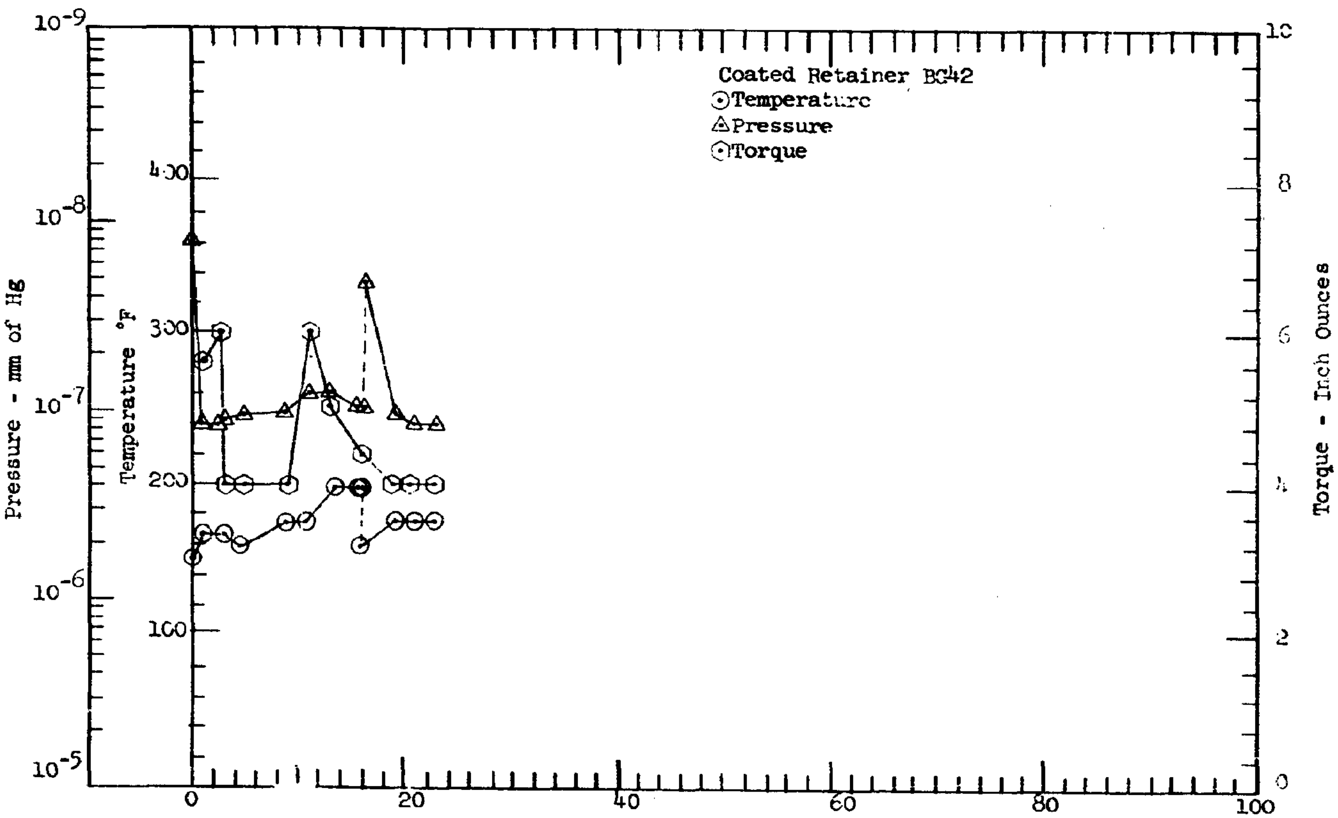

FIGURE 13

TEST CONDITIONS - BEARING TEST 4

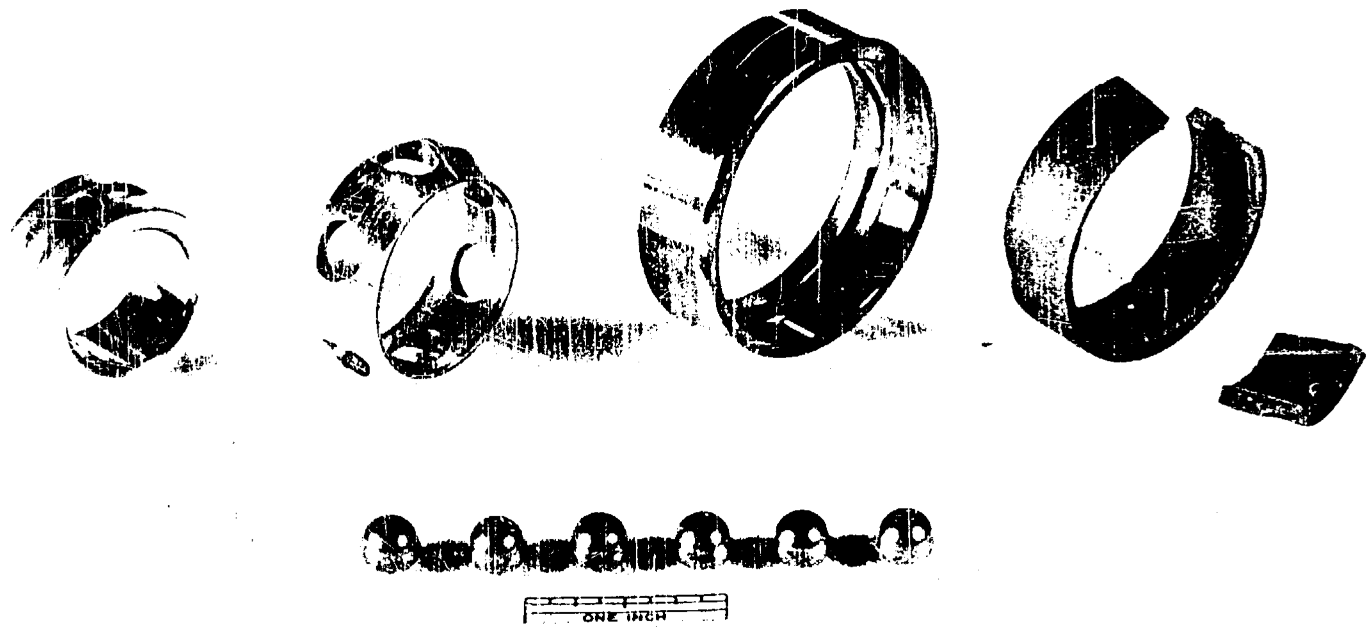

FIGURE 14

BEARING WITH INCONEL X RETAINER AND P5 RING AFTER 0.1 HOUR OPERATION — TEST 5

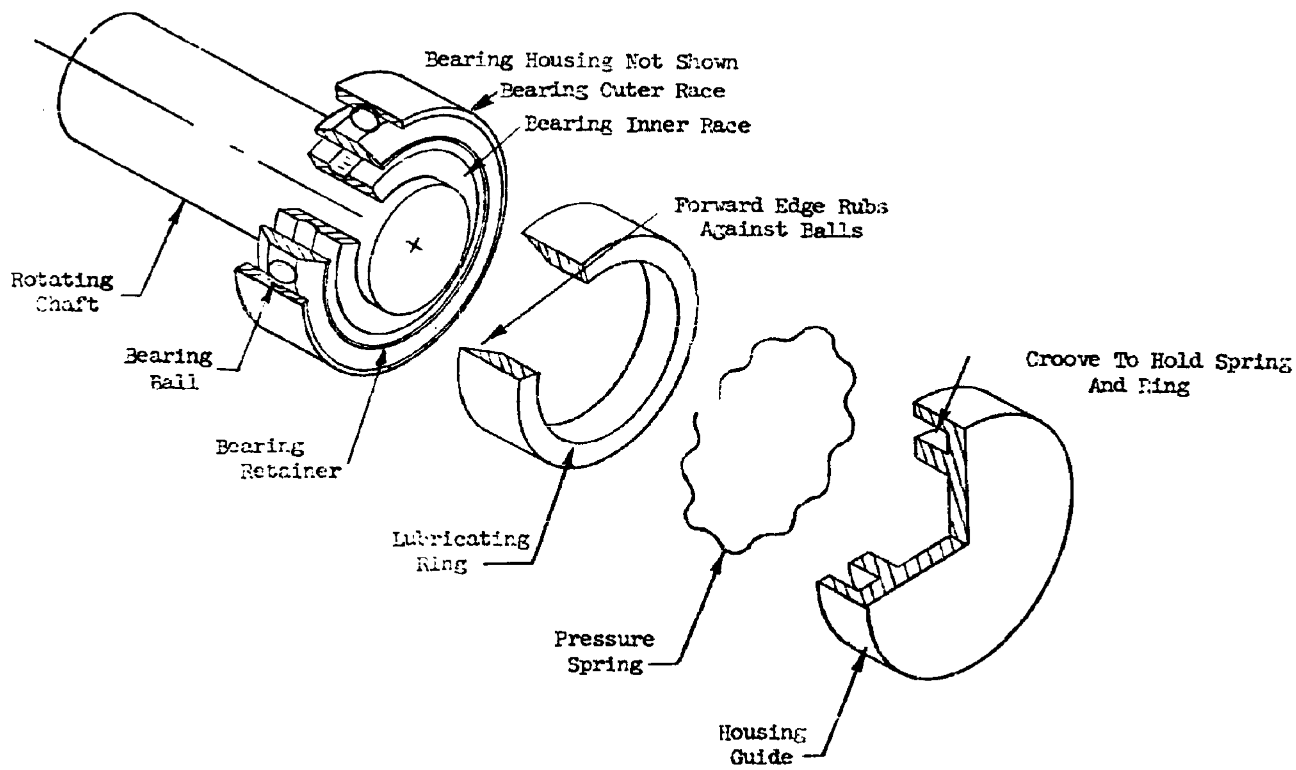

FIGURE 15

EXPLODED SCHEMATIC OF LUBRICATING RING AND BEARING COMPONENTS

FIGURE 16

BEARING WITH COATED INCONEL X RETAINER AND P5 RING
AFTER 76 HOURS OPERATION — TEST 6

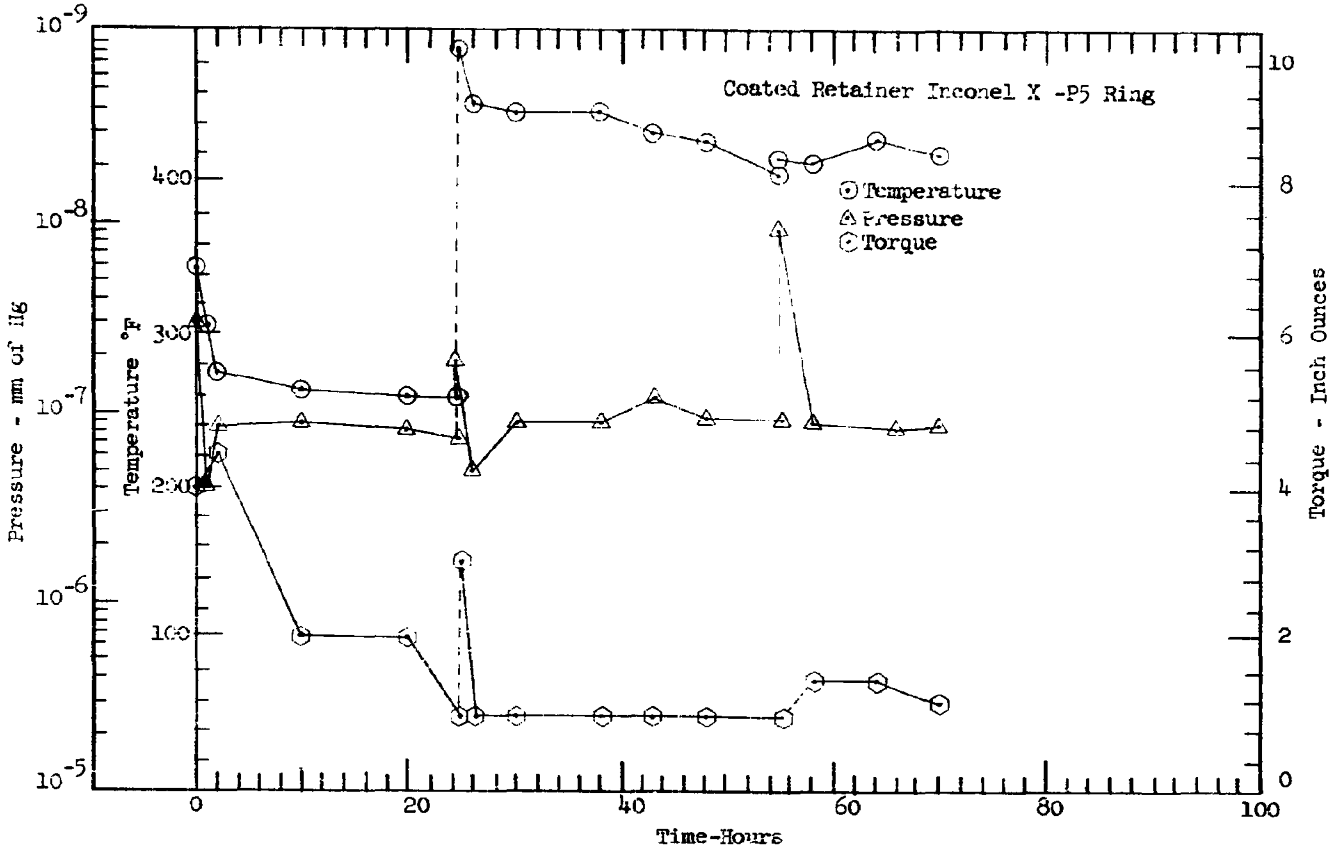

FIGURE 17

TEST CONDITIONS -- BEARING TEST 6

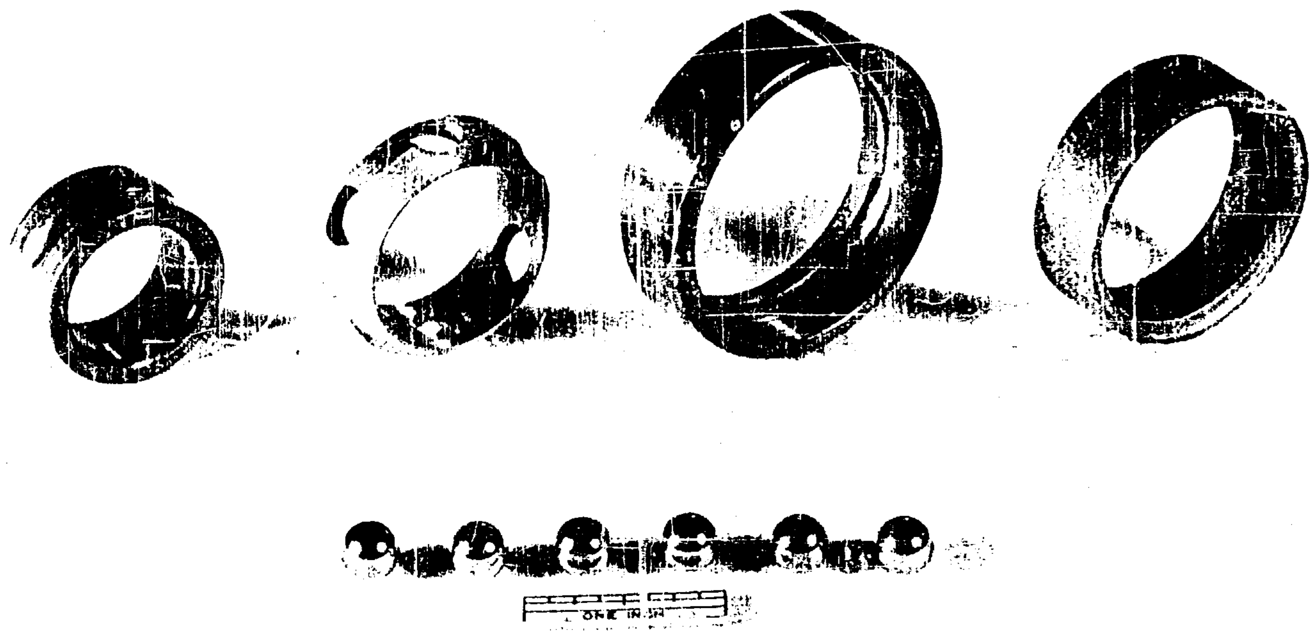

FIGURE 18

BEARING WITH COATED BG42 RETAINER AND P2W RING
AFTER 1 HOUR OPERATION — TEST 7

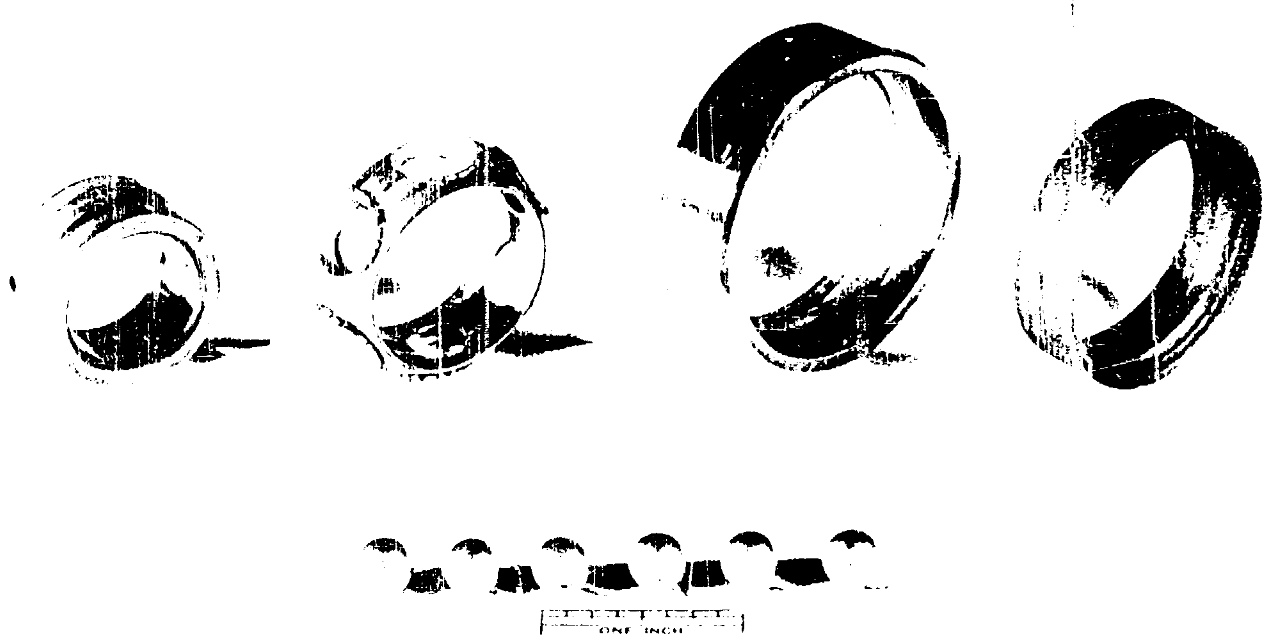

FIGURE 19

BEARING WITH COATED BG42 RETAINER AND P2W RING
AFTER 100 HOURS OPERATION — TEST 8

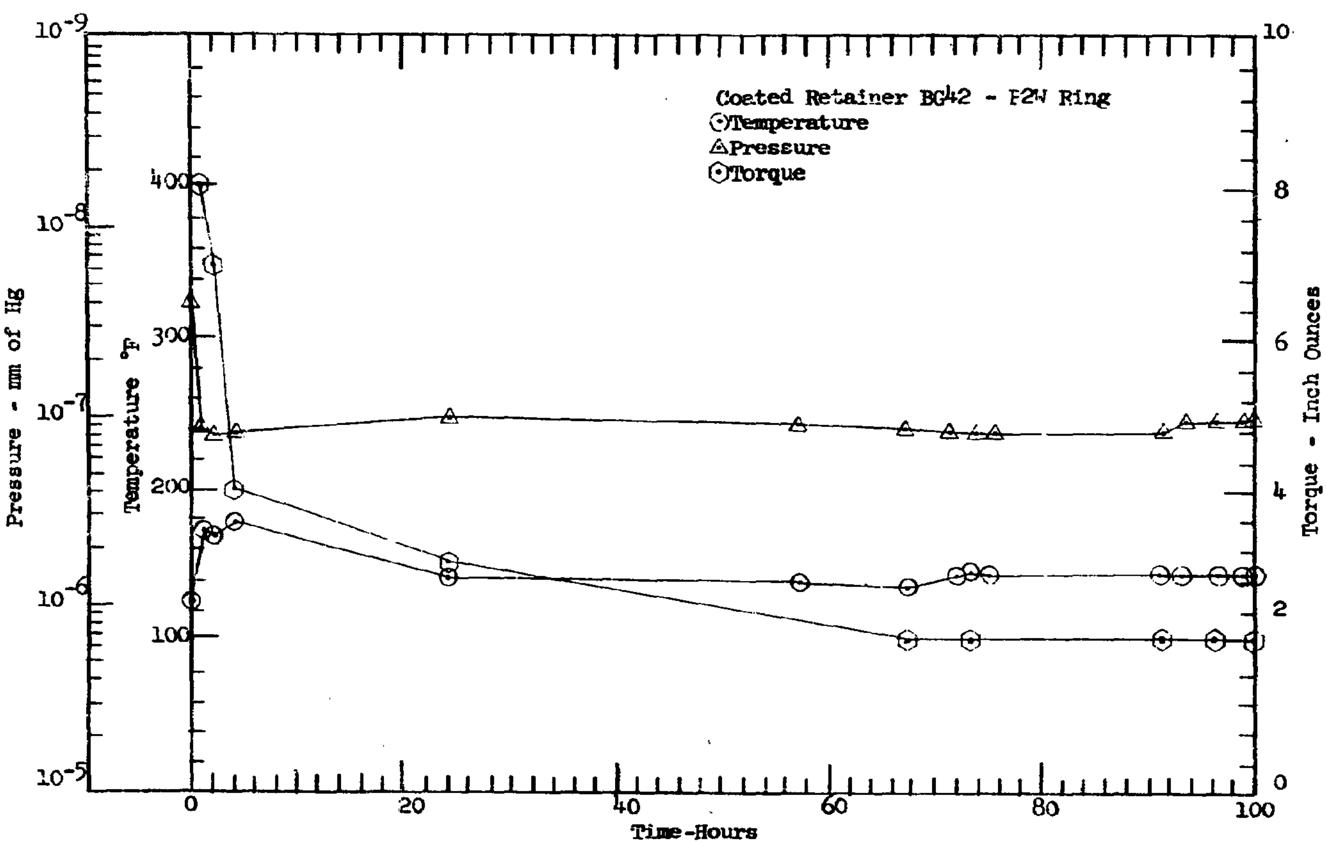

FIGURE 20

TEST CONDITIONS - BEARING TEST 8

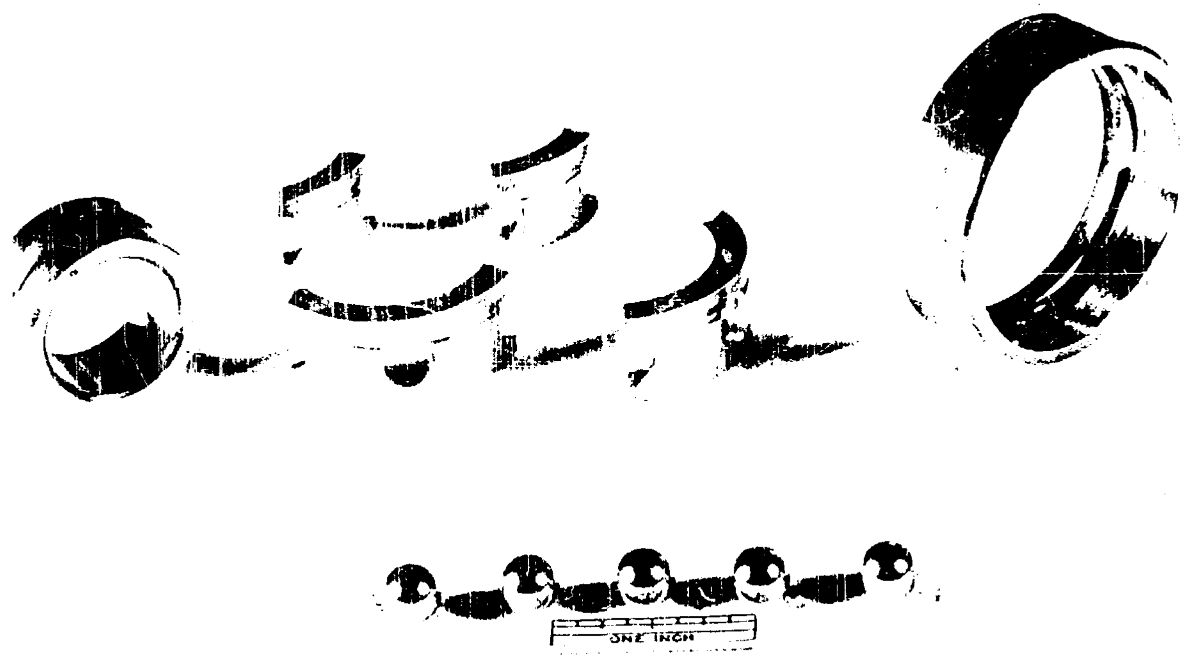

FIGURE 21

BEARING WITH SINETEX RETAINER AFTER 100 HOURS OPERATION — TEST 9

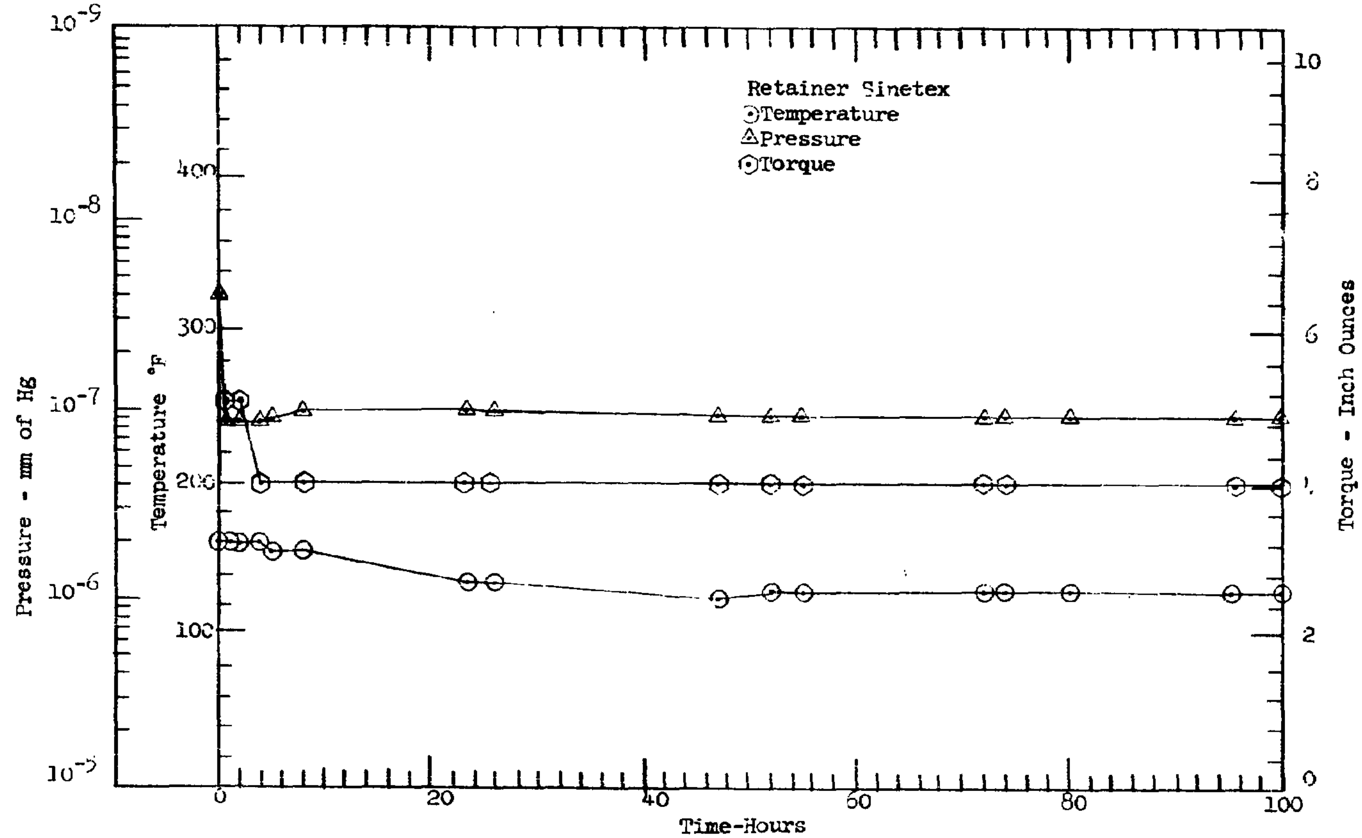

FIGURE 22

TEST CONDITIONS - BEARING TEST 9

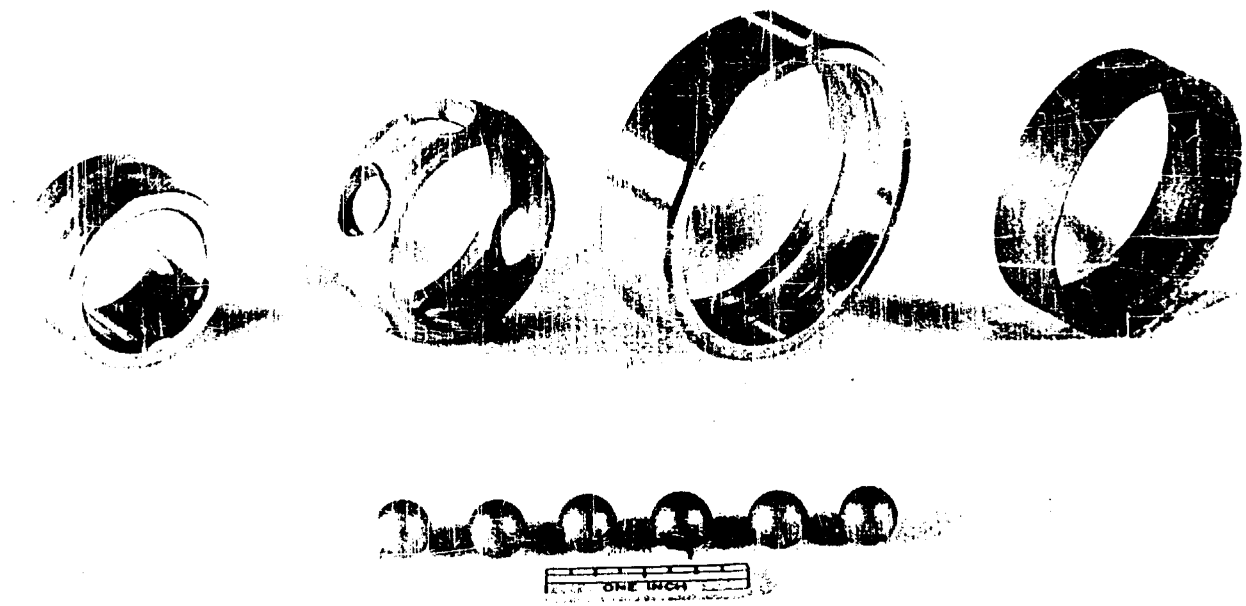

FIGURE 23

BEARING WITH COATED BG42 RETAINER AND P2W RING
AFTER 72 HOURS OPERATION — TEST 10

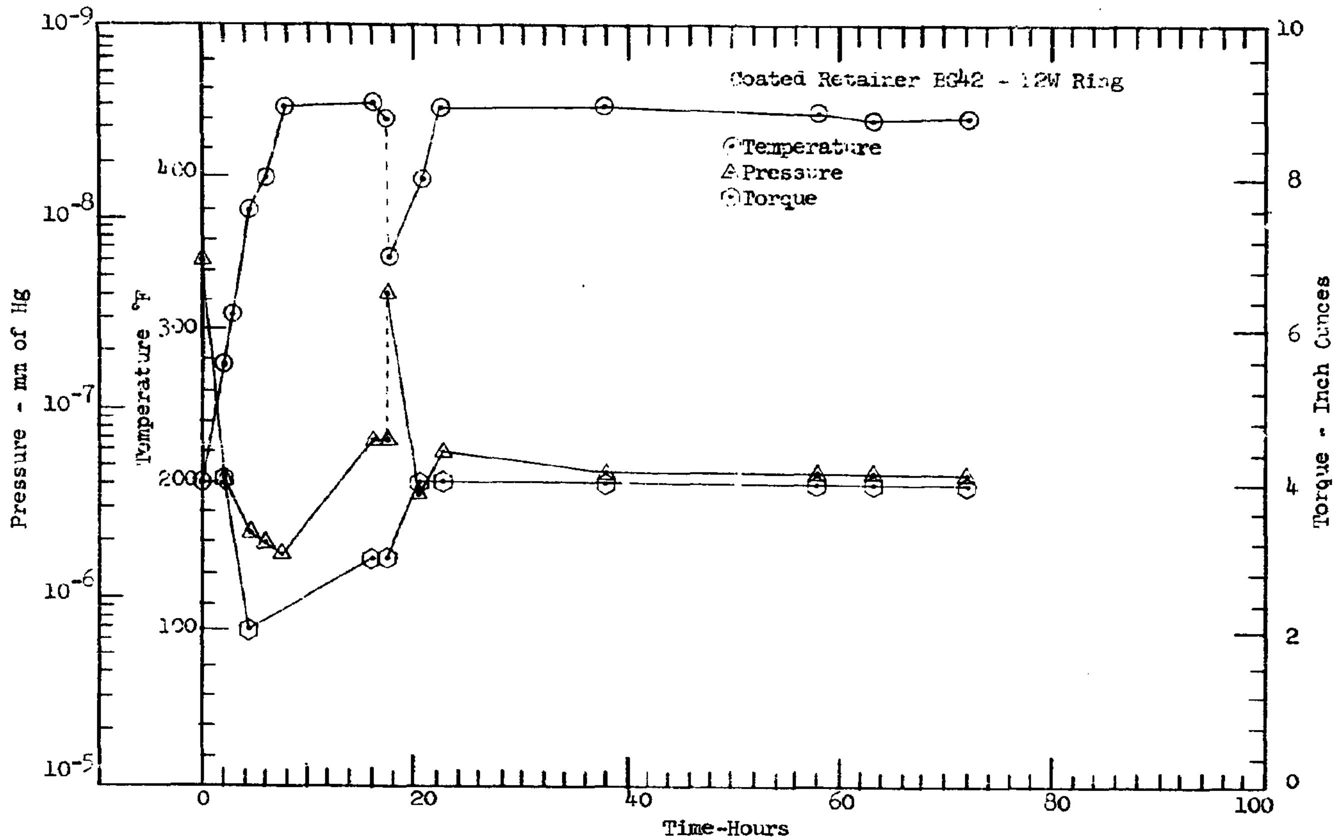

FIGURE 24

TEST CONDITIONS - BEARING TEST 10

FIGURE 25

BEARING WITH BANDED SINETEX RETAINER AFTER 100 HOURS OPERATION — TEST 11

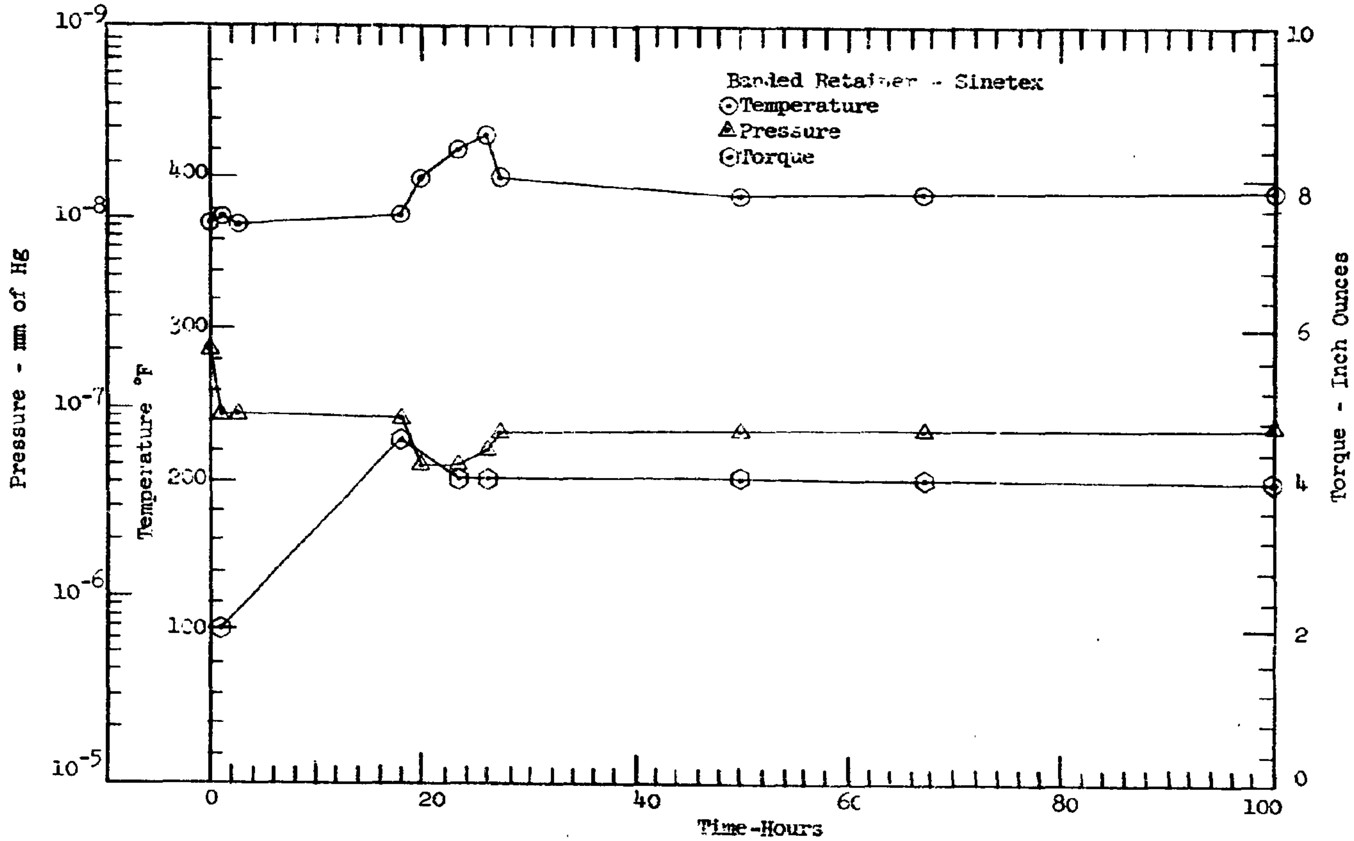

FIGURE 26

TEST CONDITIONS - BEARING TEST 11

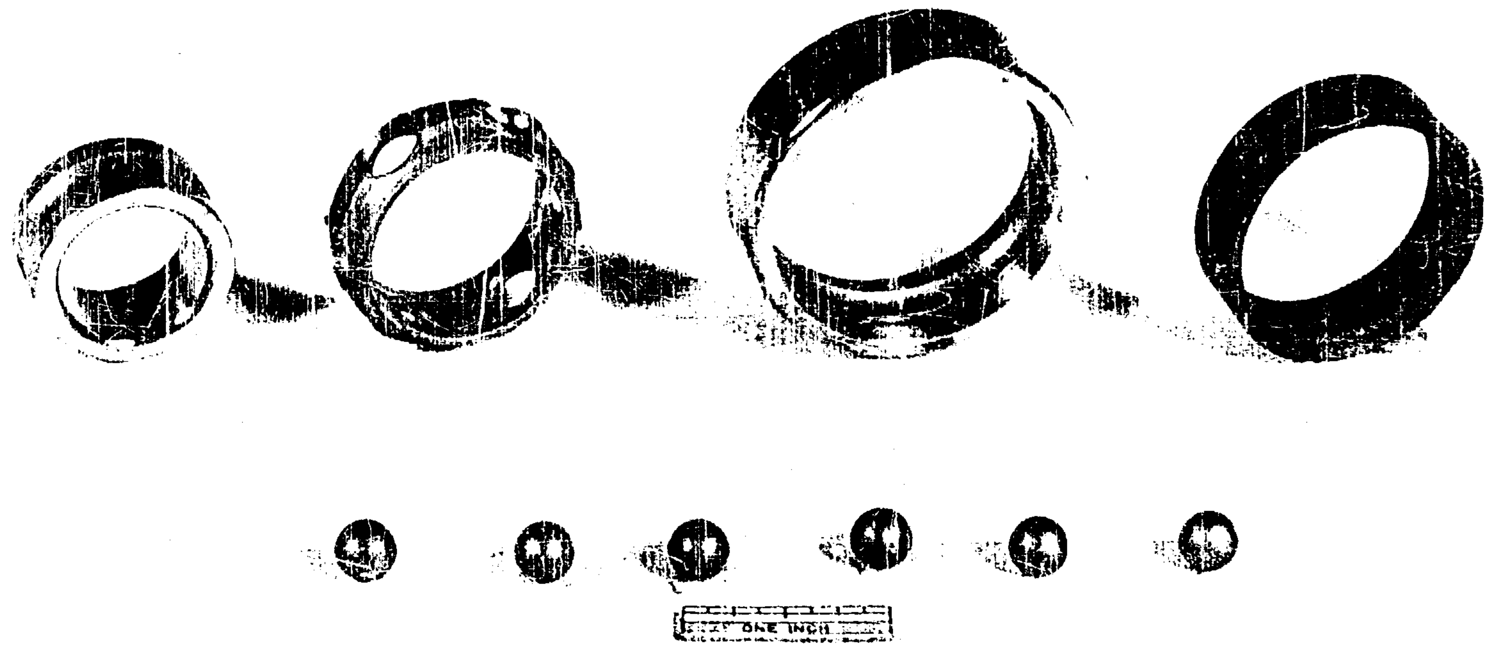

FIGURE 27

BEARING WITH COATED BG42 RETAINER AND SK278 RING
AFTER 53 HOURS OPERATION — TEST 12

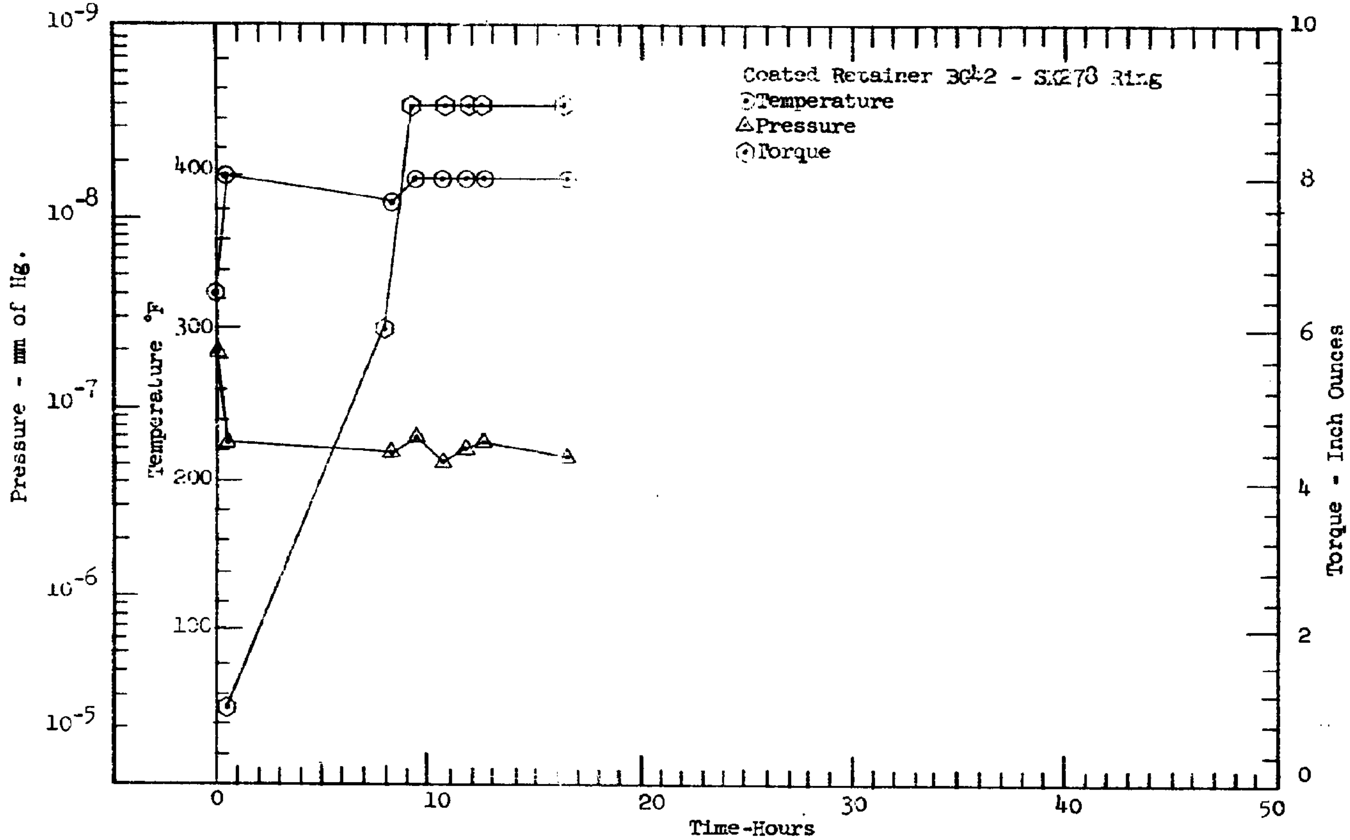

FIGURE 28

TEST CONDITIONS - BEARING TEST 12

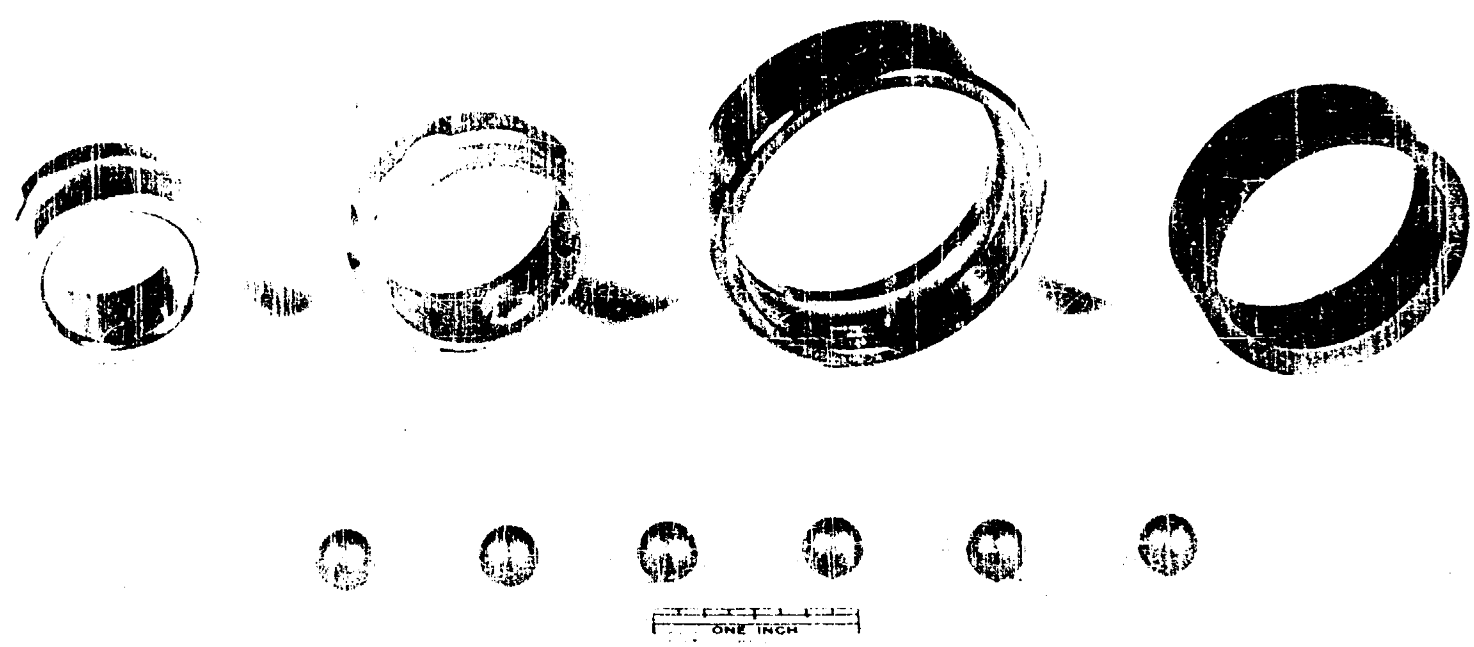

FIGURE 29

BEARING WITH COATED M—10 RETAINER AND P2W RING
AFTER 6 HOURS OPERATION — TEST 13

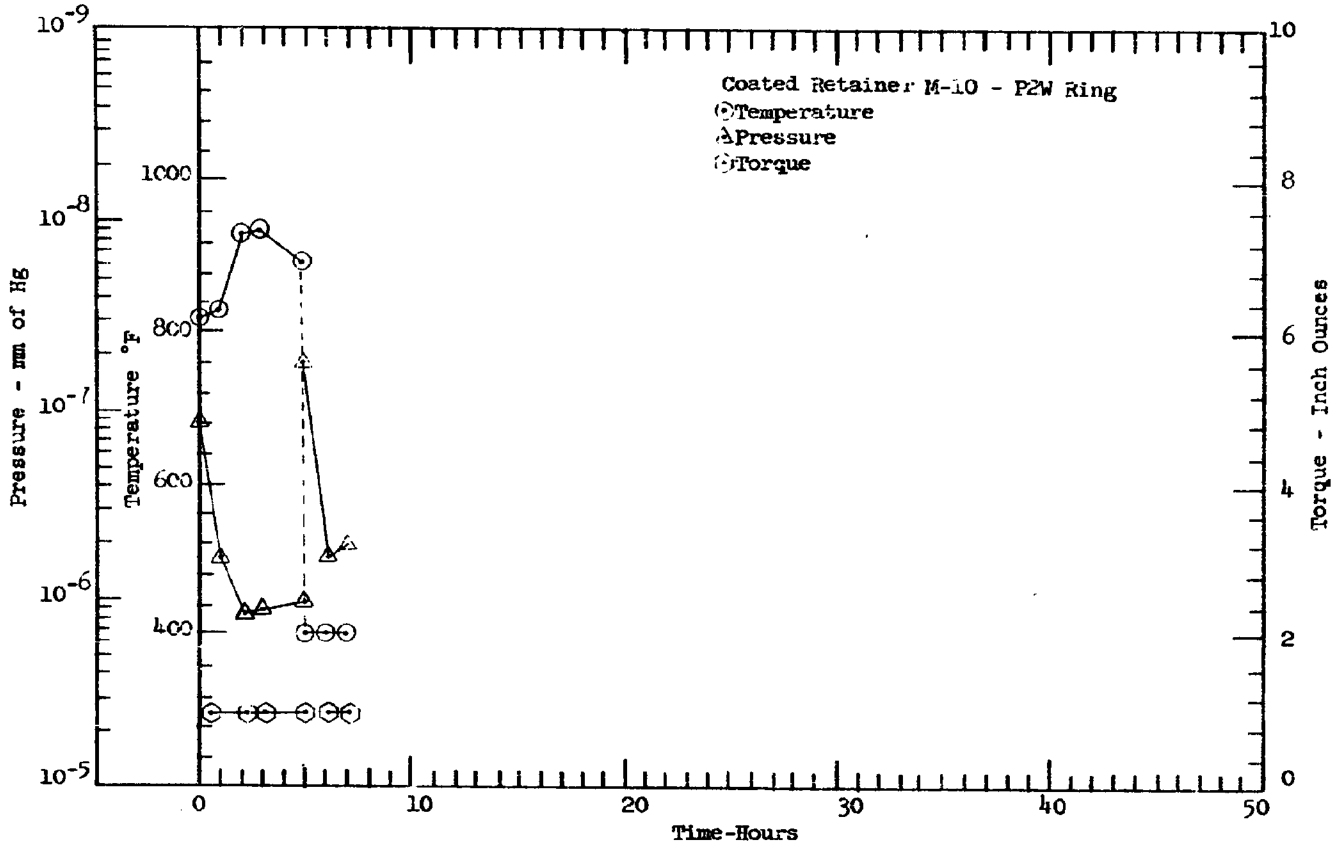

FIGURE 30

TEST CONDITIONS - BEARING TEST 13

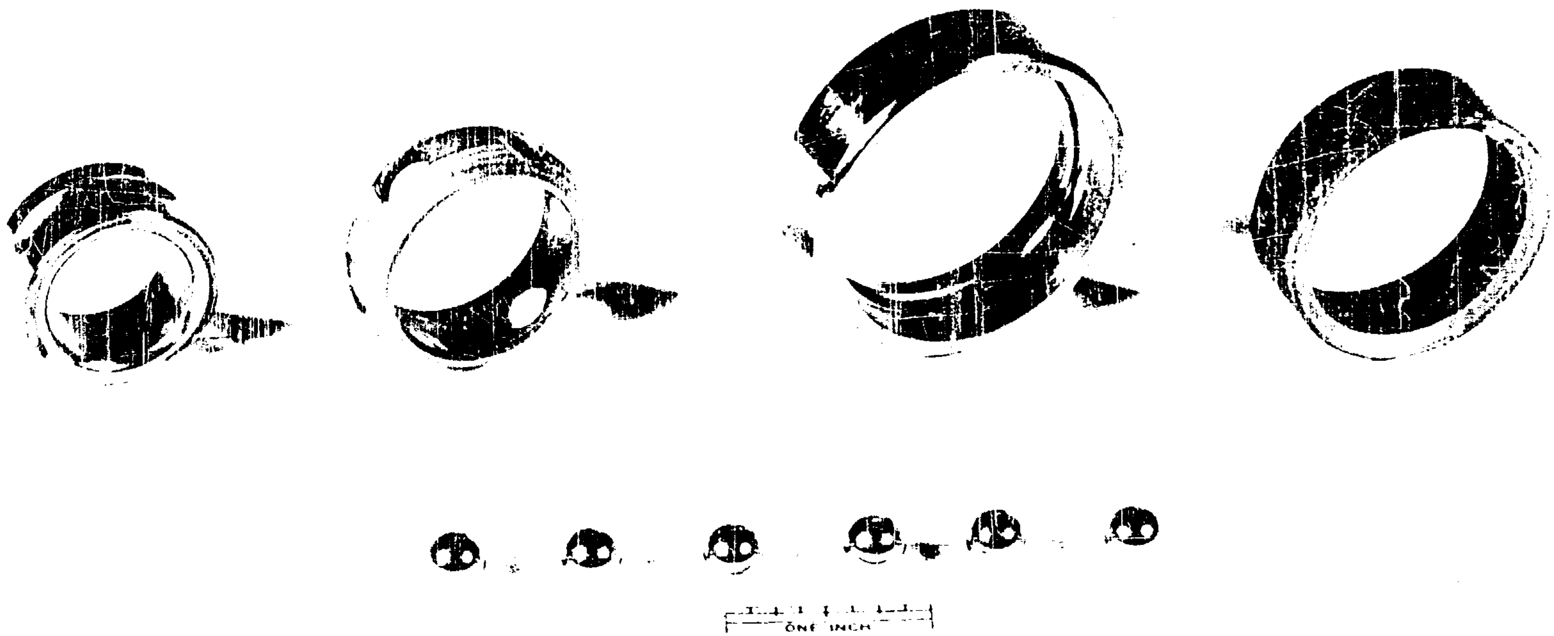

FIGURE 31

BEARING WITH COATED M–10 RETAINER AND 56HT RING
AFTER 27.6 HOURS OPERATION – TEST 14

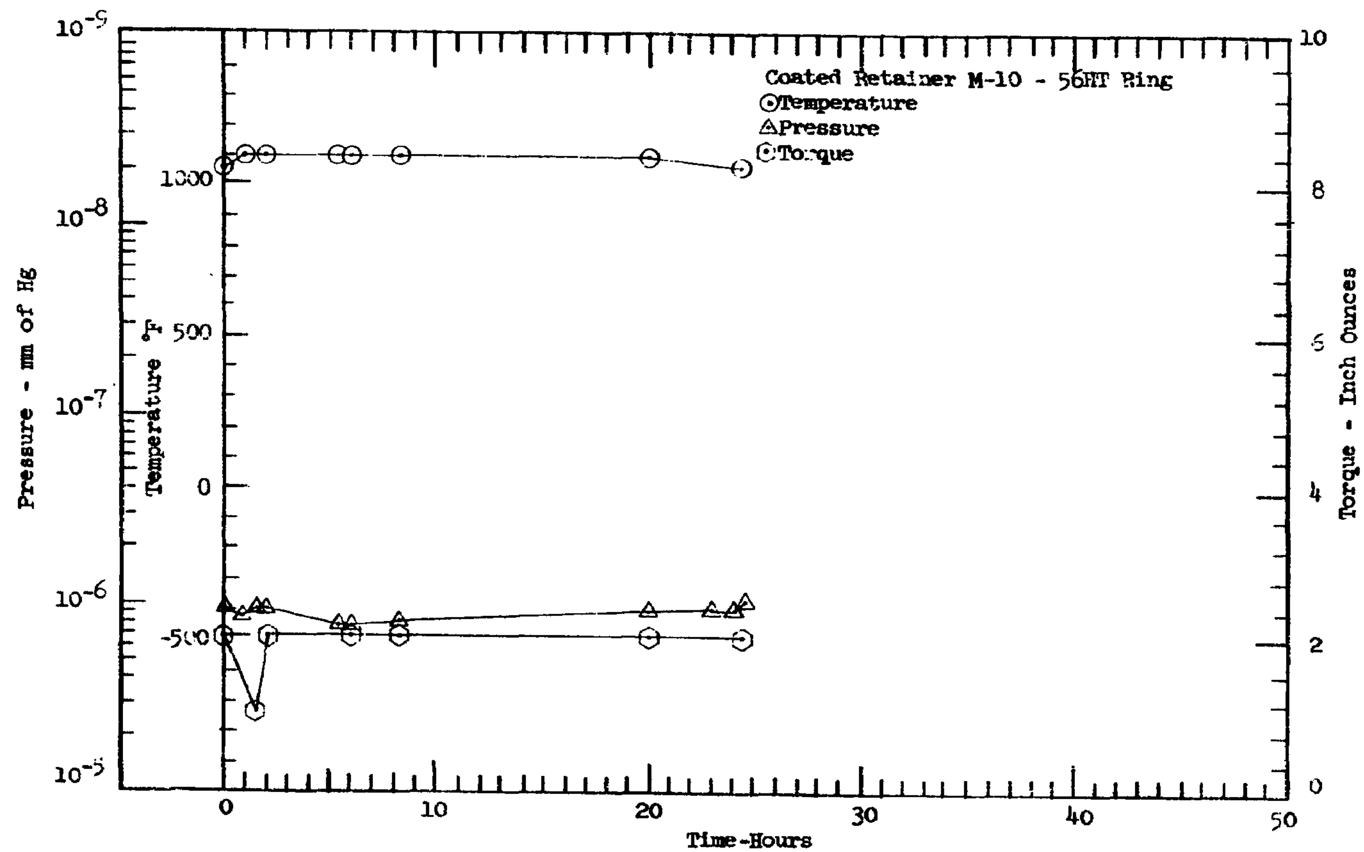

FIGURE 32

TEST CONDITIONS - BEARING TEST 14

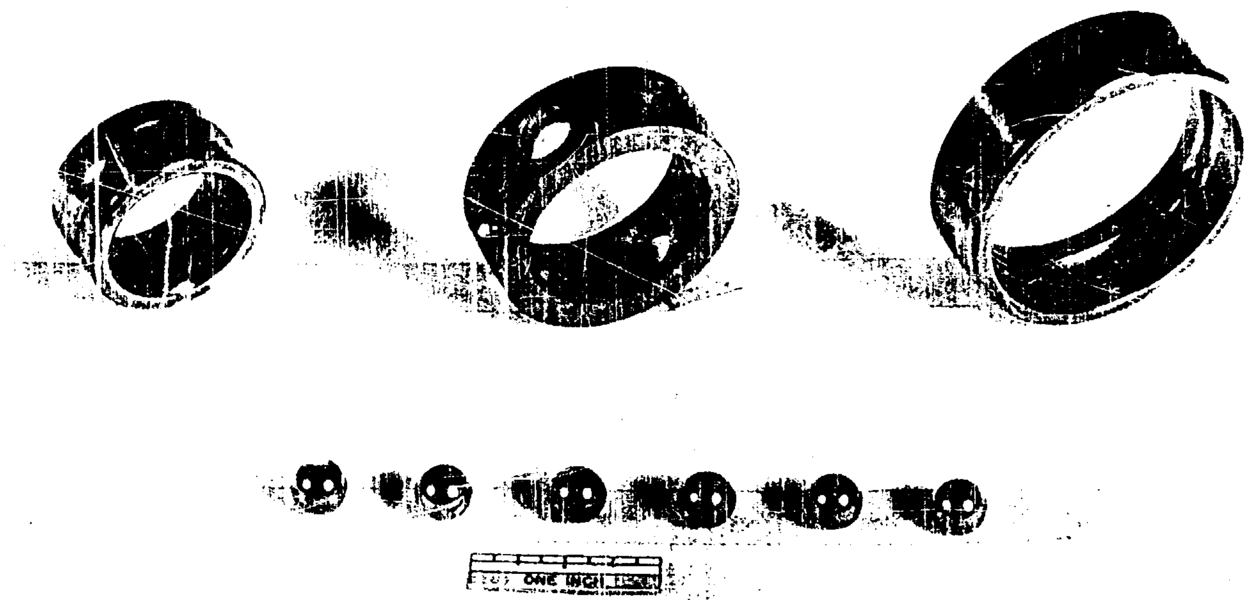

FIGURE 33

BEARING WITH BANDED SINETEX RETAINER AFTER 27.6 HOURS OPERATION — TEST 14A

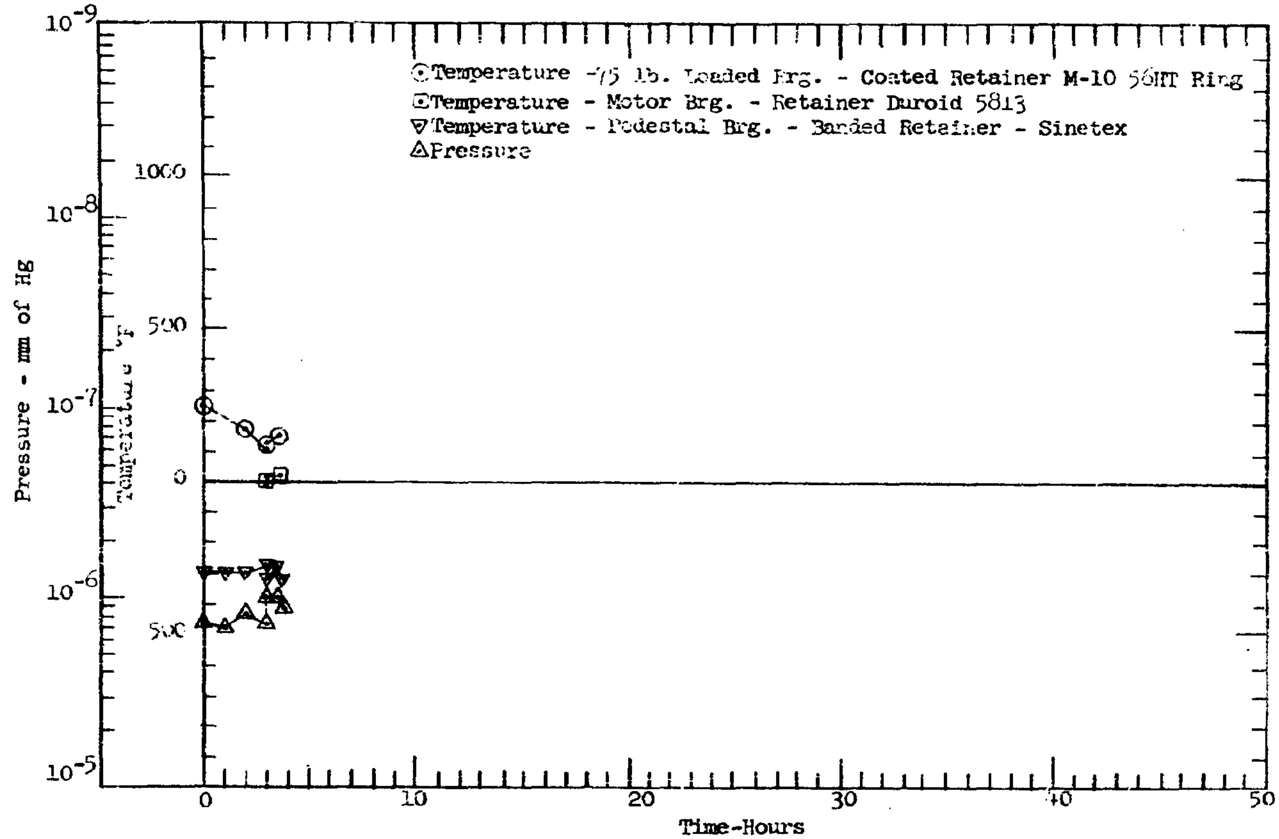

FIGURE 34

TEST CONDITIONS - BEARING TEST 14A

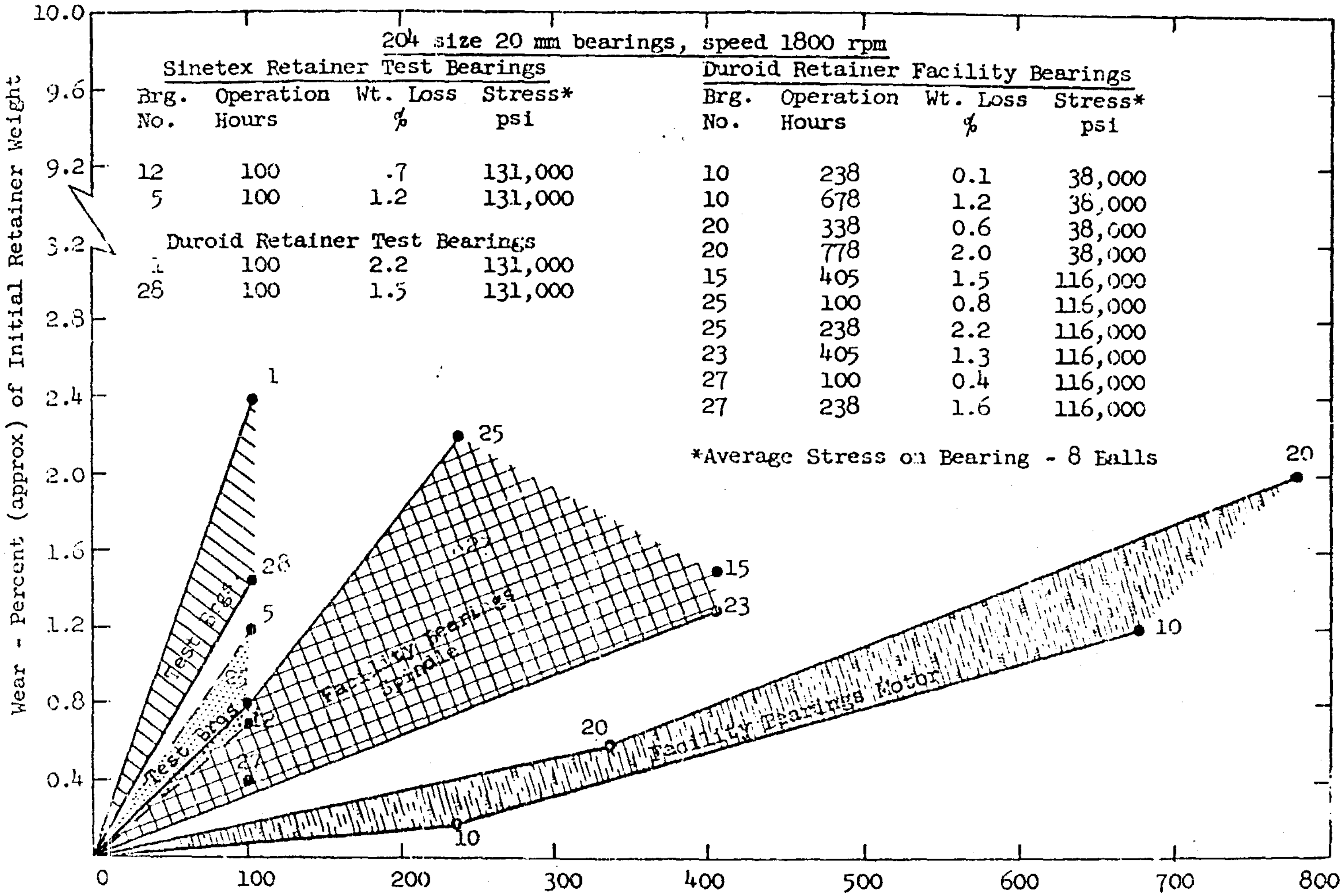

204 size 20 mm bearings, speed 1800 rpm

Sinetex Retainer Test Bearings

Brg. No.	Operation Hours	Wt. Loss %	Stress* psi
12	100	.7	131,000
5	100	1.2	131,000

Duroid Retainer Test Bearings

Brg. No.	Operation Hours	Wt. Loss %	Stress* psi
1	100	2.2	131,000
28	100	1.5	131,000

Duroid Retainer Facility Bearings

Brg. No.	Operation Hours	Wt. Loss %	Stress* psi
10	238	0.1	38,000
10	678	1.2	38,000
20	338	0.6	38,000
20	778	2.0	38,000
15	405	1.5	116,000
25	100	0.8	116,000
25	238	2.2	116,000
23	405	1.3	116,000
27	100	0.4	116,000
27	238	1.6	116,000

*Average Stress on Bearing - 8 Balls

FIGURE 35

RETAINER WEAR AS A FUNCTION OF OPERATING TIME AND LOAD

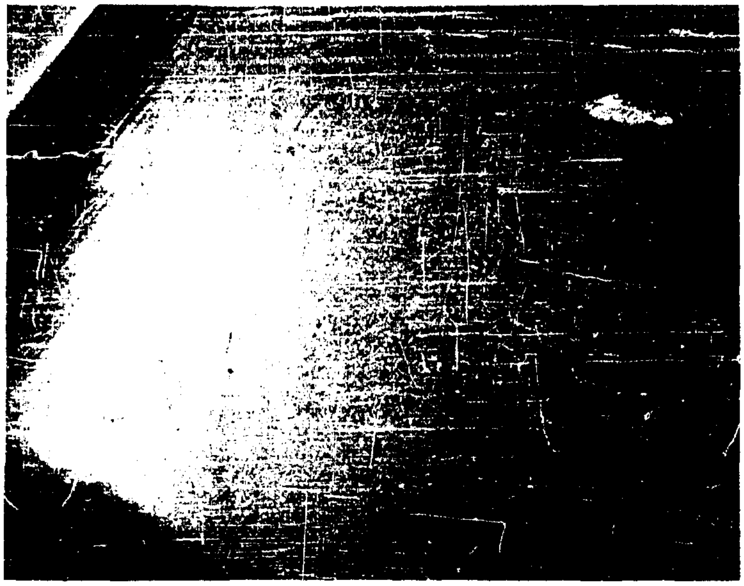

36A BALLPATH BEFORE TEST — MAG. 20X

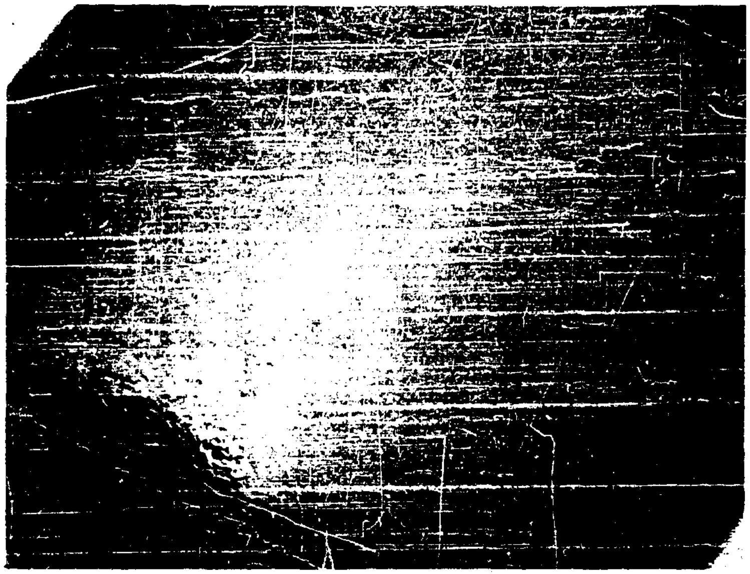

36B BALLPATH AFTER TEST — MAG. 20X

FIGURE 36

INNER RACE BALLPATH BEFORE AND AFTER TEST — TEST 9

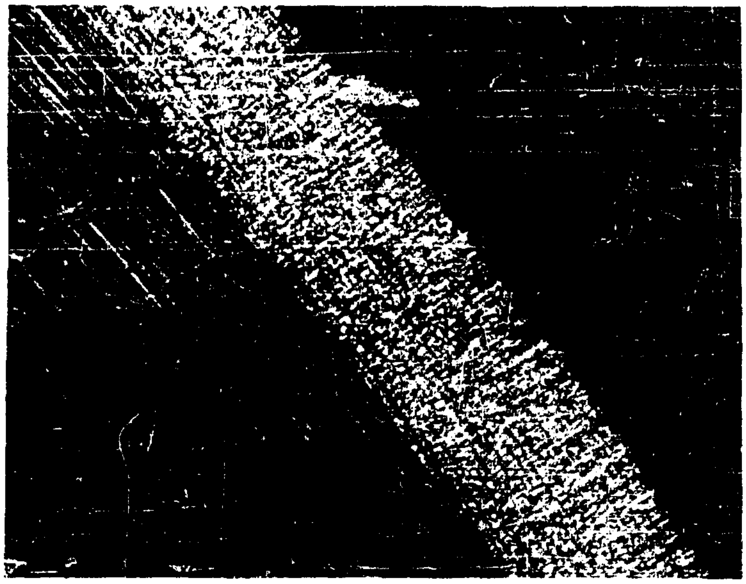

37A BALLPATH BEFORE TEST — MAG. 20X

37B BALLPATH AFTER TEST — MAG. 20X

FIGURE 37

OUTER RACE BALLPATH BEFORE AND AFTER TEST — TEST 11

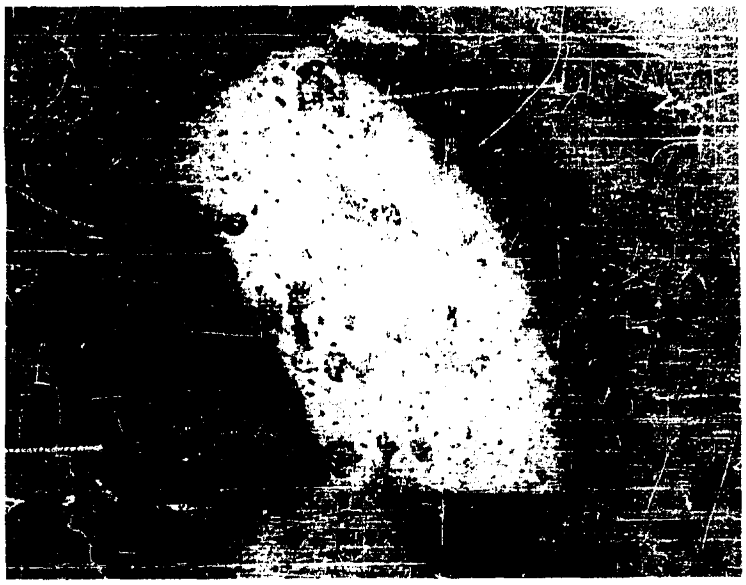

38A BALL AFTER TEST - MAG. 20X

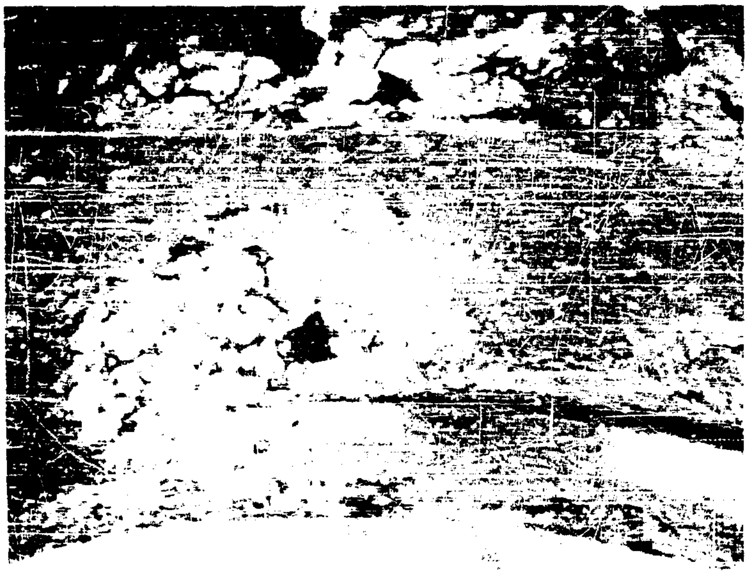

38B BALL POCKET AFTER TEST — MAG. 20X

FIGURE 38

BALL AND RETAINER POCKET AFTER TEST — TEST 11

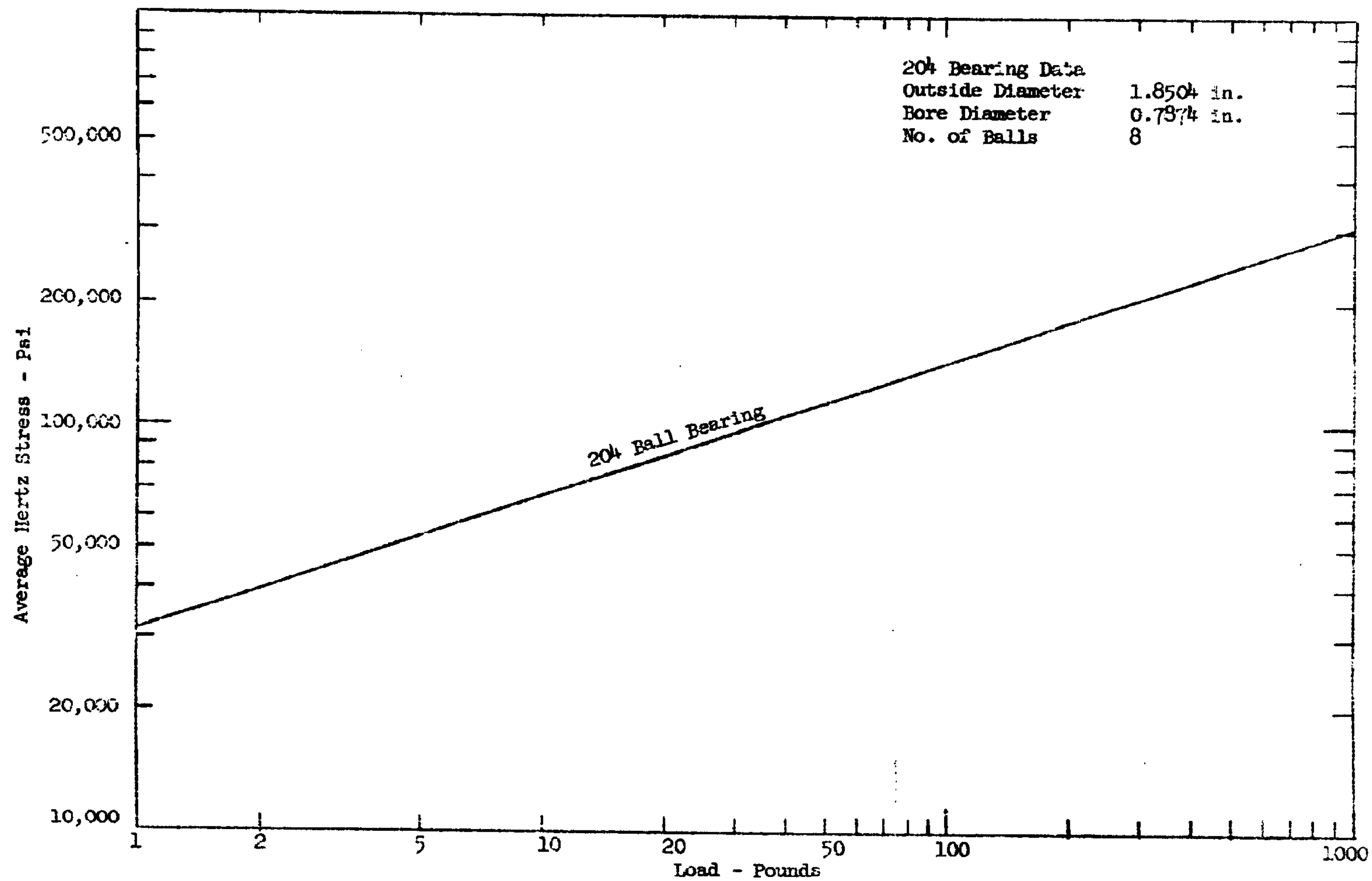

FIGURE 39

BEARING UNIT STRESS AS A FUNCTION OF LOAD

Arnold Engineering Development Center
Arnold Air Force Station, Tennessee
Rpt. No. AEDC-TDR-62-51. ANALYTICAL AND EXPERIMENTAL STUDY OF ADAPTING BEARINGS FOR USE IN AN ULTRA-HIGH VACUUM ENVIRONMENT. Phase I, II and III. February 1962, 185 p. incl illus., tables.
Unclassified Report

This report contains the results of an investigation into the lubrication of gears and bearings for use in a vacuum environment by using dry powders as a lubricant, and dry self-lubricating materials in the bearing retainer. The report is divided as follows: PHASE I, The wear and friction characteristics of various dry powders and dry self-lubricating materials for use in ball bearings were evaluated and screened in a dry inert atmosphere in laboratory test apparatus under rotating speeds and loads similar to that found in 2 to 7 h.p. electric motors. The materials evaluated included reinforced thermosetting plastics, dry lubricant filled and unfilled thermoplastics and dry lubricant filled sintered alloys. PHASE II: Dry powder and

1. Bearings
2. Lubrication
3. Vacuum systems
I. AFSC Program Area 850E, Project 7778, Task 777801
II. Contract AF 40(600)-915
III. Westinghouse Electric Corporation, East Pittsburgh, Pennsylvania
IV. Bowen, P.H.
V. Available from OTS
VI. In ASTIA collection

self-lubricating materials were subjected to the vacuum conditions in the range of 1×10^{-6} to 1×10^{-9} mm Hg, and at temperatures in the range of -60°F to 1000°F to determine the rate of the outgassing and/or decomposition of each material. PHASE III: Dry ball bearing (204 size, 22 mm bore) soaking and operating tests were conducted using retainers fabricated from the most promising materials determined in Phase II. The bearings were operated at a speed of 1800 rpm, radial load of 75 lbs., axial load of 5 lbs., and tested under the vacuum and temperature conditions described in Phase II. Special bearings and retainer materials were used for exploratory tests up to 1500°F.

Arnold Engineering Development Center
Arnold Air Force Station, Tennessee
Rpt. No. AEDC-TDR-62-51. ANALYTICAL AND EXPERIMENTAL STUDY OF ADAPTING BEARINGS FOR USE IN AN ULTRA-HIGH VACUUM ENVIRONMENT. Phase I, II and III. February 1962, 185 p. incl illus., tables.
Unclassified Report

This report contains the results of an investigation into the lubrication of gears and bearings for use in a vacuum environment by using dry powders as a lubricant, and dry self-lubricating materials in the bearing retainer. The report is divided as follows: PHASE I, The wear and friction characteristics of various dry powders and dry self-lubricating materials for use in ball bearings were evaluated and screened in a dry inert atmosphere in laboratory test apparatus under rotating speeds and loads similar to that found in 2 to 7 h.p. electric motors. The materials evaluated included reinforced thermosetting plastics, dry lubricant filled and unfilled thermoplastics and dry lubricant filled sintered alloys. PHASE II: Dry powder and

1. Bearings
2. Lubrication
3. Vacuum systems
I. AFSC Program Area 850E, Project 7778, Task 777801
II. Contract AF 40(600)-915
III. Westinghouse Electric Corporation, East Pittsburgh, Pennsylvania
IV. Bowen, P.H.
V. Available from OTS
VI. In ASTIA collection

self-lubricating materials were subjected to the vacuum conditions in the range of 1×10^{-6} to 1×10^{-9} mm Hg, and at temperatures in the range of -60°F to 1000°F to determine the rate of the outgassing and/or decomposition of each material. PHASE III: Dry ball bearing (204 size, 22 mm bore) soaking and operating tests were conducted using retainers fabricated from the most promising materials determined in Phase II. The bearings were operated at a speed of 1800 rpm, radial load of 75 lbs., axial load of 5 lbs., and tested under the vacuum and temperature conditions described in Phase II. Special bearings and retainer materials were used for exploratory tests up to 1500°F.